PROGRAMA OFICIAL DE POSGRADO

CIENCIA, TECNOLOGÍA Y GESTIÓN ALIMENTARIA

DOCTORAL THESIS

Development of active bioplastics based on wheat proteins and natural antimicrobials for food packaging applications

Mari Pau Balaguer Grimaldo

Supervisors:

Dr Pilar Hernández Muñoz

Dr Rafael Gavara Clemente

Valencia, July 2014

Dra. Pilar Hernández Muñoz, Científico Titular del Consejo Superior de Investigaciones Científicas (CSIC) en el Instituto de Agroquímica y Tecnología de Alimentos (IATA) y

Dr. Rafael Gavara Clemente, Profesor de Investigación del Consejo Superior de Investigaciones Científicas (CSIC) en el Instituto de Agroquímica y Tecnología de Alimentos (IATA).

Certifican que:

La memoria titulada "**Development of active bioplastics based on wheat proteins and natural antimicrobials for food packaging applications**" que presenta Dña. **María de la Paz Balaguer Grimaldo** para optar al grado de Doctor por la Universidad Politécnica de Valencia, ha sido realizada en el **Instituto de Agroquímica y Tecnología de Alimentos** (IATA-CSIC) bajo su dirección y que reúne las condiciones para ser defendida por su autora.

Valencia, 5 de Mayo de 2014

Fdo. Dra. P. Hernández Muñoz
Directora de la Tesis

Fdo. Dr. R. Gavara Clemente
Director de la Tesis

Av. Agustín Escardino, 7
46980 Paterna, Valencia, Spain
Tel: +34 963 90 0022
Fax: +34 963 63 6301

This work has been funded by the Spanish Ministry of Science and Innovation through the Projects AGL2006-02176, AGL2009-08776, AGL2012-39920-C03-01, and FPI fellowship BES-2008-003026.

A mis padres,

A mi hermana,

A Juan

AGRADECIMIENTOS

A la mañana siguiente me levanté y me puse a llorar.

¿Estás llorando de verdad? - me dijo.

No sabía bien porqué, ¿o sí? Era una mezcla de sensaciones. Felicidad, liberación, estrés, tristeza, satisfacción, agotamiento, nostalgia,… y agradecimiento.

Muchas gracias Rafa por concederme la oportunidad de formar parte de la familia de Envases. Por ser un genio capaz de dejar con la boca abierta a cualquiera y por tu actitud positiva frente a la vida, tengo tanto todavía de lo que aprender que me da pena alejarme. Gràcies Ramón, per tantes coses… per les teues classes magistrals sobre envasos, la teua passió contagiosa per el treball i per els teus rècords d'una vida dedicada a la investigació i combinada amb els plaers de viatjar, les aficions i la família. Y en especial gracias a Pilar, por ser la fuente de inspiración de este trabajo. Por haber sido una trabajadora incansable, por tu perseverancia, tu dedicación, tu amor por la ciencia y por todos los momentos que hemos pasado juntas. Por enseñarme que en la vida todo tiene que tener un equilibrio, que hay que disfrutar de las cosas que aunque parezcan obvias no las reconocemos cuando están delante. Por haberme motivado en muchos aspectos. Por las largas y apasionadas discusiones sobre proteínas y cinamaldehído y cinamaldehído y proteínas. ¡Y por haberme hecho disfrutar tanto de los congresos! Por todo ello gracias Pilar.

Gracias a todos mis compañeros de tesis por haber sido mucho más que eso. Por todas las risas, consejos, "picaetas" y divagaciones sobre ciencia. Gracias Carol porque si tú no hubieras estado en el lab quizás nunca hubiera comenzado esta Tesis y por tu optimismo y felicidad diarios (¡así como por amenizar el lab con tú música!). A Vir porque me llevo contigo una gran amiga y por todos los buenos momentos que hemos pasado y seguimos pasando juntas, ¡sobre todo fuera del lab! A Paula por ser mi referente, por todo lo que he aprendido de ti en muchos aspectos, y porque ¡te quiero un montón! A Joaquín por ayudarme tanto en aquellos duros inicios donde una no sabe muy bien hacia donde va. A Poliana por enseñarme que ante cualquier adversidad una puede salir victoriosa. A Josep Pasqual per la brillant ajuda rebuda sempre que l'he necessitat. A Laura por tu sabiduría y disponibilidad. Y a Gracia por haber sido una compañera más entre nosotros.

Gracias también a todos los estudiantes, chicos de prácticas y demás compañeros que han convivido también conmigo en el lab durante algún tiempo. En especial a Jader, Joan, Irene, Pili, Nerea, Alex, Javi, Belén y Carol V. por haber traído alegría y diversión.

Gracias a las vecinas de mis dos laboratorios por hacer la convivencia tan agradable, a las del 202: Marta V., Marta C., Silvia, Deni, Vicen, Maite,… y a las del 206, en especial a Clara, y a las compañeras de planta, "las chicas de sensorial", sobre todo a Laura.

También al personal del IATA: bibliotecarios, compras, limpieza, mantenimiento, administración,… por hacernos la vida más fácil.

Thanks to Dr Eva Almenar for giving me the opportunity to stay at the School of Packaging in Michigan State University. Thanks for your advice and expertise and for showing me other way to make science. I also want to thank my colleague Koushik Saha for all the help received during that 3 months in US and for his friendship. And also thanks to my 10 housemates in the coop; living with you made my stay amazing!

Merci beaucoup à la Dr Nathalie Gontard pour me recevoir dans son laboratoire de l'IATE à l'Université de Montpellier II et pour toutes les possibilités ultérieures qu'elle m'a offert. Un merci très spécial à la Dr Pascale Chalier pour son inestimable aide pendant mon stage et pour toutes les connaissances qu'elle m'a transmis. Merci aussi au Dr Stéphane Peyron, à la Dr Marie-Hélène Morel et à la Dr Emmanuelle Gastaldi. Brais, Lizeth, Céline, Clara, Mathilde, Célie, Estelle, Thibaut,… merci pour tout.

Merci au Dr Guy César pour m'avoir accueilli au sein de SERPBIO et m'avoir fait bénéficier de toutes ses compétences scientifiques sur compostabilité.

Gracias a ITENE por haberme permitido usar sus equipos e instalaciones durante la realización de esta Tesis y por haberme facilitado la terminación de la escritura durante los primeros meses de mi incorporación.

Gracias también a mis compañeros actuales en ITENE por haberme animado tanto en esta última fase, en especial a los miembros de la "Chupipandi" ¡Sin vosotros no habría podido llevarlo así de bien! Mil gracias por todo vuestro apoyo, alegría, y por ¡las fiestas!

Gràcies papà, mamà i teta per tot. Per el vostre amor, comprensió, confiança, suport, entrega i per sentir-vos tan orgullosos de mi. Crec que no podria haver crescut dins d'una família millor. Vos vull moltíssim!

Gracias Alba por la la espectacular portada de Tesis. Gracias también a mi familia y amigos de siempre por todo su apoyo. En especial a Bàrbara, Isa y Paula.

GRACIAS en mayúsculas a ti Juan. Tu confianza y apoyo me han hecho no querer dejar nunca de luchar y sacar el máximo de todo aquello que me he propuesto. Gracias por escucharme y comprenderme. Gracias por aportarme felicidad, equilibrio, risas, alegría y paz, porque he crecido más tiempo contigo que sin ti y la persona que soy lleva tu huella.

Y gracias a ti también, Tesis, por haberme hecho vivir una enriquecedora experiencia, por todos los lugares a los que me has llevado y por todas las personas que has traído para que se queden junto a mí.

DEVELOPMENT OF ACTIVE BIOPLASTICS BASED ON WHEAT PROTEINS AND NATURAL ANTIMICROBIALS FOR FOOD PACKAGING APPLICATIONS

ABSTRACT

This PhD dissertation focuses on the development of renewable and biodegradable active films based on chemically-modified wheat gliadin proteins endowed with antimicrobial capacity owing to the incorporation of naturally-occurring bioactive compounds, namely cinnamaldehyde, natamycin, and lysozyme.

Gliadin proteins were treated with cinnamaldehyde at acidic pH and films were produced by casting. The resulting protein-based films presented improved functional properties (mechanical, barrier, and water resistance), and biochemical evidence of the formation of a more compact network whose degree of cross-linking increased with the amount of cinnamaldehyde incorporated into the gliadin-ethanolic solution.

Free cinnamaldehyde not participating in the cross-linked reaction remained entrapped in the protein matrix at low relative humidity conditions. The sensitivity of the films to moisture owing to the hydrophilic character of gliadins provided a trigger and control mechanism for the release of cinnamaldehyde in moderate and high relative humidity environments, similar to conditions occurring in packaged food products.

The antimicrobial properties of the films developed were tested *in vitro* by vapor diffusion assays against common food spoilage fungi (*Penicillium expansum* and *Aspergillus niger*), showing great effectiveness. Application of these active films to the preservation of two foodstuffs, sliced bread and cheese spread, gave promising results, lengthening fungal growth lag phase and minimizing fungal growth extension.

Neither the improved functional properties nor the antimicrobial capacity hampered the inherent biodegradability of the gliadin proteins, and the resulting films were compostable, which represents a suitable and environmentally-friendly end-of-life option.

The proteinaceous matrices developed showed different swelling and water diffusivity depending on the degree of cross-linking achieved, which makes them ideal substrates for the development of carrier and release systems for active compounds. Accordingly, lysozyme and natamycin were incorporated into the cross-linked gliadin matrices. Functional, release, and antimicrobial properties were evaluated, and the results indicated the great potential of these novel matrices for active food packaging applications.

DESARROLLO DE BIOPLÁSTICOS ACTIVOS BASADOS EN PROTEÍNAS DE TRIGO Y ANTIMICROBIANOS NATURALES PARA EL ENVASADO DE ALIMENTOS

RESUMEN

En esta Tesis se ha abordado el desarrollo de películas activas, renovables y biodegradables obtenidas a partir de gliadinas de trigo modificadas químicamente y dotadas de capacidad antimicrobiana mediante la incorporación de agentes naturales bioactivos, concretamente cinamaldehído, natamicina y lisozima.

Las gliadinas fueron tratadas con cinamaldehido a pH ácido y las películas fueron producidas mediante extensión y evaporación del solvente. Las películas proteicas resultantes presentaron propiedades funcionales mejoradas (mecánicas, barrera y resistencia al agua) y evidencias bioquímicas de la formación de una red más compacta cuyo grado de entrecruzamiento aumento con la cantidad de cinamaldehído incorporado en la solución etanólica de gliadinas.

El cinamaldehído libre que no participa en la reacción de entrecruzamiento queda retenido en la matriz a bajas humedades relativas. La sensibilidad al agua de los films debida al carácter hidrofílico de las gliadinas proporciona un mecanismo para desencadenar y controlar la liberación de cinamaldehído en entornos con moderada o elevada humedad relativa, condiciones similares a las que ocurren en alimentos envasados.

Las propiedades antimicrobianas de las películas desarrolladas fueron evaluadas *in vitro* mediante ensayos de difusión en fase vapor frente a hongos que provocan deterioro en alimentos (*Penicillium expansum* y *Aspergillus niger*) mostrando una elevada efectividad. El envasado activo de dos alimentos, pan rebanado y queso de untar, dio lugar a resultados

prometedores, alargando la fase de latencia y minimizando la extensión del crecimiento fúngico.

Ni la mejora de las propiedades funcionales ni la capacidad antimicrobiana impidieron la biodegradación inherente de las gliadinas, siendo las películas resultantes compostables, lo que representa una opción de final de vida útil adecuada y respetuosa con el medio ambiente.

Las matrices proteicas desarrolladas mostraron diferente grado de hinchamiento y difusividad del agua en función del grado de entrecruzamiento conseguido, lo que las convierte en sustratos ideales para el desarrollo de sistemas portadores y liberadores de compuestos activos. En este sentido, lisozima y natamicina fueron incorporadas a las matrices de gliadinas entrecruzadas. Las propiedades funcionales, de liberación y antimicrobianas fueron evaluadas y los resultados mostraron el elevado potencial de estas novedosas matrices para ser aplicadas en envasado activo.

DESENVOLUPAMENT DE BIOPLÀSTICS ACTIUS BASATS EN PROTEÍNES DE BLAT I ANTIMICROBIANS NATURALS PER A L'ENVASAT D'ALIMENTS

RESUM

En aquesta Tesi s'ha abordat el desenvolupament de pel·lícules actives, renovables i biodegradables a partir de gliadines de blat modificades químicament i dotades amb capacitat antimicrobiana mitjançant la incorporació d'agents bioactius naturals, concretament cinamaldehid, natamicina i lisozima.

Les gliadines varen ser tractades amb cinamaldehid a pH àcid i les pel·lícules foren produïdes per extensió i evaporació del solvent. Les pel·lícules proteiques resultants presentaren propietats funcionals millorades (mecàniques, barrera i resistència al aigua) i evidencies bioquímiques de la formació d'una xarxa més compacta quin grau d'entrecreuament augmentà en funció de la quantitat de cinamaldehid incorporada a la dissolució etanólica de gliadines.

El cinamaldehid lliure que no participa a la reacció d'entrecreuament queda retingut a la matriu a baixes humitats relatives. La sensibilitat a l'aigua del films deguda al caràcter hidrofílic de les gliadines proporciona un mecanisme de desencadenament i control de l'alliberament de cinamaldehid en entorns amb moderada o elevada humitat relativa, condicions similars a les que es donen en aliments envasats.

Les propietats antimicrobianes de les pel·lícules desenvolupades varen ser avaluades *in vitro* per mitjà d'assajos de difusió en fase vapor contra fongs que provoquen deteriorament en aliments (*Penicillium expansum* i *Aspergillus niger*) mostrant una elevada efectivitat. L'envasat actiu de dos aliments, pa en llesques i formatge d'untar, donà lloc a resultats prometedors, allargant la fase de latència i minimitzant l'extensió del creixement fúngic.

Ni la millora de les propietats funcionals ni la capacitat antimicrobiana impediren la biodegradació inherent de les gliadines, sent les pel·lícules resultants compostables, la qual cosa representa una opció de final de vida útil adequada i respectuosa amb el medi ambient.

Les matrius proteiques desenvolupades mostraren diferent grau d'inflament i difusivitat de l'aigua en funció del grau d'entrecreuament aconseguit, la qual cosa les converteix en substrats ideals per al desenvolupament de sistemes portadors i alliberadors de compostos actius. En aquest sentit, lisozima i natamicina foren incorporades a les matrius de gliadines entrecreuades. Les propietats funcionals, d'alliberament i antimicrobianes foren avaluades i el resultats mostraren l'elevat potencial d'estes noves matrius per a ser aplicades en envasat actiu.

TABLE OF CONTENTS

PREFACE

DISSERTATION OUTLINE

The present Doctoral Thesis is structured in 5 sections. The INTRODUCTION section presents the state of the art in the subject of this work. The OBJECTIVES section presents the general and specific objectives of the Thesis. The CHAPTERS section consists of eight chapters which include the results obtained, presented as a collection of scientific publications. In the section named GENERAL DISCUSSION, a global discussion of the results is presented, with emphasis on the most remarkable results obtained from this Doctoral Thesis. Finally, the most important CONCLUSIONS are compiled in the last section. **Figure A** shows the structure of the present Doctoral Thesis schematically.

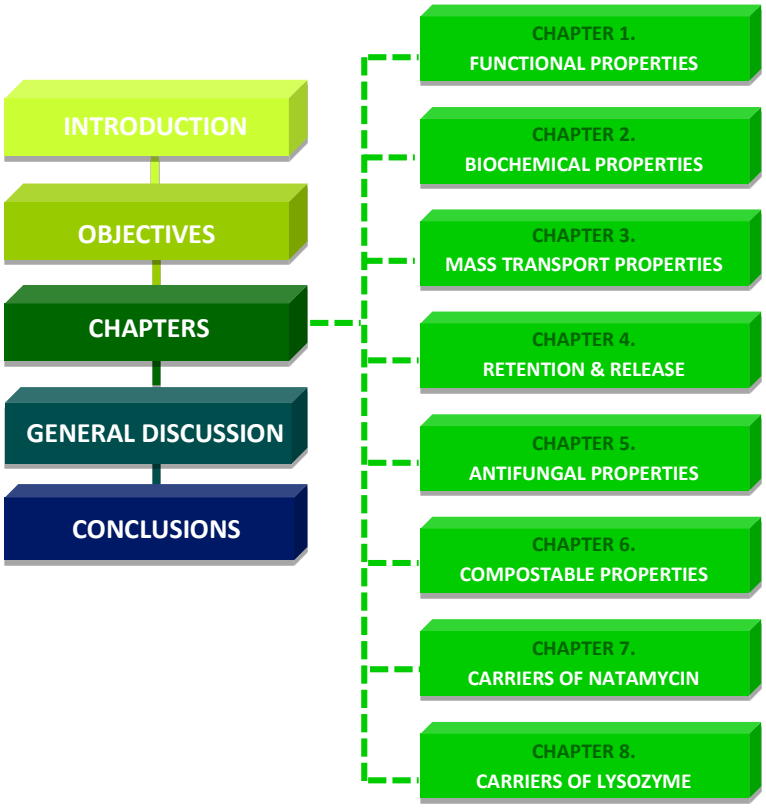

Figure A. Scheme of the Doctoral Thesis structure.

Chapter 1, entitled *Functional properties of bioplastics made from wheat gliadins modified with cinnamaldehyde*, presents new bioplastics based on chemically modified gliadins with cinnamaldehyde (3-phenylprop-2-enal), an α-β-unsaturated aldehyde and major component of cinnamon bark essential oil. Films produced from modified proteins and obtained by the solvent-casting technique improved their functional properties. In this chapter their mechanical (tensile test), thermal (modulated differential scanning calorimetry and thermogravimetric analysis), optical (CIELab color), morphological (scanning electron microscopy), and water resistance (protein solubility by bicinchoninic acid assay) properties are evaluated.

In **Chapter 2**, entitled *Biochemical properties of bioplastics made from wheat gliadins cross-linked with cinnamaldehyde*, a first insight into the cross-linking reaction mechanism of gliadins by cinnamaldehyde is given. Different assays are conducted in order to corroborate or rule out the participation of various reactive side groups present in amino acids. Biochemical evidences of the formation of a more reticulated structure (amino acid analysis, free amino groups, sodium dodecyl sulfate-polyacrylamide gel electrophoresis, enzymatic degradation, and protein solubility) are discussed.

Chapter 3, entitled *Mass transport properties of gliadin films: effect of cross-linking degree, relative humidity, and temperature*, details a complete study related to the mass transport phenomena of water vapor, oxygen, and carbon dioxide through chemically-modified gliadin films. Permeation, sorption, and diffusion are evaluated as a function of temperature, relative humidity, and degree of cross-linking of the matrix. The complexity of the mechanisms of water vapor transport through hydrophilic films is highlighted as the appearance of discontinuous and non-linear behaviors, deviating from ideal conditions, as well as the formation of clusters and plasticization of the amorphous region. Permselectivity to carbon dioxide versus oxygen is also studied. As a result of this work an exhaustive characterization of the barrier properties is given.

Retention and release of cinnamaldehyde from wheat protein matrices are evaluated in **Chapter 4**. Although cinnamaldehyde participates in the cross-linking reaction, which lets it bond covalently with protein, some amount remains free, entrapped in the matrix by weak interactions. The release of free cinnamaldehyde from the cross-linked gliadin matrix under diverse relative humidity conditions is studied and the diffusion coefficients are calculated. Moreover, new insight into the cross-linking mechanism with cinnamaldehyde is provided

by means of size exclusion–high performance liquid chromatography and attenuated total reflectance–Fourier transform infrared spectroscopy. Overall migration in food simulants according to Regulation 10/2011/EC is also analyzed.

According to the previous chapter, the films can release cinnamaldehyde, which, besides acting as a cross-linker, has been indicated as a powerful antimicrobial compound. Therefore, the antimicrobial activity of the films developed is tested *in vitro* against common food-spoilage fungi, *Penicillium expansum* and *Aspergillus niger*, and their potential as active food packaging systems to extend the microbiological shelf-life of sliced bread and cheese spread is studied. The results are compiled in **Chapter 5**: *Antifungal properties of gliadin films incorporating cinnamaldehyde and application in active food packaging of bread and cheese spread foodstuffs.*

As the films are designed for food packaging applications and are, according to their origin, inherently biodegradable, a possible and very favorable end-of-life scenario would be organic recycling. However, the improvement of their functional properties, especially water resistance, and their antimicrobial ability could endanger their compostability. **Chapter 6**, entitled *Compostable properties of antimicrobial bioplastics based on cinnamaldehyde cross-linked gliadins*, evaluates film disintegration and biodegradation in composting conditions, and ecotoxicity of the resulting compost.

As a result of modification of the degree of cross-linking of the protein matrix and consequent improvement of water resistance and swelling, the new films could be employed as carriers of other natural antimicrobials, being able to modulate their release rate. Natamycin and lysozyme were selected and incorporated into the films. The functional and release properties and antimicrobial efficacy of the resulting films are investigated and shown in **Chapter 7**, *Functional properties and antifungal activity of films based on gliadins containing cinnamaldehyde and natamycin*, and **Chapter 8**, *Chemically modified gliadins as sustained release systems for lysozyme*, respectively.

DISSEMINATION OF RESULTS

The present Doctoral Thesis gave rise to eight scientific articles published in international peer-reviewed journals:

1. **Balaguer, M.P.**; Gómez-Estaca, J.; Gavara, R.; and Hernandez-Munoz, P. **2011**. Functional properties of bioplastics made from wheat gliadins modified with cinnamaldehyde. *Journal of Agricultural and Food Chemistry*, *59*(12), 6689-6695. http://dx.doi.org/10.1021/jf200477

2. **Balaguer, M.P.**; Gómez-Estaca, J.; Gavara, R.; and Hernandez-Munoz, P. **2011**. Biochemical properties of bioplastics made from wheat gliadins cross-linked with cinnamaldehyde. *Journal of Agricultural and Food Chemistry*, 59(24), 13212-13220. http://dx.doi.org/10.1021/jf203055s

3. **Balaguer, M.P.**; Cerisuelo, J. P.; Gavara, R.; and Hernandez-Munoz, P. **2013**. Mass transport properties of gliadin films: effect of cross-linking degree, relative humidity, and temperature. *Journal of Membrane Science*, 428(0), 380-392. http://dx.doi.org/10.1016/j.memsci.2012.10.022

4. **Balaguer, M.P.**; Borne, M.H.; Chalier, P.; Gontard, N.; Morel M.-H.; Peyron, S.; Gavara, R.; and Hernandez-Munoz, P. **2013**. Retention and release of cinnamaldehyde from wheat protein matrices. *Biomacromolecules,* 14(5), 1493-502. http://dx.doi.org/10.1021/bm400158t

5. **Balaguer, M.P.**; Lopez-Carballo G.; Catala R.; Gavara, R.; and Hernandez-Munoz, P. **2013**. Antifungal properties of gliadin films incorporating cinnamaldehyde and application in active food packaging of bread and cheese spread foodstuffs. *International Journal of Food Microbiology*, 166, 369-77. http://dx.doi.org/10.1016/j.ijfoodmicro.2013.08.012

6. **Balaguer, M.P.**; Fajardo, P.; Gartner, H.; Gomez-Estaca, J.; Gavara, R.; Almenar, E.; and Hernandez-Munoz, P. **2014**. Functional Properties and Antifungal Activity of Films Based on Gliadins Containing Cinnamaldehyde and Natamycin. *International Journal of Food Microbiology*, 173(0), 62-71. http://dx.doi.org/10.1016/j.ijfoodmicro.2013.12.013

7. Fajardo, P.; Balaguer, M.P.; Gomez-Estaca, J.; Gavara, R.; and Hernandez-Munoz, P. **2014**. Chemically modified gliadins as sustained release systems for lysozyme. *Food Hydrocolloids*, 41, 53-59. http://dx.doi.org/10.1016/j.foodhyd.2014.03.019

8. Balaguer, M.P.; Villanova, J.; Cesar, G.; Gavara, R.; and Hernandez-Munoz, P. Compostable properties of antimicrobial bioplastics based on cinnamaldehyde cross-linked gliadins. **2015**. *Chemical Engineering Journal,* 262, 447-455. http://dx.doi.org/10.1016/j.cej.2014.09.099

The results were also presented at international conferences:

1. **Poster presentation** – **Balaguer, M.P.**; Gómez-Estaca, J.; Gavara, R.; and Hernandez-Munoz, P. *Cinnamaldehyde: a naturally occurring crosslinker for wheat prolamin films.* 1st International Meeting on Material Bioproduct Interactions (**MATBIM 2010**). March 3-5. Institute of Technology for Life, Food and Environmental Sciences (Agroparistech), Paris, France.

2. **Poster presentation** – **Balaguer, M.P.**; Gómez-Estaca, J.; Gavara, R.; and Hernandez-Munoz, P. *Naturally occurring cinnamaldehyde as a crosslinker to improve the physical performance of renewable gliadin films.* Institute of Food Technologists Annual Meeting and Food Expo (**IFT 2010**). July 17-20. Chicago, IL, USA.

3. **Poster presentation** – Fajardo, P.; **Balaguer, M.P.**; Vieites, J.M.; Gavara, R.; and Hernandez-Munoz, P. *Active packaging based on chemically modified gliadins as sustained release systems of natural antimicrobial compounds*. International Conference on Food Innovation (**Food Innova 2010**). October 25-29. Research Institute of Food Engineering for Development (IIAD). Polytechnic University of Valencia (UPV), Valencia, Spain.

4. **Poster presentation** – **Balaguer, M.P.**; Gavara, R.; Hernandez-Munoz, P.; Almenar, E. *Antifungal activity of biopolymers made from wheat gluten containing naturally occurring cinnamaldehyde and natamycin*. American Society for Horticultural Science Annual Conference (**ASHS 2011**). September 25-28. Waikoloa, Hawaii, USA.

5. **Poster presentation** – **Balaguer, M.P.**; Gartner, H.; Gavara, R.; Almenar, E.; and Hernandez-Munoz, P. *Effectiveness of wheat gluten-based films containing naturally*

occurring cinnamaldehyde and natamycin against the growth of main postharvest fungi. **United Fresh 2012** Convention. May 1-3. Dallas, Texas, USA.

6. **Poster presentation** – Fajardo, P.; **Balaguer, M.P.**; Gómez-Estaca, J.; Muriel-Galet, V.; Gavara, R.; Hernandez-Munoz, P. *Renewable films based on reticulated proteins for their application in antimicrobial food packaging technologies*. 18th IAPRI World Packaging Conference (**IAPRI 2012**). June 17-21. Cal Poly State University, San Luis Obispo, CA, USA.

7. **Poster presentation** – Fajardo, P.; **Balaguer, M.P.**; Gavara, R.; and Hernandez-Munoz, P. *Sustained Release of Antimicrobial Agents from Reticulated Protein films Intended for Active Packaging Applications*. 2nd International Workshop on Food Safety: Technologies and innovations applied to Food Science (**SICURA & CIGR 12**). July 5-6. IATA-CSIC, Valencia, Spain.

8. **Poster presentation** – **Balaguer, M.P.**; Gómez-Estaca, J.; Martínez-López, B.; Chalier, P.; Gontard, N.; Gavara, R.; and Hernandez-Munoz, P. *Eco-friendly antimicrobial films based on cross-linked gliadins and cinnamaldehyde*. European Federation of Food Science and Technology Annual Conference (**EFFoST 2012**). November 20-23. Montpelier, France.

9. **Poster presentation**★ **– Balaguer, M.P.**; Chalier, P.; Gontard, N.; Aucejo, S.; Gavara, R.; and Hernandez-Munoz, P. *Physical improvement of protein films with antimicrobial properties*. VII International Packaging Congress & Exhibition (**Ambalaj 2013**). May 9-11. Izmir, Turkey.

10. **Poster presentation** – **Balaguer, M.P.**; Fajardo, P.; Almenar, E.; Gavara, R.; and Hernandez-Munoz, P. *Active packaging of cheese with bioplastics based on wheat proteins and natural antimicrobials*. Institute of Food Technologists Annual Meeting and Food Expo (**IFT 2013**). July 13-16. Chicago, IL, USA.

11. **Poster** – **Balaguer, M.P.**; Aucejo, S.; Gavara, R.; and Hernandez-Munoz, P. *Compostability of cross-linked wheat protein films with antimicrobial properties*. 4th International Conference on Biodegradable Polymers and Sustainable Composites (**BIOPOL 2013**). October 1-3. Rome, Italy.

★ Winner of the Best Poster Award.

12. **Poster – Balaguer, M.P.**; Chalier, P.; Almenar, E.; Gontard, N.; Zabaleta, J.; Gavara, R.; and Hernandez-Munoz, P. *Biodegradable cross-linked gliadin films with antifungal activity for active packaging of bread*. 19th IAPRI World Packaging Conference (**IAPRI 2014**). June 15-18. Melbourne, Australia.

13. **Poster – Balaguer, M.P.**; Almenar, E.; Gavara, R.; and Hernandez-Munoz, P. Active packaging of bread with antimicrobial films based on wheat proteins and cinnamaldehyde. Institute of Food Technologists Annual Meeting and Food Expo (**IFT 2014**). June 21-24. New Orleans, LA, USA.

PREDOCTORAL STAYS AT FOREIGN INSTITUTIONS

Two predoctoral stays were carried out during the development of this Doctoral Thesis at:

- School of Packaging of Michigan State University (East Lansing, MI, USA) from June 2010 to August 2010 under the supervision of Dr Eva Almenar.
- UMR Ingénierie des Agropolymères et Technologies Emergentes at Université de Montpellier II (Montpellier, France) from September 2011 to December 2011 under the supervision of Dr Nathalie Gontard.

I. INTRODUCTION

I.1. FOOD PRODUCTS SHELF-LIFE

Food products undergo numerous physical, chemical, and microbiological changes during storage. The stability of food is a function of (i) product characteristics, including formulation and processing parameters (pH, water activity, enzymes, microorganisms, and concentration of reactive compounds); (ii) preservation treatments and packaging technology applied; and (iii) the environment to which the product is exposed during distribution and storage (temperature, RH, light, total and partial pressures of different gases, and mechanical stresses, including consumer handling) (Robertson, 2009).

According to the Institute of Food Science and Technology (IFST, UK) shelf-life can be defined as the period of time during which the food product will remain safe; be certain to retain desired sensory, chemical, physical, microbiological and functional characteristics; and comply with any label declaration of nutritional data when stored under the recommended conditions.

I.1.1. Microbial food spoilage

Microbial spoilage is a major concern for perishable foods such as fresh fruits, vegetables, meat, poultry, fish, bakery products, milk, and juices (Singh and Anderson, 2004). Potential food spoilage microorganisms include bacteria, fungi (mold and yeast), viruses, and parasites. Consequences of microbial growth in foods include consumer hazards as a result of the presence of pathogenic microorganisms or microbial toxins, as well as economic losses as a result of spoilage (Davidson, 2001). Inactivation, growth delay, and growth prevention of spoilage and pathogenic microorganisms are main objectives of food preservation (López-Malo et al., 2005).

Several factors influence microbial growth and survival; appropriate modification and/or application of these factors is the basis of food preservation technologies. Food preservation technologies work by (i) preventing or slowing down microbial growth (low temperature, reduced water activity, acidification, fermentation, modified atmosphere packaging, addition of antimicrobials, compartmentalization in water-in-oil emulsions), (ii) inactivating microorganisms (heat pasteurization and sterilization, microwave heating, ionizing radiation, high pressure, pulsed electric fields, high frequency ultrasound), and (iii) preventing or minimizing entry of microorganisms into food or removing them (aseptic

handling or packaging, centrifugation, filtration) (Gould, 1995; Sofos et al., 1998). Moreover, techniques in combination based on the hurdle technology concept (Leistner, 1995) may act by inhibiting or inactivating microorganisms.

The growth of certain microbial pathogen species may endanger consumer safety, and therefore potential proliferation should be avoided or strictly controlled (Lee, 2009). Along with pathogenic organisms, certain genera of spoilage organisms dominate the microbial flora of foods, and their growth reduces sensory quality, thus limiting shelf-life (Lee, 2009). Regulation 2073/2005/EC lays down the microbiological criteria for certain microorganisms and the implementing rules to be complied with by food business operators when implementing the general and specific hygiene measures referred to in Article 4 of Regulation 852/2004/EC. As safety criteria, certain pathogenic microbes such as *Salmonella, E. coli*, and *Listeria* should be totally absent from foods that are microbiologically perishable in nature. On the other hand, for some pathogenic bacteria such as *Bacillus cereus* and *Staphylococcus aureus*, the usual practice in food processing and distribution is to reduce the level of contamination, eliminating the potential risk of their growth to harmful levels, and thus avoiding subsequent food poisoning. However, the acceptable limit of microbial growth that determines the shelf-life of a food product is not well established. This limit differs with food type, storage conditions, and defined shelf-life.

Microbial growth in perishable foods can typically be represented as a function of time by the pattern shown in **Figure I.1**. The growth curves are usually divided into lag, exponential, stationary, and death phases. Sometimes the shelf-life of foods sensitive to microbial proliferation is taken as the lag time (Lee, 2009), which is defined as the period in which microorganisms are adapting to the medium before they start exponential growth. Storage and packaging conditions favorable for microbial spoilage result in shorter lag times and faster growth rates during the exponential phase. Microbial counts of 10^5–10^8 organisms per g or cm^2, located mostly in the linear exponential phase of **Figure I.1**, are commonly used as another convenient upper limit of quality.

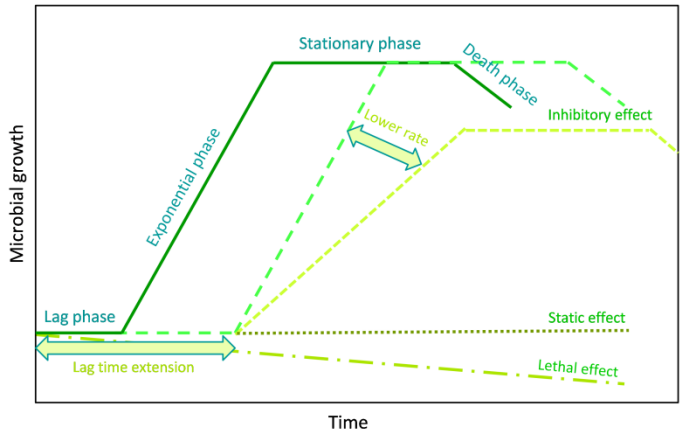

Figure I.1. Typical pattern of microbial growth in perishable food products stored under constant environmental conditions and different mechanisms of action of antimicrobials.

Regardless of the preservation technology used, packaging is an essential process in the food manufacturing chain.

I.2. FOOD PACKAGING TECHNOLOGIES

Packaging provides four basic functions (Brody et al., 2008; Marsh and Bugusu, 2007; Robertson, 2006):

1. *Containment.* The containment function involves the ability of the packaging to maintain its integrity during the handling involved in filling, sealing, processing, transportation, and dispensing of the food (Krochta, 2007).

2. *Protection.* The need for protection depends on the food product but generally includes prevention of three major classes of external influences: chemical, biological, and physical. Chemical protection minimizes compositional changes triggered by environmental influences such as exposure to gases, typically oxygen, which can allow oxidation of lipids, flavors, colors, vitamins, etc.; moisture (loss or gain, which affects microbial growth, oxidation rates, and food texture), aroma (loss or gain), heat, and light (Brody et al., 2008; Marsh and Bugusu, 2007). Biological protection provides a barrier to microorganisms (pathogens and spoiling agents), insects, rodents, and other animals, thereby preventing

disease and spoilage. Physical protection shields food from mechanical damage and includes cushioning against the shock and vibration encountered during distribution, abrasion, fracture, and/or crushing (Krochta, 2007; Marsh and Bugusu, 2007).

3. *Communication.* The information that a package provides involves meeting both legal requirements and marketing objectives (Krochta, 2007). Food labels are required to provide information on the food processor, ingredients (including possible allergens), net content, nutrient content, and country of origin. Package graphics are intended to communicate product quality, branding, and sales promotion, and thus sell the product. Bar codes and radiofrequency identification tags (RFID) allow rapid check-out and tracking of inventory.

4. *Convenience.* Providing convenience (sometimes referred to as utility of use or functionality) to consumers has become a desired function of packaging (Krochta, 2007). Range of sizes; easy handling and disposal, easy opening and dispensing; portion control; reclosability, product visibility; and food preparation in the package (ovenability/microwavability) are examples of packaging designs that provide convenience to the consumer (Han, 2014; Marsh and Bugusu, 2007).

In recent years, in order to fulfil the requirements of the modern food industry, demanding consumers, and new legislation related to food safety and the environment, novel food packaging technologies have been developed. Active and intelligent packaging systems, modified atmosphere packaging, and edible films and coatings are among the most promising ones.

I.2.1. Active food packaging

Active packaging is an innovative concept that can be defined as a mode of packaging in which package, product, and environment interact to prolong shelf-life or enhance safety and/or quality of the product (Suppakul et al., 2003)

Active packaging positively employs the mass transport phenomena that take place in polymeric materials (Catalá and Gavara, 2002). These mass transfer processes are permeation, migration, and sorption. Permeation is the process by which substances are exchanged between the external and internal packaging environments through the package walls. Migration consists of the release of low molecular weight substances from the package into the food phase. Sorption is the retention of food components within the package structure. The driving force of these processes is the lack of chemical equilibrium of various

substances that are constituents of the product/package/environment system. At the interfaces of this complex system, substances are sorbed into or desorbed from the package material. The extent of these mass exchanges depends on the affinity of a given substance for the two contacting media. Within the polymeric packaging structure, the substances diffuse from sites with high concentration to sites with lower concentration, the concentration difference acting as a driving force. **Figure I.2** schematically describes the interactions that may occur when a food product, the package, and the environment are placed in contact. Some of these possible interactions are (i) permeation of volatile components such as gases, for example oxygen and carbon dioxide, water vapor, and aroma components; (ii) sorption of food components by the packaging material (i.e. aroma scalping); and (iii) migration of package components into the food (Dury-Brun et al., 2007; Krochta, 2007).

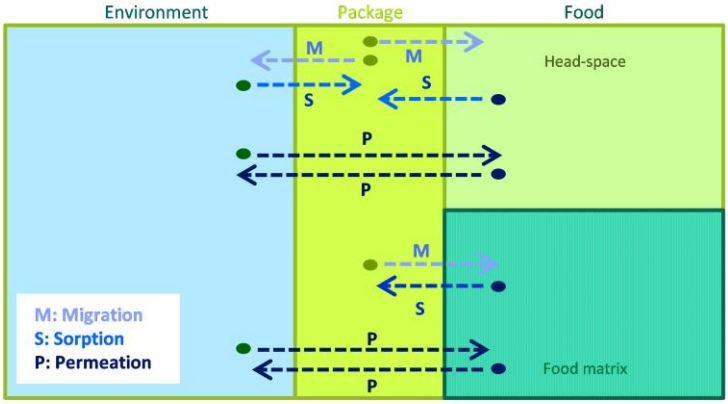

Figure I.2. Mass transport phenomena in the food/package/environment system.

Active food packaging techniques can be divided into three categories: absorbers (i.e. scavengers), releasing systems, and other systems. Absorbing systems remove undesired compounds present in the food or in the package head-space such as oxygen, carbon dioxide, ethylene, excessive water, taints, and other specific compounds. Releasing systems actively add or emit compounds to the packaged food or into the package head-space such as carbon dioxide, antioxidants, and preservatives. Other systems may have miscellaneous tasks, such as temperature control (self-heating, self-cooling, microwave susceptors and modifiers, and temperature-sensitive packaging) and preservation (UV and surface-treated

packaging materials). **Table I.1** summarizes some active food packaging applications where transport phenomena are involved in the action mechanisms.

Table I.1. Examples of active food packaging applications (Ahvenainen, 2003; Restuccia et al., 2010).

Function	Compound	Principle/ Mechanism/ Reagents	Purpose	Possible Applications
Absorbing / Scaven-ging	Oxygen	Enzymatic systems (glucose oxidase-glucose, alcohol oxidase-ethanol vapor) Chemical systems (powdered iron oxide, catechol, ferrous carbonate, iron-sulfur, sulfite salt-copper sulfate, photosensitive dye oxidation, ascorbic acid oxidation, catalytic conversion of oxygen by platinum catalyst)	Reduction/prevention of mold, yeast and aerobic bacteria growth Prevention of oxidation of fats, oils, vitamins, colors Prevention of damage by worms, insects, and insect eggs	Cheese, meat products, ready-to-eat products, bakery products, coffee, tea, nuts, milk powder
	Carbon dioxide	Iron powder-calcium hydroxide, ferrous carbonate-metal halide	Removal of carbon dioxide formed during storage in order to prevent bursting of a package	Coffee Beef jerky Dehydrated poultry products
	Ethylene	Aluminum oxide and potassium permanganate Activated carbon + metal catalyst Zeolite Clay Silicon dioxide powder Japanese oya stone	Prevention of too fast ripening and softening	Fruits like apples, apricots, banana, mango, cucumber, tomatoes, kiwifruit, avocados, persimmons and vegetables like carrots, potatoes and Brussels sprouts
	Moisture	Polyacrylates Propylene glycol Silica gel Clays Polyvinyl alcohol Diatomaceous earth	Control of excess moisture in packed food Reduction of water activity on the surface of food in order to prevent the growth of molds, yeast and spoilage bacteria	Dry and dehydrated products, meat, fish, poultry, bakery products, cuts of fruits and vegetables
	Off flavors, amines and aldehydes	Cellulose acetate film containing naringinase enzyme Ferrous salt and citric or ascorbic acid Specially treated polymers Baking soda Active carbon	Reduction of bitterness in grapefruit juice Improving the flavor of fish and oil-containing food	Fruit juices Fish Oil-containing foods (potato chips, biscuits and cereal products) Beer

Removing	Lactose	Immobilized lactase in the packaging material	Serving milk products to people suffering from lactose intolerance	Milk and other dairy products
	Cholesterol	Immobilized cholesterol reductase in the packaging material	Improving the healthiness of milk products	Milk and other dairy products
Releasing / Emitting	Carbon dioxide	Ascorbic acid Sodium hydrogen carbonate and ascorbate	Growth inhibition of Gram-negative bacteria and molds	Vegetables and fruits, fish, meat, poultry
	Ethanol	Ethanol/water mixture absorbed into silicon dioxide powder generating ethanol vapor	Growth inhibition of molds and yeast	Bakery products (preferably heated before consumption) Dry fish
	Antimicro-bial Preserva-tive	Organic acids (sorbic acid) Silver zeolite Spice and herb extracts Allyl isothiocyanate Enzymes (Lysozyme)	Growth inhibition of spoilage and pathogenic bacteria	Meat, poultry, fish, bread, cheese, fruit and vegetables
	Sulfur dioxide	Sodium metabisulfite incorporated in microporous material	Inhibition of mold growth	Fruits
	Antioxidant	BHA, BHT Tocopherol Maillard reaction Volatiles	Inhibition of oxidation of fat and oil	Dried foodstuffs Fat-containing foodstuffs
	Flavoring	Various flavors in polymers	Minimization of flavor scalping Masking off-odors Improving the flavor of food	Miscellaneous
	Pesticide	Imazalil Pyrethrins	Prevention of growth of spoilage bacteria Fungicidal or pest control	Dried, sacked foodstuffs, e.g. flour, rice, grains

Among these applications, antimicrobial packaging has attracted great interest in the last decade as a novel food preservation technology.

I.2.1.1. Antimicrobial food packaging

Antimicrobial packaging is defined as a packaging technology able to kill or inhibit spoilage and pathogenic microorganisms that are contaminating foods (Han, 2003). The antimicrobial packaging system (or material) limits or prevents microbial growth by extending the lag period, and reducing the growth rate or decreasing live counts of microorganisms (Han, 2000) [See **Figure I.1**].

The antimicrobial function can be achieved by using antimicrobial polymers and/or incorporating antimicrobial agents in the packaging system. There are basically two

methodologies for this: (i) use of independent devices such as sachets, pads, and labels that contain the antimicrobial agent aside from the food product in a conventional 'passive' package, and (ii) incorporation of the antimicrobial agent(s) in the walls of the package.

Food packaging materials with antimicrobial activity have two modes of action: (i) materials that release the antimicrobial agent onto the food surface in direct contact or into the package head-space (**Figures I.3A and I.3B,** respectively), (ii) materials that immobilize the antimicrobial agent and inhibit microbial growth on the food surface in direct contact (**Figure I.3C**) (Bastarrachea et al., 2011; Corrales et al., 2014). The release of the antimicrobial agent is controlled by a combination of mass transport phenomena that involve equilibrium and kinetic processes in the food, head-space, and packaging material (López-Carballo et al., 2012). The antimicrobial agent is partitioned in all phases, and the concentration ratio at the interfaces is given by the partition coefficient between the packaging material and the food ($K_{P/F} = C_p/C_F$), and, for volatile agents, the solubility of the antimicrobial agent in the head-space ($S_{P/HS} = C_P/P_{HS}$ and $S_{F/HS} = C_F/P_{HS}$). The release rate of the antimicrobial agent, which is defined by the diffusion coefficient (D_P), should be controlled according to the requirements of the food product. Changes in polymer chain mobility, such as those produced by plasticizers or cross-linking agents, modifications of the tortuosity of the diffusion path, for example by means of inclusion of particles in the polymer matrix, and triggered response mechanisms can modulate it.

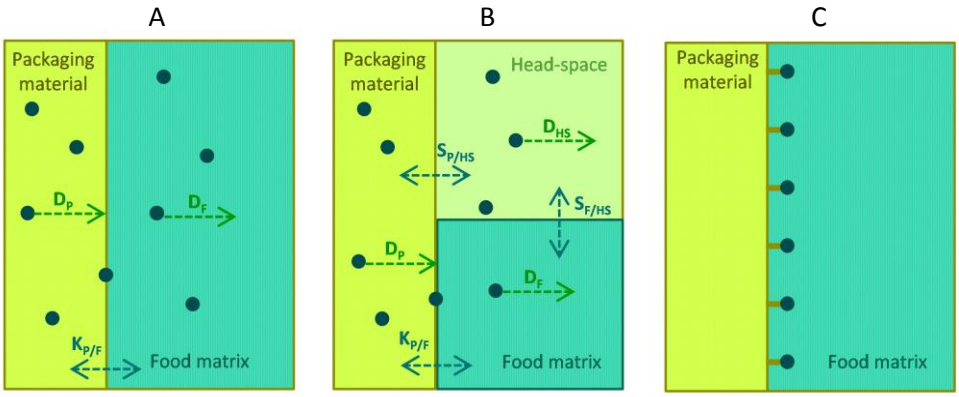

Figure I.3. Modes of action of antimicrobial food-packaging materials and mass transport phenomena taking place. (**A**) Packaging material that releases the antimicrobial agent directly onto the food surface in contact, (**B**) packaging material that releases the antimicrobial agent to the head-space and onto the food surface in direct contact, and (**C**) packaging material with the antimicrobial agent immobilized in the polymeric surface. Adapted from Han (2003) and López-Carballo et al. (2012).

Many factors related to the foodstuff, the antimicrobial agent, and the material should be considered when designing the antimicrobial packaging system. Some of them are: activity of the antimicrobial in a specific food matrix, microbial resistance, organoleptic characteristics and toxicity of antimicrobials, methods of incorporation of the antimicrobial agent in the material, release mechanisms and kinetics, chemical compatibility of the antimicrobial with the material and with the food, storage and distribution conditions, film/container processing conditions, physical and mechanical properties of the material after incorporating the antimicrobial, the effect of processing conditions on the activity of the antimicrobial, and corresponding regulations regarding developed active materials intended to come into contact with foodstuffs.

A large number of synthetic and naturally-occurring agents with antimicrobial properties such as organic acids/anhydrides, parabens, inorganic gases, metals, fungicides, bacteriocins, enzymes, chelating agents, spices, essential oils, plant extracts, etc. have been tested with the purpose of inhibiting the growth of microorganisms that can lead to deterioration of foodstuffs; however, few antimicrobial packaging systems are commercially available nowadays (**Table I.2**), and most of them are based on permeable sachets or labels in which the antimicrobial is incorporated (Appendini and Hotchkiss, 2002; Corrales et al., 2014; Pereira de Abreu et al., 2012).

Table I.2. Examples of commercial antimicrobial packaging systems for food applications (adapted from Appendini and Hotchkiss (2002); Corrales et al. (2014); Pereira de Abreu et al. (2012)).

Trade name	Active compound	Producer	Country
Piatech	Silver oxide	Daikoku Kasei Co.	Japan
Silvi Film		Nimiko Co.	Japan
Okamoto Super Wrap		Okamoto Industries, Inc.	Japan
Apacider	Silver zeolite	Sangi Co.	Japan
Zeomic		Shinanen New Ceramics Co.	Japan
Bactekiller		Kanebo Co.	Japan
Cleanaid		Gyunghyang Ind. Co.	Korea
AgIon	Silver	AgIon Technologies LLC	USA
Ageless SE		Mitsubishi Gas Chem.	Japan
MicroFree	Silver, copper oxide, zinc silicate	DuPont	USA
Novaron	Silver zirconium phosphate	Miliken Co.	USA
Surfacine	Silver halide	Surfacine Development Co.	USA
Ionpure	Silver/glass	Ishizuka Glass Co.	Japan
Microban	Triclosan	Microban Products Co.	USA
Sanitized	Triclosan and others	Sanitized AG/Clariant	Switzerland
Actigard		Thomsom Research Assoc.	Canada
Saniprot		Thomsom Research Assoc.	Canada
Ultra-Fresh		Thomsom Research Assoc.	Canada
WasaOuro	Allyl isothiocyanate	Green Cross Co.	Japan

Wasa Power		Sekisui Plastic Co.	Japan
MicroGarde	Clove and others	Rhône-Poulenc	USA
Take Guard	Bamboo extract	Takex Co.	Japan
Ethicap	Ethanol	Freund Industrial Co.	Japan
Antimold		Freund Industrial Co.	Japan
Negamold		Freund Industrial Co.	Japan
Oitech		Nippon Kayaku	Japan
Biocleanact	Antibiotics	Micro Science Tech Co.	Korea
Microsphere	Chlorine dioxide	Bernard Technologies Inc.	USA
Grape Guard	Sulfur dioxide	Química Osku S.A.	Chile
Uvasy		Grapetek	South Africa
Verifrais	Carbon dioxide	SARL Codimer	France
Bioka	Glucose oxidase (H_2O_2)	Bioka Ltd	Finland

I.2.1.1.1. Naturally-occurring antimicrobial compounds

The demand for minimally processed foods and the use of naturally-occurring bioactive ingredients is steadily rising. This is because of growing concern about the use of synthetic preservatives with limited documentation on safety and tolerance; the suspected link between the overuse of antimicrobials at various stages of the food system and the development of multi-drug resistance in microorganisms; and increased media dissemination of knowledge on diet and health (Naidu, 2000).

Numerous antimicrobial agents exist in animals and plants, where they evolved as host defense mechanisms. Naturally-occurring antimicrobials are abundant in the environment. These compounds may exhibit antimicrobial activity in foods as natural ingredients or may be used as additives in other foods (Naidu, 2000). In the case of antimicrobial packaging, these antimicrobial compounds can be incorporated into the packaging material. **Table I.3** lists some naturally-occurring antimicrobials.

Table I.3. Naturally-occurring antimicrobials for food (López-Malo et al., 2005; Naidu, 2000)

Class of natural system	Antimicrobial compounds
Lacto-antimicrobials	Lactoferrin, Lactoperoxidase, Lactoglobulins, Lactolipids
Ovo-antimicrobials	Lysozyme, Ovotransferrin, Ovoglobulin IgY, Avidin
Phyto-antimicrobials	Phyto-phenols, Saponins, Flavonoids, Thiosulfinates, Catechins, Glucosinolates, Agar
Bacto-antimicrobials	Probiotics, Nisin, Natamycin, Pediocin, Reuterin, Sakacins
Acid-antimicrobials	Lactic acid, Sorbic acid, Acetic acid, Citric acid
Milieu-antimicrobials	Sodium chloride, Polyphosphates, Chloro-cides, Ozone

However, for more extensive use of naturally-occurring antimicrobials, some points should be addressed (adapted from Sofos et al. (1998)), such as (i) efficacy and functionality in foods, (ii) toxicology and safety, (iii) interactions with food components and other preservative systems, (iv) mechanisms of action against microorganisms, (v) influences on food quality (e.g. nutritional and sensory), (vi) methods for application in commercial formulations, (vii) extraction, isolation, and economical production, and (viii) methods of incorporation in packaging materials.

In this Thesis three different naturally-occurring antimicrobials, namely cinnamaldehyde, natamycin, and lysozyme, were selected for incorporation in a biopolymer matrix with the aim of developing active materials directed at food packaging applications.

I.2.1.1.1.1. Cinnamaldehyde

Cinnamaldehyde, a naturally-occurring α,β-unsaturated aldehyde derived from cinnamon, has been shown to be a powerful antimicrobial agent against a wide range of microorganisms (Burt, 2004). It is registered in the EU flavoring list (FL no. 05.014), and the FDA has classified it as a synthetic GRAS flavoring substance for its intended use (reg no. 182.60). Minimal inhibitory concentrations (MIC) obtained by various authors are summarized in **Table I.4**. Cinnamaldehyde has been incorporated in a wide variety of matrices to give them antimicrobial activity (**Table I.5**). Moreover, active packaging systems containing cinnamaldehyde have shown promising results when tested in food (**Table I.6**).

Table I.4. Minimal inhibitory concentrations of cinnamaldehyde in various testing methods.

Method	Microorganism	MIC Original units	MIC Converted units	MIC definition	Reference
Disc vapor diffusion		mmol/dish	mg/L	The minimum concentration required to give complete control	Utama et al. (2002)
	R. stolonifer	0.42	1014		
	P. digitatum	0.09	217		
	C. musae	0.39	942		
	E. carotovora	0.11	266		
	P. aeruginosa	0.41	990		
Disc vapor diffusion		µL/L	mg/L	The minimum vapor concentration of the compound that totally inhibits growth (i.e. no detectable bacterial or fungal growth) by comparison with control	Lopez et al. (2007b)
	L. monocytogenes	21.8	22.9		
	S. choleraesuis	4.4	4.62		
	A. flavus	21.8	22.9		
	C. albicans	4.4	4.62		
Disc vapor diffusion		µmol/L	mg/L	The smallest concentration ensuring a total inhibition of mycelium growth for at least 21 days at 30 °C	Tunc et al. (2007b)
	P. notatum	3.9	0.52		
Broth liquid dilution		mg/L		The lowest concentration inhibiting any visible growth	Chan et al. (2013)
	E. coli	78.125	78.1		
	P. aeruginosa	156.25	156		
	S. aureus	78.125	78.1		
	B. subtilis	156.25	156		
Broth liquid dilution		mM	mg/L	The lowest concentration that completely inhibited bacterial growth	Helander et al. (1998)
	E. coli	3	396		
	S. typhimurium	3	396		
Broth liquid dilution		mM	mg/L	-	Zodrow et al. (2012)
	S. aureus	0.75	99		
	E. coli	3	396		
	P. aeruginosa	1	132		
Broth liquid dilution		% (v/v)	mg/L	The lowest concentration of the compound that did not permit development of turbidity	Gamage et al. (2009)
	E. coli	0.4	4.2		
	S. typhimurium	0.4	4.2		
	E. sakazakii	0.5	5.3		
	B. cereus	0.4	4.2		
Agar well diffusion		µL/mL	mg/L	The lowest concentration of the compound that resulted in a zone of inhibition	Sanla-Ead et al. (2012)
	B. cereus	3.12	3.28		
	E. faecalis	0.78	0.82		
	L. monocytogenes	6.25	6.56		
	M. luteus	6.25	6.56		
	S. aureus	1.56	1.64		
	A. hydrophila	0.78	0.82		
	E. coli	12.5	13.1		
	E. coli O157: H7	6.25	6.56		
	P. aeruginosa	12.5	13.1		
	S. enteritidis	6.25	6.56		
	C. albicans	6.25	6.56		
	S. cerevisiae	1.56	1.64		
	Z. rouxii	1.56	1.64		
Agar dilution		µg/mL	mg/L	The lowest concentration of the compound at which an absence of growth was recorded	Matan et al. (2011)
	M. dimorphosporus	25	0.025		
	Penicillium spp.	30	0.030		
	A. niger	30	0.030		
	Rhizopus spp.	30	0.030		

Table I.5. Antimicrobial effectiveness *in vitro* of cinnamaldehyde-containing packaging materials [C: Cinnamaldehyde, Cm: Cinnamon, EO: Essential oil].

Agent	Film matrix	Incorporation method	Nominal concentration	Microorganism		Effectiveness	Reference
C	SPI paper coating, Modified starch paper coating	Direct incorporation in the coating solution	10, 30, 60%	*E. coli, B. cinerea*	+++	5 mg/L, *E. coli* 4-5 log reductions, *B. cinerea* 21 days growth delay	Ben Arfa et al. (2007)
	PP coated with varnish	Direct incorporation in the coating solution	1, 2, 4%	*E. faecalis, L. monocytogenes, B. cereus, S. aureus, S. choleraesuis, Y. enterocolitica, E. coli, C. albicans, D. hansenii, Z. rouxii, B. cinerea, A. flavus, P. roqueforti, E. repens, P. islandicum, P. commune, P. nalgiovensis*	+++	Total inhibition with 4% for most fungi and some bacteria	Gutierrez et al. (2009a)
	Poly (lactic-co-glycolic acid) (PLGA)	Direct incorporation in the film-forming solution	0.1, 1%	*S. aureus, E. coli, P. aeruginosa*	+++	50% inhibition with 0.1% against *S. aureus, E. coli*. 60% inhibition with 1% against *P. aeruginosa*	Zodrow et al. (2012).
	Cellulose-based films	Direct incorporation in the film-forming solution	1%	*L. monocytogenes, S. aureus, E. coli, S. enteritidis, C. albicans, S. cerevisiae*	+		Sanla-Ead et al. (2012)
Cm EO, Cm EO + C	Paper coated with paraffin-based varnish	Direct incorporation in the coating solution		*C. albicans, A. flavus, E. repens, P. nalgiovense, P. roqueforti, B. cereus, L. monocytogenes, E. faecalis, S. aureus, S. cholerasuis, E. coli, Y. enterocolitica, P. aeruginosa*	++	Total inhibition with Cm EO +C: *C. albicans*, *A. flavus, E. repens.* Significant activity: *P. nalgiovense, P. roqueforti, S. cholerasuis, E. coli, Y. enterocolitica,* and *P. aeruginosa.* No inhibition: *B. cereus, L. monocytogenes, E. faecalis, S. aureus*	Rodriguez et al. (2007)
	PP coated with vanish, PE/EVOH coated with varnish	Direct incorporation in a coating solution	1-12%	*E. coli, Y. enterocolitica, P. aeruginosa, S. choleraesuis, L. monocytogenes, S. aureus, Bacillus cereus, E. faecalis, P. islandicum, P. roqueforti, P. nalgiovense, E. repens, A. flavus, C. albicans, D. hansenii, Z. rouxii.*	+++	Total inhibition with 4% Fungi, 8% Gram +, 10% Gram - (except *P. aeruginosa*). PP more effective than PE/EVOH	Lopez et al. (2007a),

0: No effect, -: Low effect, +: some effect, ++: high effect, +++: very high effect

Table I.6. Antimicrobial effectiveness in food products of cinnamaldehyde-containing packaging materials [C: Cinnamaldehyde, Cm: Cinnamon, EO: Essential oil].

Agent	Film	Concentration	Application	Food product	Conditions	Antimicrobial	Sensory	Reference
C	Apple-based	0.5-0.75%	Wrapping	Cooked chicken			0	Du et al. (2012)
	Apple-based	0.5, 1.5, and 3%	Wrapping	Chicken breast	4 or 23 °C, 72 h	*C. jejuni* +++		Mild et al. (2011)
	Apple-based							
	Carrot-based		Wrapping	Ham and bologna	4 °C, 7 d	*L. monocytogenes*		Ravishankar et al. (2012)
	Hibiscus-based							
	Chitosan	0.01	Film cover and vacuum packaging in EVA	Bologna, regular cooked ham, pastrami	4 °C or 10 °C, 21 d	*L. sakei* +, *S. liquefaciens* +++, *Enterobacteriaceae* +++, lactic acid bacteria 0		Ouattara et al. (2000)
	Chitosan/Pectin + β-cyclodextrin encapsulation	(2 g/100 g complex)	Layer-by-layer coating	Papaya	4 °C, 15 d	Aerobic +++, psychrotrophic ++, yeast and mold ++	0	Brasil et al. (2012)
Bark Cm EO, Leaf Cm EO	Paraffin-based paper	3-6%	Container	Cherry tomato		*A. alternata* +++	0	Rodriguez-Lafuente et al. (2010)
	Soy protein isolate coated oPP/PE laminated with LLDPE	0.6-1.2%	Pouch	Fresh sprouts (alfalfa, broccoli, and radish)	10 °C for 5 days	Total microbial counts +		Gamage et al. (2009)
Cm EO, Cm EO + C	Active paraffin-based paper			Strawberries	4 °C, 7 d	No visible fungal growth	0	Rodriguez et al. (2007)
Cm powder	Cassava starch	0.15-0.3 g/100 g suspension		Bread slices		Fungal counts 0, -		Kechichian et al. (2010)
Cm EO	PP	2, 4%	Microperforated bags	Bakery product			0	Gutierrez et al. (2009b)
	PP with an organic solvent base (ethyl acetate) coating of nitrocellulose base	0.0215, 0.0374 g/(13x10 cm)	Shelf-adhesive active label stuck inside a PE/EVOH wrap	Gluten-free bread		84% inhibition	0	Gutierrez et al. (2011)
	Paper coated with solid wax paraffin containing the active agent	1-6%	Manual packing	Bread slices		*R. stolonifer* +++		Rodriguez et al. (2008)
	Active coating of PET	0.062 g/cm^2 (324 cm^2)	Macroperforated tray (bottom active)	Calanda peaches	Room T, 12 d	Infections: 63% vs. 86% in the non-active packaging		Montero-Prado et al. (2011)
	Active coating of PP	0.54 g/cm^2 (100 cm^2)	Active label stuck at the top of PET tray			Infections: 13% vs. 86% in the non-active packaging		

0: No effect, -: Low effect, +: some effect, ++: high effect, +++: very high effect

I.2.1.1.1.2. Natamycin

Natamycin (or pimaricin) is a fungicide of the polyene macrolide group produced by several species of *Streptomyces* (Delves-Broughton et al., 2005). It is approved in the EU as a food additive (E-235) for surface treatment of some cheeses and sausages (Regulation 1333/2008/EC). It is generally applied in aqueous solutions by spraying, dipping, or painting. However, its high molecular weight (666 g/mol) and its conjugated double-bond structure make it extremely insoluble in water (30-50 mg/L), prompting its precipitation unless stirred. Moreover, some inactivation can occur when directly applied owing to interaction with food components, which reduces its effectiveness (Fajardo et al., 2010). Natamycin preparations are available commercially under the trade names Natamax™ (Danisco) and Delvocid® (DSM), both of which contain approximately 50% natamycin blended with lactose. It has no odor or taste, which is a great advantage because organoleptic alterations are avoided.

Most molds and yeasts are inhibited at concentrations ranging from 0.5 to 6 μg natamycin/mL (Delves-Broughton et al., 2005), which makes it more effective than other fungicides allowed for food applications (Koontz and Marcy, 2003). The incorporation of natamycin into various polymer matrices with the aim of controlling the amount of natamycin on the food surface has been extensively evaluated in the last decade. **Table I.7** compiles data related to the effectiveness of these materials *in vitro* and in various food products. The great variability in testing conditions (time, temperature, relative humidity, microorganism, etc.) makes it difficult to draw conclusions.

Table I.7. Effectiveness *in vitro* and in food products of natamycin-containing packaging materials.

Matrix	Manufac-ture	Amount of natamycin	Microorganism	Food product	Application/Testing method	Effectiveness	Reference
Cellulose	Laminated on Al foil by casting	2. 4%	*P. roqueforti*	Gorgonzola cheese		Hindering of fungus growth	de Oliveira et al. (2007)
						Inhibition *P. roqueforti*	
	Film casting	0.2-4%		-	Agar disc diffusion (25 °C)	>1% inhibition *P. roqueforti*	
		4% N, 4% N + 1.25% Nisin	*S. aureus*, *L. monocytogenes*, *Penicillium* spp., *Geotrichum* spp.		Agar disc diffusion (23 °C, 35 °C)	2.7 cm *S. aureus* (N+Nisin), contact area *L. monocytogenes* (N+Nisin), 4.8 cm *Penicillium* spp., 2.3 cm *Geotrichum* spp. (N, N+Nisin)	dos Santos Pires et al. (2008)
			Molds/yeasts, psychrotrophic bacteria, *Staphylococcus* spp.	Mozzarella cheese	Separator layer between slices (12 °C)	2 log reduction molds/yeasts (9 d, 12 °C) (N, N+Nisin)	
Wheat gluten	Film casting	0.02-0.2% (g N/g film-forming solution)	*A. niger*, *P. roqueforti*	-	Agar disc diffusion (30 °C)	MIC *A. niger* 0.02%, MIC *P. roqueforti* 0.01%	Ture et al. (2011) Ture et al. (2008)
Methyl cellulose				Fresh Kashar cheese	Wrapping (10 °C)	0.02% eliminates *A. niger*, no effect on *P. roqueforti*	
						0.05%-0.2%: 2-log reductions *A. niger*, no effect on *P. roqueforti*	
				-	Agar disc diffusion (30 °C)	MIC *A. niger* 0.02%, MIC *P. roqueforti* 0.01%	
Polyvinyl acetate	Commercial product with sorbate and citric acid		-	Hard cheese	Painting with brush (14 °C)	Mold growth after 6 months of ripening on 50% of surface	Suarez et al. (2012)
Polyvinyl-dichloride (PVdC)	Coating on PA/LDPE by flexography printing	16.7% N w/w + 16.7% Nisin in coating	*P. expansum*, *L. helveticus*, *F. culmorum*, *L. ivanovii*,	-	Agar disc diffusion *in vitro* (various incubation T)	Total inhibition in the contact area and small inhibition halo. Effective against *L. ivanovii*	Hanušová et al. (2010)
			B. cereus, *P. expansum*, *B. linens*	Ripened cheese (O. tvaruzky) and soft cheese (B. zlato)	Vacuum packaged (10-28 d, 23 °C)	B. zlato: *P. expansum* inhibition on cheese surface in contact. O. tvaruzky: *B. linens* inhibition	
Chitosan	Coating solution	0.5 mg/mL solution	*A. niger*, *P. crustosum*, *P. commune*, *P. roqueforti*	Semi-hard cheese (Saloio)	Spraying (7 d, 25 °C)	Complete inhibition after 7 d at 25 °C, 1.1 log reduction of yeasts/molds after 27 d at 4 °C	Fajardo et al. (2010)
		2 mg/L solution	*A. phoenicis*, *P. stoloniferum*	-	Well diffusion (6 mm)	10-11 mm inhibition zone.	Ce et al. (2012)
			-	Minimally processed pears	Coating by immersion (4 °C)	0.6 log reductions in total counts, 1.3 log reductions in yeasts/molds	
	Separate layers and bilayer film	20 mg/L in each layer	*A. alternata*, *F. semitectum*	Hami melon (30 °C, 70% RH, 20 d)	Coating by brushing	Very low mold growth (decay area 313 cm^2 vs. 17.1 cm^2 for control and coated, respectively)	Cong et al. (2007)
PE wax micro-emulsion		1.25-20 mg/L		-	Agar disc diffusion (30 °C)	*A. alternata* strong inhibition, PE wax ME more effective than chitosan film	
Whey protein	Film casting	0.002 g/mL, 0.05 g/mL	*Y. lipolytica*, *P. commune*, *P. chrysogenum*	-	Agar disc diffusion (30 °C)	Inhibition zones	Pintado et al. (2010)
Casein	Coating solution	0.07% w/w solution		Kashar cheese (90 d, 6 °C, 85% RH)	Coating by dipping	No visible mold growth in 1 month	Yildirim et al. (2006)

I.2.1.1.1.3. Lysozyme

Lysozyme is a naturally-occurring biocidal enzyme of 15 kDa effective mostly against Gram-positive bacteria; however its spectrum of activity is easily broadened to other spoilage and pathogenic organisms and even to some Gram-negative bacteria when it is used in combination with other compounds (Losso et al., 2000).

Lysozyme is ubiquitous in animal and plant kingdoms, and plays an important role in the natural defense mechanism. Lysozyme is approved as a food additive in the EU (E-1105), and it is interesting because it does not impart any organoleptic effect under normal food processing conditions, and it may not interfere with a number of organisms that are considered to be beneficial for human health. Moreover, it has been proven to be an economically viable alternative to other chemical preservatives for food applications. Lysozyme is commercially available in ready-to-use forms such as a liquid or spray-dried powder.

Lysozyme has been incorporated in a wide range of polymer matrices in order to control its dosage and maintain its activity on the food surface where most microbial contamination occurs. It has been immobilized in polyvinyl alcohol (PVOH) beads, nylon 6.6 pellets and cellulose triacetate films (Appendini and Hotchkiss, 1997), and in cross-linked PVOH films (PVOH) (Buonocore et al., 2003; Conte et al., 2006; Conte et al., 2007); incorporated in mono and multilayer cross-linked PVOH structures (Buonocore et al., 2005), composite films of plasma-treated spelt bran and cross-linked PVOH (Mastromatteo et al., 2011), low density polyethylene (LDPE), polycaprolactone (PCL), and poly(lactic acid) (PLA) (del Nobile et al., 2009), and whey protein coatings (Min et al., 2008); microencapsulated in zein (Jin et al., 2009; Zhong et al., 2009), and encapsulated in supramolecular hydrogels based on α-cyclodextrin and water-soluble PCL–poly(ethylene glycol) block copolymer (Ma et al., 2011). In these studies, the effect on the functional properties of the resulting films, and the release kinetics of lysozyme from the matrices (when appropriate) have been studied. The last assay is normally conducted following the lysis of *Micrococcus lysodeikticus* cells (Shugar, 1952), and is also indicative of the antimicrobial activity.

Table I.8 compiles data related to the effectiveness of some lysozyme carrier materials tested *in vitro* and in various food products.

Table I.8. Effectiveness *in vitro* and in food products of lysozyme-containing packaging materials.

Matrix	Manufac-ture	Amount of lysozyme	Microorganism	Food product	Application/Testing method	Effectiveness	Reference
Whey protein	Film casting	10-30 mg/g film-forming solution	*L. monocytogenes*	-	Agar disc diffusion, and inoculum spreading on film surface (37 °C)	204 mg/g film inhibited the growth of 4.4 log CFU/cm^2	Min et al. (2005)
	Coating			Smoked salmon	Coating by brushing. 4 °C-35 d + 10 °C + 28 d	25 mg/g coating solution inactivated > 2.4, 4.5, and 3 log CFU/g *L. monocytogenes*, total aerobes, and yeasts/molds, respectively.	
Fish-skin gelatin	Film casting, gel	0.001%-0.5% w/v film-forming solution	*E. coli, B. subtilis, S. cremoris*	-	Agar disc diffusion (films) Agar well diffusion (gels) 35 °C, 24 h	No effect on *E. coli* (Gram -), effect on Gram + bacteria.	Bower et al. (2006)
Zein	Film casting	1400-2800 U/cm^2 (479-958 µg/cm^2). Albumin proteins and Na_2 EDTA	*E. coli, B. subtilis,*	-	Agar disc diffusion 37 °C, 24-48 h	Effective against both microorganisms	Guçbilmez et al. (2006)
		700 µg/cm^2 + Na_2 EDTA	*L. monocytogenes, E. coli, S. typhimurium*	-	Agar disc diffusion (37 °C, 48 h)	Lysozyme film only effective against *L. monocytogenes*. Combination of lysozyme and Na_2 EDTA has synergistic effect, and films are also active against *E. coli* and *S. typhimurium*	Unalan et al. (2011)
				Ground beef patties	4 °C, 7 d	Decrease in total viable counts and total coliform counts after 5 d.	
Chitosan	Film casting, lamination on multilayer coextruded film, coating	60% w/w film-forming solution	*E. coli, L. monocytogenes, P. fluorescens*, molds and yeast	Mozzarella cheese	10 °C, 14 d for bacteria, and 30 d for fungi	Treated cheese produced 0.43 to 1.25, 0.40 to 1.40, and 0.32 to 1.35 log reductions in *E. coli, P. fluorescens,* and *L. monocytogenes*, respectively. Growth of mold was completely inhibited in cheese packaged with films, while 0.24 to 1.90 and 0.06 to 0.50 log reductions in molds were observed in cheese packaged with laminated films and coatings, respectively. All packaging applications resulted in 0.01 to 0.64 log reduction in yeasts.	Duan et al. (2007)
	Film casting	20, 60, 100% w/w chitosan.	*E. coli, S. faecalis*	-	Broth liquid dilution (37 °C, 6, 12, 24 h)	Films with 60% L produced 3.8 log reduction in *S. faecalis* and 2.7 log reduction in *E. coli*	Park et al. (2004)
Cellulose acetate	Film casting	1.5% w/w film-forming solution. Na_2 EDTA	*E. coli, B. amyloliquefaciens*	-	Agar disc diffusion (37 °C and 30 °C, respectively, 2 d)	Combination of L and Na_2 EDTA produced clear zones around films for *E. coli. B. amyloliquefaciens* was only inhibited on the contact surface.	Gemili et al. (2009)

I.2.1.2. Legal issues of active packaging

Regulation 1935/2004/EC on materials and articles intended to come into contact with food (revoking Directives 80/590/EEC and 89/109/EEC) offered the opportunity for active packaging to be used in Europe for the first time. The principle underlying this Regulation is to provide the basis for securing a high level of protection of human health and the interests of consumers. It establishes that materials and articles shall be manufactured in compliance with good manufacturing practice so that, under normal or foreseeable conditions of use, they do not transfer their constituents to food in quantities which could: (a) endanger human health; or (b) bring about an unacceptable change in the composition of the food; or (c) bring about a deterioration in the organoleptic characteristics thereof.

The general requirements stated in Regulation 1935/2004/EC for the safe use of active packaging have been integrated in Regulation 450/2009/EC on active and intelligent materials and articles intended to come into contact with food. This Regulation establishes specific requirements for their marketing. Active materials and articles are defined as "materials and articles that are intended to extend the shelf-life or to maintain or improve the condition of packaged food; they are designed to deliberately incorporate components that would release or absorb substances into or from the packaged food or the environment surrounding the food". Active materials and articles may only be placed on the market if they: (a) are suitable and effective for the intended purpose of use; (b) comply with the general and specific requirements set out in Regulation 1935/2004/EC; and (c) comply with the specific requirements of Regulation 450/2009/EC. Only substances that are included in the 'Community list' of authorized substances may be used as components of active materials. The Community list shall specify the substance type, its function, and if necessary, the conditions of use of the substance and of the resulting material, and the possible restrictions and/or specifications associated. On the other hand, to allow identification by the consumer of non-edible parts, active materials and articles or parts thereof shall be labelled, whenever they are perceived as edible, with the words "DO NOT EAT". The active substance released shall be considered as an ingredient within the meaning of Article 6(4)(a) of Directive 2000/13/EC on labelling, presentation, and advertising of foodstuffs, that is, any substance, including additives, used in the manufacture or preparation of a foodstuff and still present in the finished product, even if in altered form. Therefore, the requirements of Regulations 1333/2008/EC on food additives and/or 1334/2008/EC on flavorings and certain

food ingredients with flavoring properties for use in and on foods should be respected where applicable. Finally, a declaration of compliance shall be issued by the business operator.

I.2.1.3. Future trends in active packaging

The future trend in active packaging is directed toward the use of absorbing or releasing compounds incorporated in packaging films or in adhesive labels to get rid of separate objects in packaging, avoiding consumer rejection. Consumer preferences for minimally processed and naturally preserved foods as well as food industry willingness to invest in product quality and safety are the main drivers for active food packaging development.

Antimicrobial packaging materials can help to decrease the amount of preservative needed, and to deliver it more precisely where microbial growth and spoilage mainly occur, i.e. on the food surface (Ahvenainen, 2003). However, effective materials are still rather scarce on the market and need much research and development work. The most significant challenges in developing these materials are (i) to find new physical, chemical, and biological methods to incorporate preservatives effectively into packaging materials, maintaining the preservatives' activity, or to modify packaging materials and polymers to become antimicrobial; and (ii) to achieve a broader-spectrum activity of packaging materials against various spoilage and pathogenic microorganisms by incorporating several preservatives into the same packaging system. Moreover, these novel materials should present adequate functional properties, such as proper permeability and mechanical resistance when used as wall packaging, good appearance, reasonable cost, suitability for packaging machines already used in the food industry, and suitability for normal sealing procedures if required.

I.3. FOOD PACKAGING MATERIALS

I.3.1. Materials used in food packaging

Materials that have traditionally been used in food packaging include glass, metals (aluminum, tinplate, and tin-free steel), paper and paperboards, and plastics. Nowadays, food packages often combine several materials to exploit each material's functional or aesthetic properties. **Table I.9** summarizes key properties of packaging materials used in food packaging (Coles et al., 2003). The right selection of packaging materials and technologies can guarantee product quality and freshness during distribution and storage.

Table I.9. Key properties of food packaging materials (Coles et al., 2003).

Glass	Aluminum and tinplate	Paper and paperboard	Plastics
- Inert with respect to foods - Transparent to light and may be colored - Impermeable to gases and vapors - Rigid - Can be easily returned and reused - Brittle and breakable - Needs a separate closure - Widely in use for both single and multi-trip packaging	- Rigid material with a high density for steel and a low density for aluminum - Good tensile strength - An excellent barrier to light, liquids, and foods - Needs closures, seams, and crimps to form packs - Used in many packaging applications: food and beverage cans, aerosols, tubes, trays - Can react with product causing dissolution of the metal	- Low-density materials - Poor barriers to light without coatings or laminations - Poor barriers to liquids, gases, and vapors unless they are coated or laminated - Good stiffness - Can be grease resistant - Absorbent to liquids and moisture vapor - Can be creased, folded, and glued - Tear easily - Not brittle, but not so high in tensile strength - Excellent substrates for inexpensive printing	- Wide range of barrier properties - Permeable to gases and vapors to varying degrees - Low density materials with a wide range of physical and optical properties - Usually have low stiffness - Tensile and tear strengths are variable - Can be transparent - Functional over a wide range of temperatures depending on the type of plastic - Flexible and, in certain cases, can be creased

Among the materials used in food packaging, plastics (rigid and flexible) accounted for 37% of all global packaging sales in 2010, the largest market share (**Figure I.4**). The global production of plastic materials in 2012 rose to 288 million tons, of which nearly 40% was employed in the packaging sector.

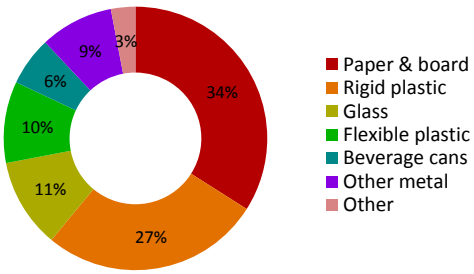

Figure I.4. Market share of food packaging materials [Source: Pira International Ltd, 2010]

Plastics are defined as polymers to which additives or other substances may have been added, and that present viscoelastic mechanical behavior. Polymer means, according to

Directive 10/2011/EC, any macromolecular substance obtained by: (a) a polymerization process such as polyaddition or polycondensation, or by any other similar process of monomers and other starting substances; or (b) chemical modification of natural or synthetic macromolecules; or (c) microbial fermentation.

Traditionally they originated in the petrochemical industry, making them non-biodegradable and non-renewable. With the current focus on exploring alternatives to petroleum and emphasis on reduced environmental impact, research is increasingly being directed to the development of biodegradable plastic materials from renewable resources (Tang et al., 2012).

I.3.1.1. Bioplastics

According to the European Bioplastics association the term bioplastics encompasses a whole family of materials that are biobased, biodegradable, or both.

A **biobased** material or product is one that wholly or partially derives from renewable resources. According to their origin, biobased polymers can be grouped into three classes (Mensitieri et al., 2011; Queiroz and Collares-Queiroz, 2009):

i) Polymers extracted directly from biomass, with or without modification.
ii) Polymers synthesized from monomers obtained from biomass.
iii) Polymers produced by microorganisms.

The first type of biopolymers includes those based on polysaccharides (starch, cellulose…), and proteins (wheat gluten, soy protein, gelatin…). The second group of biopolymers covers a wide range of materials, such as poly(lactic acid) (PLA), produced from lactic acid obtained by fermentation of, for example, sugar cane; biopolyethylene (BioPE), from the polymerization of ethylene produced from bioethanol; bionylons via diacids from biomass; and bio-polyurethanes, incorporating polyols of vegetable origin. The third type refers to biopolymers that are produced directly by microorganisms, such as polyhydroxyalkanoates (PHA). **Figure I.5** depicts the different types of biopolymers based on renewable sources and the various pathways for obtaining them by means of renewable monomers (adapted from Narayan (-) and based on Shen et al. (2009), Harmsen and Hackmann (2013)). Only a part of these biopolymers is currently available on a commercial scale.

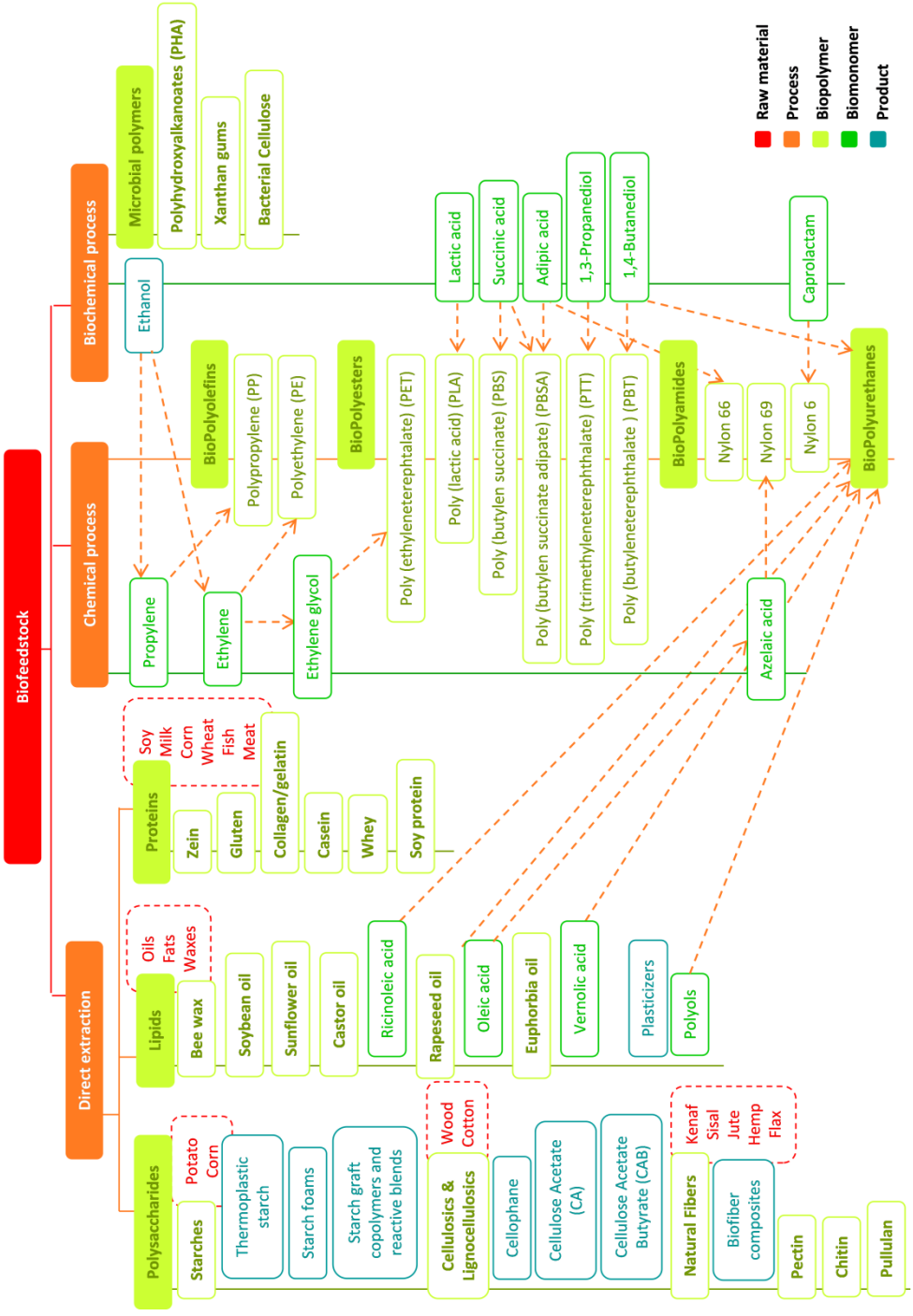

Figure I.5. Polymers, monomers, and intermediaries obtained from annually renewable feedstocks for the production of bioplastics.

According to ASTM D6866, the biobased content in a polymer is measured by using ^{14}C radiation to separate modern carbon (biogenic carbon derived from biomass) from fossil carbon (petrochemical). Fossil carbon is carbon that contains no radiocarbon or ^{14}C, since the age of fossil carbon (millions of years) is much greater than the half-life of ^{14}C, which is 5730 years (Kijchavengkul and Auras, 2008).

The term **biodegradable** refers to a biochemical process during which microorganisms that are available in the environment convert materials into water, carbon dioxide, and biomass. The process of biodegradation depends on the surrounding environmental conditions (e.g. location or temperature), on the material itself, and on the application. There are diverse environments for biodegradation of materials, such as soil, soil surface, landfill, water, marine environment, digester plants, household composting units, and industrial composting facilities, among which a possible and favorable end-of-life scenario for biodegradable packaging materials can be composting or anaerobic digestion.

According to ISO 17088 and EN 13432, a compostable plastic is a plastic that undergoes degradation by biological processes during composting to yield carbon dioxide, water, inorganic compounds, and biomass at a rate consistent with other known compostable materials, and that leaves no visually distinguishable or toxic residues. Thus the evaluation of compostability deals with material characteristics, biodegradation, disintegration, and compost quality.

Figure I.6 illustrates the composting route for the disposal of biobased and biodegradable plastics, and the cradle to cradle concept.

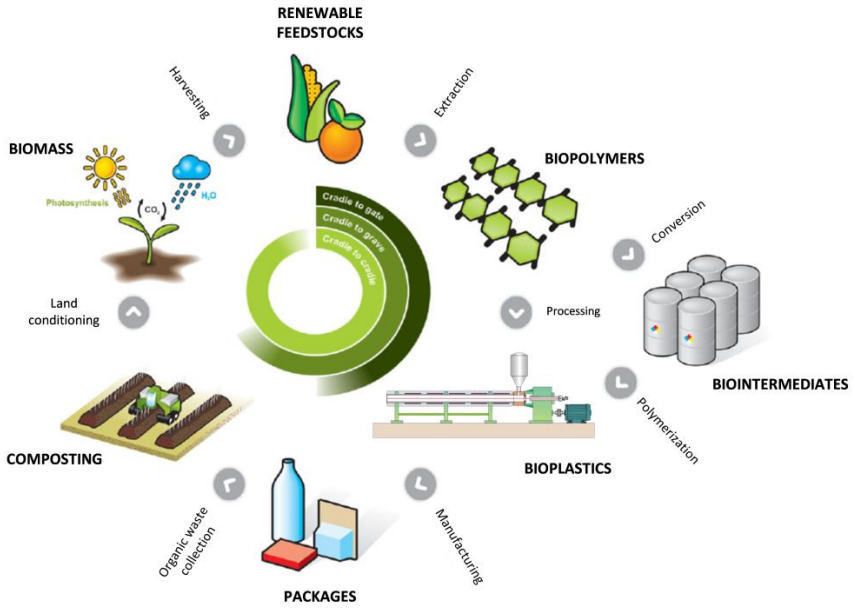

Figure I.6. Production, consumption, and disposal of biobased and biodegradable polymers via composting [Adapted from Kijchavengkul and Auras (2008)].

For durable products where biodegradability is not a required element for reasons of performance, safety, and product life, alternative methods of disposal such as energy recovery, and chemical or mechanical recycling can be suitable (Song et al., 2009a).

New bioplastic materials, compounds, and masterbatches are being developed daily and an increasing number of production facilities are coming on-stream. According to the European Bioplastics association the global production of bioplastics is expected to increase by around 400% by 2017 (**Figure I.7**). Global production capacities in 2012 positioned Bio-PET as the material with the highest percentage, followed by Bio-PE, both non-biodegradable. PLA and other biodegradable polyesters accounted for the highest production capacities among the biodegradable materials.

The market drivers are related to external factors such as the price increase of fossil materials, the dependence on fossil resources, the effects of climate change, the waste associated with non-biodegradable plastics, the high consumer acceptance, associated legislation, etc.; and with internal factors such as their advanced technical properties and functionality, the lower environmental impact, the use of renewable and highly available sources, their capability of being organically or mechanically recycled, etc.

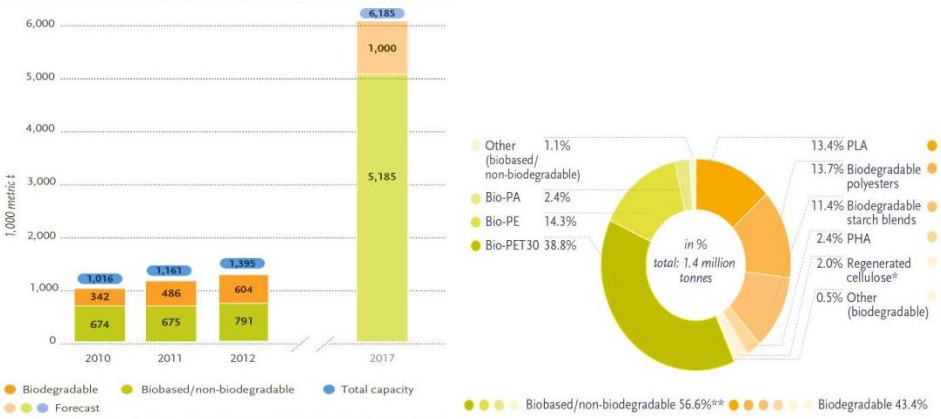

Figure I.7. Global production capacity of bioplastics by year and material types produced in 2012 [Source: European Bioplastics, 2014].

Bioplastics currently available in the market and their producers are listed in **Table I.10**.

Table I.10. Bioplastics currently available in the market and producers.

Biodegradability	Origin		Polymer	Brand	Producer
Biodegradable	Renewable	Obtained directly from biomass	Starch	Mater Bi	Novamont
				Bioplast	Biotec GmbH & Co. KG
				Biolice	Limagrain Céréales Ingrédients
				Cereplast	Cereplast Inc
				Biopar	Biopolymer Technologies
				Solanyl	Rodenburg Biopolymers
				Vegeplast	Vegemat
				EverCorn	Japan Corn Starch Co.
			Cellulose	Biograde	Fkur
				Tenite	Eastman
				Fasal	Fasal Wood Keg
				Bioceta	Mazzucchelli
				NaturFlex	Innovia Films
		Produced by microor-ganisms	PHB/PHV	Biopol	Metabolix
				Enmat	Tiana
				Biocicle	PHB-ISA
				Mirel	Metabolix-ADM
		Synthesized from bio-monomers	PLA	PLA-Ingeo	Nature Works LLC
				Cereplast	Cereplast Inc.
				Lacea	Mitsui Chemicals
				Lacty	Shimadzu
				Eco plastic	Toyota
				Heplon	Chronopol
				Ecoloju	Mitsubishi
				Hycail	Hycail
				Revode	Hysun Biomaterials Co. Ltd
				Ecovio	BASF
				Bio-flex	FKuR

				Bioshrink	Alesco GmbH & Co. KG
	Non-renewable	Synthetic	PCL	Tone	Union Carbide Corporation
				Capa	Solvay
				Celgreen	Daycel
				Pvaxx	Reliance Industries
			PVOH	Nichigo G-Polymer	Nippon Goshei
				Elvanol	DuPont
			PBS/PBSA	Bionolle	Showa Highpolymer Co.
				Sky Green BDP	SK Polymers
			PBAT	Ecoflex	BASF
				Ecovio	BASF
				Biopar	Biopolymer Technologies AG
Non-biodegradable	Renewable	Synthetic	Bio-PE		Braskem
					Dow
			Bio-PP		Braskem
			Bio-PET		Braskem
			Bio-PVC		Solvay Indupa
			Bio-PA	Rilsan PA 11	Arkema
				Ultramid	BASF
				Amilan	Toray

In this Thesis, proteins have been selected as a renewable and biodegradable raw material for the development of active bioplastics incorporating naturally-occurring antimicrobials aimed at food packaging applications.

I.3.1.1.1. Proteins

Proteins are heteropolymers, with α-amino acids being their monomer units. Most proteins contain 100–500 amino acid residues. Depending on the sequential order of the amino acids (primary structure of the protein), the protein will assume different structures along the polymer chain (secondary structure of the protein), based on van der Waals forces, hydrogen bonding, electrostatic and hydrophobic interactions, and disulfide bridges among the amino acid units (Cheftel et al., 1985). The tertiary protein structure reflects how the secondary structures organize relative to each other, based on the same types of interactions, to form an overall globular, fibrous, or random protein structure. Finally, quaternary structure occurs when whole proteins interact with each other into associations to provide a unique structure or biological activity (Krochta, 2002).

The inherent properties of proteins make them excellent materials for the production of films (Dangaran et al., 2009). The secondary, tertiary, and quaternary structures of proteins can be modified by various physical and chemical agents, including heat, shear, pressure, irradiation, lipid interfaces, acids and alkalis, cross-linkers, enzymes, and metal ions. Such

agents can be used in the formation of protein films and coatings to optimize protein configuration, protein interactions, and the functional properties of the films developed (Krochta, 2002).

Protein film-forming materials derived from animal sources include collagen, gelatin, myofibrillar protein, keratin, egg white protein, casein, and whey protein, among others (Lacroix and Cooksey, 2005). Protein film-forming materials derived from plant sources include corn zein, wheat gluten, soy protein, and cottonseed protein, among others (Buffo and Han, 2005; Gällstedt et al., 2011). **Table I.11** gives a brief overview of the sources that are available to make protein-based films.

Table I.11. Protein film-forming materials (Buffo and Han, 2005; Gällstedt et al., 2011; Lacroix and Cooksey, 2005).

Origin	Protein	Source
Animal	Myofibrillar proteins (Myosin, Actin, and others)	Muscle (mammalian or fish)
	Collagen (α, β), Gelatin (Type A and B)	Bones, tendons, connective tissue, skin, ligaments, vascular system
	Keratin	Wool, feathers, nails, hooves, epidermis, hair, horn
	Egg white proteins (ovoalbumin, ovotransferrin, ovomucoid, and others)	Egg
	Casein (α_s-, β-, κ-, γ-)	Milk
	Whey proteins (β-lactoglobulin, α-lactalbumin, Bovine serum albumin, Immunoglobulins) (concentrate and isolate)	Milk
Plant	Gluten, Glutenins, Gliadins	Wheat
	Zein	Corn
	Soy proteins (Glycinin, β-Conglycinin)	Soy
	Rapeseed protein	Rapeseed
	Kafirin	Sorghum
	Avenin	Oat
	Rice bran protein	Rice
	Secalin	Rye
	Sunflower protein	Sunflower
	Peanut proteins (Arachin and Conarachin) (concentrate and isolate)	Peanut
	Pistachio protein	Pistachio
	Pea protein	Pea
	Cottonseed proteins (Gossypin, congossypin, and others)	Cottonseed
	Lupin seed protein isolate	Lupin

Two processes have been developed to produce protein-based films and coatings: wet processing and dry processing (Cuq et al., 1998). The wet process involves dispersing or solubilizing the protein in a solvent, followed by separation of the proteins from the solvent phase by precipitation or phase changes due to: i) changes in solvent conditions (polarity or pH changes, electrolyte additions); ii) thermal treatments (heating); or iii) solvent removal (drying) (Cuq et al., 1998). In the solvent process, casting is used for the production of films, and spraying, dipping and surface covering are used for the production of coatings. The dry process is based on the thermoplastic properties of proteins under low moisture conditions. Using plasticizers and/or heating amorphous proteins above the glass transition temperature produce rubbery materials that can be shaped using compression molding, extrusion, or injection molding (Cuq et al., 1998; Verbeek and van den Berg, 2010).

Protein films are brittle owing to extensive interactions between protein chains. Relatively low molecular weight hydrophilic plasticizers are usually added, which mainly compete for hydrogen bonding and electrostatic interactions with protein chains (Krochta, 2002). Plasticizers reduce protein chain-to-chain interactions, decrease protein glass transition temperature, and improve film handling and flexibility. Moreover, film elongation increases, and film strength decreases. Unfortunately, plasticizers generally also decrease the protein film's ability to act as a barrier to moisture, oxygen, aroma, and oils. Plasticizers generally used for protein films include glycerol, propylene glycol, sorbitol, sucrose, polyethylene glycol, fatty acids, and monoglycerides. Water also acts as a ubiquitous plasticizer for protein-based materials. Thus, film moisture content, as affected by the surrounding environment's relative humidity, has a large effect on film properties.

Protein-based films possess moderate mechanical properties in comparison with conventional synthetic films, and good oxygen barrier properties at low or intermediate relative humidities exceeding those of polyolefins (Gennadios et al., 1994). In contrast, water vapor permeability of protein-based films is relatively high owing to their hydrophilic character (Gontard et al., 1994). This hydrophilic character also prompts a good barrier to aroma and lipids owing to the low affinity for apolar compounds, and hence they present a reduced tendency to cause flavor scalping (Balaguer et al., 2012). Their water sensitivity can also be used as a trigger mechanism for the release of entrapped molecules in the protein network, and therefore they represent promising matrices for the delivery and controlled release of active compounds. Some proteins are also water soluble, depending on the type and density of the intermolecular interactions present in the proteinaceous network.

However, the final properties of protein-based films are heavily influenced not only by the protein type and source, but also by the processing conditions. **Table I.12** summarizes various interesting properties of protein materials for use in the food packaging sector.

Table I.12. Properties of proteins, needs, and applications with high potential in the food packaging sector (Dangaran et al., 2009; Guilbert and Gontard, 2005).

Properties	Need	Application
Biobased	- Reduction of petroleum-based plastics	- Production of biobased plastics
Compostable	- Reduction of municipal waste - Replenish organic carbon cycle - Short-durable packaging - Sustainable packaging	- Compostable bags, containers, trays, etc. - Packaging of fresh or minimally processed fruits and vegetables, dairy products, and organically grown products
Edible	- Wraps, internal layers, and protective barriers for food	- Films and coatings
Water soluble	- Pre-dosed compounds	- Sachets for ingredients and additives
Water sensitive	- Triggered response to moisture - Controlled release	- Active packaging
Barrier (O_2, CO_2, aroma)	- Reduction of lipid oxidation - Limitation of oil penetration - Minimization of aroma loss - Gas exchange control	- Films and coatings for fresh food, oxidizable products, and eggs
Gas selective	- Reduction of browning and ripening of fresh-cut produce	- Films and coatings for gas exchange control
Carrier/Delivery systems	- Controlled release - Enhancement of compound stability - Extend food product shelf-life - Reduction of spoiled food	- Vehicles for agrochemicals, pharmaceuticals, and food additives - Active packaging (antimicrobials, antioxidants) - Encapsulation

Gliadins from wheat have been selected in the present Thesis for the production of bioplastic films with a capacity to retain and release antimicrobial compounds. In the following section properties of gluten and its fractions, gliadins and glutenins, and literature related to the production and improvement of wheat protein-based materials are reviewed.

I.3.1.1.1.1. Gluten, Gliadins, and Glutenins

Gluten is defined as the cohesive, viscoelastic, proteinaceous material obtained as a by-product during the isolation of starch from wheat flour. **Figure I.8** shows a diagram of gluten extraction from wheat flour by the Martins process. In this process, extensive washing of wheat flour yields two fractions: (a) starch and other water-soluble substances, and (b)

gluten. The aggregated gluten is then disintegrated in a pin mill and hot-air dried at mild temperature.

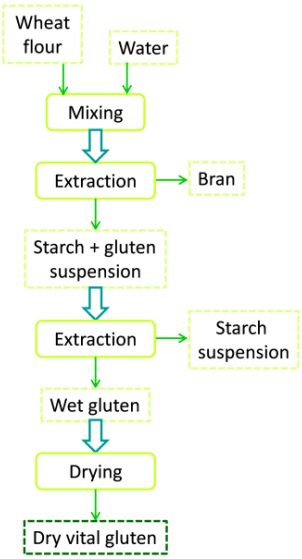

Figure I.8. Gluten extraction by the Martins process.

Wheat gluten consists of a mixture of proteins that can be classified into monomeric gliadins, which give gluten its viscous character, and polymeric glutenins, which are responsible for its elasticity. Gliadins are a heterogeneous group of single polypeptide chains with molecular weights of between 30 and 50 kDa, which are associated via hydrogen bonding and hydrophobic interactions (Cornell and Hoveling, 1998). Glutenins comprise unassociated fractions with molecular weights of 15 to 150 kDa and fractions linked via interchain disulfide bonds with molecular weights ranging from 150 to several million kDa (Cornell and Hoveling, 1998).

Gluten films can be produced by solvent and thermoplastic processes (**Table I.13**). Wheat gluten films produced by casting require a complex solvent system with basic or acidic conditions in the presence of alcohol and disulfide bond-reducing agents, because gluten proteins are insoluble in water (Guilbert et al., 2002). Changing the pH of the medium disrupts hydrogen and ionic interactions, alcohol disrupts hydrophobic interactions, and reducing agents cleave covalent disulfide bonds and reduce them to sulfhydryl groups. These disruptive agents evaporate during drying, and solvent removal gives rise to an increase in gluten protein concentration. Consequently, active sites for bond formation become free

and close enough to each other to create new interactions (Buffo and Han, 2005). New hydrogen bonds, hydrophobic interactions, and disulfide bonds link polypeptide chains together, contributing to the film structure (Gennadios et al., 1994). Processing of wheat gluten using heat combined with pressure and shear modifies the protein structure, and, unlike thermoplastic polymers, gluten viscosity does not decrease upon heating but rather levels off or increases owing to cross-linking reactions (Attenburrow et al., 1990; Kokini et al., 1994). The formation of sulfhydryl-disulfide intermolecular reactions creates a covalently cross-linked network (Morel et al., 2002). Therefore, the extrusion of proteins is, in general, only possible in a limited window of operating conditions, and the material properties of extrudates depend on the processing conditions in a complex way (Jerez et al., 2005; Redl et al., 1999).

Table I.13. Wheat gluten films studied in the literature and production methods.

Method of production	References
Casting	Cherian et al. (1995); Gennadios and Weller (1990); Gontard et al. (1992); Heralp et al. (1995); Jerez et al. (2005); Roy et al. (1999)
Compression-molding or thermoforming	Chen et al. (2012); Gällstedt et al. (2004); Gómez-Martínez et al. (2009); Mangavel et al. (2004); Pallos et al. (2006); Sun et al. (2008b); Zhang et al. (2008)
Extrusion	Cuq et al. (2000); Redl et al. (1999); Ullsten et al. (2009); Ullsten et al. (2006)
Injection-molding	Cho et al. (2011)
Blends	Kim (2008); Mohamed et al. (2008); Mohamed and Xu (2007); Park and Bae (2006); Zeng et al. (2011); Zuo et al. (2009)
Composites	Angellier-Coussy et al. (2013); Angellier-Coussy et al. (2008); Fakhouri et al. (2004); Gontard et al. (1994); Olabarrieta et al. (2006); Song et al. (2008); Song et al. (2009d); Tunc et al. (2007a)
Laminates	Cho et al. (2010); (Gontard et al., 1995); Tanada-Palmu et al. (2000)

To improve the properties of the resulting films, chemical (Hager et al., 2012; Kurniawan et al., 2009; Micard et al., 2000; Tropini et al., 2004; Tropini et al., 2000; Zhang et al., 2010; Zhang et al., 2006), physical (Koehler et al., 2010; Lee et al., 2005; Micard et al., 2000; Rhim et al., 1999), and enzymatic treatments (Larré et al., 2000) have been applied. Blends with higher performance polymers, incorporation of fillers, and development of polymer nanocomposites can also be used for this purpose (for references see **Table I.13**).

Gliadin and glutenin films can be prepared after extraction of both proteins from wheat gluten. Gliadins can be solubilized in 70% aqueous ethanol, one of the steps of the Osborne fractionation of wheat proteins, and the residue after this extraction is glutenins (Day, 2011).

Properties of films made from glutenin-rich fraction (Hernandez-Munoz et al., 2003; Hernandez-Munoz et al., 2004d; Song and Zheng, 2008; Song et al., 2009c) and gliadin-rich fraction (Sánchez et al., 1998; Sun et al., 2008a) have been characterized extensively (Chen et al., 2012; Hernandez-Munoz et al., 2003; Hernandez-Munoz et al., 2004e; Mangavel et al., 2002). In the case of gliadin films, various procedures have been employed in order to maximize their potential, including chemical cross-linking (Hernandez-Munoz et al., 2005; Hernandez-Munoz et al., 2004a; Hernandez-Munoz et al., 2004b; Hernandez-Munoz et al., 2004c; Reddy and Yang, 2010; Soares et al., 2009; Soares and Soldi, 2010; Song et al., 2009b), blends with other polymers (Li et al., 2010), and enzymatic cross-linking (Michon et al., 1999).

I.3.1.1.2. Future trends in bioplastics

The processing of bioplastics obtained from proteins should be done by means of the conventional ways of processing traditional plastics. In this regard, the polymer industry usually prefers dry processing to wet processing. At the same time, improving the performance of the biopolymers obtained directly from biomass by various techniques (cross-linking, blending, multi-layers, etc.) would make their functional properties as good as required by the final application, especially in conditions of high relative humidity. In terms of marketing, their environmental friendliness may not compensate sufficiently for their current relatively high price, but well-defined demands and new legislative frameworks could overcome these hurdles. A recovery chain needs to be established and well-informed consumers are also necessary. Despite these requirements, biodegradable and renewable bioplastics present a noteworthy potential for a wide range of applications such as packaging, drug delivery, and tissue engineering that forecast a dynamic market in the future.

I.4. REFERENCES

Ahvenainen, R. 2003. Active and intelligent packaging: An introduction. In *Novel Food Packaging Techniques*, Woodhead Publishing Limited: Cambridge, England.

Angellier-Coussy, H., Gastaldi, E., Da Silva, F. C., Gontard, N., and Guillard, V. 2013. Nanoparticle size and water diffusivity in nanocomposite agro-polymer based films. *European Polymer Journal, 49*(2), 299-306.

Angellier-Coussy, H., Torres-Giner, S., Morel, M. H., Gontard, N., and Gastaldi, E. 2008. Functional properties of thermoformed wheat gluten/montmorillonite materials with respect to formulation and processing conditions. *Journal of Applied Polymer Science, 107*(1), 487-496.

Appendini, P., and Hotchkiss, J. H. 1997. Immobilization of lysozyme on food contact polymers as potential antimicrobial films. *Packaging Technology & Science, 10*(5), 271-279.

Appendini, P., and Hotchkiss, J. H. 2002. Review of antimicrobial food packaging. *Innovative Food Science & Emerging Technologies, 3*(2), 113-126.

Attenburrow, G., Barnes, D. J., Davies, A. P., and Ingman, S. J. 1990. Rheological properties of wheat gluten. *Journal of Cereal Science, 12*(1), 1-14.

Balaguer, M. P., Gavara, R., and Hernandez-Munoz, P. 2012. Food aroma mass transport properties in renewable hydrophilic polymers. *Food Chemistry, 130*(4), 814-820.

Bastarrachea, L., Dhawan, S., and Sablani, S. S. 2011. Engineering properties of polymeric-based antimicrobial films for food packaging. *Food Engineering Reviews, 3*(2), 79-93.

Ben Arfa, A., Preziosi-Belloy, L., Chalier, P., and Gontard, N. 2007. Antimicrobial paper based on a soy protein isolate or modified starch coating including carvacrol and cinnamaldehyde. *Journal of Agricultural and Food Chemistry, 55*(6), 2155-2162.

Bower, C. K., Avena-Bustillos, R. J., Olsen, C. W., McHugh, T. H., and Bechtel, P. J. 2006. Characterization of fish-skin gelatin gels and films containing the antimicrobial enzyme lysozyme. *Journal of Food Science, 71*(5), 141-145.

Brasil, I. M., Gomes, C., Puerta-Gomez, A., Castell-Perez, M. E., and Moreira, R. G. 2012. Polysaccharide-based multilayered antimicrobial edible coating enhances quality of fresh-cut papaya. *LWT-Food Science and Technology, 47*(1), 39-45.

Brody, A. L., Bugusu, B., Han, J. H., Sand, C. K., and McHugh, T. H. 2008. Innovative food packaging solutions. *Journal of Food Science, 73*(8), 107-116.

Buffo, R. A., and Han, J. H. 2005. 17 - edible films and coatings from plant origin proteins. In *Innovations in Food Packaging*, J.H. Han, Ed. Academic Press: London; 277-300.

Buonocore, G. G., Conte, A., Corbo, M. R., Sinigaglia, M., and Del Nobile, M. A. 2005. Mono- and multilayer active films containing lysozyme as antimicrobial agent. *Innovative Food Science & Emerging Technologies, 6*(4), 459-464.

Buonocore, G. G., Del Nobile, M. A., Panizza, A., Bove, S., Battaglia, G., and Nicolais, L. 2003. Modeling the lysozyme release kinetics from antimicrobial films intended for food packaging applications. *Journal of Food Science, 68*(4), 1365-1370.

Burt, S. 2004. Essential oils: Their antibacterial properties and potential applications in foods - a review. *International Journal of Food Microbiology, 94*(3), 223-253.

Catalá, R., and Gavara, R. 2002. Mass transfer in food/plastic packaging systems. In *Engineering and food for the 21st century*, CRC Press: Boca Raton, FL, USA.

Ce, N., Norena, C. P. Z., and Brandelli, A. 2012. Antimicrobial activity of chitosan films containing nisin, peptide p34, and natamycin. *Cyta-Journal of Food, 10*(1), 21-26.

Chan, A. C., Ager, D., and Thompson, I. P. 2013. Resolving the mechanism of bacterial inhibition by plant secondary metabolites employing a combination of whole-cell biosensors. *Journal of Microbiological Methods, 93*(3), 209-217.

Cheftel, J. C., Cuq, J.-L., and Lorient, D. 1985. Amino acids, peptides, and proteins. In *Food Chemistry*, O.R. Fennema, Ed. Marcel Dekker: New York, NY, USA; 245-369.

Chen, L., Reddy, N., Wu, X., and Yang, Y. 2012. Thermoplastic films from wheat proteins. *Industrial Crops and Products, 35*(1), 70-76.

Cherian, G., Gennadios, A., Weller, C., and Chinachoti, P. 1995. Thermomechanical behavior of wheat gluten films - effect of sucrose, glycerin, and sorbitol. *Cereal Chemistry, 72*(1), 1-6.

Cho, S. W., Gällstedt, M., and Hedenqvist, M. S. 2010. Properties of wheat gluten/poly(lactic acid) laminates. *Journal of Agricultural and Food Chemistry, 58*(12), 7344-7350.

Cho, S. W., Gällstedt, M., Johansson, E., and Hedenqvist, M. S. 2011. Injection-molded nanocomposites and materials based on wheat gluten. *Int J Biol Macromol, 48*(1), 146-152.

Coles, R., McDowell, D., and Kirwan, M., 2003. *Food packaging technology*. Blackwell Publishing, CRC Press: Oxford, Egland.

Cong, F., Zhang, Y., and Dong, W. 2007. Use of surface coatings with natamycin to improve the storability of hami melon at ambient temperature. *Postharvest Biology and Technology, 46*(1), 71-75.

Conte, A., Buonocore, G. G., Bevilacqua, A., Sinigaglia, M., and Del Nobile, M. A. 2006. Immobilization of lysozyme on polyvinylalcohol films for active packaging applications. *Journal of Food Protection, 69*(4), 866-870.

Conte, A., Buonocore, G. G., Sinigaglia, M., and Del Nobile, M. A. 2007. Development of immobilized lysozyme based active film. *Journal of Food Engineering, 78*(3), 741-745.

Cornell, H. J., and Hoveling, A. W., 1998. *Wheat: Chemistry and utilization*. Technomic Publishing Company, Inc: Lancaster, PA, USA.

Corrales, M., Fernández, A., and Han, J. H. 2014. Chapter 7 - antimicrobial packaging systems. In *Innovations in food packaging (second edition)*, J.H. Han, Ed. Academic Press: San Diego, CA, USA; 133-170.

Cuq, B., Boutrot, F., Redl, A., and Lullien-Pellerin, V. 2000. Study of the temperature effect on the formation of wheat gluten network: Influence on mechanical properties and protein solubility. *Journal of Agricultural and Food Chemistry, 48*(7), 2954-2959.

Cuq, B., Gontard, N., and Guilbert, S. 1998. Proteins as agricultural polymers for packaging production. *Cereal Chemistry, 75*(1), 1-9.

Dangaran, K., Tomasula, P. M., and Qi, P. 2009. Structure and function of protein-based edible films and coatings. In *Edible Films and Coating for Food Applications*. Springer: London 25-56.

Davidson, P. M. 2001. Chemical preservatives and natural antimicrobial compounds. In *Food microbiology. Fundamentals and frontiers*, 2nd ed.; M.P. Doyle, L.R. Beuchat, and T.J. Montville, Eds. ASM Press: Washington, DC; 593-628.

de Oliveira, T. M., de Fátima Ferreira Soares, N., Pereira, R. M., and de Freitas Fraga, K. 2007. Development and evaluation of antimicrobial natamycin-incorporated film in Gorgonzola cheese conservation. *Packaging Technology and Science, 20*(2), 147-153.

del Nobile, M. A., Conte, A., Buonocore, G. G., Incoronato, A. L., Massaro, A., and Panza, O. 2009. Active packaging by extrusion processing of recyclable and biodegradable polymers. *Journal of Food Engineering, 93*(1), 1-6.

Delves-Broughton, J., Thomas, L. V., Doan, C. H., and Davidson, P. M. 2005. Natamycin. In *Antimicrobials in food, third edition*, CRC Press: 275-289.

dos Santos Pires, A. C., Ferreira Soares, N. d. F., de Andrade, N. J., Mendes do Silva, L. H., Camilloto, G. P., and Bernardes, P. C. 2008. Development and evaluation of active packaging for sliced Mozzarella preservation. *Packaging Technology and Science, 21*(7), 375-383.

Du, W.-X., Avena-Bustillos, R. J., Woods, R., Breksa, A. P., McHugh, T. H., Friedman, M., Levin, C. E., and Mandrell, R. 2012. Sensory evaluation of baked chicken wrapped with antimicrobial apple and tomato edible films formulated with cinnamaldehyde and carvacrol. *Journal of Agricultural and Food Chemistry, 60*(32), 7799-7804.

Duan, J., Park, S., Daeschel, M., and Zhao, Y. 2007. Antimicrobial chitosan-lysozyme (CL) films and coatings for enhancing microbial safety of Mozzarella cheese. *Journal of Food Science, 72*(9), M355-M362.

Dury-Brun, C., Chalier, P., Desobry, S., and Voilley, A. 2007. Multiple mass transfers of small volatile molecules through flexible food packaging. *Food Reviews International, 23*(3), 199-255.

Fajardo, P., Martins, J. T., Fucinos, C., Pastrana, L., Teixeira, J. A., and Vicente, A. A. 2010. Evaluation of a chitosan-based edible film as carrier of natamycin to improve the storability of saloio cheese. *Journal of Food Engineering, 101*(4), 349-356.

Fakhouri, F. M., Tanada-Palmu, P. S., and Grosso, C. R. F. 2004. Characterization of composite biofilms of wheat gluten and cellulose acetate phthalate. *Brazilian Journal of Chemical Engineering, 21*, 261-264.

Gällstedt, M., Hedenqvist, M. S., and Ture, H. 2011. Production, chemistry and properties of proteins. In *Biopolymers – new materials for sustainable films and coatings*, John Wiley & Sons, Ltd: Chichester, 107-132.

Gällstedt, M., Mattozzi, A., Johansson, E., and Hedenqvist, M. S. 2004. Transport and tensile properties of compression-molded wheat gluten films. *Biomacromolecules, 5*(5), 2020-2028.

Gamage, G. R., Park, H. J., and Kim, K. M. 2009. Effectiveness of antimicrobial coated oriented polypropylene/polyethylene films in sprout packaging. *Food Research International, 42*(7), 832-839.

Gemili, S., Yemenicioglu, A., and Altinkaya, S. A. 2009. Development of cellulose acetate based antimicrobial food packaging materials for controlled release of lysozyme. *Journal of Food Engineering, 90*(4), 453-462.

Gennadios, A., McHugh, T. H., Weller, C. L., and Krochta, J. M. 1994. Edible coatings and films based on proteins. In *Edible coatings and films to improve food quality*, J.M. Krochta, E.A. Baldwin, and M.O. Nisperos-Carriedo, Eds. CRC Press: Boca Raton, 201-277.

Gennadios, A., and Weller, C. L. 1990. Edible films and coatings from wheat and corn proteins. *Food Technology, 44*(10), 63-69.

Gómez-Martínez, D., Partal, P., Martínez, I., and Gallegos, C. 2009. Rheological behaviour and physical properties of controlled-release gluten-based bioplastics. *Bioresource Technology, 100*(5), 1828-1832.

Gontard, N., Duchez, C., Cuq, J.-L., and Guilbert, S. 1994. Edible composite films of wheat gluten and lipids: Water vapour permeability and other physical properties. *International Journal of Food Science & Technology, 29*(1), 39-50.

Gontard, N., Guilbert, S., and Cuq, J. L. 1992. Edible wheat gluten films - influence of the main process variables on film properties using response-surface methodology. *Journal of Food Science, 57*(1), 190-&.

Gontard, N., Marchesseau, S., Cuq, J. L., and Guilbert, S. 1995. Water-vapor permeability of edible bilayer films of wheat gluten and lipids. *International Journal of Food Science and Technology, 30*(1), 49-56.

Gould, G. W. 1995. Overview. In *New methods of food preservation*, Blackie Academic & Professional: Glasgow; xv-xix.

Guçbilmez, C. M., Yemenicioglu, A., Arslanoglu, A., Elmaci, Z. S., Korel, F., and Cetin, A. E. 2006. Incorporation of partially purified hen egg white lysozyme into zein films for antimicrobial food packaging. *Food Research International, 39*(1), 12-21.

Guilbert, S., and Gontard, N. 2005. Agro-polymers for edible and biodegradable films: Review of agricultural polymeric materials, physical and mechanical characteristics. In *Innovations in Food Packaging*, J.H. Han, Ed. Elsevier: London.

Guilbert, S., Gontard, N., Morel, M. H., Chalier, P., Micard, V., and Redl, A. 2002. Formation and properties of wheat gluten films and coatings. In *Protein-Based Films and Coatings*, CRC Press: Boca Raton.

Gutierrez, L., Batlle, R., Andujar, S., Sanchez, C., and Nerin, C. 2011. Evaluation of antimicrobial active packaging to increase shelf life of gluten-free sliced bread. *Packaging Technology and Science, 24*(8), 485-494.

Gutierrez, L., Escudero, A., Batlle, R., and Nerin, C. 2009a. Effect of mixed antimicrobial agents and flavors in active packaging films. *Journal of Agricultural and Food Chemistry, 57*(18), 8564-8571.

Gutierrez, L., Sanchez, C., Batlle, R., and Nerin, C. 2009b. New antimicrobial active package for bakery products. *Trends in Food Science & Technology, 20*(2), 92-99.

Hager, A. S., Vallons, K. J. R., and Arendt, E. K. 2012. Influence of gallic acid and tannic acid on the mechanical and barrier properties of wheat gluten films. *Journal of Agricultural and Food Chemistry, 60*(24), 6157-6163.

Han, J. H. 2000. Antimicrobial food packaging. *Food Technology, 54*(3).

Han, J. H. 2003. Antimicrobial food packaging. In *Novel food packaging techniques*, R. Ahvenainen, Ed. Woodhead Publishing Limited: Cambridge.

Han, J. H. 2014. Chapter 1 - a review of food packaging technologies and innovations. In *Innovations in food packaging (second edition)*, J.H. Han, Ed. Academic Press: San Diego; 3-12.

Hanušová, K., Šťastná, M., Votavová, L., Klaudisová, K., Dobiáš, J., Voldřich, M., and Marek, M. 2010. Polymer films releasing nisin and/or natamycin from polyvinyldichloride lacquer coating: Nisin and natamycin migration, efficiency in cheese packaging. *Journal of Food Engineering, 99*(4), 491-496.

Harmsen, P., and Hackmann, M. (2013). Green building blocks for biobased plastics. *Green Raw Materials*: Wageningen.

Helander, I. M., Alakomi, H.-L., Latva-Kala, K., Mattila-Sandholm, T., Pol, I., Smid, E. J., Gorris, L. G. M., and von Wright, A. 1998. Characterization of the action of selected essential oil components on Gram-negative bacteria. *Journal of Agricultural and Food Chemistry, 46*(9), 3590-3595.

Heralp, T. J., Gnanasambandam, R., McGuire, B. H., and Hachmeister, K. A. 1995. Degradable wheat gluten films - preparation, properties and applications. *Journal Food Science, 60*(5), 1147-&.

Hernandez-Munoz, P., Kanavouras, A., Lagaron, J. M., and Gavara, R. 2005. Development and characterization of films based on chemically cross-linked gliadins. *J Agric Food Chem, 53*(21), 8216-8223.

Hernandez-Munoz, P., Kanavouras, A., Ng, P. K. W., and Gavara, R. 2003. Development and characterization of biodegradable films made from wheat gluten protein fractions. *Journal of Agricultural and Food Chemistry, 51*(26), 7647-7654.

Hernandez-Munoz, P., Kanavouras, A., Villalobos, R., and Chiralt, A. 2004a. Characterization of biodegradable films obtained from cysteine-mediated polymerized gliadins. *Journal of Agricultural and Food Chemistry, 52*(26), 7897-7904.

Hernandez-Munoz, P., Lagaron, J. M., Lopez-Rubio, A., and Gavara, R. 2004b. Gliadins polymerized with cysteine: Effects on the physical and water barrier properties of derived films. *Biomacromolecules, 5*(4), 1503-1510.

Hernandez-Munoz, P., Lopez-Rubio, A., Lagaron, J. M., and Gavara, R. 2004c. Formaldehyde cross-linking of gliadin films: Effects on mechanical and water barrier properties. *Biomacromolecules, 5*(2), 415-421.

Hernandez-Munoz, P., Villalobos, R., and Chiralt, A. 2004d. Effect of cross-linking using aldehydes on properties of glutenin-rich films. *Food Hydrocolloids, 18*(3), 403-411.

Hernandez-Munoz, P., Villalobos, R., and Chiralt, A. 2004e. Effect of thermal treatments on functional properties of edible films made from wheat gluten fractions. *Food Hydrocolloids, 18*(4), 647-654.

Jerez, A., Partal, P., Martínez, I., Gallegos, C., and Guerrero, A. 2005. Rheology and processing of gluten based bioplastics. *Biochemical Engineering Journal, 26*(2–3), 131-138.

Jin, M., Davidson, P. M., Zivanovic, S., and Zhong, Q. 2009. Production of corn zein microparticles with loaded lysozyme directly extracted from hen egg white using spray drying: Extraction studies. *Food Chemistry, 115*(2), 509-514.

Kechichian, V., Ditchfield, C., Veiga-Santos, P., and Tadini, C. C. 2010. Natural antimicrobial ingredients incorporated in biodegradable films based on cassava starch. *LWT-Food Science and Technology, 43*(7), 1088-1094.

Kijchavengkul, T., and Auras, R. 2008. Perspective compostability of polymers. *Polymer International, 57*(6), 793-804.

Kim, S. 2008. Processing and properties of gluten/zein composite. *Bioresource Technology, 99*(6), 2032-2036.

Koehler, P., Kieffer, R., and Wieser, H. 2010. Effect of hydrostatic pressure and temperature on the chemical and functional properties of wheat gluten III. Studies on gluten films. *Journal of Cereal Science, 51*(1), 140-145.

Kokini, J. L., Cocero, A. M., Madeka, H., and de Graaf, E. 1994. The development of state diagrams for cereal proteins. *Trends in Food Science & Technology, 5*(9), 281-288.

Koontz, J. L., and Marcy, J. E. 2003. Formation of natamycin: Cyclodextrin inclusion complexes and their characterization. *Journal of Agricultural and Food Chemistry, 51*(24), 7106-7110.

Krochta, J. M. 2002. Proteins as raw materials for films and coatings. In *Protein-based films and coatings*, CRC Press: Boca Raton.

Krochta, J. M. 2007. Food packaging. In *Handbook of food engineering*, D.R. Heldman, and D.B. Lund, Eds. CRC Press: Boca Raton, FL.

Kurniawan, L., Qiao, G. G., and Zhang, X. 2009. Formation of wheat-protein-based biomaterials through polymer grafting and crosslinking reactions to introduce new functional properties. *Macromolecular Bioscience, 9*(1), 93-101.

Lacroix, M., and Cooksey, K. 2005. 18 - edible films and coatings from animal origin proteins. In *Innovations in food packaging*, J.H. Han, Ed. Academic Press: London; 301-317.

Larré, C., Desserme, C., Barbot, J., and Gueguen, J. 2000. Properties of deamidated gluten films enzymatically cross-linked. *Journal of Agricultural and Food Chemistry, 48*(11), 5444-5449.

Lee, D. S. 2009. Packaging and the microbial shelf life of food. In *Food packaging and shelf life: A practical guide*, CRC Press: Boca Raton, Florida; 55-79.

Lee, S., Lee, M., and Song, K. 2005. Effect of gamma-irradiation on the physicochemical properties of gluten films. *Food Chemistry, 92*(4), 621-625.

Leistner, L. 1995. Principles and applications of hurdle technology. In *New methods of food preservation*, G.W. Gould, Ed. Springer US: 1-21.

Li, Y., Guo, X., Lin, P., Fan, C., and Song, Y. 2010. Preparation and functional properties of blend films of gliadins and chitosan. *Carbohydrate Polymers, 81*(2), 484-490.

López-Carballo, G., Gómez-Estaca, J., Catalá, R., Hernández-Muñoz, P., and Gavara, R. 2012. Active antimicrobial food and beverage packaging. In *Emerging food packaging technologies*, K.L. Yam, and D.S. Lee, Eds. Woodhead Publishing Limited: Londo, 27-54.

López-Malo, A., Palou, E., and Alzamora, S. M. 2005. Naturally occurring compounds - plant sources. In *Antimicrobials in food, third edition*, CRC Press: Boca Raton, 429-451.

Lopez, P., Sanchez, C., Batlle, R., and Nerin, C. 2007a. Development of flexible antimicrobial films using essential oils as active agents. *Journal of Agricultural and Food Chemistry, 55*(21), 8814-8824.

Lopez, P., Sanchez, C., Batlle, R., and Nerin, C. 2007b. Vapor-phase activities of cinnamon, thyme, and oregano essential oils and key constituents against foodborne microorganisms. *Journal of Agricultural and Food Chemistry, 55*(11), 4348-4356.

Losso, J. N., Nakai, S., and Charte, E. A. 2000. Lysozyme. In *Natural food antimicrobial systems*, N. AS, Ed. CRC Press: Boca Raton.

Ma, D., Zhang, L.-M., Xie, X., Liu, T., and Xie, M.-Q. 2011. Tunable supramolecular hydrogel for in situ encapsulation and sustained release of bioactive lysozyme. *Journal of Colloid and Interface Science, 359*(2), 399-406.

Mangavel, C., Barbot, J., Bervast, E., Linossier, L., Feys, M., Gueguen, J., and Popineau, Y. 2002. Influence of prolamin composition on mechanical properties of cast wheat gluten films. *Journal of Cereal Science, 36*(2), 157-166.

Mangavel, C., Rossignol, N., Perronnet, A., Barbot, J., Popineau, Y., and Gueguen, J. 2004. Properties and microstructure of thermo-pressed wheat gluten films: A comparison with cast films. *Biomacromolecules, 5*(4), 1596-1601.

Marsh, K., and Bugusu, B. 2007. Food packaging - roles, materials, and environmental issues. *J Food Sci, 72*(3), 39-55.

Mastromatteo, M., Lecce, L., De Vietro, N., Favia, P., and Del Nobile, M. A. 2011. Plasma deposition processes from acrylic/methane on natural fibres to control the kinetic release of lysozyme from PVOH monolayer film. *Journal of Food Engineering, 104*(3), 373-379.

Matan, N., Saengkrajang, W., and Matan, N. 2011. Antifungal activities of essential oils applied by dip-treatment on areca palm (*areca catechu*) leaf sheath and persistence of their potency upon storage. *International Biodeterioration & Biodegradation, 65*(1), 212-216.

Mensitieri, G., Di Maio, E., Buonocore, G. G., Nedi, I., Oliviero, M., Sansone, L., and Iannace, S. 2011. Processing and shelf life issues of selected food packaging materials and structures from renewable resources. *Trends in Food Science & Technology, 22*(2–3), 72-80.

Micard, V., Belamri, R., Morel, M. H., and Guilbert, S. 2000. Properties of chemically and physically treated wheat gluten films. *Journal of Agricultural and Food Chemistry, 48*(7), 2948-2953.

Michon, T., Wang, W., Ferrasson, E., and Guéguen, J. 1999. Wheat prolamine crosslinking through dityrosine formation catalyzed by peroxidases: Improvement in the modification of a poorly accessible substrate by “indirect” catalysis. *Biotechnology and Bioengineering, 63*(4), 449-458.

Mild, R. M., Joens, L. A., Friedman, M., Olsen, C. W., McHugh, T. H., Law, B., and Ravishankar, S. 2011. Antimicrobial edible apple films inactivate antibiotic resistant and susceptible *Campylobacter jejuni* strains on chicken breast. *Journal of Food Science, 76*(3), 163-168.

Min, S., Harris, L. J., Han, J. H., and Krochta, J. M. 2005. *Listeria monocytogenes* inhibition by whey protein films and coatings incorporating lysozyme. *Journal of Food Protection, 68*(11), 2317-2325.

Min, S., Rumsey, T. R., and Krochta, J. M. 2008. Diffusion of the antimicrobial lysozyme from a whey protein coating on smoked salmon. *Journal of Food Engineering, 84*(1), 39-47.

Mohamed, A., Finkenstadt, V. L., Gordon, S. H., Biresaw, G., Palmquist, D. E., and Rayas-Duarte, P. 2008. Thermal properties of PCL/gluten bioblends characterized by TGA, DSC, SEM, and infrared-PAS. *Journal of Applied Polymer Science, 110*(5), 3256-3266.

Mohamed, A. A., and Xu, J. 2007. Thermal and kinetic properties of poly(lactic acid) and transglutaminase-crosslinked wheat gluten blends. *Journal of Applied Polymer Science, 106*(1), 214-219.

Montero-Prado, P., Rodriguez-Lafuente, A., and Nerin, C. 2011. Active label-based packaging to extend the shelf-life of "calanda" peach fruit: Changes in fruit quality and enzymatic activity. *Postharvest Biology and Technology, 60*(3), 211-219.

Morel, M. H., Redl, A., and Guilbert, S. 2002. Mechanism of heat and shear mediated aggregation of wheat gluten protein upon mixing. *Biomacromolecules, 3*(3), 488-497.

Naidu, A. S. 2000. Overview. In *Natural food antimicrobial systems*, A.S. Naidu, Ed. CRC Press: Boca Raton, Florida.

Narayan, R. (-). Biobased & biodegradable plastics: East Lansing, Michigan State University.

Olabarrieta, I., Gallstedt, M., Ispizua, I., Sarasua, J. R., and Hedenqvist, M. S. 2006. Properties of aged montmorillionite-wheat gluten composite films. *Journal of Agricultural and Food Chemistry, 54*(4), 1283-1288.

Ouattara, B., Simard, R. E., Piette, G., Begin, A., and Holley, R. A. 2000. Inhibition of surface spoilage bacteria in processed meats by application of antimicrobial films prepared with chitosan. *International Journal of Food Microbiology, 62*(1-2), 139-148.

Pallos, F. M., Robertson, G. H., Pavlath, A. E., and Orts, W. J. 2006. Thermoformed wheat gluten biopolymers. *Journal Agriculture and Food Chemistry, 54*(2), 349-352.

Park, S., Daeschel, M., and Zhao, Y. 2004. Functional properties of antimicrobial lysozyme-chitosan composite films. *Journal of Food Science, 69*(8), M215-M221.

Park, S. K., and Bae, D. H. 2006. Antimicrobial properties of wheat gluten-chitosan composite film in intermediate-moisture food systems. *Food Science and Biotechnology, 15*(1), 133-137.

Pereira de Abreu, D. A., Cruz, J. M., and Paseiro Losada, P. 2012. Active and intelligent packaging for the food industry. *Food Reviews International, 28*(2), 146-187.

Pintado, C. M. B. S., Ferreira, M. A. S. S., and Sousa, I. 2010. Control of pathogenic and spoilage microorganisms from cheese surface by whey protein films containing malic acid, nisin and natamycin. *Food Control, 21*(3), 240-246.

Queiroz, A. U. B., and Collares-Queiroz, F. P. 2009. Innovation and industrial trends in bioplastics. *Polymer Reviews, 49*(2), 65-78.

Ravishankar, S., Jaroni, D., Zhu, L., Olsen, C., McHugh, T., and Friedman, M. 2012. Inactivation of *Listeria monocytogenes* on ham and bologna using pectin-based apple, carrot, and hibiscus edible films containing carvacrol and cinnamaldehyde. *Journal of Food Science, 77*(7), M377-M382.

Reddy, N., and Yang, Y. Q. 2010. Developing water stable gliadin films without using crosslinking agents. *Journal of Polymers and the Environment, 18*(3), 277-283.

Redl, A., Morel, M. H., Bonicel, J., Vergnes, B., and Guilbert, S. 1999. Extrusion of wheat gluten plasticized with glycerol: Influence of process conditions on flow behavior, rheological properties, and molecular size distribution. *Cereal Chemistry, 76*(3), 361-370.

Restuccia, D., Spizzirri, U. G., Parisi, O. I., Cirillo, G., Curcio, M., Iemma, F., Puoci, F., Vinci, G., and Picci, N. 2010. New EU regulation aspects and global market of active and intelligent packaging for food industry applications. *Food Control, 21*(11), 1425-1435.

Rhim, J. W., Gennadios, A., Fu, D., Weller, C. L., and Hanna, M. A. 1999. Properties of ultraviolet irradiated protein films. *Lebensmittel-Wissenschaft und - Technologie, 32*(3), 129-133.

Robertson, G., 2006. *Food packaging: Principles and practice*. 2nd ed.; CRC Press: Taylor & Francis Group: Boca Raton.

Robertson, G. L. 2009. Food packaging and shelf life. In *Food packaging and shelf life: A practical guide*, G.L. Robertson, Ed. CRC Press: Boca Raton.

Rodriguez-Lafuente, A., Nerin, C., and Batlle, R. 2010. Active paraffin-based paper packaging for extending the shelf life of cherry tomatoes. *Journal of Agricultural and Food Chemistry, 58*(11), 6780-6786.

Rodriguez, A., Batlle, R., and Nerin, C. 2007. The use of natural essential oils as antimicrobial solutions in paper packaging. Part II. *Progress in Organic Coatings, 60*(1), 33-38.

Rodriguez, A., Nerin, C., and Batlle, R. 2008. New cinnamon-based active paper packaging against *Rhizopus stolonifer* food spoilage. *Journal of Agricultural and Food Chemistry, 56*(15), 6364-6369.

Roy, S., Weller, C. L., Gennadios, A., Zeece, M. G., and Testin, R. F. 1999. Physical and molecular properties of wheat gluten films cast from heated film-forming solutions. *J Food Sci, 64*(1), 57-60.

Sánchez, A. C., Popineau, Y., Mangavel, C., Larré, C., and Guéguen, J. 1998. Effect of different plasticizers on the mechanical and surface properties of wheat gliadin films. *Journal of Agricultural and Food Chemistry, 46*(11), 4539-4544.

Sanla-Ead, N., Jangchud, A., Chonhenchob, V., and Suppakul, P. 2012. Antimicrobial activity of cinnamaldehyde and eugenol and their activity after incorporation into cellulose-based packaging films. *Packaging Technology and Science, 25*(1), 7-17.

Shen, L., Haufe, J., and Patel, M. K. (2009). Product overview and market projection of emerging bio-based plastics (PRO-BIP 2009). Universiteit Utrecht, The Netherlands.

Shugar, D. 1952. The measurement of lysozyme activity and the ultra-violet inactivation of lysozyme. *Biochimica et Biophysica Acta, 8*(3), 302-309.

Singh, R. P., and Anderson, B. 2004. The major types of food spoilage: An overview. In *Understanding and measuring the shelf-life of food*, R. Steele, Ed. Woodhead Publishing Limited: Cambridge, England; 3-19.

Soares, R. M. D., Maia, G. S., Rayas-Duarte, P., and Soldi, V. 2009. Properties of filmogenic solutions of gliadin crosslinked with 1-(3-dimethyl aminopropyl)-3-ethylcarbodiimidehydrochloride/N-hydroxysuccinimide and cysteine. *Food Hydrocolloids, 23*(1), 181-187.

Soares, R. M. D., and Soldi, V. 2010. The influence of different cross-linking reactions and glycerol addition on thermal and mechanical properties of biodegradable gliadin-based film. *Materials Science and Engineering: C, 30*(5), 691-698.

Sofos, J. N., Beuchat, L. R., Davidson, P. M., and Johnson, E. A. 1998. Naturally occurring antimicrobials in food. *Regulatory Toxicology and Pharmacology , 28*(2), 71-72.

Song, J. H., Murphy, R. J., Narayan, R., and Davies, G. B. 2009a. Biodegradable and compostable alternatives to conventional plastics. *Philosophical Transactions of the Royal Society B: Biological Sciences, 364*(1526), 2127-2139.

Song, Y., Li, L., and Zheng, Q. 2009b. Influence of epichlorohydrin modification on structure and properties of wheat gliadin films. *Journal of Agricultural and Food Chemistry, 57*(6), 2295-2301.

Song, Y., and Zheng, Q. 2008. Preparation and properties of thermo-molded bioplastics of glutenin-rich fraction. *Journal of Cereal Science, 48*(1), 77-82.

Song, Y., Zheng, Q., and Liu, C. 2008. Green biocomposites from wheat gluten and hydroxyethyl cellulose: Processing and properties. *Industrial Crops and Products, 28*(1), 56-62.

Song, Y., Zheng, Q., and Zhang, Q. 2009c. Rheological and mechanical properties of bioplastics based on gluten- and glutenin-rich fractions. *Journal of Cereal Science, 50*(3), 376-380.

Song, Y., Zheng, Q., and Zhou, W. 2009d. Preparation and properties of wheat gluten/silica composites. *Science in China Series B: Chemistry, 52*(3), 257-260.

Suarez, V. B., Tremmel, G. J., Rivera, M., Reinheimer, J. A., and Meinardi, C. A. 2012. Polyphosphates as inhibitors of surface mould growth on hard cheese during ripening. *International Journal of Dairy Technology, 65*(3), 410-415.

Sun, S., Song, Y., and Zheng, Q. 2008a. Morphology and mechanical properties of thermo-molded bioplastics based on glycerol-plasticized wheat gliadins. *Journal of Cereal Science, 48*(3), 613-618.

Sun, S., Song, Y., and Zheng, Q. 2008b. Thermo-molded wheat gluten plastics plasticized with glycerol: Effect of molding temperature. *Food Hydrocolloids, 22*(6), 1006-1013.

Suppakul, P., Miltz, J., Sonneveld, K., and Bigger, S. W. 2003. Active packaging technologies with an emphasis on antimicrobial packaging and its applications. *Journal of Food Science, 68*(2), 408-420.

Tanada-Palmu, P., Helen, H., and Hyvonen, L. 2000. Preparation, properties and applications of wheat gluten edible films. *Agricultural and Food Science in Finland, 9*(1), 23-35.

Tang, X. Z., Kumar, P., Alavi, S., and Sandeep, K. P. 2012. Recent advances in biopolymers and biopolymer-based nanocomposites for food packaging materials. *Critical Reviews in Food Science and Nutrition, 52*(5), 426-442.

Tropini, V., Lens, J. P., Mulder, W., and Silvestre, F. 2004. Wheat gluten films cross-linked with 1-ethyl-3-(3-dimethylaminopropyl) carbodiimide and N-hydroxysuccinimide. *Industrial Crops and Products, 20*(3), 281-289.

Tropini, V., Lens, J. P., Mulder, W. J., and Silvestre, F. 2000. Cross-linking of wheat gluten using a water-soluble carbodiimide. *Cereal Chemistry, 77*(3), 333-338.

Tunc, S., Angellier, H., Cahyana, Y., Chalier, P., Gontard, N., and Gastaldi, E. 2007a. Functional properties of wheat gluten/montmorillonite nanocomposite films processed by casting. *Journal of Membrane Science, 289*(1-2), 159-168.

Tunc, S., Chollet, E., Chalier, P., Preziosi-Belloy, L., and Gontard, N. 2007b. Combined effect of volatile antimicrobial agents on the growth of *Penicillium notatum*. *International Journal of Food Microbiology, 113*(3), 263-270.

Ture, H., Eroglu, E., Ozen, B., and Soyer, F. 2011. Effect of biopolymers containing natamycin against aspergillus niger and penicillium roquefortii on fresh kashar cheese. *International Journal of Food Science and Technology, 46*(1), 154-160.

Ture, H., Eroglu, E., Soyer, F., and Ozen, B. 2008. Antifungal activity of biopolymers containing natamycin and rosemary extract against *Aspergillus niger* and *Penicillium roquefortii*. *International Journal of Food Science and Technology, 43*(11), 2026-2032.

Ullsten, N. H., Cho, S. W., Spencer, G., Gallstedt, M., Johansson, E., and Hedenqvist, M. S. 2009. Properties of extruded vital wheat gluten sheets with sodium hydroxide and salicylic acid. *Biomacromolecules, 10*(3), 479-488.

Ullsten, N. H., Gällstedt, M., Johansson, E., Graslund, A., and Hedenqvist, M. S. 2006. Enlarged processing window of plasticized wheat gluten using salicylic acid. *Biomacromolecules, 7*(3), 771-776.

Ünalan, I. U., Korel, F., and Yemenicioglu, A. 2011. Active packaging of ground beef patties by edible zein films incorporated with partially purified lysozyme and Na(2)EDTA. *International Journal of Food Science and Technology, 46*(6), 1289-1295.

Utama, I. M. S., Wills, R. B. H., Ben-Yehoshua, S., and Kuek, C. 2002. In vitro efficacy of plant volatiles for inhibiting the growth of fruit and vegetable decay microorganisms. *Journal of Agricultural and Food Chemistry, 50*(22), 6371-6377.

Verbeek, C. J. R., and van den Berg, L. E. 2010. Extrusion processing and properties of protein-based thermoplastics. *Macromolecular Materials and Engineering, 295*(1), 10-21.

Yildirim, M., Gulec, F., Bayram, M., and Yildirim, Z. 2006. Properties of kashar cheese coated with casein as a carrier of natamycin. *Italian Journal of Food Science, 18*(2), 127-138.

Zeng, M., Huang, Y. W., Lu, L. Y., Fan, L. R., Mangavel, C., and Lourdin, D. 2011. Mechanical properties of thermo-moulded biofilms in relation to proteins/starch interactions. *Food Biophysics, 6*(1), 49-57.

Zhang, Q., Song, Y., and Zheng, Q. 2008. Influences of acid and alkali on mechanical properties of compression-molded gluten bioplastics. *Cereal Chemistry, 85*(3), 379-383.

Zhang, X., Do, M. D., Kurniawan, L., and Qiao, G. G. 2010. Wheat gluten-based renewable and biodegradable polymer materials with enhanced hydrophobicity by using epoxidized soybean oil as a modifier. *Carbohydrate Research, 345*(15), 2174-2182.

Zhang, X., Hoobin, P., Burgar, I., and Do, M. D. 2006. Chemical modification of wheat protein-based natural polymers: Cross-linking effect on mechanical properties and phase structures. *Journal of Agricultural and Food Chemistry, 54*(26), 9858-9865.

Zhong, Q., Jin, M., Davidson, P. M., and Zivanovic, S. 2009. Sustained release of lysozyme from zein microcapsules produced by a supercritical anti-solvent process. *Food Chemistry, 115*(2), 697-700.

Zodrow, K. R., Schiffman, J. D., and Elimelech, M. 2012. Biodegradable polymer (PLGA) coatings featuring cinnamaldehyde and carvacrol mitigate biofilm formation. *Langmuir, 28*(39), 13993-13999.

Zuo, M., Song, Y., and Zheng, Q. 2009. Preparation and properties of wheat gluten/methylcellulose binary blend film casting from aqueous ammonia: A comparison with compression molded composites. *Journal of Food Engineering, 91*(3), 415-422.

II. OBJECTIVES

II.1. DISSERTATION AIM AND OBJECTIVES

II.1.1. General objective

The main objective of the present Doctoral Thesis is the development and characterization of new biodegradable films based on chemically modified gliadins with improved functional properties and antimicrobial capacity intended to be used in active food packaging.

II.1.2. Specific objectives

The specific objectives are:

- To develop novel renewable and biodegradable bioplastics based on gliadin proteins with improved functional properties by means of chemical cross-linking with cinnamaldehyde.
- To characterize the most important engineering properties of the films developed (mechanical, thermal, barrier, optical, morphological, water resistance, compostability, etc.), and to evaluate the influence of environmental conditions (relative humidity, temperature) and degree of cross-linking of the matrices on some of their most important properties.
- To inquire into the cross-linking reaction mechanism established between cinnamaldehyde and gliadins by means of biochemical techniques.
- To determine the free cinnamaldehyde entrapped in the modified gliadin matrix, and the effect of environmental conditions on its release.
- To evaluate the antimicrobial activity of the new films, based on the release of free cinnamaldehyde, against common food spoilage microorganisms; and their application in diverse active packaging systems designed for foodstuffs.
- To study the potential of these films as carriers and release systems for the antimicrobials natamycin and lysozyme, and to evaluate the effect of their incorporation on film functional properties and antimicrobial efficacy.

III. CHAPTERS

CHAPTER 1

FUNCTIONAL PROPERTIES OF BIOPLASTICS MADE FROM WHEAT GLIADINS MODIFIED WITH CINNAMALDEHYDE

Balaguer, M.P.; Gómez-Estaca, J.; Gavara, R.; and Hernandez-Munoz, P.

Journal of Agricultural and Food Chemistry, 2011, *59*(12), 6689-6695

Cinnamaldehyde is a naturally occurring α,β-unsatured aldehyde. Its potential as a natural cross-linker to improve the physical performance of cast wheat gliadin films was evaluated. The cross-linking reaction was found to be dependent on the pH of the reaction medium, with pH 2 as the optimum. The water resistance (weight loss after immersion), mechanical properties (Young's modulus, tensile strength and elongation at break), thermal properties (T_g and decomposition behavior), optical properties and morphology of films were evaluated. Cross-linked films showed high transparency, maintained their integrity after immersion, and displayed significant improvements in tensile strength and Young's modulus without impairment of their elongation properties. These effects, which were proportional to the amount of cinnamaldehyde added, highlight the possible formation of intermolecular covalent bonds between "monomeric" gliadins, leading to a polymerized network. Thus, this treatment could provide a new alternative to the toxic cross-linkers commonly employed and so extend the use of gliadin films.

1.1. INTRODUCTION

The use of renewable raw materials for the manufacture of biodegradable and environmentally friendly plastics is a new technological goal for efficient and sustainable development. Biobased polymers made from different proteins have been researched and developed over the past 20 years for a number of purposes, including the formation of films and coatings for packaging applications. Attention has focused on plant proteins such as wheat gluten, corn zein and soy, and animal proteins such as casein, whey, collagen, keratin and egg albumen. These biomaterials are not intended to replace traditional plastics but to target niche markets in which their short lifecycle is suitable. In food packaging, applications in fresh or minimally processed fruits and vegetables, dairy products, organically grown products, and catering facilities are good candidates (Guilbert and Gontard, 2005). These biopolymers have also led to great interest in the development of sustained release devices for active packaging purposes.

Protein-based films possess moderate mechanical properties in comparison to conventional synthetic films, and good oxygen barrier properties at low or intermediate relative humidities exceeding those of polyolefins (Gennadios et al., 1994). Nevertheless, one of their greatest limitations as packaging materials is their loss of mechanical and barrier properties at high relative humidity levels. In order to overcome this water sensitivity, some modification of the protein is required.

Since amino acids have a large number of reactive side groups (NH_2, COOH, SH, etc.) that are susceptible to physical, chemical or enzymatic modification, covalent cross-linking of polypeptide chains provides a means for improving the physical integrity of these networks and consequently enhancing the functionality of the resulting films.

The food value of wheat is well recognized, as shown by the large volume of wheat-derived breakfast cereals and different types of breads and pasta. However, wheat is now also well established as a raw material for the manufacture of starch. The economics of starch manufacture from wheat depend on the returns from the gluten, the proteinaceous material comprising gliadins and glutenins obtained as a by-product of isolating the starch from the wheat flour. Wheat gluten has a market in bakery products, especially for protein enrichment, and in the breakfast-cereal industry. As the markets for wheat starch increase, manufacturers are looking to expand the outlets for the concomitant gluten production. This

situation, and the general interest in developing environmentally friendly products based on renewable resources, has prompted investigation on non-food uses for wheat gluten. Wheat gluten presents important viscoelasticity, thermoplasticity, film-forming and other properties which endow this biomaterial with a noteworthy potential for a wide range of technological applications, particularly as a food packaging material (Cornell and Hoveling, 1998). However, gluten presents poor solubility in water and in ethanolic solutions; in addition high molecular weight glutenin subunits tend to form large aggregates hindering gluten processability. In this sense gliadins, with lower molecular weight, have been selected due to their ready extractability in ethanolic solutions in which they show long-term stability and excellent film-forming properties.

Previous studies on gluten proteins have shown that gliadins and glutenins can be exploited separately in order to maximize their range of industrial uses (Hernandez-Munoz et al., 2003). Films made from gliadins are very glossy and transparent but have poor mechanical resistance and lose their integrity upon immersion in water, which limits their use in specific industrial applications such as packaging materials (Hernandez-Munoz et al., 2003). Gliadin films obtained by casting have been subjected to thermal curing treatments (Hernandez-Munoz et al., 2004d) and have been blended with other renewable polymers that possess superior mechanical strength, such as chitosan (Hernandez-Munoz et al., 2009), with the aim of improving their functional properties. Chemical agents such as cysteine (Hernandez-Munoz et al., 2004a; Hernandez-Munoz et al., 2004b; Soares et al., 2009) and cross-linking agents such as formaldehyde, glutaraldehyde and glyoxal (Hernandez-Munoz et al., 2005; Hernandez-Munoz et al., 2004c), 1-ethyl-3-(3-dimethylaminopropyl) carbodiimide/N-hydroxysuccinimide (Soares et al., 2009) and epichlorhydrin (Song et al., 2009) have also been employed. However, the inherent toxicity of some of these compounds has to be considered when these materials are used in food packaging applications.

Cinnamaldehyde is a naturally occurring aromatic α,β-unsaturated aldehyde derived from cinnamon that has antimicrobial properties (Burt, 2004). Due to its chemical structure (**Figure 1.1**), it could also act as a cross-linking agent for proteins. However, it is uncertain which proteins or other macromolecules react with cinnamaldehyde, and among those that do, which groups have the greatest potential to react (Weibel and Hansen, 1989).

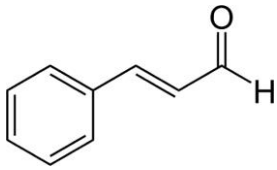

Figure 1.1. Chemical structure of cinnamaldehyde.

The aim of this study is to explore the potential of cinnamaldehyde as a cross-linking agent to improve the physical performance of gliadin films.

1.2. MATERIALS AND METHODS

1.2.1. Materials

Crude wheat gluten (≥80% protein, 7% fat and 8% moisture content on a dry basis), glycerol, ethanol, hydrochloric acid and cinnamaldehyde (3-phenylprop-2-enal), all laboratory grade, were supplied by Sigma (Madrid, Spain).

1.2.2. Gliadin-rich fraction extraction from wheat gluten

The gliadin-rich fraction was extracted from wheat gluten according to the method described by Hernandez-Munoz and Hernandez (2001). Briefly, 100 g of wheat gluten was dispersed in 400 mL of 70% (v/v) ethanol/water mixture, stirred overnight at room temperature and centrifuged at 5000 rpm for 20 min at 20 °C. The supernatant containing the gliadin-rich fraction was collected and used as the film-forming solution.

1.2.3. Chemical modification of gliadins

The capacity of cinnamaldehyde to modify gliadins and improve the physical performance of the resulting films was studied in relation to the pH of the gliadin solution. For this purpose 5% (g/100 g of dry protein) of cinnamaldehyde was incorporated into the gliadin solution prior to adjustment of its pH to 1, 1.5, 2, 2.5, 3, 4 or 5 or maintenance of the original pH 6 of the gliadin solution. Glycerol was added as a plasticizer at 25% (g/100 g dry protein) and the solution was stirred for 1 h at room temperature. The films were cast, dried at 37 °C for 24 h and conditioned at 23 °C and 50% relative humidity (RH). The effectiveness of the cinnamaldehyde at the different pH levels was evaluated by measuring the films' resistance

to disintegration in water. In order to establish the pH value at which the loss of proteinaceous film material in water is minimal, the protein solubility of the films which were resistant to water was measured as indicated below. The physical properties of the cinnamaldehyde-modified gliadin films were then determined at the pH at which the films maintained their integrity in water and the protein solubility was minimal; the effect of the cinnamaldehyde content on the properties of the films was evaluated at cinnamaldehyde concentrations of 1.5, 3 and 5% (g/100 g of dry protein).

The samples were coded as follows: G (gliadin), XC, where X is the percentage of cinnamaldehyde (C), and _pHY, where Y is the pH of the reaction.

1.2.4. Film thickness

The thickness of the films was measured using a micrometer (Mitutoyo, Kanagawa, Japan) with a sensitivity of ± 2 μm. The mean thickness was calculated from measurements taken at ten different locations on each film sample.

1.2.5. Protein solubility

Protein solubility of the films in phosphate buffer was determined by the bicinchoninic acid protein assay kit (Sigma, Madrid, Spain) (Smith et al., 1985). The film samples were stored in a desiccator over silica gel for 10 days before being immersed in test tubes containing 10 mL of 0.1 M sodium phosphate buffer (pH 7). The tubes were shaken at 180 rpm at 25 °C for 24 h. Aliquots of 1 mL from each test tube were centrifuged at 13000 g for 10 min and 0.1 mL of each supernatant was added to 2 mL of the protein determination reagent and heated at 37 °C for 30 min. After cooling to ambient temperature, the absorbance of the solutions was measured at 562 nm in comparison with a reagent blank. Protein content was calculated from a standard curve constructed using bovine serum albumin solution standards (from 0 to 1000 μg/mL). Protein solubility was expressed as milligrams of protein dissolved in the buffer per gram of dry film. Three replications were carried out for each film and the experiment was repeated three times with reproducible results.

1.2.6. Film Color

Film color was measured using a Konica Minolta CM-3500d spectrophotometer (Konica Minolta Sensing, Inc., Osaka, Japan) set to D65 illuminant/10° observer. Film specimens were measured against on the surface of a standard white plate, and the CIELAB color space was used to obtain the color coordinates L* [black (0) to white (100)], a* [green (-) to red (+)] and b* [blue (-) to yellow (+)]. The color was expressed using the polar coordinates L*C*h°, where L* is the same as above, C* is the chroma and h° is the hue angle. Simple transformations were used to convert L*a*b* coordinates to L*C*h° coordinates:

$$C^* = \sqrt{a^{*2} + b^{*2}} \qquad (\mathbf{1.1})$$

$$h^\circ = arctg\left(\frac{b^*}{a^*}\right) \qquad (\mathbf{1.2})$$

Eight measurements were taken of each sample and three samples of each film were measured.

1.2.7. Mechanical properties

A universal machine Mecmesin model MultiTest 1-í (Landes Poli Ibérica, S.L., Barcelona, Spain) equipped with a 100 N static load cell was used to evaluate the maximum tensile strength (σ_m), percentage of elongation at break (ε_b) and Young's modulus (*E*) of the films according to ASTM standard method D882 (ASTM, 2009). The films were conditioned at 50% and 75% RH for at least 1 week prior to testing. Film samples were cut into strips 2.54 cm wide and 10 cm long. The grip separation was set at 5.08 cm and the cross-head speed at 25 $mm \cdot min^{-1}$. At least 10 replicates from each sample were tested. The tensile properties were calculated from the plot of stress (tensile force/initial cross-section area) versus strain (elongation as a fraction of the original length).

1.2.8. Weight loss

Film specimens (3 × 3 cm^2) were dried in a desiccator over silica gel for ten days, at which point a moisture content close to zero was assumed. The dry films were weighed accurately (initial dry weight, W_i) and immersed in test tubes containing 10 mL of 0.1 M sodium phosphate buffer (pH 7) with or without 2% 2-mercaptoethanol (2-ME). The tubes were

shaken at 180 rpm at 25 °C for 24 h. The films were then removed from the buffer solutions, and the remaining water was eliminated from the surface with absorbent paper. The films were weighed and placed in the desiccator again until they reached a constant weight (final dry weight, W_f). The percentage weight loss (WL) of the films was calculated from the following equation:

$$WL\,\% = \frac{W_i - W_f}{W_i} \cdot 100 \qquad (\mathbf{1.3})$$

1.2.9. Modulated differential scanning calorimetry (MDSC)

Measurements of the glass transition temperature (T_g) of gliadin films made without glycerol and conditioned at 0% RH at 23 °C were determined by modulated differential scanning calorimetry. It is well-known that, when using conventional DSC, during the first heating of gluten proteins an endothermic peak is superimposed on the glass transition phenomenon, preventing correct measurement of the glass transition temperature. This peak can be eliminated during the second heating, but the protein can be modified as a result due to thermal cross-linking. A more reliable measurement of T_g can be obtained using MDSC. This technique makes it possible to separate reversing thermal events from non-reversing ones in a single scan and thus to separate T_g from the endothermic relaxation in gluten proteins. The glass transition of the films was measured using a TA Instruments DSC Q2000 (TA Instruments Inc., New Castle, DE, USA) equipped with Universal Analysis 2000 software. Nitrogen was used as a purge gas at a flow rate of 50 mL/min. Temperature calibration of the instrument was performed with indium. The heating rate was 2 °C/min, the modulation period was 60 s and the amplitude of modulation was 0.32 °C. The glass transition temperature was recorded from the inflection point of the reversing heat flow signal. The films were dried over P_2O_5 at 23 °C for 2 weeks before testing. Dry samples of approximately 5 mg were placed in aluminum pans with inverted lids to achieve optimum thermal conductivity. These were sealed, punctured three times and kept over P_2O_5 for a further week prior to scanning. All samples were measured in triplicate.

1.2.10. Thermogravimetric analysis (TGA)

TGA of gliadin films without glycerol was carried out using a Mettler Toledo TGA/SDTA/851 (Mettler Toledo, Columbus, OH, USA). Samples of approximately 10 mg were heated from room temperature to 800 °C at 10 °C/min and held at an isotherm for 3 min. The TGA data

were plotted as the weight percentage versus temperature, and the decomposition temperature was obtained from the first derivative of weight percentage versus temperature (DTGA).

1.2.11. Morphology

The films were fractured under liquid nitrogen, and their cross-section surface morphology was studied by scanning electron microscopy (SEM) using a Hitachi model S-4100 with a BSE Autrata detector and an EMIP 3.0 image capture system (Hitachi, Madrid, Spain). A copper cube was used as a support for the films, which were fixed with double-sided carbon tape and silver paint. The samples were coated with gold–palladium under a vacuum in a sputter coating unit.

1.2.12. Statistical analysis

Statistical analysis of the results was performed with SPSS commercial software (SPSS Inc, Chicago, IL. USA). A one-way analysis of variance (ANOVA) was carried out. Differences between means were assessed on the basis of confidence intervals using the Tukey test at a level of significance of $p \leq 0.05$. The data were graphically plotted with Sigmaplot software (Systat Software Inc., Richmond, CA, USA).

1.3. RESULTS AND DISCUSSION

1.3.1. pH effect on the cross-linking capacity of cinnamaldehyde

The water resistance in phosphate buffer at pH 7 was determined for films modified with 5% cinnamaldehyde and cast from solutions with a pH of between 1 and 6. The films produced at pHs of between 1 and 3 maintained their integrity after immersion in water whereas those prepared at pHs of between 4 and 6 lost their physical integrity and became insoluble masses aggregated in a transparent buffer. **Figure 1.2** shows the film protein solubility of the films that were resistant to water. It can be seen that the pH 1 and 1.5 films presented the greatest protein solubility, which could be due to a possible protein degradation occurring as a result of acid hydrolysis of peptide bonds. In contrast, the lowest protein solubility value was obtained for films made at pH 2; however, there were no significant differences ($p > 0.05$) in the protein solubility of films made at pHs of between 2 and 3. This study shows that there

is an optimal pH at which cinnamaldehyde acts as a cross-linker for gliadins and that this could be considered to be between pH 2 and pH 3.

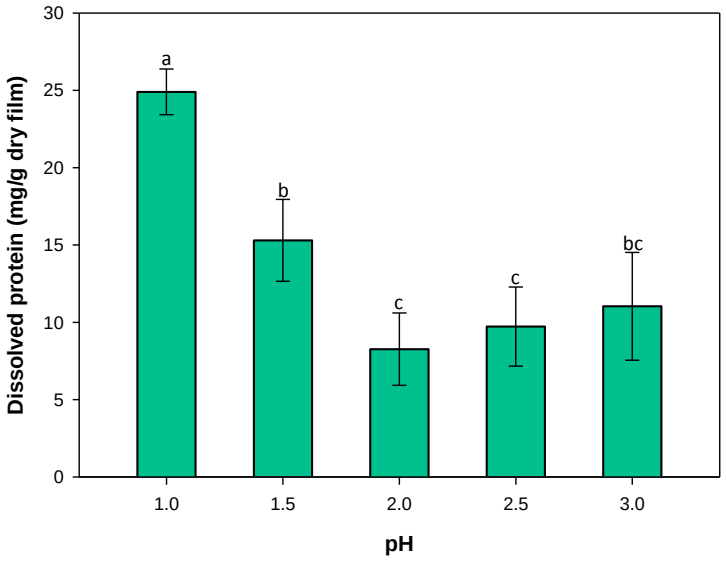

Figure 1.2. Effect of the pH of the film-forming solution on the protein solubility of water-resistant films made with 5% of cinnamaldehyde after 24 h of immersion in phosphate buffer at pH 7 and 25 °C. Different letters indicate significant differences between means ($p \leq 0.05$) according to the Tukey test.

The effect of the reaction medium pH on the color of the films measured by the L*C*h° parameters is shown in **Figure1.3** where it can be observed that the color depends on the pH of the film-forming solution. Untreated gliadin films cast at pH 6 presented a pale yellow color whereas cinnamaldehyde-treated films cast in the pH 2 to 6 range presented a yellow-green color, with hue angles falling in the second quadrant (-a, +b), at around 105°. Gliadin films prepared at pH 6 without cinnamaldehyde presented the lowest chroma. The addition of cinnamaldehyde to gliadins cast at pHs of between 2 and 3 gave rise to films with similar chromaticity, and at higher pHs the intensity of the films' color increased gradually with the pH, which could indicate the appearance of conjugated double bonds which account for color. The low pH films (1, 1.5) developed chroma values similar to those made at pH 5 and pH 4 respectively but presented lower hue values than the films with higher pH values. In general, all the films were very transparent as shown by their high L* values (around 87).

The only significant difference ($p \leq 0.05$) was found in those films modified with cinnamaldehyde at pH 6, which exhibited slightly lower luminosity.

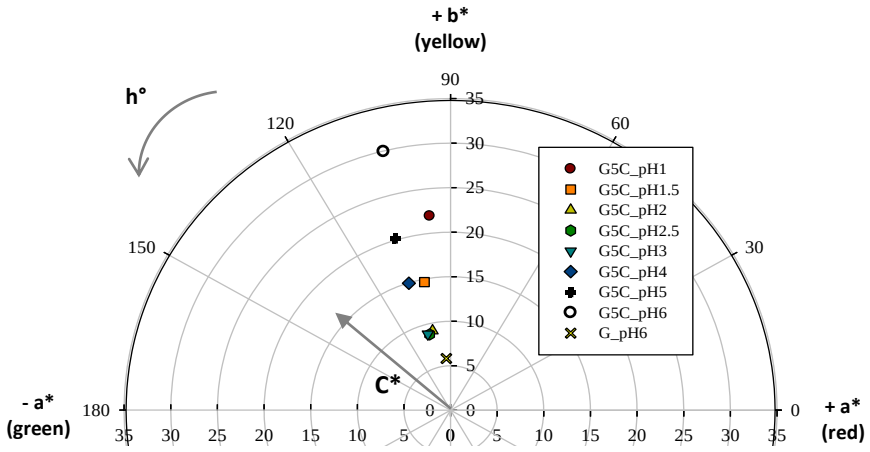

Figure1.3. Effect of the pH of the film-forming solution on the L*C*h° coordinates of films made with 5% cinnamaldehyde and a control film (G_pH6).

Following these results, the film-forming solution was adjusted to pH 2 before studying the cross-linking effect of cinnamaldehyde on the functional properties of gliadin films. The effect of cinnamaldehyde was studied at concentrations of 1.5, 3 and 5% (G1.5C_pH2, G3C_pH2, G5C_pH2). Two control films were prepared: gliadin films at pH 6 (G_pH6), and gliadin films at pH 2 (G_pH2).

1.3.2. Film color

The L*, C* and h° parameters of gliadin films modified with cinnamaldehyde at pH 2 and of the control films cast at pH 2 and 6 are shown in Table 1.1. The films made from untreated gliadins at pH 2 and 6 were very transparent, as indicated by their high L* values, and presented a slight yellowish color. The transparency of the films was not significantly altered by treatment with different amounts of cinnamaldehyde. Compared with the controls, the cinnamaldehyde-treated films all developed a similar yellow-green color, and their chromaticity increased with the amount of cinnamaldehyde incorporated.

Table 1.1. Color coordinates L*C*h° of gliadin films.

Sample	L*	C*	h°
G_pH6	87.6 ± 0.3 [a]	5.82 ± 0.58 [a]	94.4 ± 0.4 [a]
G_pH2	88.8 ± 0.9 [a]	5.23 ± 0.76 [a]	94.4 ± 1.0 [a]
G1.5C_pH2	88.0 ± 0.5 [a]	6.24 ± 0.58 [a]	100.5 ± 0.6 [b]
G3C_pH2	87.8 ± 0.5 [a]	7.31 ± 0.61 b	101.5 ± 0.4 c
G5C_pH2	87.9 ± 0.2 [a]	9.12 ± 0.17 c	102.2 ± 0.2 d

Reported values are means of three different films and eight replicates in each film ± standard deviation. Any two means in the same column followed by a different letter are significantly different ($p \leq 0.05$) according to the Tukey test.

1.3.3. Mechanical properties

The stress-strain ($\sigma - \varepsilon$) curves of the control and cinnamaldehyde-treated gliadin films are depicted in **Figure 1.4A** and **1.4B**, which correspond to measurements taken at 50% and 75% RH respectively. As can be observed in **Figure 1.4A**, the control films cast at pH 2 (G_pH2) and pH 6 (G_pH6) presented low σ_m and high ε_b which is in accordance with the viscous nature of gliadins (Shewry et al., 1986). The rupture of interpeptidic non-covalent interactions (hydrophobic interactions and hydrogen bonding) due to equibiaxial extension and the formation of new associations allows considerable deformation to occur (Song and Zheng, 2008). Chemical treatment with cinnamaldehyde at pH 2 modified the typically viscous behavior of the gliadin films, giving rise to a different mechanical profile. The stiffness of the films increased, and they presented a greater elastic component. The σ_m of modified gliadin films gradually increased with the amount of cinnamaldehyde incorporated into the film-forming solution, indicating the formation of a cross-linked protein network. Strain hardening was observed after the plateau zone which follows the elastic region. In polymers, strain hardening is due to the straightening of polymer segments between entanglements: the progressive orientation of polymer chains under equibiaxial extension in the direction of flow entails a continued increase of the tensile strength (Song and Zheng, 2008). The new anchor points created in the cross-linked gliadin films produced this phenomenon during the stretching process.

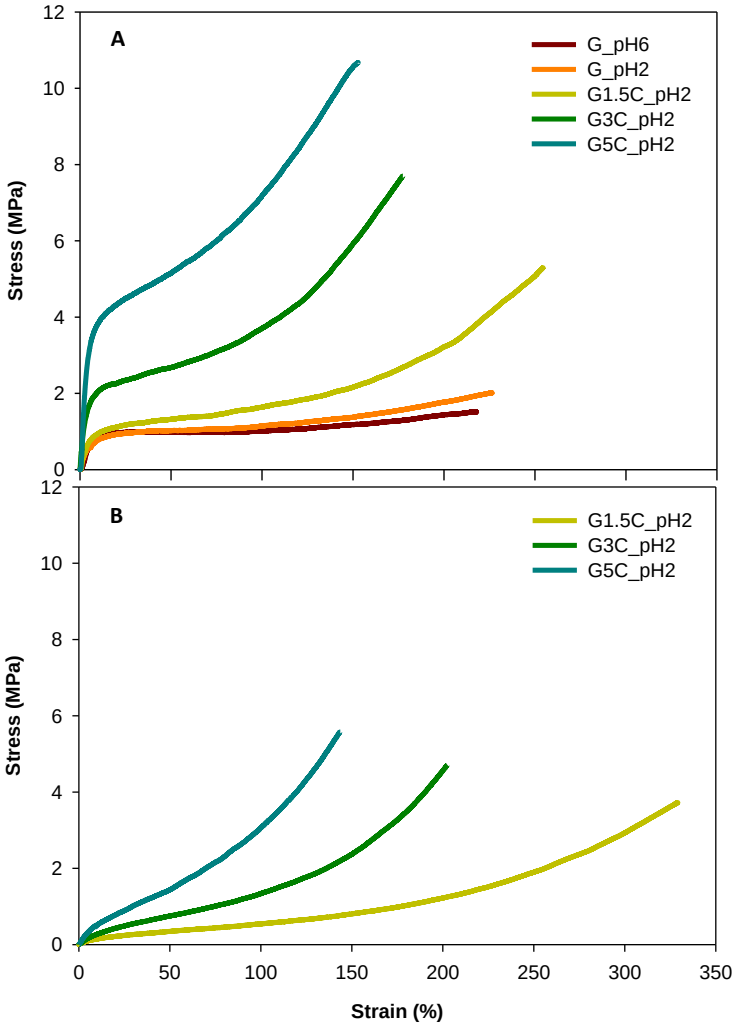

Figure 1.4. Stress-strain curves of gliadin films at 50% RH **(A)** and 75% RH **(B)**.

The mechanical properties of non-cross-linked films at 75% RH could not be measured due to the high moisture sensitivity of the gliadin control films. The addition of water generated a high level of plasticity in the polymeric matrix that hindered their manipulation. In **Figure 1.4B** the mechanical profiles of cross-linked films conditioned at 75% RH can be observed. The great plasticization of films caused by environmental humidity reduces the intermolecular forces between the polypeptide chains because of the disruption of the hydrogen bonding, which increases the chain segmental mobility and the free volume of the

network (Lefèvre et al., 2005; Lieberman and Gilbert, 1973). Consequently, the films become weaker and more extensible (Gennadios et al., 1993).

The mechanical parameters (σ_m, *E*, and ε_b) of the control and treated films conditioned at 50% and 75% RH are shown in Table 1.2. The gliadin control films conditioned at 50% RH all presented similar values for these mechanical parameters. The incorporation of cinnamaldehyde into the film-forming solution at pH 2 gave rise to a considerable increase in the σ_m and the *E*, and a decrease in the ε_b of gliadin films. The σ_m and elasticity of the films increased with the percentage of cinnamaldehyde, suggesting a greater degree of cross-linking in the protein matrix. Thus, both the σ_m and the *E* of the gliadin films made with 5% cinnamaldehyde and conditioned at 50% RH increased 6-fold compared to the control films while the ε_b only decreased 1.5-fold, and the film continued to exhibit good elongation properties. The σ_m values for the cross-linked gliadin films with 3% (7.7 ± 0.8 MPa) and 5% (9.9 ± 1.2 MPa) cinnamaldehyde were higher than those obtained for cross-linked gliadin films with 40% epichlorohydrin (6.5 ± 0.6 MPa) (Song et al., 2009), or 4% formaldehyde, glutaraldehyde or glyoxal (6.5 ± 0.7 MPa, 2.8 ± 0.8 MPa, and 2.1 ± 0.2 MPa respectively) (Hernandez-Munoz et al., 2005). The cross-linked films conditioned at 75% RH followed a similar pattern regarding σ_m and *E* parameters, but the great plasticization effect caused by water brought about a 2-fold reduction in the σ_m of these films with respect to those conditioned at 50% RH, and the *E* decreased dramatically, around 16-fold, compared to the cross-linked films conditioned at 50% RH. Although the ε_b of the cross-linked films conditioned at 75% RH could be expected to be higher than that of the films conditioned at 50% RH, this increase was only observed for the films treated with 1.5% cinnamaldehyde whereas the ε_b of the films with higher levels of cinnamaldehyde was similar to the level of those conditioned at 50% RH.

Table 1.2. Mechanical properties of films tested at 50% and 75% RH.

Sample	σ_m (MPa)		ε_b (%)		*E* (MPa)	
	50% HR	75% HR	50% HR	75% HR	50% HR	75% HR
G_pH6	1.60 ± 0.24 ^{a}	-	226 ± 32 ^{cd}	-	24.3 ± 4.9 ^{ab}	-
G_pH2	1.63 ± 0.39 ^{a}	-	212 ± 30 ^{bcd}	-	19.3 ± 7.7 ^{a}	-
G1.5C_pH2	5.23 ± 0.83 ^{b}	3.55 ± 0.42^{a}	248 ± 14 ^{d}	319 ± 15 ^{c}	34.9 ± 6.5 ^{b}	2.10 ± 0.74 ^{a}
G3C_pH2	7.74 ± 0.83 ^{c}	4.63 ± 0.59 ^{b}	180 ± 8 ^{ab}	197 ± 11 ^{b}	63.9 ± 21.7 ^{c}	4.67 ± 0.83 ^{b}
G5C_pH2	9.93 ± 1.21 ^{d}	5.11 ± 0.90 ^{c}	146 ± 12 ^{a}	144 ± 10 ^{a}	112.1 ± 10.9 ^{d}	6.73 ± 1.41 ^{c}

σ_m: Maximum tensile strength, ε_b: Elongation at break, E: Young's modulus.

Reported values are means of 10 replicates ± standard deviation. Any two means in the same column followed by a different letter are significantly different ($p \leq 0.05$) according to the Tukey test.

1.3.4. Weight loss

The control films (G_pH2, G_pH6) could not be recovered after immersion in an aqueous medium because they lost their integrity. The lack of intermolecular covalent bonds between the polypeptide chains in the film matrix was responsible for the films' low water resistance (Hernandez-Munoz et al., 2003) in spite of the low solubility of gliadin proteins in water. Nevertheless, due to the high content of non-polar amino acids and the low content of polar ionizable amino acids present in gliadins (Cornell and Hoveling, 1998), the films did not dissolve. The films made from the gliadin solution with cinnamaldehyde at pH 2 (G1.5C_pH2, G3C_pH2 and G5C_pH2) maintained their integrity after 24 h of immersion in water.

Table 1.3 shows the weight loss of the different films in a buffer medium at pH 7 and in the same medium with 2% 2-ME. In the buffer, the loss of weight of the gliadin films treated with different amounts of cinnamaldehyde was around 20%, without any significant differences being found between them ($p > 0.05$). Adding 2-ME to the buffer did not change this pattern, which suggests that the possible formation of disulfide bonds during the drying process does not play a major role in the water resistance of films. The loss of weight of the films was mainly due to the diffusion of hydrophilic glycerol into the aqueous medium and, to a lower extent, the loss of polypeptide chains from the reticulated matrix. The loss of glycerol was confirmed not only by the lack of flexibility of the films after drying but also by glycerol accounting for 20% of the dry weight of the film (20 g of glycerol/100 g of dry film).

Table 1.3. Weight loss (%) after 24 h immersion at 25 °C in phosphate buffer at pH 7 and phosphate buffer containing 2% 2-ME.

Sample	Weight Loss (%)	
	Phosphate Buffer pH 7	Phosphate Buffer pH 7 + 2% 2-ME
G1.5C_pH2	21.43 ± 0.68	20.53 ± 1.38
G3C_pH2	21.08 ± 0.43	19.88 ± 1.22
G5C_pH2	20.10 ± 1.63	20.23 ± 0.75

Reported values are means of triplicates of three different films ± standard deviation. No significant differences between means ($p > 0.05$) in the same column were found by the Tukey test.

1.3.5. Modulated differential scanning calorimetry (MDSC)

Polymer processing can result in internal molecular stresses which are relieved on reheating. The release of these stresses appears as a small endothermic relaxation peak, which can even occur after the glass transition. The close proximity of the endotherm to the glass

transition can prevent the correct evaluation of T_g. In standard DSC, thermal history effects can be eliminated by heating the material once above the T_g, slowly cooling it before evaluation, and then heating it a second time to measure the T_g value. Nevertheless, this type of pretreatment could induce changes such as curing or cross-linking that would alter the results. MDSC, however, separates the thermodynamic and kinetic contributions in a single scan (Gill et al., 1993).

Gliadin proteins are amorphous biopolymers capable of undergoing a glass transition from a glassy to a rubbery state. Apart from their chemical structure and the presence of added plasticizers, the T_g of polymers is governed by other structural features such as molecular weight, chain branching, crystallinity and the extent of cross-linking. For this test, the films were made without glycerol since the aim of the thermal analysis was to observe whether cross-linking imparts some modification to the T_g of proteins cast into films without any additional effects of glycerol or water. As can be seen in **Table 1.4**, the T_g of the pH 6 gliadin control film (G_pH6) had a value of 164 ± 3 °C, in agreement with those obtained by several authors (Ferrari and Johari, 1997; Micard and Guilbert, 2000). For the film cast at a lower pH (G_pH2), the T_g decreased significantly ($p \leq 0.05$). This change in the T_g of the protein could be related to denaturation. At pHs far from the isoelectric point, for example 8.1 for gliadins (Wu and Dimler, 1963), side-chain repulsion of induced net charges leads to conformational changes in the structure due to possible unfolding, rupture of hydrogen bonds and alteration of hydrophobic interactions (Chourpa et al., 2006; Sun et al., 2008), facilitating chain mobility and prompting a lower T_g. Modification of gliadins with cinnamaldehyde at pH 2 produced the expected increase in T_g as the concentration of cinnamaldehyde increased, which can be explained by a restriction of polymer chain mobility due to increases in both the cross-linking density and the molecular weight of the polymer.

Table 1.4. Thermal properties. Glass transition temperature (T_g) obtained by DSC and peak decomposition temperature obtained by TGA.

Sample	T_g (°C)	Decomposition T (°C)
G_pH6	164.0 ± 3.0 ^{ab}	323.0 ± 0.5 ^{c}
G_pH2	158.4 ± 2.4 ^{a}	302.1 ± 2.0 ^{a}
G1.5C_pH2	164.2 ± 0.2 ^{ab}	306.7 ± 0.5 ^{ab}
G3C_pH2	168.7 ± 1.5 ^{bc}	309.4 ± 5.8 ^{ab}
G5C_pH2	172.9 ± 0.1 ^{c}	313.7 ± 3.1 ^{b}
cinnamaldehyde	-	211.6 ± 0.2

Reported values are means of three replicates ± standard deviation. Any two means in the same column followed by a different letter are significantly different ($p \leq 0.05$) according to the Tukey test.

1.3.6. Thermogravimetric Analysis (TGA)

All the samples showed a one-step decomposition profile with a single transition temperature, as demonstrated by TGA (**Figure 1.5A**) and the derivative plots (DTGA) (**Figure 1.5B**). The degradation onset temperatures were very similar in all the films, starting at approximately 245 °C, and resulted in a char residue of approximately 20%. **Table 1.1** shows the peak decomposition temperatures of the gliadin films and of cinnamaldehyde. The G_pH6 control film showed a peak decomposition temperature of 323 ± 0.5 °C, slightly lower than that found by Song et al. (Song et al., 2009) for films with 20% glycerol (331 °C). The peak decomposition temperature (302 ± 2 °C) of the control film cast at pH 2, G_pH2, was significantly lower ($p \leq 0.05$), showing that it possessed lower thermal stability than the films made at pH 6. This may be attributed to protein denaturation at low pH. Compared with G_pH2, the incorporation of cinnamaldehyde at pH 2 led to increases in the degradation temperature of these films in proportion to the amount of cross-linker added. The peak decomposition temperature of cinnamaldehyde is 212 ± 0.2 °C, with a sharp drop in its decomposition profile. **Figure 1.5B1** shows a detail of the DTGA of the cross-linked films. A slight slope can be detected in the region of cinnamaldehyde decomposition as a function of cinnamaldehyde content. This small loss of weight could be attributed to the free cinnamaldehyde which does not participate in the formation of the cross-linked matrix.

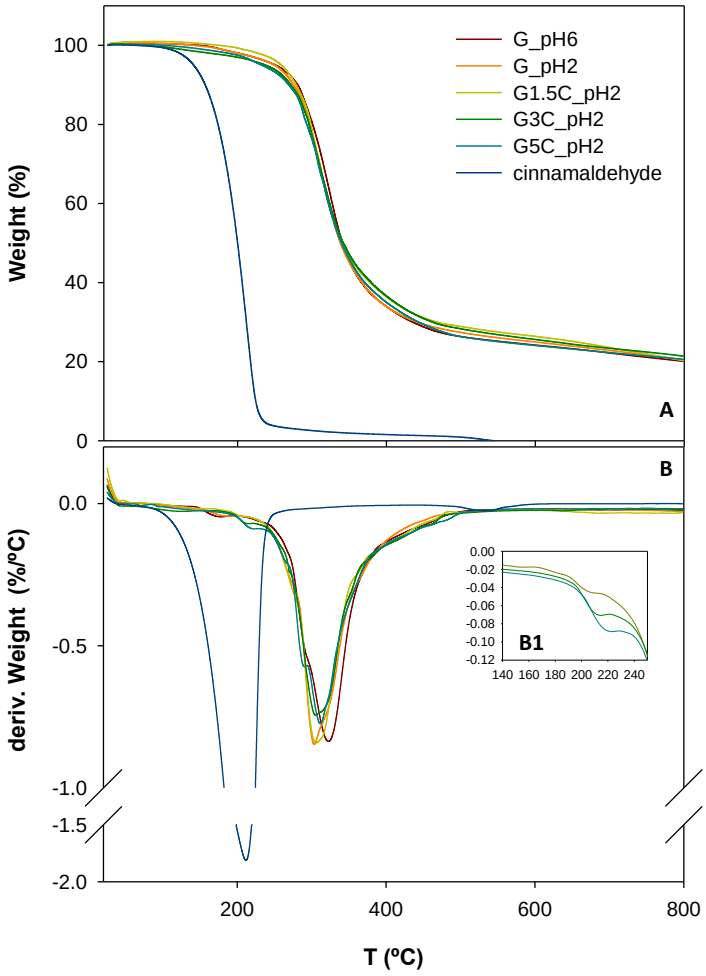

Figure 1.5. (A) Thermogravimetric (TGA), and **(B)** derivative thermogravimetric (DTGA) profiles of gliadin films and cinnamaldehyde. **(B1)** DTGA detail of the region of cinnamaldehyde degradation, cross-linked films only.

1.3.7. Morphology

Figure 1.6 shows SEM images of cryofractured cross sections of the G_pH6 control film and the film treated with 5% cinnamaldehyde at a low pH (G5C_pH2). This type of fracturing process allows soft materials to be cut without surface deformation, providing useful information on the structure of the polymer, the formation of different phases and the distribution of the added component. The control films presented a smooth surface with a

nonporous structure, and no phase separation was appreciated. No differences were observed compared to the films formed when cinnamaldehyde was added to the film-forming solution at pH 2, indicating great miscibility of cinnamaldehyde with gliadins.

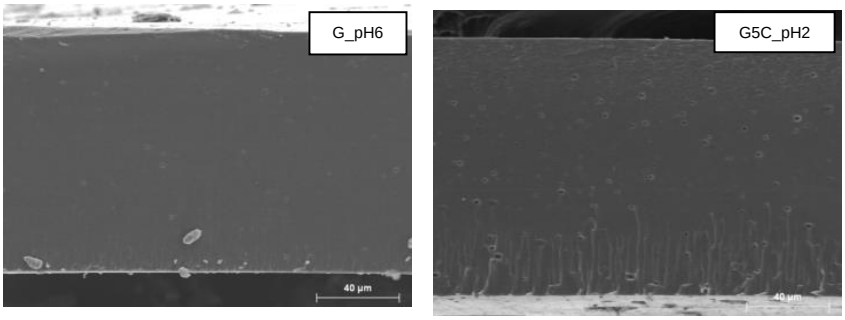

Figure 1.6. SEM micrograph of the cryofractured cross-section of films G_pH6 and G5C_pH2 (magnification × 600).

1.4. CONCLUSION

The present work has proved the suitability of cinnamaldehyde as a natural cross-linker for gliadin films, presumably due to the formation of intermolecular covalent bonds among polypeptide chains that polymerize the "monomeric" gliadins and reticulate the protein matrix. The cross-linking capacity of cinnamaldehyde has been found to be dependent on the pH of the reaction medium, with pH 2 being the optimum. The cross-linking effect, which was proportional in its intensity to the amount of cinnamaldehyde added, was evidenced by a great improvement in the mechanical strength of the films without impairment of their elongation properties; complete resistance after water immersion with negligible loss of weight attributable to protein; and an increase in the T_g compared to the control films. The use of a natural compound such as cinnamaldehyde is a valuable alternative to toxic cross-linking agents for improving the physical performance of renewable films made from gliadins and so extending their use in food packaging applications, as well as in other areas of interest such as agrochemistry, pharmacy, cosmetics, etc.

1.5. REFERENCES

ASTM. 2009. D882. Standard test method for tensile properties of thin plastic sheeting.

Burt, S. 2004. Essential oils: Their antibacterial properties and potential applications in foods - a review. *International Journal of Food Microbiology, 94*(3), 223-253.

Cornell, H. J., and Hoveling, A. W., 1998. *Wheat: Chemistry and utilization*. Technomic Publishing Company, Inc: Lancaster, PA, USA.

Chourpa, I., Ducel, V., Richard, J., Dubois, P., and Boury, F. 2006. Conformational modifications of alpha gliadin and globulin proteins upon complex coacervates formation with gum arabic as studied by raman microspectroscopy. *Biomacromolecules, 7*(9), 2616-2623.

Ferrari, C., and Johari, G. P. 1997. Thermodynamic behaviour of gliadins mixture and the glass-softening transition of its dried state. *International Journal of Biological Macromolecules, 21*(3), 231-241.

Gennadios, A., Brandenburg, A. H., Weller, C. L., and Testin, R. F. 1993. Effect of pH on properties of wheat gluten and soy protein isolate films. *Journal of Agricultural and Food Chemistry, 41*(11), 1835-1839.

Gennadios, A., McHugh, T. H., Weller, C. L., and Krochta, J. M. 1994. Edible coatings and films based on proteins. In *Edible Coatings and Films to Improve Food Quality*, J.M. Krochta, E.A. Baldwin, and M.O. Nisperos-Carriedo, Eds. CRC Press: Boca Raton, 201-277.

Gill, P. S., Sauerbrunn, S. R., and Reading, M. 1993. Modulated differential scanning calorimetry. *Journal of Thermal Analysis, 40*(3), 931-939.

Guilbert, S., and Gontard, N. 2005. Agro-polymers for edible and biodegradable films: Review of agricultural polymeric materials, physical and mechanical characteristics. In *Innovations in Food Packaging*, J.H. Han, Ed. Elsevier: London.

Hernandez-Munoz, P., and Hernandez, R. J. 2001. *Glutenin and gliadin films from wheat gluten: Preparation and properties.* Paper presented at the IFT Annual Meeting, New Orleans, Louisiana.

Hernandez-Munoz, P., Kanavouras, A., Lagaron, J. M., and Gavara, R. 2005. Development and characterization of films based on chemically cross-linked gliadins. *Journal of Agricultural and Food Chemistry, 53*(21), 8216-8223.

Hernandez-Munoz, P., Kanavouras, A., Ng, P. K. W., and Gavara, R. 2003. Development and characterization of biodegradable films made from wheat gluten protein fractions. *Journal of Agricultural and Food Chemistry, 51*(26), 7647-7654.

Hernandez-Munoz, P., Kanavouras, A., Villalobos, R., and Chiralt, A. 2004a. Characterization of biodegradable films obtained from cysteine-mediated polymerized gliadins. *Journal of Agricultural and Food Chemistry, 52*(26), 7897-7904.

Hernandez-Munoz, P., Lagaron, J. M., Lopez-Rubio, A., and Gavara, R. 2004b. Gliadins polymerized with cysteine: Effects on the physical and water barrier properties of derived films. *Biomacromolecules, 5*(4), 1503-1510.

Hernandez-Munoz, P., Lopez-Rubio, A., Lagaron, J. M., and Gavara, R. 2004c. Formaldehyde cross-linking of gliadin films: Effects on mechanical and water barrier properties. *Biomacromolecules, 5*(2), 415-421.

Hernandez-Munoz, P., Villalobos, R., Cerisuelo, J. P., Balaguer, M. P., and Gavara, R. (2009). *Physical performance improvement of wheat prolamin films by modification with chitosan.* Paper presented at the BIOPOL, Alicante.

Hernandez-Munoz, P., Villalobos, R., and Chiralt, A. 2004d. Effect of thermal treatments on functional properties of edible films made from wheat gluten fractions. *Food Hydrocolloids, 18*(4), 647-654.

Lefèvre, T., Subirade, M., and Pézolet, M. 2005. Molecular description of the formation and structure of plasticized globular protein films. *Biomacromolecules, 6*(6), 3209-3219.

Lieberman, E. R., and Gilbert, S. G. 1973. Gas permeation of collagen films as affected by cross-linkage, moisture, and plasticizer content. *Journal of Polymer Science: Polymer Symposia, 41*(1), 33-43.

Micard, V., and Guilbert, S. 2000. Thermal behavior of native and hydrophobized wheat gluten, gliadin and glutenin-rich fractions by modulated DSC. *International Journal of Biological Macromolecules, 27*(3), 229-236.

Shewry, P. R., Tatham, A. S., Forde, J., Kreis, M., and Miflin, B. J. 1986. The classsification and nomenclature of wheat gluten proteins - a reassessment. *Journal of Cereal Science, 4*(2), 97-106.

Smith, P. K., Krohn, R. I., Hermanson, G. T., Mallia, A. K., Gartner, F. H., Provenzano, M. D., Fujimoto, E. K., Goeke, N. M., Olson, B. J., and Klenk, D. C. 1985. Measurement of protein using bicinchoninic acid. *Analytical Biochemistry, 150*(1), 76-85.

Soares, R. M. D., Maia, G. S., Rayas-Duarte, P., and Soldi, V. 2009. Properties of filmogenic solutions of gliadin crosslinked with 1-(3-dimethyl aminopropyl)-3-ethylcarbodiimidehydrochloride/N-hydroxysuccinimide and cysteine. *Food Hydrocolloids, 23*(1), 181-187.

Song, Y., and Zheng, Q. 2008. Influence of gliadin removal on strain hardening of hydrated wheat gluten during equibiaxial extensional deformation. *Journal of Cereal Science, 48*(1), 58-67.

Song, Y. H., Li, L. F., and Zheng, Q. 2009. Influence of epichlorohydrin modification on structure and properties of wheat gliadin films. *Journal of Agricultural and Food Chemistry, 57*(6), 2295-2301.

Sun, S., Song, Y., and Zheng, Q. 2008. Ph-induced rheological changes for semi-dilute solutions of wheat gliadins. *Food Hydrocolloids, 22*(6), 1090-1096.

Weibel, H., and Hansen, J. 1989. Interaction of cinnamaldehyde (a sensitizer in fragance) with protein. *Contact Dermatitis, 20*(3), 161-166.

Wu, Y. V., and Dimler, R. J. 1963. Hydrogen ion equilibria of wheat glutenin and gliadin. *Archives of Biochemistry and Biophysics, 103*(3), 310-318.

CHAPTER 2

BIOCHEMICAL PROPERTIES OF BIOPLASTICS MADE FROM WHEAT GLIADINS CROSS-LINKED WITH CINNAMALDEHYDE

Balaguer, M.P.; Gómez-Estaca, J.; Gavara, R.; and Hernandez-Munoz, P.

Journal of Agricultural and Food Chemistry, 2011, 59(24), 13212-13220

The aim of this work has been to study the modification of gliadin films with cinnamaldehyde as a potential cross-linker agent. The molecular weight profile and cross-linking density showed that cinnamaldehyde increased reticulation in the resulting films. The participation of free amino groups of the protein in the new entanglements created could be a possible mechanism of connection between the polypeptidic chains. The combination of a Schiff base and a Michael addition is a feasible approach to understanding this mechanism. The protein solubility in different media pointed to lower participation by both non-covalent and disulfide bonds in stabilizing the structure of the cross-linked films. The new covalent bonds formed by the cinnamaldehyde treatment hampered water absorption and weight loss, leading to more water-resistant matrices which had not disintegrated after 5 months. The properties of this novel bioplastic could be modified to suit the intended application by using cinnamaldehyde, a naturally occurring compound.

2.1. INTRODUCTION

There is increasing interest in the search for new added-value uses of cereal by-products from the food industry. Most of these by-products consist of agro-polymers such as polysaccharides (cellulose, starch, arabinoxylans) (Guilbert and Gontard, 2005) or proteins (zein, gluten) (Cuq et al., 1998) with potential applications in the design of bioplastics. In addition, these materials are renewable and hence contribute to environmental sustainability. Wheat gluten proteins are a by-product of the extraction of starch from wheat flour. Gluten is commonly used in bakery products and other foods as an ingredient that provides functional properties. Wheat gluten consists of a mixture of proteins that can be classified into monomeric gliadins, which confer gluten its viscous character, and polymeric glutenins, which are responsible for its elasticity. Gliadins consist of a heterogeneous group of single polypeptide chains with molecular weights (MW) of between 30 and 50 kDa, which associate via hydrogen bonding and hydrophobic interactions (Cornell and Hoveling, 1998). Glutenins comprise unassociated fractions with MW of 15 to 150 kDa and fractions linked via interchain disulfide bonds with MW ranging from 150 to several million kDa (Cornell and Hoveling, 1998). Low-quality gluten, which is unsuitable for flour improvement in bread-making, can be used for preparing plastic films (Mangavel et al., 2002), since it presents attractive properties such as viscoelasticity, adhesiveness, thermoplasticity and good film-forming behavior. However, gluten presents poor solubility in water and the glutenins hinder its processability, since they tend to aggregate upon shearing and heating. From this point of view, gliadins have a lower MW and are highly soluble and highly stable in ethanol solutions for long periods of time. Nonetheless, some functional aspects of gliadin-derived films such as their mechanical, water-barrier and water-resistance properties need to be improved.

Chemical cross-linking provides a mechanism for enhancing the performance of the biopolymers currently being investigated. The most commonly-used general cross-linking reagents are symmetrical bifunctional compounds with reactive groups that may possess chemical specificity for a particular class of functional group on the macromolecules (Peters and Richards, 1977). The cross-linkers generally used for proteins include aldehydes such as formaldehyde, glutaraldehyde and glyoxal (Galietta et al., 1998; Hernandez-Munoz et al., 2005; Marquie, 2001), diisocyanates and carbodiimides (Tropini et al., 2004; Tropini et al., 2000), epoxy compounds (Song et al., 2009; van Wachem et al., 1999), sulfhydryl reagents

such as cysteine (Soares et al., 2009), etc. Nowadays, much less toxic cross-linking agents are being explored, especially when films are intended for food applications: those being investigated include genipin (Bispo et al., 2010; Butler et al., 2003; Sung et al., 1999), proanthocyanidin (Kim et al., 2005), carboxylic acids such as citric or malic acid (Reddy et al., 2009), and ferulic and tannic acid (Cao et al., 2007; Zhang et al., 2010).

Cinnamaldehyde is a naturally occurring aromatic α,β-unsaturated aldehyde derived from cinnamon. Recently, it has been used as an antimicrobial/antifungal agent in active packaging applications (Becerril et al., 2007; Ben Arfa et al., 2007; Rodriguez et al., 2008). Due to its chemical structure (the molecule consists of a phenyl group attached to an unsaturated aldehyde) it can also act as a cross-linking agent for proteins. A previous work demonstrated the suitability of cinnamaldehyde as a natural cross-linker for gliadin films, an effect that was assumed to be attributable to the formation of intermolecular covalent bonds between polypeptide chains, which polymerizes the 'monomeric' gliadins and reticulates the protein matrix (Balaguer et al., 2011). Cinnamaldehyde can be viewed as a derivative of acrolein or crotonaldehyde, whose mechanism of reaction with proteins has been completely elucidated (Monsan et al., 1976; Peters and Richards, 1977). However, it is uncertain which proteins or other macromolecules react with cinnamaldehyde, and among those that do, which groups have the greatest potential to react (Weibel and Hansen, 1989). Majeti and Suskind found that cinnamaldehyde reacts with amino groups on protein side chains, giving rise to the corresponding Schiff base derivatives (Majeti and Suskind, 1977; Suskind and Majeti, 1976). Weibel and Hansen (1989) claimed that thiol groups in cysteine residues were the most common binding sites on bovine serum albumin. Dupuis and Benezra (1982) suggested that a conjugate is formed by a Michael addition (1.4-addition) of cinnamaldehyde to the free amino groups in lysine residues. It is also well known that phenols condense readily with aldehydes at their ortho- and para-positions, forming resinous materials (Akabori and Ohno, 1950; Zigon et al., 1987). This kind of reaction could also take place between tyrosine residues and cinnamaldehyde. Another possible cross-linking reaction is believed to occur at acidic pH levels, below pH 2 to 3, since some methylene cross-linking may occur between pairs of amide groups, leading to a doubling of the molecular weight in gliadins (Fraenkel-Conrat and Mecham, 1949).

The main objective of the present work was to investigate the nature of the chemical modification of wheat gliadins by cinnamaldehyde. A further objective was to study the long term stability in water of the cross-linked films, as well as their enzymatic degradation

kinetics under simulated gastric or intestinal conditions, as a function of the degree of cross-linking.

2.2. MATERIALS AND METHODS

2.2.1. Reagents

Crude wheat gluten (≥ 80% protein), glycerol, ethanol, hydrochloric acid, and cinnamaldehyde, all laboratory grade, were supplied by Sigma (Madrid, Spain).

2.2.2. Gliadin-rich fraction extraction from wheat gluten

The gliadin-rich fraction was extracted from the wheat gluten according to the method described by Hernandez-Munoz and Hernandez (2001). Briefly, 100 g of wheat gluten were dispersed in 400 mL of 70% (v/v) ethanol/water mixture, stirred overnight at room temperature, and centrifuged at 5000 rpm for 20 min at 20 °C. The supernatant containing the gliadin-rich fraction was collected and used as the film-forming solution.

2.2.3. Chemical modification of gliadins

In preliminary studies (Balaguer et al., 2011), the use of cinnamaldehyde as a protein cross-linker was found to be strongly dependent on the pH. Initially, the pH of the gliadin film forming solution was brought to 2 with HCl as the most suitable for polymerization. Then, chemical modification of gliadins was conducted by adding different cinnamaldehyde concentrations to the film-forming solution, namely 1.5% (G1.5C_pH2), 3% (G3C_pH2) and 5% (G5C_pH2) (g cinnamaldehyde/100 g protein), and incubation at 23 °C for 30 minutes under gentle stirring. Glycerol was added as plasticizer to the film-forming solution at 25% (g glycerol/100 g protein) and stirred for 15 minutes. Control samples were prepared at the original pH 6 of the gliadin solution (G_pH6), at pH 2, the level at which chemical modification occurs (G_pH2), and in some cases at pH 6 with 5% of cinnamaldehyde (G5C_pH6).

2.2.4. Film formation and conditioning

Measured volumes of the film-forming solution were poured onto a horizontal flat Pyrex tray to allow water and ethanol to evaporate. The films were dried at 37 °C for 24 h. The dried films were peeled off the casting surface and preconditioned in a chamber at 23 °C and the desired relative humidity (RH) for at least 1 week prior to testing. The film thickness was measured using a micrometer (Mitutoyo, Kanagawa, Japan) with a sensitivity of ± 2.54 μm. The mean thickness was calculated from measurements taken at ten different locations on each film sample.

2.2.5. Sodium Dodecyl Sulfate - Polyacrylamide Gel Electrophoresis (SDS-PAGE)

The molecular weight distributions of the proteins in the gliadin films with and without cinnamaldehyde treatment were analyzed by SDS-PAGE performed in a vertical electrophoresis unit (Bio-Rad Laboratories, Hercules, CA, USA). The procedure employed was that of Laemmli (1970) with some minor modifications. The samples were first denatured by treating 50 μg of ground film with 1 mL of denaturing buffer (2.5% SDS, 10 mM Tris-HCl, 1 mM EDTA, 6% glycerol, 0.01% bromophenol blue, with or without 5% β-mercaptoethanol). Each sample-buffer mixture was allowed to stand at room temperature for 2 h with occasional shaking and centrifuged at 13 000 g for 10 min. A 15 μL quantity of the clear top layer of each sample was then loaded into each slot in the gel. The stacking gel was 4% acrylamide and the resolving gel 12% acrylamide. Electrophoresis was carried out at 25 mA/gel for 1.5 h and the gels were stained with Coomassie brilliant blue R-250. The molecular weight composition of the standard protein mixture (Bio-Rad Laboratories, Hercules, CA, USA) run for comparison was 199 kDa (myosin), 116 kDa (β-galactosidase), 97 kDa (bovine serum albumin), 53 kDa (ovalbumin), 37 kDa (carbonic anhydrase), 29 kDa (soybean trypsin inhibitor), 20 kDa (lysozyme) and 7 kDa (aprotinin).

2.2.6. Cross-link density (CLD)

The concentration of elastically effective chains (υ_e), known as the cross-link density (CLD), was assessed from the stress-strain curves. The following relationship (Sekkar et al., 2007) exists between Young's modulus (*E*), determined from the initial slope of the stress-strain curves, and CLD:

$$E = 3\upsilon_e RT \qquad (\mathbf{2.1})$$

where R is the universal gas constant (8.314 J/(mol·K)) and T the absolute temperature (K).

A Mecmesin MultiTest 1-í universal test machine (Landes Poli Ibérica, S.L, Barcelona, Spain) equipped with a 100 N static load cell was used to evaluate the Young's modulus (*E*) of the films according to ASTM D882 (2009). The films were conditioned at 50% RH for one week before testing. Sample films were cut into 2.54 cm wide strips at least 10 cm long. The grip separation was set at 5 cm and the cross-head speed at 25 mm·min^{-1}. At least 10 replicates from each sample were tested.

2.2.7. Amino acid Analysis

A 10 mg/mL quantity of dry film was dissolved in HCl, and the samples (20 µL) were dried and hydrolyzed in vacuum-sealed glass tubes at 110 °C for 24 h in the presence of continuously boiling 5.7 N HCl containing 0.1% phenol with norleucine as the internal standard. After hydrolysis, the samples were vacuum-dried, dissolved in the application buffer, and injected onto a Biochrom 30 (Biochrom Ltd., Cambridge, UK) analyzer which employs a method based on ion exchange chromatography with post column derivatization with ninhydrin (Pharmacia, Barcelona, Spain).

2.2.8. Determination of the free amino group content

The primary amino group content of cross-linked and non-cross-linked gliadin films was determined using 2,4,6-trinitrobenzenesulfonic acid (TNBS) (Adler-Nissen, 1979; Habeeb, 1966), adapting the method as described by Tropini et al. (2000) for low water soluble proteins. To a film sample of approximately 10 mg, 1 mL of phosphate buffer (0.2 M, pH 8.5) and 1 mL of a freshly prepared TNBS solution (0.5% (w/v)) were added. After keeping this mixture for 4 h at 50°in the dark, 8 mL of 50% sulfuric acid was added. This mixture was vigorously shaken at room temperature in the dark for 1 h and left to stand at 50 °C for 30 min to obtain a clear solution. An aliquot of 1 mL of the solution was diluted with 3 mL of 50% sulfuric acid, after which the absorbance was measured at 345 nm. A blank was prepared by applying the same procedure without adding gliadin film. Separately, gliadin films underwent the same procedure without the addition of TNBS. The blank value consisted of the addition of the values of the two last readings. The free amino group content was calculated using a molar absorption coefficient of 14600 L/(mol·cm) for trinitrophenyl lysine.

2.2.9. Swelling

Film specimens were dried for 10 days in a desiccator over silica gel (0% RH). The samples (<150 mg) were immersed in test tubes containing 10 mL of two different buffer solutions: 0.1 M sodium phosphate buffer (pH 7) with and without 2% 2-mercaptoethanol (2-ME). The tubes were shaken at 180 rpm and 25 °C for 24 h. The films were removed from the buffer solutions and the remaining water was removed from the film surface with absorbent paper before weighing (final wet weight, W_w^f). The films were then replaced in the desiccator until they reached a constant weight (final dry weight, W_d^f). The percentage of water uptake (ΔW) was calculated as follows:

$$\Delta W\ (\%) = \frac{W_w^f - W_d^f}{W_d^f} \cdot 100 \qquad (\mathbf{2.2})$$

2.2.10.Protein solubility

The protein solubility of the films in a phosphate buffer (pH 7) and in the same buffer with 2% SDS or 2% 2-ME was determined by the bicinchoninic acid protein assay kit (Sigma, Madrid) (Smith et al., 1985). The film samples were stored in a desiccator over silica gel for 10 days before being immersed in test tubes containing 10 mL of 0.1 M sodium phosphate buffer (pH 7). The tubes were shaken at 180 rpm at 25 ºC for 24 h. Aliquots of 1 mL from each test tube were centrifuged at 13000 g for 10 min and 0.1 mL of each supernatant was added to 2 mL of the protein determination reagent and heated at 37 °C for 30 min. Due to the fact that 2-ME causes false positives with the kit, the samples that contained this solution were vacuum-dried and resuspended with a sodium phosphate buffer (Makkar et al., 1980). After cooling to ambient temperature, the absorbance of the solutions was measured at 562 nm in comparison with a reagent blank. The protein content was calculated from a standard curve constructed using standard bovine serum albumin solution (from 0 to 1000 µg/mL). The protein solubility was expressed as milligrams of protein dissolved in the buffer per gram of dry film. Three replications were carried out for each film and the experiment was repeated three times with reproducible results.

2.2.11.Evaluation of the long term stability of cross-linked films in water

Film specimens were cut into circles with a diameter of 2.5 cm (initial diameter, $\emptyset^i$), and dried for 10 days in a desiccator over silica gel (0% RH). It is assumed that at this point the

film samples were close to zero moisture. They were weighed (initial dry weight, W_d^i), and their thickness was measured (initial thickness, l^i) with a micrometer. Then they were immersed in test tubes containing distilled water and shaken occasionally. The films were removed from the solution at different time intervals over 140 days. The remaining water was removed from the film surface with absorbent paper before weighing (final wet weight, W_w^f), and the diameter (final diameter, $\emptyset^f$) and thickness (final thickness, l^f) were measured. The films were replaced in the desiccator until they reached a constant weight (final dry weight, W_d^f). The percentage of water uptake (ΔW) was calculated by equation 3.2, where the weight loss (WL), diameter gain ($\Delta\emptyset$), and thickness gain (Δl) were calculated as follows:

$$WL\ (\%) = \frac{W_d^i - W_d^f}{W_d^i} \cdot 100 \quad (\mathbf{2.3})$$

$$\Delta\emptyset\ (\%) = \frac{\emptyset^f - \emptyset^i}{\emptyset^i} \cdot 100 \quad (\mathbf{2.4})$$

$$\Delta l\ (\%) = \frac{l^f - l^i}{l^i} \cdot 100 \quad (\mathbf{2.5})$$

2.2.12.Enzymatic degradation under simulated gastric and intestinal conditions

The enzymatic degradation method used was based on the methods of Laparra (2003) and Chen et al. (2008), modified and adapted for the films under study. To a dry gliadin film 2.5 cm in diameter (60 mg aprox.), 80 mL of cellular grade water was added. The pH was adjusted to 1.2 (gastric pH) with 6 M HCl. After 10 min, the pH value was checked and if necessary readjusted to pH 1.2, then, 2 ml of freshly prepared pepsin solution (10% pepsin in 0.1 M HCl) was added. The sample was made up to 100 g with water and incubated in a shaking water bath at 37 °C for 6 h. Aliquots of 1 mL were withdrawn from the dissolution medium at various time intervals, and replaced with an equal volume of fresh dissolution medium (with or without enzyme) to maintain same conditions. To distinguish the effect of the gastric and intestinal enzymes from the dissolution properties of the films, a control without any enzyme was prepared in order to subtract the soluble protein in the medium. The same preparation was made for the intestinal digestion step. In this case, the pH was raised to 7.4 by adding 1 M $NaHCO_3$, then the pancreatin-bile extract mixture (0.2 g of pancreatin and 1.25 g of bile extract in 50 mL of 0.1 M $NaHCO_3$) was added. The experiment

was performed in triplicate for each sample. After centrifuging the withdrawn aliquots, the soluble protein was determined at different time intervals by the bicinchoninic acid (BCA) protein assay (Smith et al., 1985) as described above.

2.2.13.Statistical analysis

Statistical analysis of the results was performed with SPSS commercial software (SPSS Inc., Chicago, IL, USA). A one-way analysis of variance (ANOVA) was carried out. Differences between means were assessed on the basis of confidence intervals using the Tukey test at a $p \leq 0.05$ significance level. The data were plotted with Sigmaplot software (Systat Software Inc., Richmond, CA. USA).

2.3. RESULTS AND DISCUSSION

2.3.1. Cross-linking wheat gliadins with cinnamaldehyde

The suitability of cinnamaldehyde as a natural cross-linker for improving the functional properties of gliadin films has been shown in a previous study (Balaguer et al., 2011). The resulting films showed high transparency, maintained their integrity after immersion in aqueous media, and displayed significant improvements in maximum tensile strength and Young's modulus without impairment of their elongation properties. Furthermore, the cross-linking effect appeared to be dependent on the amount of the added cross-linker. In the present study, SDS-PAGE analysis was used to assess changes in the molecular weight profile of gliadins treated with cinnamaldehyde. Both the gliadin film-forming solutions and the resulting films were assayed. In the first case typical gliadin bands were observed between 35 and 50 kDa, and no differences were found between samples with and without cinnamaldehyde (results not shown). However, clear differences were observed among the gliadins extracted from the different films, according to whether or not the reducing agent 2-ME was present (**Figure 2.1**). This difference between the SDS-PAGE profiles of the gliadins in the film-forming solutions and in the films would indicate that the cross-linking reaction caused by the cinnamaldehyde could take place while the film is drying. **Figure 2.1**. Sodium dodecyl sulfate-polyacrylamide gel electrophoresis (SDS-PAGE) patterns of non-reduced gliadin films (A) and 2-ME reduced gliadin films (B). Lane 1: marker (molecular weight in kDa);

lane 2: G1.5C_pH2; lane 3: G3C_pH2; lane 4: G5C_pH2; lane 5: G_pH2; lane 6: G5C_pH6; and lane 7: G_pH6.

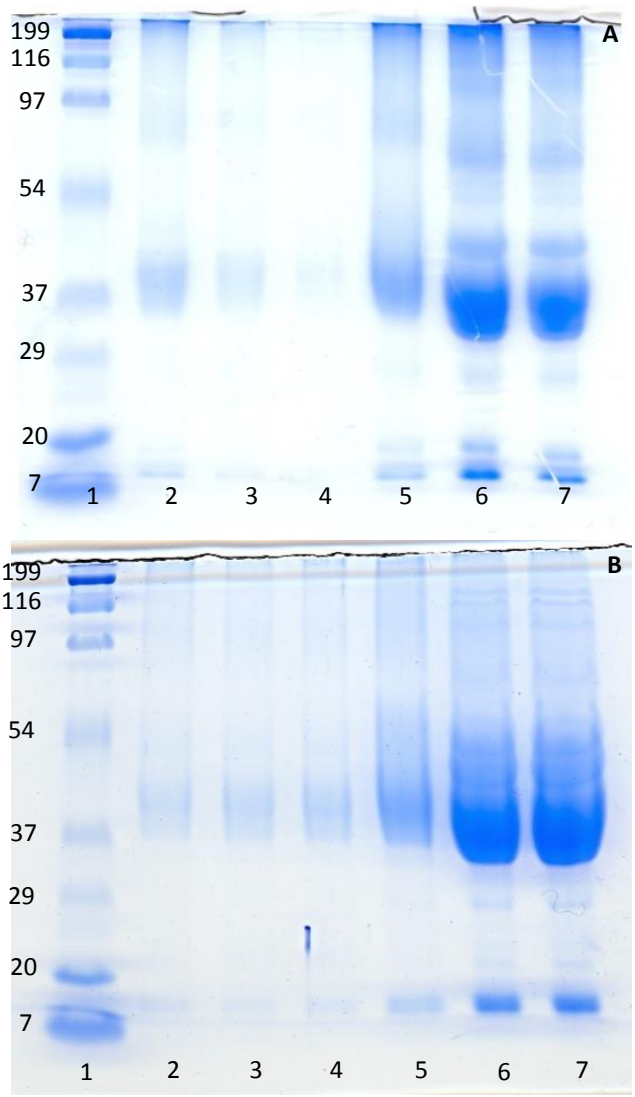

Figure 2.1. Sodium dodecyl sulfate-polyacrylamide gel electrophoresis (SDS-PAGE) patterns of non-reduced gliadin films **(A)** and 2-ME reduced gliadin films **(B)**. Lane 1: marker (molecular weight in kDa); lane 2: G1.5C_pH2; lane 3: G3C_pH2; lane 4: G5C_pH2; lane 5: G_pH2; lane 6: G5C_pH6; and lane 7: G_pH6.

In the non-reduced control film G_pH6 (lane 7 of **Figure 2.1A**), typical bands corresponding to molecular mobilities in the region of gliadin were detected. Moreover, a great quantity of

protein was noted as a blur band in the 54-199 kDa range and aggregates of high molecular weight were found on the top of the gel. The same results were found for G_pH2 and G5C_pH6 (lanes 5 and 6, respectively). These high MW fractions were probably the result of a certain number of disulfide bonds' forming through sulfhydryl-disulfide interchange reactions during drying, as they disappeared when the films were subjected to reduction with 2-ME (**Figure 2.1B**). When combining the pH reduction and the cinnamaldehyde addition (Figure 1A, G1.5C_pH2, lane 2; G3C_pH2, lane 3; G5C_pH2, lane 4), a noticeable decrease in the density of the bands and high MW aggregates was observed. This effect can be attributed to the cross-linking capacity of cinnamaldehyde, which gives rise to lower protein extraction. In fact, these samples were highly insoluble in the denaturing buffer. The addition of 2-ME to the denaturing buffer did not alter the observed electrophoretic profile of the cross-linked films (**Figure 2.1B**), showing that disulfide bonds in the gliadins were not implicated in the cross-linking of the films with cinnamaldehyde. Therefore, the results of the present experiment provide biochemical evidence of the cross-linking of gliadins with cinnamaldehyde, as well as demonstrating that the reaction occurs in acidic conditions (pH 2). Both are in accordance with previous findings (Balaguer et al., 2011).

The cross-link density (CLD) was determined to evaluate the changes in the degree of cross-linking according to the amount of cross-linker added (**Table 2.1**). The G_pH6 film showed a CLD at 50% RH of 3.20 ± 0.68 mol/m^3. This value rose progressively as the amount of cinnamaldehyde in the film increased, reaching 15.2 ± 1.5 mol/m^3 for the G5C_pH2 film, so the cross-linking density was directly proportional to the amount of cinnamaldehyde added.

The swelling of a cross-linked polymer gives an insight into cross-linking density. **Table 2.1** shows the swelling measured as water uptake percentage in a buffered medium at pH 7 and in the presence of 2% of 2-ME. The cinnamaldehyde-treated films at pH 2 (G1.5C_pH2, G3C_pH2 and G5C_pH2) maintained their integrity after 24 h of immersion in aqueous solutions. The swelling values were in accordance with the CLD values. The higher the cinnamaldehyde content the lower the swelling obtained, which indicates that a greater reticulation of the polymeric matrix was hampering chain mobility and water absorption. Disulfide bridges seemed not to be fundamental in the cross-linking, as 2-ME addition did not produce the loss of integrity of any film.

Table 2.1. Cross-linking density (CLD) at 50% RH and swelling, measured as water uptake (%) after 24 h of immersion at 25 °C in a pH 7 phosphate buffer or a pH 7 phosphate buffer with 2% of 2-ME.

Sample	CLD (mol/m³) at 50% RH	Water Uptake (%)	
		Phosphate Buffer pH 7	Phosphate Buffer pH 7 + 2% 2-ME
G_pH6	3.20 ± 0.60 [a]	-	-
G_pH2	2.61 ± 1.04 [a]	-	-
G1.5C_pH2	4.72 ± 0.82 [b]	64.37 ± 7.94 [c]	67.63 ± 7.07 [c]
G3C_pH2	9.75 ± 1.87 [c]	46.22 ± 3.28 [b]	48.87 ± 4.14 [b]
G5C_pH2	15.19 ± 1.48 [d]	32.99 ± 0.17 [a]	38.82 ± 2.92 [a]*

Values reported are the means ± standard deviations (n = 10, 95% confidence interval).
[a-d] Different lowercase letters in the same column indicate a statistically significant difference between films ($p \leq 0.05$)
* In the same row indicates a statistically significant difference ($p \leq 0.05$)

Protein solubility after the immersion of the films in the buffers was determined as an indirect way of analyzing the kind of links established among gliadins as a result of the addition of cinnamaldehyde. **Figure 2.2** shows the amount of protein dissolved in the buffered medium at pH 7, and in the same buffer with 2% of SDS or 2% of 2-ME. An increase in protein solubility in the phosphate buffer at pH 7 was observed when the pH of the films was reduced from 6 (G_pH6) to 2 (G_pH2). This was because protein solubility increases when the pH is far from the isoelectric point (8.1 for gliadins (Wu and Dimler, 1963)). When the films were treated with cinnamaldehyde at pH 2, however, a drop in the protein solubility was observed, corresponding to the three-dimensionally stabilized structure obtained by means of cross-linking. Adding SDS to the medium greatly increased the protein solubility of the non-cross-linked films, indicating that the integrity of gliadin films is maintained mainly by non-covalent bonds. This finding, which agrees with those of other authors (Tatham and Shewry, 1985), explains the lack of water resistance found in the swelling analysis of the control films. Cross-linked films (G1.5C_pH2, G3C_pH2, G5C_pH2) did not release a significantly higher ($p \leq 0.05$) amount of protein into the medium when exposed to SDS than when this agent was absent, showing that the participation of non-covalent bonds in the stabilization of the film structure is negligible.

When 2-ME was added to the medium, a slight but not significant increase ($p \leq 0.05$) was observed when compared to the buffer alone. A feasible explanation for this is the reduction of the intermolecular S-S bonds in gliadins generated during film drying and the subsequent release of small protein fragments.

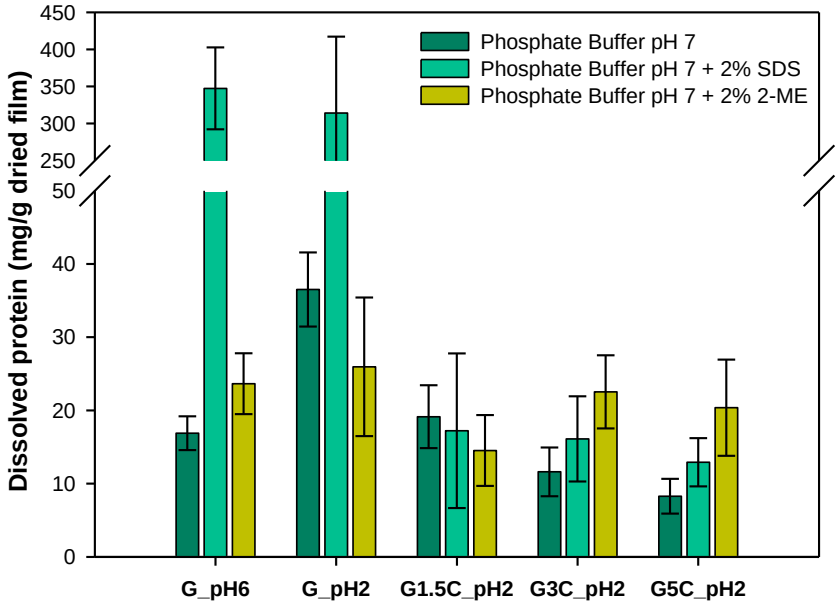

Figure 2.2. Protein solubility after 24 h of immersion at 25 °C in phosphate buffer at pH 7, in buffer with 2% SDS and in buffer with 2% 2-ME.

The study of protein solubility in different buffers revealed the limited participation of non-covalent bonds, as well as disulphide bridges, in stabilizing the cross-linked protein structure. A possible means of gliadin-cinnamaldehyde interaction may involve amino groups. It is well known that aldehydes react with primary amines to give rise to condensation products known as imines or Schiff bases. It has also been demonstrated that cinnamaldehyde reacts with amino groups present in the side chain of the amino acids (Majeti and Suskind, 1977). Cross-linking, however, requires another anchor point that lets cinnamaldehyde act as an interchain bridge. Therefore, a second bond that could be forming would involve a Michael addition in which the amino group joins the double bond of the α,β-unsatured molecule (1,4-addition) (Peters and Richards, 1977; Sebenik, 1994; Sebenik and Osredkar, 1988). **Figure 2.3** shows a possible reaction between gliadins and cinnamaldehyde involving the formation of a Schiff base by means of a hemiaminal as an intermediary, and the formation of a new bond via Michael addition. Furthermore, the resulting imine could react with more amino groups to give rise to an aminal (Sebenik and Osredkar, 1988), and the derived products could continue reacting among themselves to form 3-point cross-links.

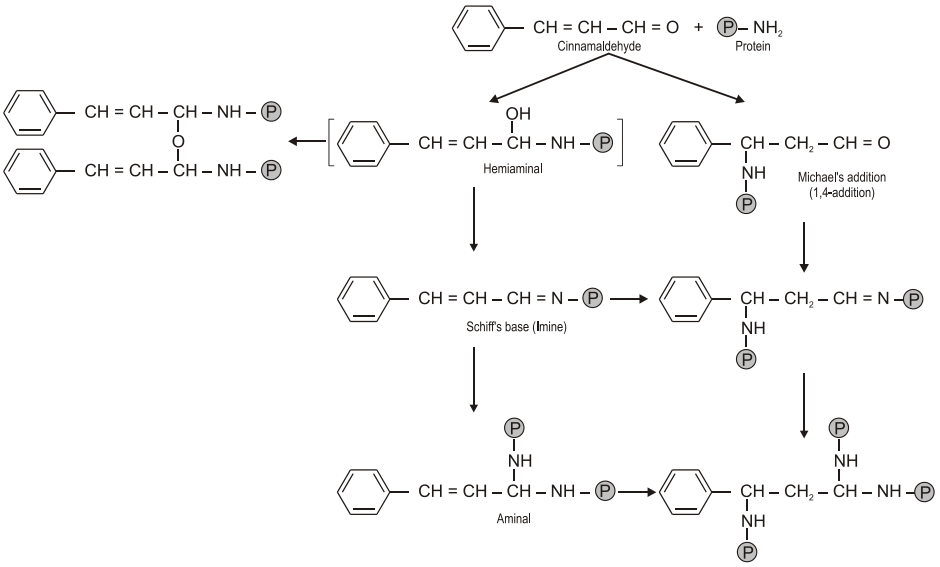

Figure 2.3. Possible reactions between cinnamaldehyde and the amino groups of the protein.

Determination of the free amino groups may be a useful way to investigate whether the reaction mechanisms proposed in **Figure 2.3** are taking place. Firstly, because of the pH dependence of the cross-linking reaction, the effect of the pH of the film-forming solution on the free amino groups of the resulting films was evaluated (**Figure 2.4A**).

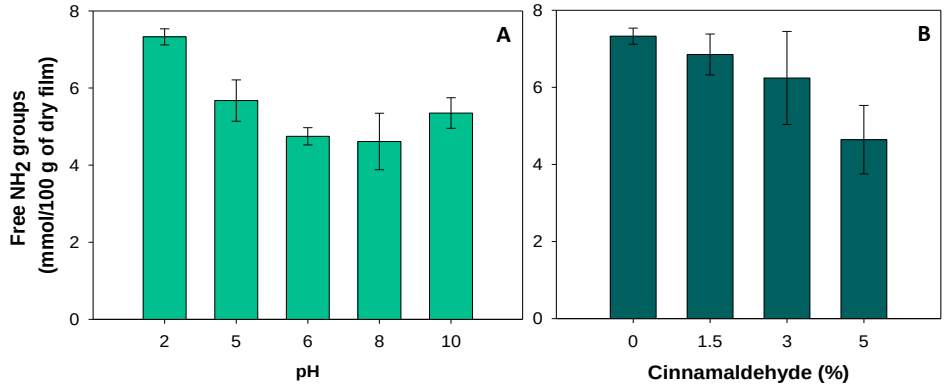

Figure 2.4. (A) Effect of the pH of the film-forming solution on the amount of free NH_2 groups in the derived gliadin film. **(B)** Effect of cinnamaldehyde content on the amount of free NH_2 groups in the derived gliadin film obtained at pH 2.

The free amino group content increased from 4.6 ± 0.7 mmol/100 g of film for pH 8, the closest to the isoelectric point, to 7.3 ± 0.2 mmol/100 g of film for pH 2. It is known that at

pHs far from the isoelectric point, side-chain repulsion of induced net charges leads to conformational changes in the protein structure due to possible unfolding, rupture of hydrogen bonds and alteration of hydrophobic interactions (Chourpa et al., 2006; Sun et al., 2008). These changes in the native conformation of the protein favor the exposure of groups that otherwise remain unexposed.

In a second experiment, in which different amounts of cinnamaldehyde were added to the film-forming solution at pH 2, a downwards tendency in the free amino group content was observed as the cinnamaldehyde concentration increased, as compared to the control at pH 2 (**Figure 2.4B**). Both experiments are indicative of the implication of free amino groups in the gliadins-cinnamaldehyde cross-linking mechanism. However, the participation of other reactive side groups in the cross-linking, such as thiol in cysteine or phenol in tyrosine, cannot be not ruled out.

The amino acid analysis was carried out in order to evaluate possible changes in the molar fraction of the amino acids that could be reacting with the cinnamaldehyde. **Figure 2.5** shows the amino acid molar composition for the different gliadin films. The values obtained were very similar to those found by Lasztity (1984). Wheat gliadin proteins contain very high molar fractions of glutamine (~35%) and proline (~20%) and low levels of the basic amino acids arginine, lysine, and histidine. Glutamic acid and aspartic acid are mostly amidated, but the amino acid analysis technique detects both as the respective acids.

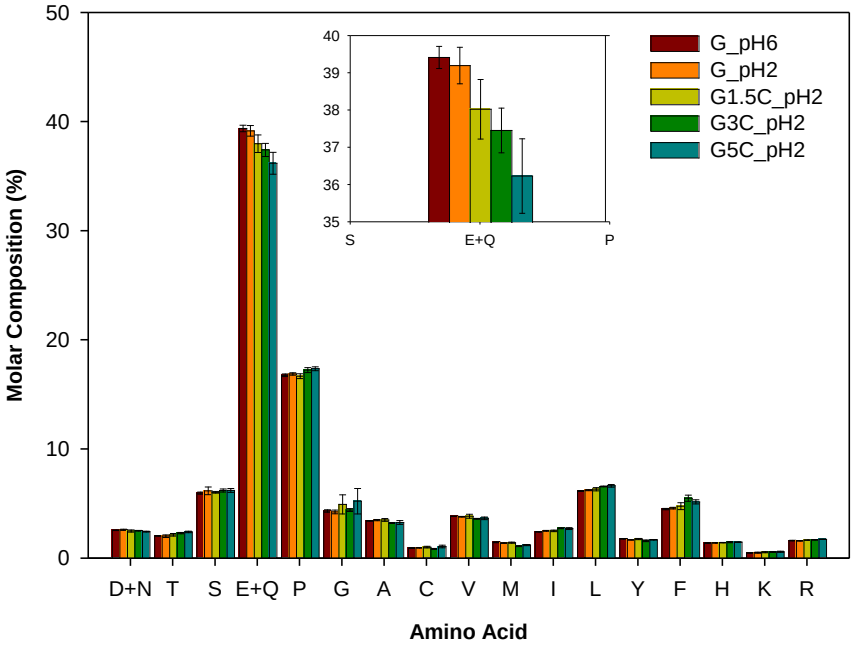

Figure 2.5. Amino acid analysis of gliadin films. Inset graph: Detail of glutamic acid molar composition.

The downwards tendency in the molar fraction of glutamine when cinnamaldehyde treatment at pH 2 was applied to the films can be seen in the inset graph in **Figure 2.5**. A possible approach to explaining this fact is that some amino groups from the glutamine residue could be reacting with cinnamaldehyde and preventing its complete determination. In this regard, Fraenkel-Conrat and Mecham (1949) found that with formaldehyde treatment at pHs below 3 to 2, some methylene cross-linking may occur between pairs of amide groups, doubling the molecular weight of gliadins. The lower content in other residues with amino groups in the side chain which can react with cinnamaldehyde, such as lysine, asparagine, arginine, or histidine was probably responsible for the lack of a more noticeable variation in content in the molar composition of the films. In the same way, the participation of other reactive side groups such as phenol in tyrosine or thiol in cysteine could not be corroborated.

2.3.2. Long term stability of cross-linked films in water

Figure 2.6 shows the water uptake (**A**), weight loss (**B**), diameter gain (**C**), and thickness gain (**D**) over time (140 days) for the films containing 1.5%, 3%, and 5% of cinnamaldehyde. The percentage of water uptake after 24 hours of immersion in water (the first point in **Figure 2.6A**) followed the same trend as that observed with the phosphate buffer (**Table 2.1**), being inversely related to the amount of cinnamaldehyde added to the gliadin film-forming solution. The weight loss after 24 h (the first point in **Figure 2.6B**) was similar for all the films, irrespective of the cross-linker concentration. This weight loss was around 22% and was mainly due to the loss of hydrophilic glycerol to the aqueous medium and, to a lesser extent, to the freeing of short polypeptide chains from the reticulated matrix. The loss of glycerol was confirmed by the lack of flexibility of the films after drying. In fact, the proportion of glycerol incorporated into the film in relation to the protein content was 25% (25 g of glycerol / 100 g of protein), corresponding to 20 g of glycerol /100 g of dry film.

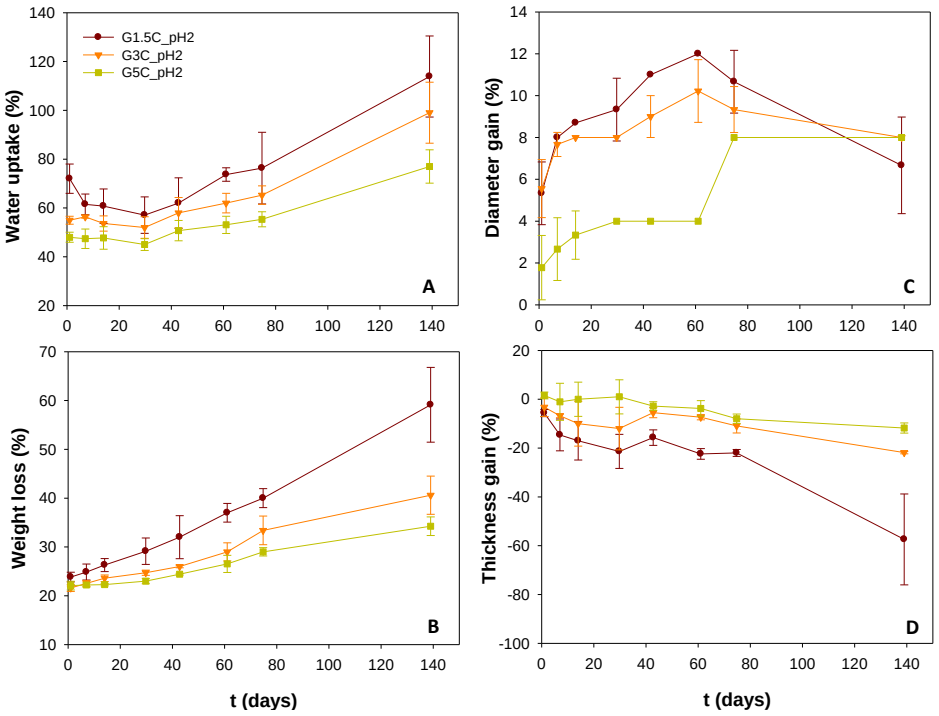

Figure 2.6. Physical changes in gliadin films kept in aqueous medium through 140 days of storage at ambient temperature**. (A)** Water uptake (%), **(B)** weight loss (%), (**C)** diameter gain (%), and **(D)** thickness gain (%).

The water uptake and the loss of weight of all the films increased progressively and the differences among them became more acute over time, reflecting changes in the structure of the protein matrix. After 140 days, films G1.5C_pH2, G3C_pH2, and G5C_pH2 had absorbed 113.84 ± 16.6, 99.0 ± 12.5, and 77.0 ± 6.8 g of water/100 g of film respectively. The weight loss after 140 days was 59.1 ± 7.7, 40.6 ± 3.9, and 34.3 ± 1.9 g/100 g of film, respectively. These findings draw attention to the improvement in the physical performance of cross-linked matrices, which enables the films with the greatest cross-linking to withstand water immersion conditions for longer periods of time.

Diameter and thickness variations are plotted in **Figures 2.6C** and **2.6D** respectively. The most cross-linked film (G5C_pH2) only gained 4% in diameter after 60 days of immersion in water, after which a step change took place, resulting in a final value of 8%. The diameter of G1.5C_pH2 and G3C_pH2 increased by up to a maximum of 12 and 10% respectively, after which it decreased, probably due to degradation of the films, as shown by their weight loss. With regard to thickness, after 24 h the only film in which it had increased was G5C_pH2 (1.56 ± 1.42%), while films G3C_pH2 and G1.5C_pH2 showed a reduction in thickness of 3.24 ± 3.82 and 5.63 ± 1.47% respectively. This decrease in the thickness of the films was higher for the films with less cross-linking but was a consistent tendency for all the films over the period studied, and was also correlated with the loss of weight (**Figure 2.6B**).

2.3.3. Enzymatic degradation of cross-linked films under simulated gastric and intestinal conditions

The bioplastics developed in this study presented considerable resistance over long periods of immersion in water. As these films may be potentially edible and could also act as carriers of bioactive compounds, their dissolution over time under simulated gastric or intestinal conditions was studied. The results are shown in **Figure 2.7**. A different behavior pattern was observed for gliadin films subjected to simulated gastric and intestinal conditions. Under simulated gastric fluid (SGF) the cross-link density influenced the film dissolution: as is well-known, the greater the cross-link density, the lower the film dissolution. This can be attributed to the development of a more rigid and compact structure in films treated with a greater amount of cinnamaldehyde, leading to a decrease in the penetration of digestive enzymes into the network. In contrast, under simulated intestinal conditions (SIF) the cinnamaldehyde-treated gliadin films were scarcely affected by the digestive enzymes, whatever the cross-link density. This is in agreement with the specificity of the proteolytic

enzymes pepsin and trypsin, present in the simulated gastric and intestinal fluids, respectively. Pepsin cleaves the peptide bonds in which hydrophobic amino acids are involved (Yon-Kahn and Hervé, 2010), and this group comprises about 45% of the total amino acids present in gliadin. In contrast, trypsin mainly cleaves peptide chains on the carboxyl side of the amino acids lysine and arginine (Yon-Kahn and Hervé, 2010), which together account for only about 2.5% of the total amino acids in gliadin.

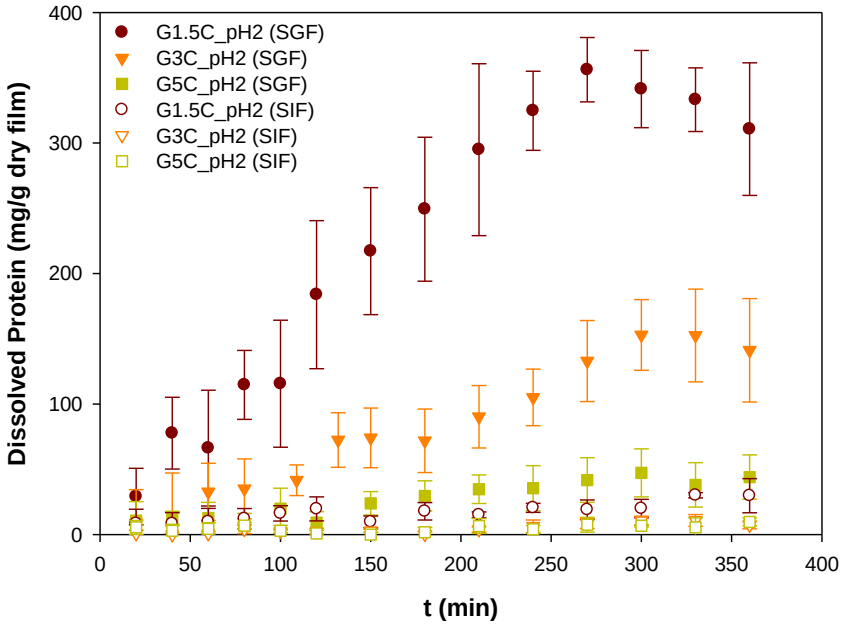

Figure 2.7. Dissolved protein under simulated gastric fluid (SGF) (pH 1.2 and pepsin) and simulated intestinal fluid (SIF) (pH 7.4 and pancreatin-bile extract).

According to these results, the gliadin films may be digested in the stomach, although the extent of digestion would depend on the cross-link density. In this respect, the most cross-linked film, G5C_pH2, retained its integrity after the enzymatic treatment under SGF, while the least cross-linked film, G1.5C_pH2, was completely degraded. If these edible films were used as matrices to release active compounds into the gastrointestinal tract, they would be very useful when release in the stomach is required, as the degree of cross-linking can be modified in order to regulate the erosion kinetics of the film.

2.4. CONCLUSION

In the present work, the possible mechanism of wheat gliadin cross-linking by cinnamaldehyde was studied. Furthermore, the long term stability of the films in water and their behavior under simulated gastrointestinal conditions was evaluated. Protein solubility studies in different media (phosphate buffer, SDS, 2-mercaptoethanol) ruled out the participation of either non-covalent or disulfide bridges in the stabilization of the film structure. The amino acid analysis and the evaluation of free amino groups showed their possible implication in the reticulation of the protein matrix. The combination of a Schiff base and a Michael addition between the amino groups of the protein and the cinnamaldehyde presents itself as a feasible cross-linking mechanism, although the participation of other reactive groups cannot be ruled out. The resulting films were not found to disintegrate after 5 months in distilled water, although a weight loss was recorded, depending on the amount of cinnamaldehyde added. The films were partially degraded when subjected to simulated gastric conditions, and the lower the degree of cross-linking, the higher this effect, whereas all the films were highly resistant to simulated intestinal conditions. The different degradation behavior of the films according to the degree of cross-linking reveals their interest as a valuable biomaterial for a wide range of novel applications.

2.5. REFERENCES

Adler-Nissen, J. 1979. Determination of the degree of hydrolysis of food protein hydrolysates by trinitrobenzenesulfonic acid. *Journal of Agricultural and Food Chemistry, 27*(6), 1256-1262.

Akabori, S., and Ohno, K. 1950. On the splitting of the side chain from tyrosine by the action of aldehydes. Osaka University. *26*(6), 39-41.

Balaguer, M. P., Gómez-Estaca, J. n., Gavara, R., and Hernandez-Munoz, P. 2011. Functional properties of bioplastics made from wheat gliadins modified with cinnamaldehyde. *Journal of Agricultural and Food Chemistry, 59*(12), 6689-6695.

Becerril, R., Gomez-Lus, R., Goni, P., Lopez, P., and Nerin, C. 2007. Combination of analytical and microbiological techniques to study the antimicrobial activity of a new active food packaging containing cinnamon or oregano against *E. coli* and *S. aureus*. *Analytical and Bioanalytical Chemistry, 388*(5-6), 1003-1011.

Ben Arfa, A., Preziosi-Belloy, L., Chalier, P., and Gontard, N. 2007. Antimicrobial paper based on a soy protein isolate or modified starch coating including carvacrol and cinnamaldehyde. *Journal of Agricultural and Food Chemistry, 55*(6), 2155-2162.

Bispo, V. M., Mansur, A. A. P., Barbosa-Stancioli, E. F., and Mansur, H. S. 2010. Biocompatibility of nanostructured chitosan/poly(vinyl alcohol) blends chemically cross linked with genipin for biomedical applications. *Journal of Biomedical Nanotechnology, 6*(2), 166-175.

Butler, M. F., Ng, Y. F., and Pudney, P. D. A. 2003. Mechanism and kinetics of the crosslinking reaction between biopolymers containing primary amine groups and genipin. *Journal of Polymer Science Part a-Polymer Chemistry, 41*(24), 3941-3953.

Cao, N., Fu, Y. H., and He, J. H. 2007. Mechanical properties of gelatin films cross-linked, respectively, by ferulic acid and tannin acid. *Food hydrocolloids, 21*(4), 575-584.

Cornell, H. J., and Hoveling, A. W., 1998. *Wheat: Chemistry and utilization*. Technomic publishing Company, Inc.: Lancaster, PA, USA.

Cuq, B., Gontard, N., and Guilbert, S. 1998. Proteins as agricultural polymers for packaging production. *Cereal Chemistry, 75*(1), 1-9.

Chen, L. Y., Remondetto, G., Rouabhia, M., and Subirade, M. 2008. Kinetics of the breakdown of cross-linked soy protein films for drug delivery. *Biomaterials, 29*(27), 3750-3756.

Chourpa, I., Ducel, V., Richard, J., Dubois, P., and Boury, F. 2006. Conformational modifications of alpha gliadin and globulin proteins upon complex coacervates formation with gum arabic as studied by raman microspectroscopy. *Biomacromolecules, 7*(9), 2616-2623.

D882, ASTM. 2009. Standard test method for tensile properties of thin plastic sheeting.

Dupuis, G., and Benezra, C., 1982. *Allergic contact dermatitis to simple chemicals, a molecular approach.* Marcel Dekker: New York.

Fraenkel-Conrat, H., and Mecham, D. K. 1949. The reaction of formaldehyde with proteins. Vii. Demonstration of cross-linking by means of osmotic pressure measurements *Journal of Biological Chemistry, 177*(1), 477-486.

Galietta, G., Di Gioia, L., Guilbert, S., and Cuq, B. 1998. Mechanical and thermomechanical properties of films based on whey proteins as affected by plasticizer and crosslinking agents. *Journal of Dairy Science, 81*(12), 3123-3130.

Guilbert, S., and Gontard, N. 2005. Agro-polymers for edible and biodegradable films: Review of agricultural polymeric materials, physical and mechanical characteristics. In *Innovations in Food Packaging*, J.H. Han, Ed. Elsevier: London.

Habeeb, A. F. S. A. 1966. Determination of free amino groups in proteins by trinitrobenzenesulfonic acid. *Analytical Biochemistry, 14*(3), 328-336.

Hernandez-Munoz, P., and Hernandez, R. J. 2001. *Glutenin and gliadin films from wheat gluten: Preparation and properties.* Paper presented at the IFT Annual Meeting, New Orleans, Louisiana.

Hernandez-Munoz, P., Kanavouras, A., Lagaron, J. M., and Gavara, R. 2005. Development and characterization of films based on chemically cross-linked gliadins. *Journal of Agricultural and Food Chemistry, 53*(21), 8216-8223.

Kim, S., Nimni, M. E., Yang, Z., and Han, B. 2005. Chitosan/gelatin-based films crosslinked by proanthocyanidin. *Journal of Biomedical Materials Research Part B-Applied Biomaterials, 75B*(2), 442-450.

Laemmli, U. K. 1970. Cleavage of structural proteins during assembly of head of bacteriophage-t4. *Nature, 227*(5259), 680-&.

Laparra, J. M. 2003. Estimation of arsenic bioaccessibility in edible seaweed by an *in vitro* digestion method. *Journal of Agricultural and Food Chemistry, 51*(20), 6080-6085.

Lasztity, R., 1984. *The chemistry of cereal proteins*. CRC Press: Boca Raton, FL, USA.

Majeti, V. A., and Suskind, R. R. 1977. Mechanism of cinnamaldehyde sensitization. *Contact Dermatitis, 3*(1), 16-18.

Makkar, H. P. S., Sharma, O. P., and Negi, S. S. 1980. Assay of proteins by Lowry method in the presence of high-concentrations of beta-mercaptoethanol. *Analytical Biochemistry, 104*(1), 124-126.

Mangavel, C., Barbot, J., Bervast, E., Linossier, L., Feys, M., Gueguen, J., and Popineau, Y. 2002. Influence of prolamin composition on mechanical properties of cast wheat gluten films. *Journal of Cereal Science, 36*(2), 157-166.

Marquie, C. 2001. Chemical. Reactions in cottonseed protein cross-linking by formaldehyde, glutaraldehyde, and glyoxal for the formation of protein films with enhanced mechanical properties. *Journal of Agricultural and Food Chemistry, 49*(10), 4676-4681.

Monsan, P., Puzo, G., and Mazarguil, H. 1976. Étude du mécanisme d'établissement des liaisons glutaraldéhyde-protéines. *Biochimie, 57*(11-12), 1281-1292.

Peters, K., and Richards, F. M. 1977. Chemical cross-linking: Reagents and problems in studies of membrane structure. *Annual Review of Biochemistry, 46*(1), 523-551.

Reddy, N., Li, Y., and Yang, Y. Q. 2009. Alkali-catalyzed low temperature wet crosslinking of plant proteins using carboxylic acids. *Biotechnology Progress, 25*(1), 139-146.

Rodriguez, A., Nerin, C., and Batlle, R. 2008. New cinnamon-based active paper packaging against *Rhizopus stolonifer* food spoilage. *Journal of Agricultural and Food Chemistry, 56*(15), 6364-6369.

Sebenik, A. 1994. Step-growth polymerization of unsatured aldehydes with aliphatic-amines. *Journal of Applied Polymer Science, 54*(8), 1013-1018.

Sebenik, A., and Osredkar, U. 1988. Investigation of urea cinnamaldehyde resin. *European Polymer Journal, 24*(9), 863-866.

Sekkar, V., Narayanaswamy, K., Scariah, K. J., Nair, P. R., Sastri, K. S., and Ang, H. G. 2007. Evaluation by various experimental approaches of the crosslink density of urethane networks based on hydroxyl-terminated polybutadiene. *Journal of Applied Polymer Science, 103*(5), 3129-3133.

Smith, P. K., Krohn, R. I., Hermanson, G. T., Mallia, A. K., Gartner, F. H., Provenzano, M. D., Fujimoto, E. K., Goeke, N. M., Olson, B. J., and Klenk, D. C. 1985. Measurement of protein using bicinchoninic acid. *Analytical Biochemistry, 150*(1), 76-85.

Soares, R. M. D., Maia, G. S., Rayas-Duarte, P., and Soldi, V. 2009. Properties of filmogenic solutions of gliadin crosslinked with 1-(3-dimethyl aminopropyl)-3-ethylcarbodiimidehydrochloride/N-hydroxysuccinimide and cysteine. *Food hydrocolloids, 23*(1), 181-187.

Song, Y. H., Li, L. F., and Zheng, Q. 2009. Influence of epichlorohydrin modification on structure and properties of wheat gliadin films. *Journal of Agricultural and Food Chemistry, 57*(6), 2295-2301.

Sun, S., Song, Y., and Zheng, Q. 2008. Ph-induced rheological changes for semi-dilute solutions of wheat gliadins. *Food hydrocolloids, 22*(6), 1090-1096.

Sung, H. W., Huang, D. M., Chang, W. H., Huang, R. N., and Hsu, J. C. 1999. Evaluation of gelatin hydrogel crosslinked with various crosslinking agents as bioadhesives: *In vitro* study. *Journal of Biomedical Materials Research, 46*(4), 520-530.

Suskind, R. R., and Majeti, V. A. 1976. Occupational and environmental allergic problems of the skin. *Journal of Dermatology (Tokyo), 3*(1), 3-12.

Tatham, A. S., and Shewry, P. R. 1985. The conformation of wheat gluten proteins. The secondary structures and thermal stabilities of [alpha]-, [beta]-, [gamma]- and [omega]-gliadins. *Journal of Cereal Science, 3*(2), 103-113.

Tropini, V., Lens, J. P., Mulder, W., and Silvestre, F. 2004. Wheat gluten films cross-linked with 1-ethyl-3-(3-dimethylaminopropyl) carbodiimide and N-hydroxysuccinimide. *Industrial Crops and Products, 20*(3), 281-289.

Tropini, V., Lens, J. P., Mulder, W. J., and Silvestre, F. 2000. Cross-linking of wheat gluten using a water-soluble carbodiimide. *Cereal Chemistry, 77*(3), 333-338.

van Wachem, P. B., Zeeman, R., Dijkstra, P. J., Feijen, J., Hendriks, M., Cahalan, P. T., and van Luyn, M. J. A. 1999. Characterization and biocompatibility of epoxy-crosslinked dermal sheep collagens. *Journal of Biomedical Materials Research, 47*(2), 270-277.

Weibel, H., and Hansen, J. 1989. Interaction of cinnamaldehyde (a sensitizer in fragance) with protein. *Contact Dermatitis, 20*(3), 161-166.

Wu, Y. V., and Dimler, R. J. 1963. Hydrogen ion equilibria of wheat glutenin and gliadin. *Archives of Biochemistry and Biophysics, 103*(3), 310-318.

Yon-Kahn, J., and Hervé, G., 2010. *Molecular and cellular enzymology*. Springer: Berlin; Vol. I.

Zhang, X. Q., Do, M. D., Casey, P., Sulistio, A., Qiao, G. G., Lundin, L., Lillford, P., and Kosaraju, S. 2010. Chemical modification of gelatin by a natural phenolic cross-linker, tannic acid. *Journal of Agricultural and Food Chemistry, 58*(11), 6809-6815.

Zigon, M., Sebenik, A., Osredkar, U., and Vizovisek, I. 1987. Synthesis and characterization of resorcinol-cinnamaldehyde resins. *Angewandte Makromolekulare Chemie, 148*, 127-135.

CHAPTER 3

MASS TRANSPORT PROPERTIES OF GLIADIN FILMS: EFFECT OF CROSS-LINKING DEGREE, RELATIVE HUMIDITY, AND TEMPERATURE

Balaguer, M.P.; Cerisuelo, J. P.; Gavara, R.; and Hernandez-Munoz, P.

Journal of Membrane Science, 2013, 428(0), 380-392

The degree of cross-linking of gliadin films was increased by chemical treatment with cinnamaldehyde. The formation of a more reticulated network was able to achieve a simultaneous reduction of water vapor, oxygen, and carbon dioxide permeabilities, enhancing barrier properties by up to 64%, 75%, and 79%, respectively. The evaluation of solubility and diffusivity coefficients involved in water vapor permeation highlights the complexity of the mechanisms implicated in water transport through hydrophilic films. Water vapor sorption isotherms followed a non-linear profile, which was fitted with the D'Arcy and Watt model. Water vapor diffusivity was concentration-dependent, being affected by plasticization and water clustering. Temperature-dependence of water vapor permeability showed a discontinuous behavior when the Arrhenius law was applied, indicating possible changes in the matrix structure. Oxygen permeability was positively influenced by relative humidity and temperature. The higher selectivity to carbon dioxide permeation in comparison with oxygen diminished as the water content of the film increased, which is in accordance with the loss of barrier properties at high relative humidities. This study underlines the importance of the evaluation of environmental conditions during end-use applications in order to optimize the performance of biopolymer-based films.

3.1. INTRODUCTION

The new requirements of a consumer more concerned about environmental protection have boosted the development of biodegradable plastics from renewable resources for use as packaging materials. Film-forming capacities of agro-proteins have been largely investigated (Cuq et al., 1998). Wheat gliadins represent a suitable raw material for production of these new bioplastics because of their remarkable functional properties (Balaguer et al., 2011b; Hernandez-Munoz et al., 2005; Hernandez-Munoz et al., 2003; Sun et al., 2008).

The existence of mass transport through polymeric materials is well established. Permeation, migration, and sorption processes are of considerable interest when polymers are used as packaging materials where the content is sensitive to environmental conditions, as occurs in food or pharmaceutical products. The barrier properties of biopolymers based on hydrocolloids are highly dependent on temperature and especially on relative humidity (Aulin et al., 2010). The hydrophilic nature of proteinaceous films and the substantial amount of hydrophilic plasticizer added to impart adequate flexibility are responsible for their poor water vapor resistance (Gallstedt and Hedenqvist, 2002; Roy et al., 2000). However, they represent an excellent barrier against oxygen in dry conditions, deteriorating with relative humidity, and they also present selective permeation to carbon dioxide in relation with oxygen (Gontard et al., 1996).

Various strategies have been tried in order to improve the barrier properties of films produced from wheat gluten or its fractions: thermal treatments (Angellier-Coussy et al., 2010), addition of nanoclays (Tunc et al., 2007), chemical cross-linking with aldehydes (Hernandez-Munoz et al., 2005), or epichlorohydrin (Song et al., 2009), blending with other proteins (Gennadios et al., 1993a), formation of bilayer films (Foulk and Bunn, 2001; Irissin-Mangata et al., 1999), and combination or coating with lipids (Gennadios et al., 1993a; Gontard et al., 1994; Gontard et al., 1995).

A reduction of 30% in water vapor permeability was achieved by increasing the thermoforming temperature from 80 to 120 °C for a relative humidity gradient of 0%–100% at 20 °C (Angellier-Coussy et al., 2010). For the same relative humidity gradient, modification of the gluten matrix with beeswax reduced the water vapor transmission rate by 50% at 30 °C, but when beeswax was applied as a surface coating the reduction was

nearly 10-fold compared with the control. Chemical cross-linking of gliadins with formaldehyde, glutaraldehyde, or glyoxal enhanced the water barrier properties of the resulting films, decreasing water vapor permeability values by around 25%, but amounts of cross-linker greater than 1.5% did not modify permeability further (Hernandez-Munoz et al., 2005). In contrast to the effect of aldehyde cross-linking of gliadins (Hernandez-Munoz et al., 2005), the addition of epichlorohydrin did not produce significant modifications in water vapor permeability, irrespective of the percentage used (Song et al., 2009).

The only reported enhancement of oxygen barrier properties was found when wheat gluten was mixed or bilayered with other proteins or polyolefins. Films of gluten mixed with hydrolyzed keratin increased the oxygen barrier by 83%, although the improvement in the water vapor barrier was only 23% (Gennadios et al., 1993a). The formation of a soy protein isolate/wheat gluten bilayer film reduced oxygen permeance (Foulk and Bunn, 2001). Similarly, bilayer films composed of wheat gluten and functionalized polyethylene improved the oxygen and carbon dioxide barrier in comparison with a gluten film (Irissin-Mangata et al., 1999). However, neither the addition of montmorillonite (Tunc et al., 2007) nor the addition of mineral oils or sodium sulfite (Gennadios et al., 1993a) affected oxygen (and carbon dioxide) permeabilities.

The aim of this work was to study mass transport properties in gliadin-based films prepared by casting and cross-linked with cinnamaldehyde. The influence of the cross-linking degree on the permeation, sorption, and diffusion of water vapor, oxygen, and carbon dioxide was evaluated at different relative humidities and temperatures. The dependence of the size, shape, and polarity of the permeant molecule and the effect of polymer-chain segmental mobility are discussed.

3.2. MATERIALS AND METHODS

3.2.1. Materials

Crude wheat gluten (≥80% protein), glycerol, ethanol, hydrochloric acid, and cinnamaldehyde, all laboratory grade, were supplied by Sigma (Madrid, Spain).

3.2.2. Film production

A gliadin-rich film-forming solution was extracted from wheat gluten according to the method described by Hernandez-Munoz and Hernandez (Hernandez-Munoz and Hernandez, 2001). Gliadin films were prepared, following the optimal conditions established in previous works (Balaguer et al., 2011a; Balaguer et al., 2011b). Cinnamaldehyde was added as a cross-linker at different percentages, namely 1.5%, 3%, and 5% (g/100 g of protein), to the film-forming solution adjusted to pH 2. Glycerol was added as a plasticizer at 25% (g/100 g of protein). Gliadin control films without cinnamaldehyde were prepared at pH 6, the native pH of the film-forming solution.

Films were prepared by casting and drying at 37 °C for 24 h. Film thickness was measured using a micrometer (Mitutoyo, Kanagawa, Japan) with a sensitivity of ±2 µm. Mean thickness was calculated from measurements taken at ten different locations on each film sample.

3.2.3. Water vapor mass transport properties

3.2.3.1. Water vapor permeability

The water vapor transmission rates (kg/m^2·s) through the films were measured using a Mocon PERMATRAN-W® Model 3/33 (Lippke, Neuwied, Germany). It operates according to ASTM F1249 (ASTM, 2006) and uses an infrared sensor. The film samples were double-masked with aluminum foil, leaving a circular uncovered effective film area of 5 cm^2. Testing was performed at 23 °C with a relative humidity gradient of 35% to 0%, 50% to 0%, 75% to 0%, and 90% to 0% (in dry nitrogen) across the film. At least four samples of each type of film produced were measured. Although hydrophilic films exposed to relative humidity gradients are non-homogeneous due to the presence of varying amounts of water within different regions, water permeability coefficients (*P*) were estimated for comparative purposes under the selected test conditions. The water vapor permeability coefficient in (kg·m)/(m^2·s·Pa) can be calculated from the transmission rate values measured as follows:

$$P = \frac{Q \cdot l}{A \cdot t \cdot \Delta p} \qquad (\mathbf{3.1})$$

where Q is the amount of permeant (kg) passing through a film of thickness l (m) and area A (m^2), t is time (s), and Δp is the partial pressure differential across the film (Pa). Δp is calculated from the water vapor partial pressure at the temperature selected and the RH gradients.

3.2.3.2. Activation energy of water vapor permeability

For gases and vapors, the dependence of film permeability on temperature often obeys the Arrhenius relationship:

$$P = P_0 \cdot \exp\left(-\frac{E_p}{RT}\right) \qquad (\mathbf{3.2})$$

where P_0 is a pre-exponential factor, E_p is the activation energy of permeation (kcal/mol), R is the universal gas constant (1.987 kcal/mol·K), and T is the absolute temperature (K). Permeability was calculated at different temperatures, namely 10, 15, 20, 23, 30, 37, and 40 °C. E_p can be determined from the slope of the plot of $Ln\ P$ versus $1/T$.

3.2.3.3. Water vapor sorption isotherm

Water vapor sorption kinetics experiments were performed at 20 °C using a model D-200 controlled atmosphere electrobalance (Cahn Inc., Cerritos, CA, USA). The apparatus records the mass evolution with time of a sample that is exposed to an atmosphere of a specific relative humidity. The humidities are generated by mixing dry and saturated vapor gas flows in the correct proportions using gas flowmeters and a high precision hygrosensor (Newport Scientific, Jessup, MD, USA). Film samples were dried for one week prior to testing with P_2O_5. Then the sample was loaded and equilibrated at 0% RH by a continuous flow of dry nitrogen, when equilibrium was reached it was subjected to successive step changes of relative humidity from 0% to 100%, and the remoistening kinetic was followed step by step until equilibrium between the sample and the surrounding atmosphere was reached. The equilibrium water content (C_w, in g of water/g of dry film) was calculated at each relative humidity *i* using the following equation:

$$C_w^i = \frac{M_\infty^i - M_d}{M_d} \qquad (\mathbf{3.3})$$

where M_{∞}^{i} is the weight in the equilibrium at relative humidity *i*, and M_d is the dry weight of the film sample. The water vapor sorption isotherm data (the equilibrium water content) were assigned to the relative humidity reached.

3.2.3.3.1. Sorption isotherm fitting

The experimental sorption isotherms were fitted using the D'Arcy and Watt equation (**3.4**) (D'Arcy and Watt, 1970) by minimizing the root mean square deviations (RMSE) between theoretical and experimental data:

$$C_w = \frac{K_1 K_2 a_w}{1 + K_1 a_w} + K_3 a_w + \frac{K_4 K_5 a_w}{1 - K_4 a_w} \qquad (\mathbf{3.4})$$

This expression comprises three separate processes: (a) monolayer adsorption by strongly binding sites, (b) monolayer adsorption by weakly binding sites, and (c) formation of a multilayer whose extent is limited by the properties of the substrate. Component (a) has the form of the Langmuir isotherm for monolayer adsorption at surfaces, while component (c), describing the formation of a multilayer, yields a modified Langmuir-type equation. In general, component (b) can be approximated by an adsorption that is linear with relative vapor pressure (Henry's law). For some substrates, one or more of the three component isotherms may be inoperative.

3.2.3.3.2. Clustering function

In order to determine whether self-association of water molecules was occurring, the clustering function developed by Zimm and Lundberg was applied to the isotherm sorption model (Zimm and Lundberg, 1956). The clustering function in binary systems in equilibrium is written as:

$$\frac{G}{\phi_w} = -(1 - \phi_w) \frac{\partial \left(\frac{a_w}{\phi_w}\right)}{\partial a_w} - 1 \qquad (\mathbf{3.5})$$

where G is the cluster integral, and ϕ_w is the volume fraction of water calculated as $V_w/(V_P + V_w)$, V_w being the volume of water, and V_P the polymer volume. Applying **Equation 3.5** to **Equation 3.4**, the clustering function, G/ϕ_w, can be written as a function

of the K_i parameters. When the numerical value of the clustering function is greater than –1, water cluster formation is expected to occur.

3.2.3.4. Water vapor diffusivity

The mathematical theory of diffusion is represented by Fick's second law considering one-dimensional isothermal water diffusion into a thin polymer sample, and a diffusion coefficient (*D*) dependent on the concentration:

$$\frac{\partial c}{\partial t} = \frac{\partial}{\partial x}\left(D\frac{\partial c}{\partial x}\right) \qquad (\mathbf{3.6})$$

However, for each small relative humidity step established the diffusion coefficient (*D*) can be assumed as constant:

$$\frac{\partial c}{\partial t} = D\frac{\partial^2 c}{\partial x^2} \qquad (\mathbf{3.7})$$

The initial and boundary conditions for a plane sheet of thickness l where the polymer structure is initially maintained at a constant uniform water concentration C_1, and the surfaces are kept at a constant water concentration C_0, are:

$$t = 0 \qquad -\frac{l}{2} < x < \frac{l}{2} \qquad C = C_1$$

$$t > 0 \qquad x = \pm\frac{l}{2} \qquad C = C_0$$

The solution of this equation under the above-specified conditions was obtained by Crank (Crank, 1975):

$$\frac{M_t}{M_\infty} = 1 - \frac{8}{\pi^2}\sum_{n=0}^{\infty}\frac{1}{(2n+1)^2}exp\left[-\frac{(2n+1)^2\pi^2}{l^2}Dt\right] \qquad (\mathbf{3.8})$$

where M_t denotes the total amount of diffusing substance that has entered the sheet during time t (in our case it represents the water uptake), and M_∞ the corresponding

amount after infinite time (equilibrium). The mass ratio M_t/M_∞ was obtained for each relative humidity step as a function of time following (**section 3.2.3.3**). Since the model used was valid for a mass transport process with constant diffusivity, the diffusion coefficient identified was considered as an apparent diffusivity. The apparent water vapor diffusion coefficients were calculated by minimizing the root mean square deviations between simulated and experimental data.

Deviations from the theoretical behavior assumed with this model, mostly due to polymer swelling or external mass transfer resistance at the interface (Roca et al., 2008), were not taken into account, since a previous study shows insignificant size deformations with these cross-linked matrices when immersed in water (Balaguer et al., 2011a) and the external mass transfer coefficient for the geometry encountered in the microbalance was negligible owing to the high flow used.

3.2.3.5. Mechanism of water vapor transport

The water diffusion mechanism can be described by:

$$\frac{M_t}{M_\infty} = kt^n \qquad (\mathbf{3.9})$$

where M_t/M_∞ is the fraction of water absorbed after time t relative to the amount of water absorbed at infinite time, k is a constant incorporating the characteristics of the macromolecular network system and the penetrant, and n is the diffusional exponent, indicative of the transport mechanism, the value of which lies between 0.5 and 1. **Equation 3.9** is valid for $M_t/M_\infty \leq 0.6$ (Ritger and Peppas, 1987).

Alfrey et al. (1966) proposed a useful classification according to the solvent diffusion rate and the polymer relaxation rate. Three classes are distinguished:

a) Case I (n = 0.5): Fickian diffusion, in which the rate of diffusion is much less than that of relaxation, so that the diffusion process controls the sorption process.

b) Case II (n = 1): the other extreme, in which diffusion is very rapid compared with the relaxation process and the latter controls the sorption process.

c) Non-Fickian diffusion or anomalous diffusion (0.5 < n < 1): which occurs when the diffusion and relaxation rates are comparable.

3.2.4. Oxygen mass transport properties

3.2.4.1. Oxygen permeability

The oxygen transmission rates ($m^3/m^2 \cdot s$) through the films were measured using a Mocon OX-TRAN® Model 2/21 (Lippke, Neuwied, Germany). It operates according to ASTM D3985 (ASTM, 2005) and uses a coulometric sensor (COULOX®). The film samples were double-masked with aluminum foil, leaving a circular uncovered effective film area of 5 cm^2. Testing was performed at 23 °C and constant relative humidities of 35%, 50%, 75%, and 90%. At least four samples of each type of film produced were measured. Transmission rate values are reported as oxygen permeability coefficient in $(m^3 \cdot m)/(m^2 \cdot s \cdot Pa)$, calculated as in **Equation 3.1**.

3.2.4.2. Oxygen diffusivity

Continuous permeation experiments were carried out to determine the oxygen diffusion coefficient (*D*) using the OX-TRAN® equipment. Taking the transmission rate values measured during the unsteady state, the value of *D* was assessed from the solution to Fick's second law for the boundary conditions of an isostatic permeation experiment by minimizing the root mean square deviations between simulated and experimental data (Gavara and Hernandez, 1993):

$$\frac{F_t}{F_\infty} = \frac{4}{\sqrt{\pi}}\left(\sqrt{\frac{l^2}{4Dt}}\right)\sum_{n=1,3,5\ldots}^{\infty} exp\left[-\frac{n^2 l^2}{4Dt}\right] \qquad (\mathbf{3.10})$$

where F_t/F_∞ denotes the flow of permeant exiting from the film through the surface exposed to the low permeant pressure environment at time *t* and after infinite time (equilibrium).

3.2.5. Carbon dioxide permeability

The carbon dioxide permeation rates of the materials were determined at 35%, 50%, and 75% RH and 23 °C using an isostatic permeation test (Gavara et al., 1996). In brief: a stainless-steel cell with two chambers separated by the film to be tested was used. A constant gas stream was passed through each chamber. The permeant gas, carbon dioxide, flowed through the upper chamber while the carrier gas, nitrogen, flowed through the

lower chamber (both flow streams at the required relative humidity) and drove the permeated molecules to the detector system. To humidify the gases, the gas streams bubbled through a gas washing bottle filled with water and then mixed with a second stream of dry gas. Flowmeters (Dakota Instruments, Orangeburg, USA), needle valves (Swagelok, Solon, OH, USA), and digital hygrometers were used to adjust and control the gas streams. At the exit from the lower chamber, the carrier gas flow rate was measured by a mass flowmeter (Dakota Instruments, Orangeburg, USA). The concentration of CO_2 in this stream was analyzed by gas chromatography. An HP5890 gas chromatograph (Agilent Technologies, Barcelona, Spain) equipped with a manual injection valve and a 500-µL injection loop, a Chromosorb 102, 80/100 mesh, 12'×1/8" column (Teknokroma, Barcelona, Spain), and a thermal conductivity detector were used. The GC was calibrated by injecting known amounts of carbon dioxide (r^2 = 0.9993). Once the cell had been assembled, the carrier gas was passed through both chambers for at least 24 h to remove all gases present in the cell during handling and equilibrate the film to the humidity of the test. At time zero, the permeant gas started to flow into the upper chamber. The concentration of carbon dioxide in the lower chamber was monitored until constant, that is to say, until the steady state was established. The gas permeability (P) was calculated as follows:

$$P = \frac{c_{CO_2} \cdot f \cdot l}{A \cdot \Delta P} \qquad (\mathbf{3.11})$$

where c_{CO_2} is the volume concentration of CO_2 in the steady state, f is the carrier gas flow in m^3/s, l is the film thickness in m, A is the film area in m^2, and ΔP is the difference in the partial pressure of CO_2 in the stationary state between the two chambers, measured in Pa.

3.3. RESULTS AND DISCUSSION

The control and cinnamaldehyde-treated films were very transparent, without discontinuities, and flexible. A full description of optical, morphological, and mechanical properties of the films obtained has already been reported (Balaguer et al., 2011b).

3.3.1. Water vapor mass transport properties

3.3.1.1. Water vapor permeability

Permeability is an intensive magnitude related to the transmission rate of a permeant through a resisting material which involves a multi-mode process. First, the permeant molecules dissolve in the film matrix on the high-concentration side; second, they diffuse through the film, driven by a permeant concentration gradient; and third, they desorb and evaporate from the other side of the film (Kester and Fennema, 1986). Thus the permeability coefficient (*P*) incorporates the solubility coefficient (*S*), corresponding to the thermodynamic component involved in the sorption and desorption processes at the matrix surfaces, and the diffusivity coefficient (*D*), corresponding to the kinetic component that describes molecular movement in the bulk of the polymer material:

$$P = D \cdot S \qquad (\mathbf{3.12})$$

This definition applies only when Fick's and Henry's laws fully apply, that is, when the diffusion coefficient is constant, and the sorption isotherm is linear. However, for most biomaterials, water vapor interacts strongly with the polymer, which results in diffusion and solubility coefficients dependent on the water vapor partial pressure. Thus, in this case, a layered-like material appeared as a consequence of the water vapor entrance, and the term permeability would be erroneously applied, since the mass transport properties varies throughout the film thickness, in contrast with homogeneous materials (Schwartzberg, 1986). However, for comparison purposes transmission rates were multiplied by the film thickness (and divided by the relative humidity gradient). To better apply this assumption the films were selected with a thickness of 110 μm ± 10 to minimize its effect. Therefore, water vapor permeability of hydrophilic films is a characteristic of the film-permeant couple under given environmental conditions (i.e., % relative humidity and temperature) (Kester and Fennema, 1986).

Water vapor permeabilities obtained at 23 °C and at relative humidity gradients of 35–0%, 50–0%, 75–0%, and 90–0% are shown in **Figure 3.1.** The values of water vapor permeability coefficients for the gliadin films ranged from $0.66 \cdot 10^{-14}$ to $33.9 \cdot 10^{-14}$ (kg·m)/(m^2·s·Pa) and were dependent on the cross-linking degree and on the humidity to which the film was

exposed (the concentration of the permeant on the surface in contact with the high-humidity environment).

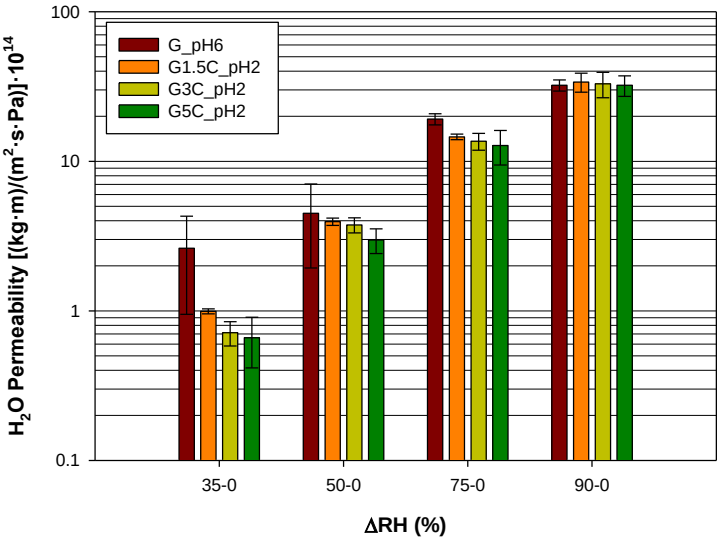

Figure 3.1. Water vapor permeability coefficients of gliadin films at different relative humidity gradients and 23 °C.

Increasing the relative humidity gradient from 35–0% to 90–0% raised permeability around 50-fold for all the types of films. This was due to the hydrophilic behavior of gliadin films, conferred by their high content of amide groups (~40%), which establish hydrogen bonds with water molecules, and, to a lesser extent, by the presence of the glycerol added, which either plasticizes or retains water, owing to its intensely hygroscopic character. As environmental humidity increases, the amount of water dissolved in the biopolymer increases more than the proportionality expressed by Henry's law, deviating positively, as shown below. Also, the entry of water molecules and their interaction with the amide groups of the polymer progressively reduce the cohesive energy of the polymer through interchain hydrogen bonds, resulting in plasticization of the matrix and increasing the diffusion coefficient. Consequently, permeability of water vapor through these hydrophilic film matrices increases greatly as the relative humidity to which the film is exposed is raised. This behavior has been largely observed in protein and carbohydrate films (Fabra et al., 2012; Gontard et al., 1993; Hambleton et al., 2012; Lai and Padua, 1998).

When the gliadin films were cross-linked with cinnamaldehyde, water vapor permeation resistance improved in comparison with the gliadin control film, G_pH6. The greater the amount of cinnamaldehyde added, the higher the water vapor barrier of the treated film. In this way, a reduction of 75% in water vapor permeability coefficient at a relative humidity gradient of 35–0% was achieved for the film cross-linked with 5% cinnamaldehyde (G5C_pH2) in comparison with the control film (G_pH6). This reduction in permeability gradually diminished as the relative humidity gradient increased.

Since water vapor sorption was similar for all the films evaluated in the relative humidity range studied, as will be shown in section 4.3.1.3., the reduction in permeability might be attributable to the formation of a more reticulated polymeric network that imposes restraints on chain mobility and reduces diffusivity. The diminishing difference in the water vapor barrier of the cinnamaldehyde-treated films in comparison with the control as the relative humidity increases might be related to the substantial water uptake of gliadin films. In hydrophilic matrices, water acts as a plasticizer, reducing intermolecular interactions, increasing free volume, and prompting polymer chain mobility, which raises permeability in all the films despite the higher cross-linking degree achieved. This effect is more important as the humidity increases, decreasing the effect of the constraints imposed by the cross-links.

Although the values obtained for water vapor permeability are in all cases higher than for those for good water vapor barriers such as polyolefin, they are indicative that this treatment can improve water resistance at low relative humidities, and therefore it might be sufficient to protect food for short-term applications, which is in accordance with the biodegradable properties of the film and its intended uses.

Important remarks on the method used. An important point that should be highlighted is that since the method involves different relative humidity conditions on each side of the film, a water concentration gradient appears across the film thickness. Thus, on the side exposed to high relative humidity the water sorbed produces considerable plasticization of the film, favoring chain mobility, but on the other side, at low relative humidity, a different behavior controlled by small movements of water molecules in a rigid chain structure is more feasible. Consequently, regions could appear below and above the T_g, owing to the different moisture contents, which completely changes the diffusion mechanism. Therefore the diffusion mechanism obtained by **Equation 3.8** would be an average of all

these film states, and the diffusion coefficient calculated should be considered as an apparent diffusivity.

Another important point is that the dependence of water concentration on the water vapor permeability was evaluated by varying the relative humidity on only one side of the film, owing to the method used, which imposes 0% RH on one of the sides. Consequently, the gradient in water partial pressure (ΔP) across the film (the driving force) was fixed at 0.98, 1.40, 2.11, and 2.53 MPa for the relative humidity gradients of 35–0%, 50–0%, 75–0%, and 90–0%, respectively, at 23 °C. However, it must be emphasized that identical pressure gradients at different high and low humidities (i.e. 100–50% instead of 50–0%) would have resulted in different permeability values, since the gradient water content would be different. Consequently, the relative humidity gradient to which the film is exposed should be stated when water vapor permeability values are given.

3.3.1.2. Activation energy of water vapor permeability

Water vapor permeability was evaluated at different temperatures in the range of 10 to 40 °C for a fixed relative humidity gradient of 50–0% for the most cross-linked film (G5C_pH2) and for the film without cross-linking (G_pH6) and the logarithms of the *P* values are plotted versus the reciprocal of the absolute temperature in **Figure 3.2**. When the temperature increased, the water vapor permeability also increased, as occurs in every kinetic process. In the whole temperature range, the control film presented higher water vapor permeabilities than the cinnamaldehyde-treated film. The previously mentioned reduction in chain mobility imposed by cross-linking might be mainly responsible for this reduction in *P*.

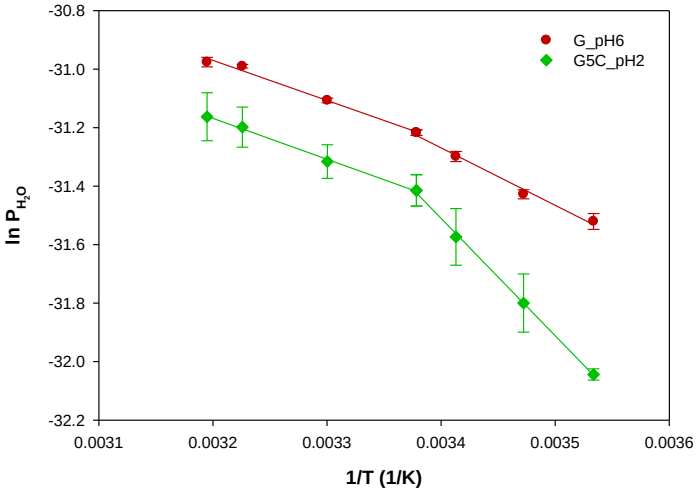

Figure 3.2. Effect of temperature on water vapor permeability of gliadin films at a relative humidity gradient of 50–0%.

The activation energy determined from the slope of the plots in **Figure 3.2** (**Equation 3.2**) represents an inherent property of a material in the presence of a specific gas or vapor. As can be seen, the permeability constant decreases from 40 to 23 °C and from 23 to 10 °C. At about 23 °C, there is a change in the slope of **Equation 3.2.** This discontinuous behavior of permeability with temperature has also been observed in pullulan-starch blends (Biliaderis et al., 1999), in natural rubbers (Doty et al., 1946), and in polyvinyl acetate (Meares, 1954), and might reflect changes in material structure due to thermal transitions such as crystallization or glass transition.

Table 3.1 shows E_p and P_0 calculated from the Arrhenius law (**Equation 3.2**) at both ranges. At the high temperature range, the activation energy is about 2.8 kcal/mol for both films. Below the transition point the decrease is faster but the activation energy differs from one film to the other. The E_p for the gliadin films treated with cinnamaldehyde doubled that of the control film, 8.0 compared with 3.9 kcal/mol. This demonstrates that cross-linking decreases permeability by increasing activation energy, but its effect is more noticeable at lower temperatures.

Table 3.1. Water vapor permeability parameters of Arrhenius fitting.

Sample	E_p (kcal/mol)		P_0 [(kg·m)/(m²·s·Pa)]	
	High T	Low T	High T	Low T
G_pH6	2.71 ± 0.23	3.90 ± 0.19	$2.93 \cdot 10^{-12}$	$2.15 \cdot 10^{-11}$
G5C_pH2	2.78 ± 0.29	7.98 ± 1.19	$2.76 \cdot 10^{-12}$	$4.08 \cdot 10^{-8}$

From the permeability definition (**Equation 3.12**), E_p is the sum of the activation energy for diffusion (E_d) and the heat of solution (ΔH_s):

$$E_p = E_d + \Delta H_s \qquad (\mathbf{3.13})$$

The diffusion of a gas molecule through a membrane is considered a thermally activated process following the Arrhenius law, and E_d is always positive since the diffusion coefficient always increases with temperature. Hydrophilic polymers, however, tend to have lower E_d values, owing to the lower activation energy for water diffusion in a swollen polymer network (Barrie, 1968). E_d is usually higher at temperatures above T_g since the diffusion process is controlled by long-range motions of polymer chains that have larger activation energies, while below T_g diffusion is controlled by local motions of the polymer and movement of water (Barrie, 1968). Therefore, above T_g polymer segments become more mobile and oscillate with greater freedom from inter-polymer constraints, forming vacant spaces or "holes" with greater frequency and facilitating water diffusion (Kumins et al., 1957). Typical E_d values of gases and vapors migrating through polymers are in the range of 0 to 18 kcal/mol (Doty et al., 1946; Meares, 1954).

Solubility is a two-step process. The first step involves condensation of the gas molecule in the polymer, followed by the creation of molecular-scale "holes" to accommodate the gas molecules. Thus, ΔH_s can be expressed as the sum of heat condensation, ΔH_c, and the heat of mixing, ΔH_m:

$$\Delta H_s = \Delta H_c + \Delta H_m \qquad (\mathbf{3.14})$$

For condensable vapors such as water, ΔH_c is negative (–44.17 kJ/mol at 20 °C), while ΔH_m is positive for hydrophobic polymers, since the interaction between the gas molecule and the polymer is weak, and near zero or negative for hydrophilic polymers, so that an increase in temperature causes a decrease in solubility. Thus, if the absolute value of ΔH_s becomes higher than E_d, E_p could be negative for hydrophilic polymers (Shogren, 1997). For proteins, ΔH_s values fall in the range of 0 to –7 kcal/mol, and they are dependent on the number of water molecules sorbed (the first molecules of water sorbed release a higher amount of heat) (McLaren and Rowen, 1951), but, as far as we know, no studies report its behavior in the thermal transitions that occur in proteins.

Generally, gases migrating through films have E_p values of 3 to 15 kcal/mol (Donhowe and Fennema, 1994). The greater the E_p of a film, the more sensitive its permeability to temperature changes. Since the E_p values obtained for water vapor permeating through the gliadin films were in the range of 3 to 8 kcal/mol, the water vapor permeability was not highly temperature-dependent, especially at higher temperatures. This behavior implies that temperature fluctuations do not have a significant impact on water vapor permeability, which is a favorable property in terms of storage (packaging).

As **Figure 3.2** shows, with cross-linking an increase in E_p was observed, especially at low temperatures. This effect should have been anticipated since, on the one hand, the formation of a more compact structure could result in a reduction of $-\Delta H_s$ because more heat has to be supplied to separate the chains surrounding the free volume cavities where sorption takes place, hence a lower amount of heat is liberated; and, on the other hand, the inclusion of covalent bonds between protein chains results in a more rigid structure that increases E_d, since a higher amount of energy is needed to confer mobility to the polymer chains. The effect is greater at lower temperatures because, despite the fact that in this region most of the polymer segments are prevented from oscillating by strong bonding forces, it is feasible that if the segments are weakly bonded to each other they may take part in "hole" formation if sufficient energy is available to the system. If there are no constraints the inter-segmental forces are weak and consequently E_d for a non-cross-linked film is lower. The same effect has been reported for unplasticized films (Kumins et al., 1957).

The increase in E_p with cross-linking was also in accordance with the increase in the P_0 term for the range at lower temperatures. This pre-exponential factor represents the probability of a water molecule colliding with a protein macromolecule (Stenesh, 1993). This suggests that a denser structure may occur in the cross-linked films as compared with the control, whose lower cohesive energy reduces the flow resistance to permeating molecules (Birley et al., 1992). At higher temperatures, the protein chains become flexible and the difference in water permeation imposed by cross-linking is less relevant.

The unusual reduction in E_p at higher temperatures and its equality for both matrices might be indicative of a high increase in $-\Delta H_s$ that compensates the possible increase in E_d. The thermal expansion of the matrix with temperature is reflected as an increase in

free volume that facilitates water vapor entry, reducing the amount of energy needed to open the matrix, which results in a higher amount of energy released.

There are some important features of the method used that should be mentioned. Although the relative humidity gradient was constant (50%–0% RH), the temperature increase produces an increase in gradient partial pressure (**Table 3.2**). Although this change is taken into account when calculating the values of water vapor permeability in **Equation 3.1**, in the case of hydrophilic films this implies a modification of the water content of the film. This makes it difficult to distinguish clearly between the contributions of the change of intrinsic transport properties of the material with temperature, and the apparent increase in water vapor transport rates due simply to the higher water vapor pressure at higher temperatures (or the consequent increase in water gained by the polymer); that is to say, in the experiments presented in this work, temperature-dependent effects on mass transport phenomena were not separated from concentration-dependent effects.

Table 3.2. Gradient of water vapor partial pressures across the film (driving forces imposed) for a relative humidity gradient of 50-0% as a function of temperature.

T (°C)	P_v (MPa)	ΔP (MPa) at 50–0% RH
10	0.00123	0.00061
15	0.00170	0.00085
20	0.00234	0.00117
23	0.00281	0.00140
30	0.00424	0.00212
37	0.00627	0.00314
40	0.00737	0.00369

3.3.1.3. Water vapor solubility

Water vapor sorption isotherms in the gliadin films were determined gravimetrically at 20 °C. The equilibrium water content expressed as a percentage of the dry weight of the sample is shown as a function of relative humidity in **Figure 3.3**. Sorption curves were typical of water vapor sensitive polymers, the initial portion of the isotherm being convex, and the final portion concave. The sorption levels were within the range reported for cellulose films and protein-based films (Cuq et al., 1997; Debeaufort et al., 1994; Park and Chinnan, 1995). The water content of the films remained low for relative humidities under

50% and increased sharply above 65%, as expected from the hydrophilic nature of these materials.

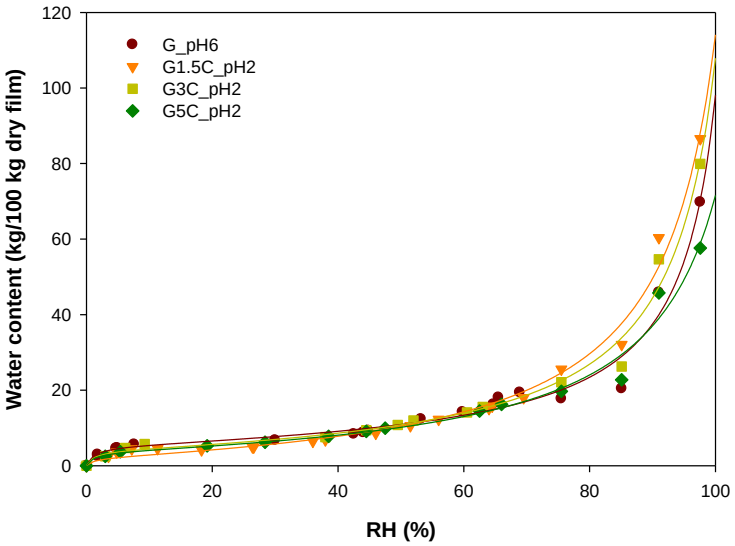

Figure 3.3. Water vapor sorption isotherms of gliadin films at 20 °C. Experimental points and theoretical curves obtained from D'Arcy and Watt equation fitted with *K* parameters from **Table 3.3**.

Cross-linking of the gliadin-based films had no significant effect on water sorption at low relative humidities. The effect of cinnamaldehyde was only noticeable at relative humidities higher than 75%, where the films cross-linked with the higher amount of cinnamaldehyde sorbed a lower quantity of water. The formation of intermolecular covalent bonds between monomeric gliadins, leading to a polymerized network with a higher cross-linking degree, was responsible for the reduction in the capability of water sorption at higher relative humidities.

The amount of water sorbed by the cinnamaldehyde-treated films at pH 2 compared with the control film at pH 6, in the range of high relative humidities, indicates that the maintenance of the original pH of the film-forming solution prevents a higher interaction of water molecules with the matrix. This effect might be related to the proximity of the isoelectric point of the protein at pH 6. At pH 2, side-chain repulsions of induced net charges produce unfolding of the protein, rupture of hydrogen bonds, and alteration of hydrophobic interactions (Chourpa et al., 2006), increasing the number of water molecules

that could be held by the matrix. Only for the last point at 97.6% RH was the effect of cross-linking with 5% cinnamaldehyde enough to reduce the amount of water sorbed compared with the control.

Similar results were observed in a previous study for the water uptake of films immersed in water, where water uptake by gliadins reduced with the concentration of the cross-linking agent. In contrast, control films lost their integrity in liquid water (Balaguer et al., 2011b). The values obtained for liquid water uptake after 24 h of immersion (around 72%, 55%, and 48%, for G1.5C_pH2, G3C_pH2, and G5C_pH2, respectively) are lower than those obtained for water vapor sorption (around 87%, 80%, and 58%, for G1.5C_pH2, G3C_pH2, and G5C_pH2, respectively, at a RH of 97.6%), probably owing to erosion of the film surface and loss of glycerol, reducing the capability to absorb more liquid water.

The sorption isotherms were adjusted to different models and the best fit was found for the D'Arcy and Watt equation (**Equation 3.4**) (D'Arcy and Watt, 1970). This model considers that sorbed water may be associated with polar side chains, with peptide and amide groups at low humidities, while at high humidities a portion of water uptake constitutes a hydrogen-bonded network. At low humidities the amount of water associated with each polar group of the protein matrix is described by an isotherm of the Langmuir type (first term of the equation), and water associated with peptide bonds is linearly related to the relative vapor pressure (second term of the equation). At high humidities the average mobility of the water increases and a hydrogen-bonded network is formed, resulting in water multilayers. Much of the water in this network will probably be associated with other water molecules at sorption sites and is unlikely to be directly associated with the substrate (third term of equation) (D'Arcy and Watt, 1970).

The sets of values for the *K* parameters in **Equation 3.4** that provided the best fits to the experimental points are given in **Table 3.3**. **Figure 3.4** represents the contributions of each term of the D'Arcy and Watt equation in the water vapor sorption isotherm of the control film, G_pH6, as an example. As can be observed in the inset graph, the Langmuir contribution is very important in the initial part of the isotherm and it becomes less important as the a_w increases. K_1 and K_2 are related to the number of active sites and the bonding energy involved in the Langmuir adsorption isotherm. The drop in the values of K_2 observed with the increasing cinnamaldehyde content implies a reduction of the active sites available, which is in accordance with the tendency to a closer, denser matrix as the

cinnamaldehyde content increases. The term represented by the Henry's law contribution, corresponding to the solubility of the penetrant in the solid, was never predominant in the isotherms. This term took a small value in the control film, G_pH6, while it was negligible for the treated polymer. Finally, the term including the deviations was dominant on the extreme right of the isotherm. The parameters K_4 and K_5 are related to the substrate capacity and bonding energy of the formation of multilayers. The absolute value of this term reduced as the cross-linking degree increased, although it was greater than that of the untreated gliadin matrix, probably owing to the previously mentioned pH effect.

Table 3.3. Water isotherm parameters fitting D'Arcy and Watt equation.

Sample	K_1	K_2	K_3	K_4	K_5	RMSE
G_pH6	75.7972	0.0520	0.0197	0.9437	0.0543	0.0138
G1.5C_pH2	75.7994	0.0507	0	0.9183	0.0997	0.0108
G3C_pH2	75.7990	0.0408	0	0.9294	0.0789	0.0118
G5C_pH2	75.7933	0.0367	0	0.8926	0.0818	0.0095

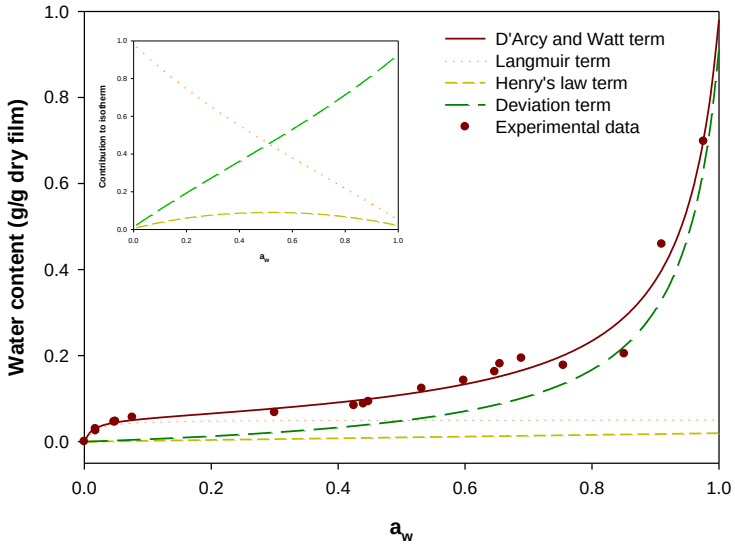

Figure 3.4. Contribution of Langmuir term, Henry's law term, and deviation term of D'Arcy and Watt equation to the water vapor sorption isotherm for G_pH6 film. **Inset graph**: Relative contributions of each term.

For water activities above 0.65 there is a step increase in the slope of the isotherm, suggesting the existence of moisture as unbound water. It is said that for hydrophilic films

clustering may be expected if the number of water molecules is greater than the quantity that can be bound to the polymer. The range of water activities in which the self-association of water molecules occurs can be determined from an isotherm sorption model by applying the clustering function developed by Zimm and Lundberg (Zimm and Lundberg, 1956). They suggested that the first water molecules to enter the polymer structure loosen the structure and make it easier for subsequent molecules to enter the neighborhood of the first rather than to go elsewhere. The value of G/ϕ_w is calculated as a function of a_w, applying **Equation 3.5** to the sorption isotherm model of the D'Arcy and Watt equation (**Equation 3.4**) and substituting the values of the *K* parameters.

The function $1 + G/\phi_w\,(1 - \phi_w)$ represents a measure of the cluster dimension. A value greater than 1 indicates the formation of water aggregates. In **Figure 3.5**, values of the cluster dimension in number of water molecules aggregated are reported as a function of water activity. A minimum value for the function can be observed for water activities around 0.05, after which the values increase steadily. Water molecules tend to cluster for water activities of 0.55 for G_pH6 and 0.47 for G5C_pH2. The higher cohesiveness among the chains of cross-linked gliadin compared with control gliadins might make the active sorption sites less accessible for water-binding molecules, thus favoring the self-association of water molecules at lower water activities. Similarly, the dimension of water clusters at high a_w is greater when the film is not cross-linked (8 molecules versus 5 molecules), owing to the higher swelling of the control film, which allows a larger number of molecules to enter the matrix.

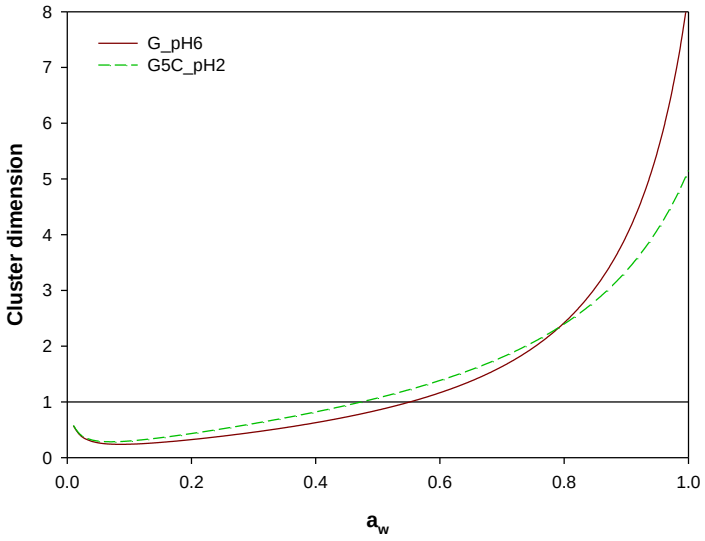

Figure 3.5. Dimension of water clusters as a function of water activity for gliadin films.

3.3.1.4. Water vapor diffusivity

The effective water vapor diffusion coefficients (D_{H_2O}) of the gliadin films at 20 °C were calculated by applying the Crank solution of Fick's second law for a plane sheet with the initial and boundary conditions of the gravimetric experiment (**Equation 3.8**). Fitting was optimized by minimizing the root mean square deviations between experimental and theoretical values of the water vapor sorption kinetic curves. Although the diffusion coefficient might vary with the relative humidity of the experiment, as already commented in the permeability results, the sorption experiment was made by steps, with small changes in the relative humidity in each experiment, and therefore a constant (apparent) diffusion coefficient can be assumed for each individual test. ∞

Figure 3.6 shows the experimental data of various water sorption kinetics tests measured with the electrobalance at different relative humidities for the film G5C_pH2. The values of D_{H_2O} calculated at different average relative humidities for the various gliadin films are shown in **Figure 3.7**. D_{H_2O} was concentration-dependent, varying with the average relative humidity, resulting in a bell-like curve. This behavior was also described for wheat gluten thermoformed films (Angellier-Coussy et al., 2010), for wheat starch biocomposite materials (Chivrac et al., 2010), and for hydrophilic synthetic polymers such as nylon–6

(Hernandez and Gavara, 1994). This evolution of D_{H_2O} with relative humidity might be related to changes in the mobility of polymer chains due to the plasticizing effect of water, and to the formation of clusters and saturation of polymer-free sites. The values obtained were in the range of $1 \cdot 10^{-14}$ to $20 \cdot 10^{-14}$ (m^2/s). Higher cross-linking degrees (G5C_pH2 > G3C_pH2 > G1.5C_pH2) resulted in a reduction in the water vapor diffusion coefficient. This highlights the formation of a more reticulated matrix with the addition of greater amounts of cinnamaldehyde. Thus the restraints imposed on the mobility of polymeric chains and the increase in the tortuosity of the path that permeant molecules had to follow owing to these new entanglements slowed down the effective diffusion.

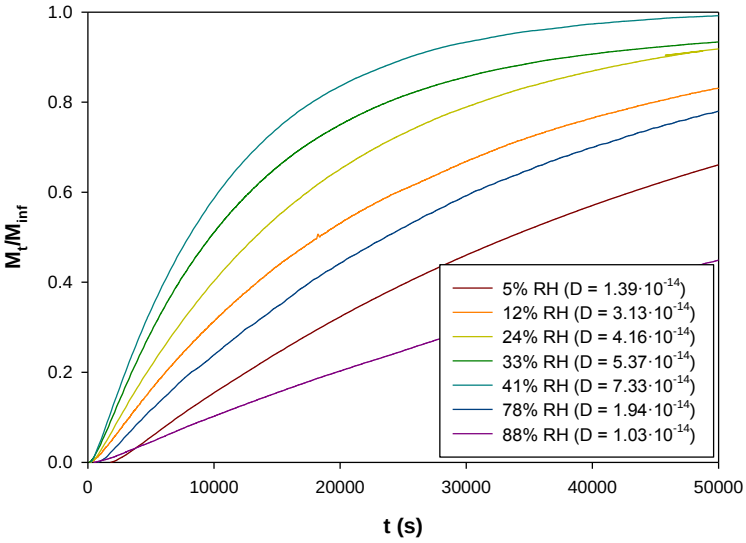

Figure 3.6. Experimental water vapor mass ratio entering G5C_pH2 film versus time obtained from the water sorption kinetic experiments at different mean relative humidities and the corresponding calculated diffusivities.

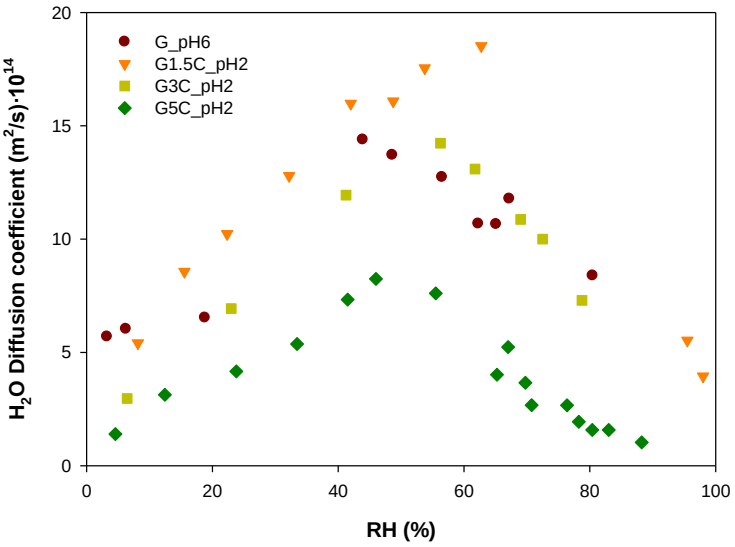

Figure 3.7. Effective diffusion coefficients of water vapor through gliadin films at 20 °C as a function of mean relative humidity.

When the gliadin films were not cross-linked (G_pH6), a D_{H_2O} value of about $6 \cdot 10^{-14}$ (m^2/s) was measured at low humidities, increasing with humidity to a maximum value near $15 \cdot 10^{-14}$ (m^2/s) at intermediate RH values. Then, coinciding with the formation of water clusters, D values decreased to values below $10 \cdot 10^{-14}$ (m^2/s) as the water clusters became larger. Similar profiles were observed for other materials. Roca et al. (2008) reported that the value of D_{H_2O} can be underestimated if the swelling due to water uptake is not considered. Nevertheless, a negligible thickness gain (less than 1.6%) was shown for the most cross-linked matrix after immersion in liquid (Balaguer et al., 2011a).

The maximum value of D_{H_2O} was observed at relative humidities of 48%, 55%, and 64%, for G5C_pH2, G3C_pH2, and G1.5C_pH2, respectively. The shift of this maximum with the cross-linking degree indicates a complex mechanism for water vapor diffusion that involves, on the one hand, cluster formation that reduces the diffusion rate owing to the greater dimension of the permeant cluster created, and, on the other hand, a plasticization effect of the polymeric matrix that reduces the interchain attractive forces and increases the free volume, which leads to an increase in the diffusion rate.

3.3.1.5. Mechanism of water vapor transport

The mechanism of water vapor transport through the films was evaluated by applying **Equation 3.9**. Independently of the relative humidity, exponent *n*, which describes the different cases of diffusion-controlling mechanisms, was found to be around 0.8–0.9. This means that the rate of diffusion of the penetrant molecule is comparable with the rate of the relaxation processes. This non-Fickian or anomalous diffusion is a consequence of the nature of the penetrant molecule, which is also what causes the swelling of the polymer and the relaxation processes. However, for higher relative humidities, when a swollen network was observed, it was expected that a diffusion-controlling mechanism would be found (n = 0.5), since the polymer would be in the rubbery state and the chains would adjust so quickly to the presence of the penetrant that they would not cause diffusion anomalies and would follow Fick's law (Crank, 1975).

3.3.2. Oxygen mass transport properties

3.3.2.1. Oxygen Permeability

The oxygen permeability coefficients obtained at 23 °C and at different relative humidities of 35, 50, 75, and 90% are shown in **Figure 3.8**. The values of oxygen permeability for the gliadin films ranged from $0.5 \cdot 10^{-19}$ to $208 \cdot 10^{-19}$ $(m^3 \cdot m)/(m^2 \cdot s \cdot Pa)$. They were similar to oxygen permeabilities found for wheat gluten by other authors (Aydt et al., 1991; Gennadios et al., 1993b; Park and Chinnan, 1995).

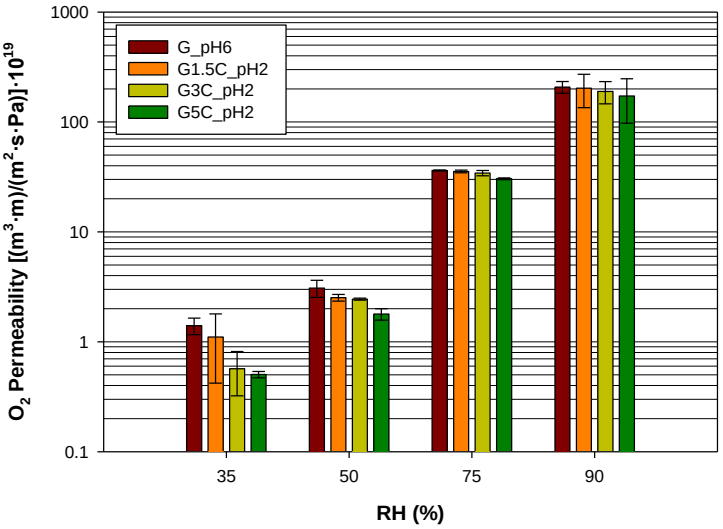

Figure 3.8. Oxygen permeability coefficients of gliadin films at different relative humidities and 23 °C.

The gliadin films presented very low oxygen permeabilities at low relative humidity compared with common polyolefin films (see **Table 3.4**). However, the variation in relative humidity had a strong influence on their barrier properties, raising the permeability 150-fold when the relative humidity was increased from 35% to 90% for the gliadin control film. This tendency was previously observed for other hydrophilic films (Gontard et al., 1996; McHugh and Krochta, 1994). This increase in oxygen permeability might be related to the higher content of sorbed water molecules, which interact with polar groups in the protein, mainly amide residues, and weaken the intermolecular and intramolecular hydrogen bonds, producing a plasticizing effect that facilitates segmental motion and thereby oxygen diffusion (see section 4.3.2.3.), but also to the increase in oxygen solubility, mostly in the water molecules sorbed by the matrix.

Table 3.4. Comparison of permeabilities to gases of some polymers used in food packaging.

Polymer	RH	P_{CO_2} [(m³·m)/(m²·s·Pa)]	P_{O_2} [(m³·m)/(m²·s·Pa)]	P_{CO_2}/P_{O_2}	References
Wheat gliadin	50%	$3.47 \cdot 10^{-18}$	$3.08 \cdot 10^{-19}$	11.26	Present study
	75%	$1.72 \cdot 10^{-17}$	$3.64 \cdot 10^{-18}$	4.7	
Wheat gluten	0%	$1.66 \cdot 10^{-19}$	$2.78 \cdot 10^{-20}$	6.0	Gontard et al. (1996)
	91%	$5.49 \cdot 10^{-16}$	$2.20 \cdot 10^{-17}$	24.9	
Sodium caseinate	11%	$1.28 \cdot 10^{-18}$	$1.68 \cdot 10^{-19}$	7.6	Fabra et al. (2012)
	85%	$1.91 \cdot 10^{-17}$	$2.53 \cdot 10^{-18}$		
Chitosan	0%	$1.93 \cdot 10^{-20}$	$3.49 \cdot 10^{-20}$	0.8	Kurek et al. (2012)
	96%	$4.13 \cdot 10^{-18}$	$5.32 \cdot 10^{-20}$	11.1	
PE	0%	$2.68 \cdot 10^{-16}$	$4.18 \cdot 10^{-17}$	6.4	Pascat (1986) at 30 °C
PP		$6.99 \cdot 10^{-17}$	$1.75 \cdot 10^{-17}$	4.0	
PS		$6.69 \cdot 10^{-17}$	$8.33 \cdot 10^{-18}$	8.0	

The cross-linking of the gliadin films reduced the oxygen permeability by up to 64% at 35% RH, comparing the most cross-linked film, G5C_pH2, with the control, G_pH6. This reduction was proportional to the amount of cinnamaldehyde added. Nevertheless, despite the cross-linking, the oxygen barrier properties decreased as relative humidity increased, as occurred in the case of water vapor. As with water vapor transport, at high relative humidity the differences between treated and control films decreased and a reduction of 17% was observed between the most cross-linked film and the control at 90% RH.

3.3.2.2. Activation energy of oxygen permeability

Oxygen permeability was evaluated at different temperatures in the range of 10 to 40 °C for a fixed relative humidity of 50% for the most cross-linked film (G5C_pH2) and for the film without cross-linking (G_pH6) (**Figure 3.9**). In the whole temperature range, the control film presented higher oxygen permeability than the cinnamaldehyde-treated film. As expected, when the temperature increased, the oxygen permeability increased exponentially. This temperature effect is due to the thermal expansion of the polymer, to the enhancement of chain mobility, and to an increased energy level of the permeating molecules with temperature. The good fit obtained between experimental data and **Equation 3.2** (evidenced by the determination coefficients, R^2, of 0.9984 and 0.9936 for G_pH6 and G5C_pH2, respectively) indicates that the oxygen permeability obeys the Arrhenius relationship. The activation energy values calculated were around 13 kcal/mol, which is in the range for most common gases diffusing through films (3–15 kcal/mol (Donhowe and Fennema, 1994)), and they were comparable to those obtained for films

made from wheat gluten (11.9 kcal/mol), corn zein (11.1 kcal/mol) (Gennadios et al., 1993b), or whey protein (10.9–12.1 kcal/mol) (Hong and Krochta, 2006). The higher value of oxygen permeability activation energy indicates that oxygen permeability is more sensitive to temperature than water vapor permeability.

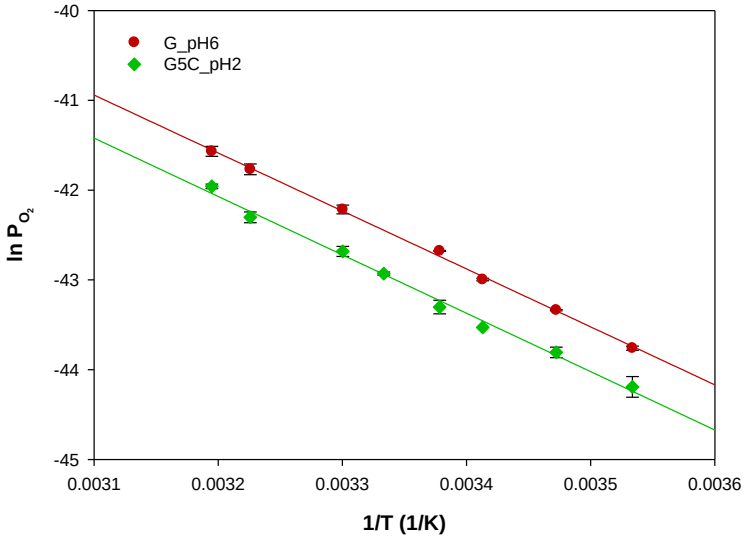

Figure 3.9. Effect of temperature on oxygen permeability of gliadin films at a relative humidity of 50%.

Arrhenius plots can be used to locate glass transition temperatures (T_g). For some polymeric materials, a discontinuity occurs in the relationship between oxygen permeability and temperature, seen as a change in the slope of the Arrhenius plot and as an increase in oxygen permeability above T_g (Biliaderis et al., 1999; Compañ et al., 1993; Meares, 1954). No such change was noticed in our case, indicating that no phase transition from a glassy to a rubbery state occurred within the range studied (10–40 °C) at 50% RH.

The cross-linking of the gliadin films did not greatly change the temperature-dependence of the oxygen permeability, since the activation energies were very similar for both films: 12.83 kcal/mol for G_pH6 and 12.92 kcal/mol for G5C_pH2.

The comparison of the changes produced in oxygen permeability when relative humidity or temperature were modified indicated that oxygen mass transport properties are more

dependent on the water content of the film than on temperature, which was also observed by Hong and Krochta (Hong and Krochta, 2006).

3.3.2.3. Oxygen diffusivity

The effective oxygen diffusion coefficients (D_{O_2}) of the gliadin films at 23 °C and at different relative humidities were calculated by applying the Crank solution of Fick's second law for a plane sheet with appropriate initial and boundary conditions (**Equation 3.10**) by minimizing the root mean square deviations between experimental and theoretical values of oxygen mass ratios through gliadin films versus time obtained from the continuous mode experiments (**Figure 3.10**). Since the model used was not representative of a prevailing mechanism of oxygen transport, the diffusion coefficient identified was considered as an apparent diffusivity.

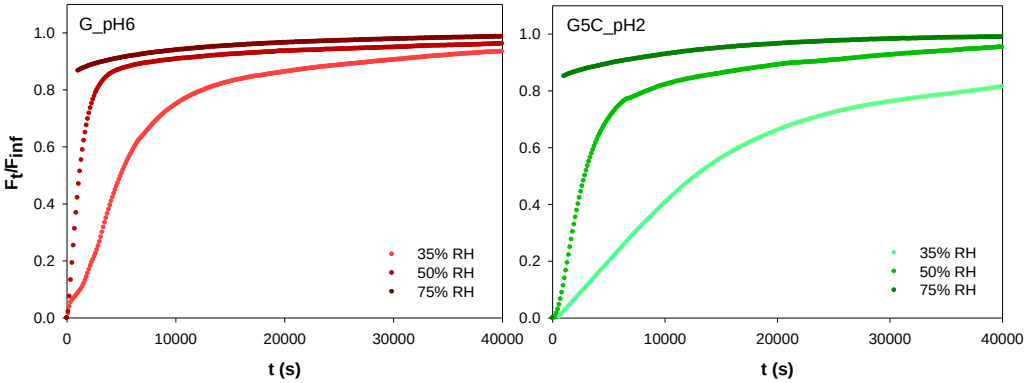

Figure 3.10. Experimental oxygen flow ratio through gliadin films versus time obtained from the continuous mode experiments as a function of relative humidity.

The values of D_{O_2} calculated at 35%, 50%, and 75% RH for the control film, G_pH6, and the most cross-linked gliadin film, G5C_pH2, are shown in **Figure 3.11**. The value of D_{O_2} at 90% RH could not be obtained because of the fast kinetic, which prevents measurement of the first points.

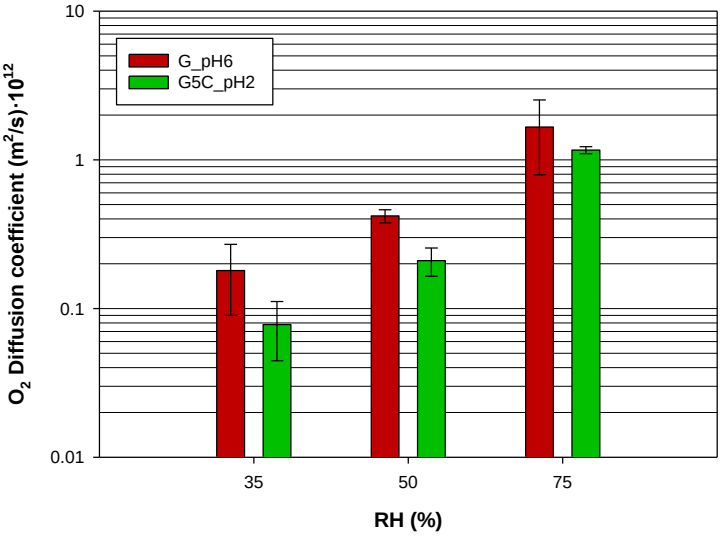

Figure 3.11. Effective diffusion coefficients of oxygen through gliadin films at 23 °C as a function of relative humidity.

D_{O_2} increased by one order of magnitude when relative humidity increased from 35% to 75%, which is in accordance with the general rule established for hydrophilic films: the diffusion coefficients for low molecular weight penetrants are roughly proportional to their diffusivity in water multiplied by the volume fraction of water in the film (Schwartzberg, 1986). Moreover, the higher water content at higher relative humidities has a plasticizing and/or swelling effect on the polymer network. A weakening of polymer-polymer interactions occurs, owing to the absorbed water molecules that interact with polar groups of the protein. Consequently, this causes widening of the path that the oxygen molecules have to follow and an increase in polymer chain mobility, which results in a much higher effective diffusion.

The D_{O_2} values obtained were in the range of $7.8 \cdot 10^{-14}$ to $1.66 \cdot 10^{-12}$ (m^2/s). At 50% RH they had a value similar to that of EVOH plasticized with 20% glycerol (López-de-Dicastillo et al., 2010).

The cross-linking of the gliadin matrix gave rise to a reduction in the oxygen diffusivity value in the entire humidity range studied, as a consequence of the creation of new joints that produce structural constraints, which hampers the mobility of polymeric chains and intensifies the tortuosity of the permeant path.

3.3.3. Carbon dioxide mass transport properties

3.3.3.1. Carbon dioxide permeability

Carbon dioxide permeability was evaluated at different relative humidities for the most cross-linked film (G5C_pH2) and for the control film (G_pH6). **Figure 3.12** shows the values of the permeability coefficients for CO_2. An exponential increase with relative humidity was observed for both films, being more acute for the control film, G_pH6. The values obtained ranged from $6.6 \cdot 10^{-19}$ to $1.7 \cdot 10^{-17}$ $(m^3 \cdot m)/(m^2 \cdot s \cdot Pa)$. They are within the range of other biopolymers such as chitosan ($4.3 \cdot 10^{-18}$ $(m^3 \cdot m)/(m^2 \cdot s \cdot Pa)$ at 96% RH (Kurek et al., 2012)), sodium caseinate ($2.13 \cdot 10^{-17}$ $(m^3 \cdot m)/(m^2 \cdot s \cdot Pa)$ at 50% RH (Fabra et al., 2012)), and wheat gluten ($1.25 \cdot 10^{-17}$ $(m^3 \cdot m)/(m^2 \cdot s \cdot Pa)$ at 91% RH (Gontard et al., 1996)).

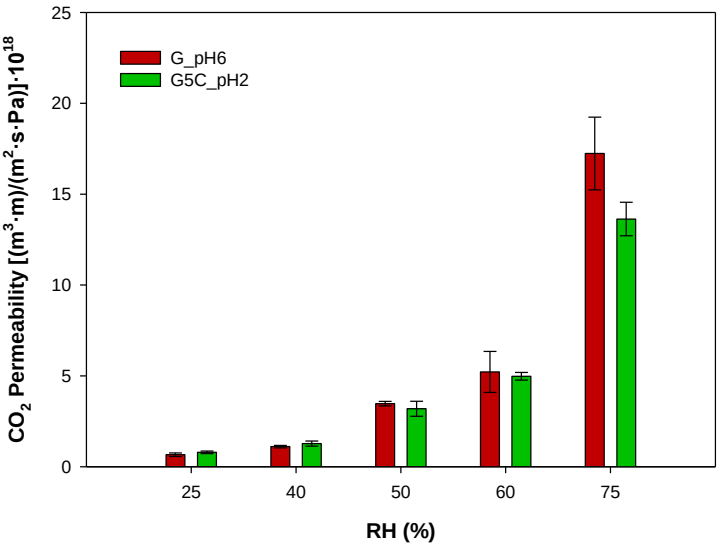

Figure 3.12. Carbon dioxide permeability coefficients of gliadin films at different relative humidities and 23 °C.

Contrary to what was found for water vapor and oxygen permeability, at low relative humidities no differences in carbon dioxide permeability were found, regardless of the degree of cross-linking. A clear reduction in carbon dioxide permeability was only achieved at 75% RH when gliadins were cross-linked with 5% cinnamaldehyde.

3.3.3.2. Permselectivity

Figure 3.13 shows oxygen and carbon dioxide permeabilities together in order to compare the tendency of permselectivity with water content. The ratio P_{CO_2}/P_{O_2} decreased from 17.8 at 50% RH (0.10 kg water/kg dry film) to 4.5 at 75% RH (0.20 kg water/kg dry film) for film G5C_pH2, and from 11.3 at 50% RH to 4.8 at 75% RH for film G_pH6 (0.11 and 0.20 kg water/kg dry film, respectively). Thus the gliadin films became less selective when relative humidity increased. The loss of permselectivity is in accordance with the loss of barrier properties of these films when relative humidity is high. The diminishing distinction between oxygen and carbon dioxide molecules might be a result of swelling of the film matrix at high relative humidities. The enlargement of the free space to permeate the molecules and the reduction of polymer-polymer interactions prevent the matrix from being selective. However, Gontard and co-authors found the opposite behavior, an increase in the P_{CO_2}/P_{O_2} ratio with relative humidity, for wheat gluten films, from 7 at 0% RH to 28 at 95% RH (Gontard et al., 1996). In a first attempt they tentatively explained this phenomenon in terms of sorption in the water trapped in the gluten protein network. In our opinion, however, although the solubility of carbon dioxide in water is greater than the solubility of oxygen in water (768 cm^3/L (Dodds et al., 1956) and 31.6 at 25 °C and 1 atm (Perry and Green, 1997), respectively), this relationship stays proportional throughout the relative humidity range, with a constant S_{CO_2}/S_{O_2} ratio of 24. Therefore the increase in carbon dioxide permeability with relative humidity cannot be completely explained by the carbon dioxide sorbed in the water contained in the film. In a second attempt, the authors suggested that the enhancement of carbon dioxide sorption observed could be explained by a structural modification of the protein matrix and by potential interactions between the film and the carbon dioxide (Pochat-Bohatier et al., 2006). We think that if these interactions occur a reduction in the effective permeability observed could be taking place, since some of the carbon dioxide that is expected to cross the film and be detected on the low concentration side would remain attached to the film matrix.

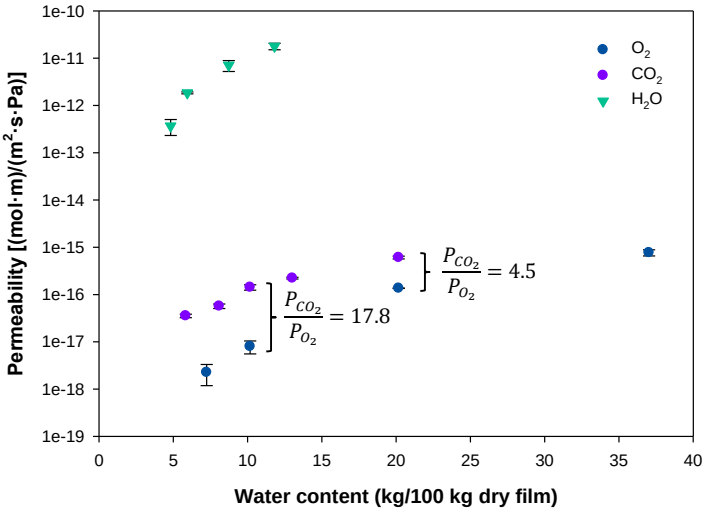

Figure 3.13. Comparison of permeability coefficients and permselectivity of G5C_pH2 film.

For most plastic films, carbon dioxide permeability is from 2 to 6 times greater than that of oxygen (Hernandez, 1997). Thus the gas selectivity coefficient is greater for gliadin films at relative humidities lower than 70%, but it remains in the same range for higher relative humidities.

Gas selectivity is related to some molecular parameters associated with mass transport properties. The oxygen molecule is smaller than the carbon dioxide molecule (2.98 and 3.34 molecular diameter (Å), respectively (Weast, 1987)), which translates into a higher diffusivity of oxygen in water in comparison with carbon dioxide ($2.94 \cdot 10^{-9}$ and $1.95 \cdot 10^{-9}$ (m^2/s) (EPA)). Although carbon dioxide diffusivity in the film was not analyzed, it is expected to be lower than that of oxygen according to the principle that the diffusion coefficients for low molecular weight penetrants are roughly proportional to their diffusivity in water multiplied by the volume fraction of water in the film (Schwartzberg, 1986). This difference in diffusivity should be even larger at high relative humidity, compensating the higher solubility of carbon dioxide in the polymer. Further studies are needed to determine the solubility of both molecules in films.

3.3.4. Potential of cinnamaldehyde as an improver of gliadin films barrier properties

An important achievement of the present work is that chemical modification of gliadins by means of cross-linking with an α,β-unsaturated aldehyde was able to reduce oxygen and

water vapor permeabilities simultaneously. Other strategies employed to improve the barrier properties of hydrophilic films, such as lipid addition, combination of layers, etc., lead to opposite effects in the barrier properties of gases and vapors, owing to their different affinity.

For example, lipid addition in sodium caseinate films reduced water vapor permeability but had the negative effect of increasing oxygen and carbon dioxide permeabilities, as shown in a work by Fabra et al. (2012). Coating polyethylene with chitosan to enhance its barrier against oxygen promoted its water vapor permeability, since the hygroscopic chitosan layer acts as a water reservoir on the polyethylene surface (Kurek et al., 2012)

3.4. CONCLUSION

Permeation of water vapor through hydrophilic films deviates substantially from the ideal behavior, and therefore the study of the mass transport properties of water vapor is a far more difficult task than the study of other gas permeants. A hydrophilic film exposed to a relative humidity gradient generates a non-linear profile of water concentration throughout the film's thickness, owing to the shape of the sorption isotherm. The amount of water sorbed strongly influences the state of the amorphous phase (rubbery or glassy), which changes the transport mechanism. Water diffusivities are concentration-dependent and are influenced by a high number of simultaneously occurring phenomena, such as plasticization of the matrix, water clustering, availability of free active sites, chain segmental motion, modification of free volume, etc.

An increase in temperature and/or relative humidity is accompanied by a loss in barrier properties, permeability being influenced more by relative humidity changes than by temperature changes, and oxygen permeability being more sensitive than water vapor permeability. It is difficult to distinguish between temperature-dependent effects and concentration-dependent effects on water vapor mass transport phenomena, because changes in temperature produce changes in water vapor concentration.

Consequently, environmental conditions during end-use applications must be considered in order to optimize the performance of these hydrophilic films.

The transport of various penetrants concurrently in the same direction or in opposite directions may induce different resulting permeabilities. Further studies are needed to clarify this.

Increasing the cross-linking degree by means of chemical modification with cinnamaldehyde seems a feasible way to improve the barrier properties of gliadin films produced by casting.

3.5. REFERENCES

Alfrey, T., Gurnee, E. F., and Lloyd, W. G. 1966. Diffusion in glassy polymers. *Journal of Polymer Science Part C: Polymer Symposia, 12*(1), 249-261.

Angellier-Coussy, H., Gastaldi, E., Gontard, N., and Guillard, V. 2010. Influence of processing temperature on the water vapour transport properties of wheat gluten based agromaterials. *Industrial Crops and Products*.

ASTM. 2005. D3985. Standard test method for oxygen gas transmission rate through plastic film and sheeting using coulometric sensor.

ASTM. 2006. F1249. Standard test method for water vapor transmission rate through plastic film and sheeting using a modulated infrared sensor.

Aulin, C., Gallstedt, M., and Lindstrom, T. 2010. Oxygen and oil barrier properties of microfibrillated cellulose films and coatings. *Cellulose, 17*(3), 559-574.

Aydt, T. P., Weller, C. L., and Testin, R. F. 1991. Mechanical and barrier properties of edible corn and wheat protein films. *Transactions of the American Society of Agricultural Engineers, 34*(1), 207-211.

Balaguer, M. P., Gómez-Estaca, J., Gavara, R., and Hernandez-Munoz, P. 2011a. Biochemical properties of bioplastics made from wheat gliadins cross-linked with cinnamaldehyde. *Journal of Agricultural and Food Chemistry, 59*(24), 13212-13220.

Balaguer, M. P., Gómez-Estaca, J., Gavara, R., and Hernandez-Munoz, P. 2011b. Functional properties of bioplastics made from wheat gliadins modified with cinnamaldehyde. *Journal of Agricultural and Food Chemistry, 59*(12), 6689-6695.

Barrie, J. A. 1968. Water in polymers. In *Diffusion in Polymers*, J.a.P. Crank, G.S., Ed. Academic Press: London; 259-308.

Biliaderis, C. G., Lazaridou, A., and Arvanitoyannis, I. 1999. Glass transition and physical properties of polyol-plasticised pullulan–starch blends at low moisture. *Carbohydrate Polymers, 40*(1), 29-47.

Birley, A. W., Haworth, B., and Batchelo, J., 1992. *Physics of plastics. Processing, properties, and materials engineering.* Hanser Publishers: Königsfeld, Germany.

Compañ, V., Lopez, M. L., Monferrer, L., Garrido, J., Riande, E., and San Roman, J. 1993. Determination of the glass transition temperature of poly(cyclohexyl acrylate) from oxygen permeability measurements. *Polymer, 34*(14), 2971-2974.

Crank, J., 1975. *The Mathematics of Diffusion*. 2nd ed.; Oxford University Press, London: 44-69.

Cuq, B., Gontard, N., Cuq, J. L., and Guilbert, S. 1997. Selected functional properties of fish myofibrillar protein-based films as affected by hydrophilic plasticizers. *Journal of Agricultural and Food Chemistry, 45*(3), 622-626.

Cuq, B., Gontard, N., and Guilbert, S. 1998. Proteins as agricultural polymers for packaging production. *Cereal Chemistry, 75*(1), 1-9.

Chivrac, F., Angellier-Coussy, H., Guillard, V., Pollet, E., and Avérous, L. 2010. How does water diffuse in starch/montmorillonite nano-biocomposite materials? *Carbohydrate Polymers, 82*(1), 128-135.

Chourpa, I., Ducel, V., Richard, J., Dubois, P., and Boury, F. 2006. Conformational modifications of alpha gliadin and globulin proteins upon complex coacervates formation with gum arabic as studied by raman microspectroscopy. *Biomacromolecules, 7*(9), 2616-2623.

D'Arcy, R. L., and Watt, I. C. 1970. Analysis of sorption isotherms of non-homogeneous sorbents. *Transactions of the Faraday Society, 66*.

Debeaufort, F., Voilley, A., and Meares, P. 1994. Water-vapor permeability and diffusivity through methylcellulose edible films. *Journal of Membrane Science, 91*(1-2), 125-133.

Dodds, W. S., Stutzman, L. F., and Sollami, B. J. 1956. Carbon dioxide solubility in water. *Industrial & Engineering Chemistry Chemical & Engineering Data Series, 1*(1), 92-95.

Donhowe, I. G., and Fennema, O. 1994. Edible films and coatings: Characteristics, formation, definitions, and testings methods. In *Edible Coatings and Films to Improve Food Quality.* J. Krochta, E. Baldwin, and M. Nisperos-Carriedo, Eds. CRC Press, Boca Raton, FL, USA.

Doty, P. M., Aiken, W. H., and Mark, H. 1946. Temperature dependence of water vapor permeability. *Industrial & Engineering Chemistry, 38*(8), 788-791.

EPA. On-line Tools for Site Assessment Calculation. http://www.epa.gov/athens/learn2model/part-two/onsite/index.html (accessed on october 2012).

Fabra, M. J., Talens, P., Gavara, R., and Chiralt, A. 2012. Barrier properties of sodium caseinate films as affected by lipid composition and moisture content. *Journal of Food Engineering, 109*(3), 372-379.

Foulk, J. A., and Bunn, J. M. 2001. Physical and barrier properties of developed bilayer protein films. *Applied Engineering in Agriculture, 17*(5), 635-641.

Gällstedt, M., and Hedenqvist, M. S. 2002. Oxygen and water barrier properties of coated whey protein and chitosan films. *Journal of Polymers and the Environment, 10*(1-2), 1-4.

Gavara, R., Catalá, R., Hernández-Muñoz, P. M., and Hernández, R. J. 1996. Evaluation of permeability through permeation experiments: Isostatic and quasi-isostatic methods compared. *Packaging Technology and Science, 9*(4), 215-224.

Gavara, R., and Hernandez, R. J. 1993. Consistency test for continuous flow permeability experimental data. *Journal of Plastic Film and Sheeting, 9*(2), 126-138.

Gennadios, A., Weller, C. L., and Testin, R. F. 1993a. Modification of physical and barrier properties of edible wheat gluten-based films. *Cereal Chemistry, 70*(4), 426-429.

Gennadios, A., Weller, C. L., and Testin, R. F. 1993b. Temperature effect on oxygen permeability of edible protein-based films. *Journal of Food Science, 58*(1), 212-+.

Gontard, N., Duchez, C., Cuq, J.-L., and Guilbert, S. 1994. Edible composite films of wheat gluten and lipids: Water vapour permeability and other physical properties. *International Journal of Food Science & Technology, 29*(1), 39-50.

Gontard, N., Guilbert, S., and Cuq, J. L. 1993. Water and glycerol as plasticizers affect mechanical and water-vapor barrier properties of an edible wheat gluten film. *Journal of Food Science, 58*(1), 206-211.

Gontard, N., Marchesseau, S., Cuq, J.-L., and Guilbert, S. 1995. Water vapour permeability of edible bilayer films of wheat gluten and lipids. *International Journal of Food Science & Technology, 30*(1), 49-56.

Gontard, N., Thibault, R., Cuq, B., and Guilbert, S. 1996. Influence of relative humidity and film composition on oxygen and carbon dioxide permeabilities of edible films. *Journal of Agricultural and Food Chemistry, 44*(4), 1064-1069.

Hambleton, A., Perpiñan-Saiz, N., Fabra, M. J., Voilley, A., and Debeaufort, F. 2012. The schroeder paradox or how the state of water affects the moisture transfer through edible films. *Food Chemistry, 132*(4), 1671-1678.

Hernandez-Munoz, P., and Hernandez, R. J. 2001. *Glutenin and gliadin films from wheat gluten: Preparation and properties.* Paper presented at the IFT Annual Meeting, New Orleans, Louisiana.

Hernandez-Munoz, P., Kanavouras, A., Lagaron, J. M., and Gavara, R. 2005. Development and characterization of films based on chemically cross-linked gliadins. *Journal of Agricultural and Food Chemistry, 53*(21), 8216-8223.

Hernandez-Munoz, P., Kanavouras, A., Ng, P. K. W., and Gavara, R. 2003. Development and characterization of biodegradable films made from wheat gluten protein fractions. *Journal of Agricultural and Food Chemistry, 51*(26), 7647-7654.

Hernandez, R. J. 1997. Food packaging materials, barrier properties and selection. In *Handbook of food engineering practice*, K.J. Valentas, E. Rotstein, and R.P. Singh, Eds. CRC Press: Boca Raton, FL, USA; 291-360.

Hernandez, R. J., and Gavara, R. 1994. Sorption and transport of water in nylon-6 films. *Journal of Polymer Science Part B: Polymer Physics, 32*(14), 2367-2374.

Hong, S. I., and Krochta, J. M. 2006. Oxygen barrier performance of whey-protein-coated plastic films as affected by temperature, relative humidity, base film and protein type. *Journal of Food Engineering, 77*(3), 739-745.

Irissin-Mangata, J., Boutevin, B., and Bauduin, G. 1999. Bilayer films composed of wheat gluten and functionalized polyethylene: Permeability and other physical properties. *Polymer Bulletin, 43*(4), 441-448.

Kester, J. J., and Fennema, O. R. 1986. Edible films and coatings - a review. *Food Technology, 40*(12), 47-59.

Kumins, C. A., Rolle, C. J., and Roteman, J. 1957. Water vapor diffusion through vinyl chloride–vinyl acetate copolymer. *The Journal of Physical Chemistry, 61*(10), 1290-1296.

Kurek, M., Ščetar, M., Voilley, A., Galić, K., and Debeaufort, F. 2012. Barrier properties of chitosan coated polyethylene. *Journal of Membrane Science, 403–404*(0), 162-168.

Lai, H. M., and Padua, G. W. 1998. Water vapor barrier properties of zein films plasticized with oleic acid. *Cereal Chemistry, 75*(2), 194-199.

López-de-Dicastillo, C., Gallur, M., Catalá, R., Gavara, R., and Hernandez-Muñoz, P. 2010. Immobilization of β-cyclodextrin in ethylene-vinyl alcohol copolymer for active food packaging applications. *Journal of Membrane Science, 353*(1–2), 184-191.

McLaren, A. D., and Rowen, J. W. 1951. Sorption of water vapor by proteins and polymers - a review. *Journal of Polymer Science, 7*(2-3), 289-324.

McHugh, T. H., and Krochta, J. M. 1994. Sorbitol- vs glycerol-plasticized whey protein edible films: Integrated oxygen permeability and tensile property evaluation. *Journal of Agricultural and Food Chemistry, 42*(4), 841-845.

Meares, P. 1954. The diffusion of gases through polyvinyl acetate. *Journal of the American Chemical Society, 76*(13), 3415-3422.

Park, H. J., and Chinnan, M. S. 1995. Gas and water vapor barrier properties of edible films from protein and cellulosic materials. *Journal of Food Engineering, 25*(4), 497-507.

Pascat, B. 1986. Study of some factors affecting permeability. In *Food packaging and preservation: Theory and practice*, M. Mathlouthi, Ed. Elsevier Applied Science Publishers: New York.

Perry, R. H., and Green, D. W., 1997. *Perry's chemical engineers handbook*. 7th ed.; Mc Graw Hill Professional, New York.

Pochat-Bohatier, C., Sanchez, J., and Gontard, N. 2006. Influence of relative humidity on carbon dioxide sorption in wheat gluten films. *Journal of Food Engineering, 77*(4), 983-991.

Ritger, P. L., and Peppas, N. A. 1987. A simple equation for description of solute release I. Fickian and non-fickian release from non-swellable devices in the form of slabs, spheres, cylinders or discs. *Journal of Controlled Release, 5*(1), 23-36.

Roca, E., Guillard, V., Broyart, B., Guilbert, S., and Gontard, N. 2008. Effective moisture diffusivity modelling versus food structure and hygroscopicity. *Food Chemistry, 106*(4), 1428-1437.

Roy, S., Gennadios, A., Weller, C. L., and Testin, R. F. 2000. Water vapor transport parameters of a cast wheat gluten film. *Industrial Crops and Products, 11*(1), 43-50.

Schwartzberg, H. G. 1986. Modelling of gas and vapor transport through hydrophilic films. In *Food packaging and preservation: Theory and practice*, M. Mathlouthi, Ed. Elsevier Applied Science: London; 115–135.

Shogren, R. 1997. Water vapor permeability of biodegradable polymers. *Journal of Polymers and the Environment, 5*(2), 91-95.

Song, Y. H., Li, L. F., and Zheng, Q. 2009. Influence of epichlorohydrin modification on structure and properties of wheat gliadin films. *Journal of Agricultural and Food Chemistry, 57*(6), 2295-2301.

Stenesh, J., 1993. *Core topics in biochemistry*. Cogno Press: Kalamazoo, MI.

Sun, S. M., Song, Y. H., and Zheng, Q. 2008. Morphology and mechanical properties of thermo-molded bioplastics based on glycerol-plasticized wheat gliadins. *Journal of Cereal Science, 48*(3), 613-618.

Tunc, S., Angellier, H., Cahyana, Y., Chalier, P., Gontard, N., and Gastaldi, E. 2007. Functional properties of wheat gluten/montmorillonite nanocomposite films processed by casting. *Journal of Membrane Science, 289*(1-2), 159-168.

Weast, R. C., 1987. *Handbook of chemistry and physics*. 68th ed.; CRC Press: Boca Raton, Florida

Zimm, B. H., and Lundberg, J. L. 1956. Sorption of vapors by high polymers. *Journal of Physical Chemistry, 60*(4), 425-428.

CHAPTER 4

RETENTION AND RELEASE OF CINNAMALDEHYDE FROM WHEAT PROTEIN MATRICES

Balaguer, M.P.; Borne, M.H.; Chalier, P.; Gontard, N.; Morel M.-H.; Peyron, S.; Gavara, R.; and Hernandez-Munoz, P.

Biomacromolecules, 2013, 14(5), 1493-502

Cinnamaldehyde treatment of gliadin films provided a means of decreasing their solubility, increasing their molecular weight profile, and reducing their overall migration into food simulants as a consequence of the high degree of polymerization achieved. Despite losses incurred in the film manufacturing process, and the amount that remained covalently bonded with protein because of cross-linking, the addition of 1.5, 3, and 5% of cinnamaldehyde (g/100 g protein) to gliadins at pH 2 rendered 1.8, 4.8, and 11.0 mg cinnamaldehyde/g film, respectively, available to be released, and therefore to exert antimicrobial activity. Cinnamaldehyde diffusivity was largely dependent on environmental conditions, increasing from $0.49 \cdot 10^{-15}$ m^2/s at 30% RH to $13.1 \cdot 10^{-15}$ m^2/s at 90% RH and 23 °C. This water sensitivity of films provides a mechanism with a noteworthy potential to retain the compound before its use, to trigger its release when needed, and to modulate the release rate according to the product humidity.

4.1. INTRODUCTION

The design of new bioplastics based on natural resources has become a suitable way to achieve sustainable development in many sectors. The food industry needs to simultaneously reduce i) the waste produced because of deterioration of perishable products, without incorporating synthetic preservatives directly into the food, and ii) the volume of petroleum-based plastic materials used in food packaging. One promising way to accomplish these objectives comes from active packaging with biopolymers. Despite the fact that naturally occurring macromolecules such as gluten, soy proteins, starch, etc. show excellent film-forming capacity (Cuq et al., 1998), their functional properties must be improved to fulfill the requirements when used as packaging materials. Chemical cross-linking, thermal treatments, addition of nanoparticles, blending, and formation of multi-layers are among the methods commonly employed to enhance their properties (Angellier-Coussy et al., 2008; Pereda et al., 2008; Rhim and Ng, 2007; Zhang and Do, 2009).

Gliadins represent a group of proteins found in wheat. They can easily be extracted from wheat gluten in 70% (v/v) ethanol, and because of their monomeric character (they lack of intermolecular disulfide bridges) the solution obtained is highly stable over time. Various authors have shown methods for overcoming the major drawbacks of films made from gliadins: poor mechanical properties and low water resistance (Chen et al., 2012; Hernandez-Munoz et al., 2005; Soares and Soldi, 2010; Song et al., 2009). Among these methods, cross-linking has been shown to be an effective means to improve the functional properties of gliadin films. However, when the applications are aimed at food, the toxicity of the chemical cross-linkers used must be taken into account.

Cinnamaldehyde, the main component of cinnamon essential oil, has been described as an effective cross-linker (Balaguer et al., 2011a; Balaguer et al., 2011b; Kim et al., 2006; Kyoungju et al., 2007). Moreover, this compound possesses antimicrobial properties (Burt, 2004; Friedman et al., 2002), and has been included in various systems to be released and exert antimicrobial activity against pathogenic and spoilage microorganisms, with promising results (Ben Arfa et al., 2007; Gomes et al., 2011; Rojas-Grau et al., 2007; Sanla-Ead et al., 2012). Minimum inhibitory concentrations (MIC) of cinnamaldehyde for bacteria range from 22.89 mg/L for *Listeria monocytogenes* in vapor phase (Lopez et al., 2007), to 4.2 mg/L for *Escherichia coli* and *Salmonella typhimurium* in broth dilution (Gamage et al., 2009). For fungi in vapor phase, it ranges from 0.52 mg/L for *Penicillium notatum* (Tunc et

al., 2007), to 22.89 mg/L for *Aspergillus flavus* (Lopez et al., 2007), and to 4.62 mg/L for *Candida albicans* (Lopez et al., 2007).

The potential of cinnamaldehyde to be used as a cross-linker, improving the water resistance, mechanical, and barrier properties of gliadin protein films has been demonstrated in previous works (Balaguer et al., 2013; Balaguer et al., 2011a; Balaguer et al., 2011b). Its capacity was found to be strongly dependent on pH, and pH 2 was established as the most suitable for polymerization. It is believed that only a small amount of the cinnamaldehyde added to the protein matrix acts as a cross-linker and is irreversibly attached to the protein. However, a considerable amount of the compound can remain in the matrix, and can be released under appropriate conditions of humidity and temperature.

The objectives of the present work are to give new insight into the interactions established between cinnamaldehyde and gliadin proteins, and to evaluate the quantity of free cinnamaldehyde able to be released, and thus able to exert antimicrobial activity.

4.2. MATERIALS AND METHODS

4.2.1. Reagents

Crude wheat gluten (≥80% protein), glycerol, ethanol, hydrochloric acid, and cinnamaldehyde, all laboratory grade, were supplied by Sigma (Madrid, Spain).

4.2.2. Gliadin-rich fraction extraction from wheat gluten

The gliadin-rich fraction was extracted from the wheat gluten according to the method described by Hernandez-Munoz and Hernandez (2001). Briefly, 100 g of wheat gluten was dispersed in 400 mL of 70% (v/v) ethanol/water mixture, stirred overnight at room temperature, and centrifuged at 5000 rpm for 20 min at 20 °C. The supernatant containing the gliadin-rich fraction was collected and used as the film-forming solution. The amount of protein extracted was around 12–14% (g protein/100 g film-forming solution).

4.2.3. Chemical modification of gliadins

Different cinnamaldehyde concentrations were added to the gliadin film-forming solution, namely 1.5% (G1.5C_pH2), 3% (G3C_pH2) and 5% (G5C_pH2) (g cinnamaldehyde/100 g protein). HCl was used to adjust the pH. Control samples were prepared at the original pH 6 of the gliadin solution (G_pH6), at pH 2, the level at which chemical modification occurs (G_pH2), and in some cases at pH 6 with 5% of cinnamaldehyde (G5C_pH6). Glycerol, as plasticizer, was added to the film-forming solutions at 25% (g glycerol/100 g protein). The mixture containing the protein, the glycerol, and the cinnamaldehyde at the chosen pH was maintained under stirring for 30 min.

4.2.4. Film formation

The film-forming solution was poured onto a horizontal flat Pyrex tray to allow water and ethanol to evaporate. The weight of film-forming solution used to form the film was calculated in order to obtain a density of 0.01 g of protein per cm^2. The films were dried at 37 °C and 50% RH for 24 h, after which they were peeled off the casting surface.

4.2.5. Film thickness determination

The film thickness was measured using a micrometer (Mitutoyo, Kanagawa, Japan) with a sensitivity of ± 2 µm. The mean thickness was calculated from measurements taken at ten different locations on each film sample.

4.2.6. Film moisture content determination

The moisture content of the films conditioned at 50% RH was evaluated after drying them for 1 week in a desiccator containing P_2O_5. The weight loss was assumed to correspond to the moisture content only.

4.2.7. Evaluation of gliadin cross-linking with cinnamaldehyde

4.2.7.1. Size exclusion high performance liquid chromatography (SE-HPLC)

Changes in the molecular size distribution of the gliadin proteins were characterized by size exclusion high performance liquid chromatography. A detailed presentation of the method was specified by Redl et al. (1999). Briefly, samples were ground in the presence of liquid nitrogen using a laboratory ball mill (Prolabo, France) and then blended with soluble wheat

starch (1/5 w/w). Upon mixing, starch progressively absorbs the glycerol from the gluten, thereby increasing the material glass transition temperature, making it easier to grind. The powders obtained (160 mg) were stirred for 80 min at 60 °C in the presence of 20 mL of 0.1 M sodium phosphate buffer (pH = 6.9) containing 1% sodium dodecyl sulfate (SDS). The SDS-soluble protein extract was recovered by centrifugation (30 min at 39000 g and 20 °C) and a 20 µL sample was submitted to SE-HPLC fractionation (first extract). The pellet was suspended in 5 mL of SDS-phosphate buffer containing 20 mM dithioerythritol (DTE). After shaking for 60 min at 60 °C, the sample was sonicated (Vibra Cell 20 kHz, Bioblock Scientific) for 3 min at 30% power setting. Disulfide and weak bonds are disrupted by DTE and SDS, respectively, whose efficiencies are further increased by ultrasonic waves. Thus, the chemical and physical treatments brought insoluble protein aggregates into solution. After centrifugation (30 min, 39000 g, 20 °C), a part of the supernatant was then mixed with an equivalent volume of SDS-phosphate buffer containing 40 mM iodoacetamide in order to alkylate thiol groups. The reaction was carried out for 1 h in darkness, at room temperature. 20 µL of this solution was submitted to SE-HPLC fractionation (second extract).

The SE-HPLC apparatus was a Waters model (Alliance) controlled by Millennium software (Waters). A TSK G4000-SWXL (Tosoh Biosep) size exclusion analytical column (7.8 mm × 300 mm) was used with a TSK SWXL (Tosoh Biosep) guard column (6 mm × 40 mm). The columns were eluted at ambient temperature with 0.1 M sodium phosphate buffer (pH = 6.9) containing 0.1% SDS. The flow rate was 0.7 mL/min, and absorbance was measured at 214 nm to identify and quantify proteins. The apparent molecular weight of proteins was estimated by calibrating the column with protein standards (Morel et al., 2002b). The SDS-insoluble protein fraction (Fi), second extract, was expressed as percent of the total extractable protein, estimated from the sum of the areas of the two extracts, after correcting them for their different solid to solvent ratios. To estimate the percentage of recoverable protein, the total area of the extractable proteins was expressed as a percentage of the area of the native gliadin, on the same gliadin weight basis.

4.2.7.2. Attenuated total reflectance – Fourier transform infrared spectroscopy (ATR-FTIR)

The film-forming solutions, adjusted to different pHs and with or without cinnamaldehyde, were analyzed by ATR-FTIR during the drying step at 37 °C for 24 h. The sample was place in an autoheatable Golden Gate single reflection diamond ATR accessory (Teknokroma,

Barcelona, Spain) and the spectra were recorded with a Bruker Tensor 27 FTIR Spectrometer (Bruker Española S.A., Barcelona, Spain). The resolution was 4 cm^{-1} in the range of 4000 to 600 cm^{-1} and 128 scans were recorded per test. Results were recorded in duplicate.

4.2.7.3. Overall migration tests in food simulants

The overall migration into different aqueous food simulants of gliadin film cross-linked with 5% of cinnamaldehyde (G5C_pH2) was analyzed in accordance with the conditions set out in Regulation 10/2011/EC, which establishes specific requirements for plastic materials and articles intended to come into contact with food. The food simulants employed are listed in **Table 4.1**, and they are assigned for different types of food. Food simulants A, B, and C are assigned for foods that have a hydrophilic character and are able to extract hydrophilic substances. Food simulant B is used for those foods that have a pH below 4.5. Food simulant C is used for alcoholic foods with an alcohol content of up to 20% and those foods that contain a relevant amount of organic ingredients that render the food more lipophilic. Food simulant D1 is assigned for foods that have a lipophilic character and are able to extract lipophilic substances and it is used for alcoholic foods with an alcohol content of above 20% and for oil in water emulsions. The regulation does not include an overall migration test for dried food.

Table 4.1. List of food simulants employed in the overall migration tests.

Food	Food simulant	Food simulant abbreviation
Aqueous	Ethanol 10% (v/v)	A
Acid (pH ≤ 4.5)	Acetic acid 3% (w/v)	B
Alcoholic ≤ 20% **Containing a relevant amount of organic ingredients**	Ethanol 20% (v/v)	C
Alcoholic > 20% **Oil in water emulsions**	Ethanol 50% (v/v)	D1

Overall migration tests were performed under the standardized testing conditions set out in the regulation for the intended food contact conditions. The testing conditions were set at 10 days of contact at 40 °C (test number OM2); this test is used for food products with long term storage at room temperature or below, including heating up to 70 °C for up to 2 hours, or heating up to 100 °C for up to 15 minutes.

The regulation setting of migration limits takes into account a conventional assumption that 1 kg of food is consumed daily by a person of 60 kg bodyweight and that the food is packaged in a cubic container of 6 dm^2 surface area releasing the substance. Accordingly, four specimens of gliadin film G5C_pH2, 16 mm in diameter, were immersed in glass tubes containing 26.8 mL of food simulant. The films were threaded onto a stainless steel wire and were separated by glass beads in order to have both film surfaces in contact with the liquid medium (total surface area in contact 0.1608 dm^2).

After the contact period, the assembly with the films was removed and the liquid simulants were evaporated, firstly at low temperature to avoid strong bubbling and then at 105 °C until a constant weight was reached.

4.2.8. Evaluation of free cinnamaldehyde release from cross-linked gliadin films

4.2.8.1. Kinetics of cinnamaldehyde release from gliadin films

Films were cut into small disks, each 2 cm in diameter, and they were weighed and placed in three different chambers maintained at 23 °C and at a constant RH of 30, 50, or 90% ± 5%. The RH was adjusted by using a humidified air flow (30 mL/min) through the chamber (volume about 370 cm^3). Air was humidified by bubbling in a gas washing bottle containing water and placed in a cryostat at controlled temperature. The temperature differential imposed between the cryostat and the chambers allowed the air flux to reach the selected humidity. During each experiment, the chamber humidity was controlled using a hygrometer probe (Rotronic, Bassersdorf, Switzerland). Pieces of film were picked out of the chambers at prescribed time intervals for analysis; cinnamaldehyde content was immediately determined by the extraction method described below.

4.2.8.2. Extraction of remaining cinnamaldehyde from gliadin films

Cinnamaldehyde was extracted from films by immersing three pieces of film in 10 mL of n-pentane containing 100 µL of internal standard solution under continuous magnetic stirring for 24 h at 500 rpm and ambient temperature. Different extraction methods were tested in order to maximize the amount of cinnamaldehyde extracted. Mixtures (50/50) of water/n-pentane, water/dichloromethane, and water/ethanol, and also the pure solvents were used at different pHs (2, 6, and 9) in an attempt to raise the solubility of the films, and hence increase the extraction yield. However, the films were highly insoluble in all the

media, and the best extraction results were obtained using pure n-pentane. The internal standard used was 2-nonanol (10 mg/mL in ethanol). The organic phase containing cinnamaldehyde and 2-nonanol was removed and dried over anhydrous sodium sulfate and analyzed by gas chromatography. Analyses were performed by a Varian 3800 GC (Les Ulis, France) equipped with a DB-WAX column (J&W Scientific) (30 m × 0.32 mm, film thickness 0.25 µm) and a flame ionization detector (FID). Hydrogen was used as carrier gas with a flow rate of 2 mL/min. The oven temperature was programmed to rise from 60 to 150 °C at 4 °C/min, then from 150 to 250 °C at 15 °C/min, and held at 250 °C for 10 min. Injector and detector temperatures were maintained at 250 °C. Injections were done in split mode with a 1:20 ratio. Quantification of cinnamaldehyde was performed using the internal standard and after determination of the response coefficient, which was equal to 0.990 ± 0.008. The extraction efficiency was estimated by depositing a known quantity of cinnamaldehyde on a gliadin control film (without the compound) and by applying the extraction procedure described above. The extraction yield was found to be 75% ± 1%. For each time and RH, the extraction was done in triplicate from two different films. Results were expressed in terms of remaining cinnamaldehyde at time *t* per gram of film conditioned at 50% RH (the weight just after the drying step).

The initial theoretical quantity of cinnamaldehyde in the films was calculated taking into account the surface density of cinnamaldehyde (0.15, 0.3, and 0.5 mg of cinnamaldehyde/cm^2 of film for the films G1.5C_pH2, G3C_pH2, and G5C_pH2, respectively) and the surface density of the film (around 0.017 g/cm^2). For instance, for the gliadin film G5C_pH2 the theoretical quantity is equal to: 0.5/0.017 = 29.4 mg cinnamaldehyde/g film.

4.2.8.3. Mathematical modeling of cinnamaldehyde release from gliadin films

The mathematical model was based on the one previously presented by Chalier et al. (2009) and Mascheroni et al. (2011) for modeling carvacrol release from agro-based materials toward humidified atmosphere. Because the experimental conditions applied in this study are similar, the same hypothesis, summarized below, can be considered to model our system:

1) The film placed in the chamber is a plane sheet of thickness l.
2) The antimicrobial film is assumed to be instantaneously in equilibrium with the surrounding RH.
3) The antimicrobial agent release is unidirectional, in the axial direction, with the axis origin at the interface between the glass tray and the film.
4) The diffusivity is an apparent diffusivity (D) and represents the overall transport of cinnamaldehyde in the film without a prevailing mechanism of transport. In a first approximation, the apparent diffusivity is assumed to be constant whatever the antimicrobial agent concentration.

The internal diffusion of active agent in the film was modeled using Fick's second law:

$$\forall x, \quad 0 < x < l, \quad \forall t, \quad \frac{\partial C}{\partial t} = D\frac{\partial^2 C}{\partial x^2} \qquad (\mathbf{4.1})$$

The boundary conditions were:

a) The flux was considered as null at the interface between the glass tray and the film:

$$x = 0, \quad \forall t, \quad \frac{\partial C(0,t)}{\partial x} = 0 \qquad (\mathbf{4.2})$$

b) The cinnamaldehyde concentration in the atmosphere was considered as null because the air flow blew through the chamber, enabling a purge of the air at each time t. The cinnamaldehyde concentration on the upper side of the film was assumed to be in equilibrium with the atmosphere and null:

$$x = l, \quad \forall t, \quad C(l,t) = 0 \qquad (\mathbf{4.3})$$

And the initial condition was written as follows:

$$0 < x < l, \quad t = 0, \quad C(x,0) = C_0 = constant \qquad (\mathbf{4.4})$$

In these conditions, and if C_t denotes the cinnamaldehyde concentration in the film (mg/g of dry film) at time t, and C_∞ the active agent concentration in the film at time assumed to

be infinite, the particular solution of the systems of **Equations (4.1)–(4.4)** is given by Crank (1975):

$$\frac{C_t - C_0}{C_\infty - C_0} = 1 - \frac{8}{\pi^2}\sum_{n=0}^{\infty}\frac{1}{(2n+1)^2}exp\left[\frac{-D(2n+1)^2\pi^2}{l^2}t\right] \qquad (\mathbf{4.5})$$

4.2.8.4. Determination of apparent diffusivity of cinnamaldehyde

Cinnamaldehyde diffusivity was determined from experimental release kinetics by fitting predicted curves of cinnamaldehyde concentration evolution with time using the model just described. Diffusivity was determined for each formulation (G1.5C_pH2, G3C_pH2 and G5C_pH2) and for the G5C_pH2 formulation for each relative humidity tested (30, 50, 90%). The Levenberg-Marquardt algorithm (Gill et al., 1981) was used for the optimization procedure, using a dedicated MATLAB® (The Mathworks Inc., Natick, Mass, USA) function, "lsqnonlin". The root mean square error (RMSE) was used to estimate the quality of model fitting and was calculated as follows (**Equation 4.6**):

$$RMSE = \sqrt{\frac{(\hat{y} - y)^2}{(N - p)}} \qquad (\mathbf{4.6})$$

where y and $\hat{y}$ are, respectively, the experimental and predicted residual cinnamaldehyde content (g/g of dry film), N is the number of cinnamaldehyde content measurements, and p the number of identified parameters.

4.2.9. Statistical analysis

Statistical analysis of the results was performed with SPSS commercial software (SPSS Inc, Chicago, IL, USA). A one-way analysis of variance (ANOVA) was carried out. Differences between means were assessed on the basis of confidence intervals using the Tukey test at a level of significance of $p \leq 0.05$.

4.3. RESULTS AND DISCUSSION

4.3.1. Evaluation of gliadin cross-linking with cinnamaldehyde

4.3.1.1. SE-HPLC

Figures 4.1 and **4.2** depict the size distribution profiles determined by SE-HPLC of the gliadin film-forming solutions and the resulting gliadin films, respectively. The absorbance is represented vs. both the elution time and the molecular weights assigned by calibration. The size distribution profiles of the SDS-soluble fraction and the SDS-insoluble fraction (brought into solution after sonication and DTE reduction treatment) correspond to **Figures 4.1A** and **4.1B**, respectively. Morel et al. (2002a) classified the native gluten SE-HPLC profile in terms of different fractions: fractions F1 and F2 consisted of glutenin polymers and large protein aggregates, and fractions F3 to F5 consisted mainly of gliadin monomers of decreasing size (ω, γ, β, and α), and some remaining soluble proteins. The molecular weight (Da) of the fractions was above 680000 (F1), ranging from 95000 to 680000 (F2), from 55000 to 95000 (F3), and from 20000 to 55000 (F4), and salt-soluble protein from 6000 to 20000 (F5).

The elution profile of the gliadin film-forming solution (**Figure 4.1**) was similar to the elution profile of gluten obtained by Redl et al. (1999) The major and expected difference was the small area obtained for fractions F1 and F2, mostly corresponding to glutenin polymers and large protein aggregates. The appearance of high molecular weight units in the gliadin profile could be related with the procedure for gliadin extraction from wheat gluten, which entailed the extraction of some glutenin polymers, and to the presence of some protein aggregates in the solution.

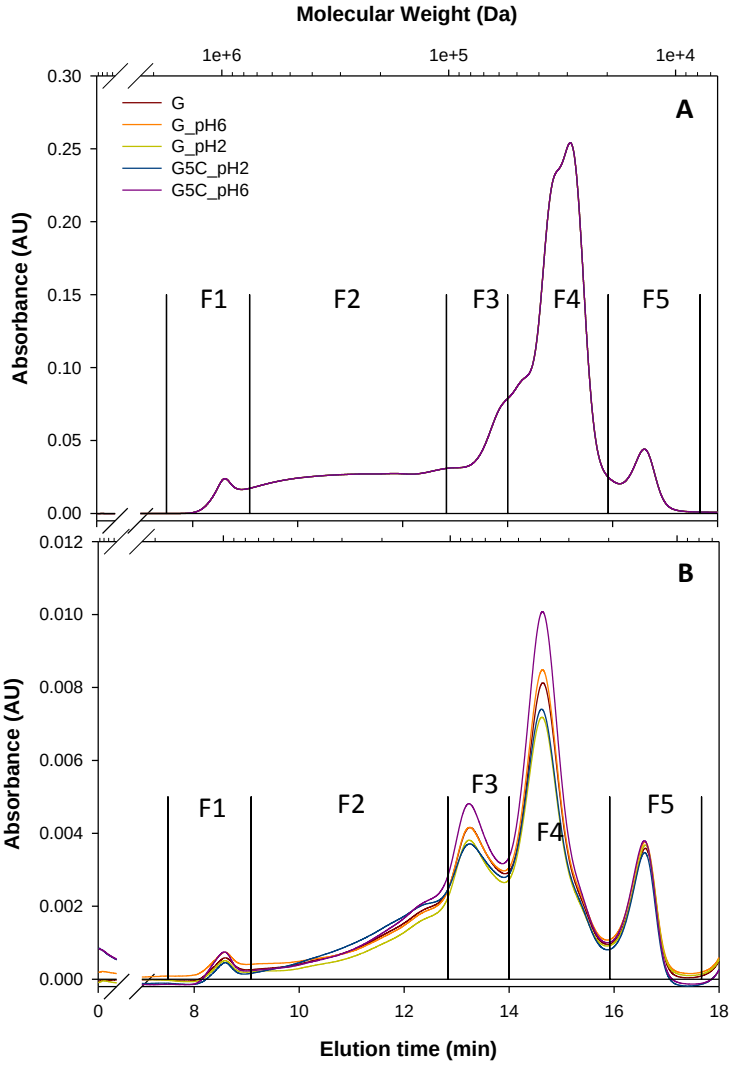

Figure 4.1. Size exclusion distribution profiles of gliadin film-forming solutions: (**A**) SDS-soluble fraction, (**B**) SDS-insoluble fraction extracted with sonication and DTE reduction treatment. Fractions F1 to F5 include: glutenin polymers and large protein aggregates above 680000 Da (F1), and ranging from 95000 to 680000 Da (F2); gliadin monomers ranging from 55000 to 95000 Da (F3), and from 20000 to 55000 Da (F4); and saline-soluble proteins from 6000 to 20000 Da (F5).

Table 4.2 shows the total extractable area, and the corresponding percentages of soluble fraction in SDS, insoluble fraction in SDS extracted with sonication and DTE reduction treatment, and insoluble fraction in SDS and DTE with sonication treatment.

Table 4.2. Results of size exclusion high performance liquid chromatography (SE-HPLC): total extractable area, and percentages of soluble fraction in SDS, insoluble fraction in SDS extracted with sonication and DTE reduction treatment, and insoluble fraction in SDS and DTE with sonication treatment.

Sample		Total extractable area	% SDS-soluble fraction	% SDS-insoluble+DTE-soluble fraction	% SDS+DTE-insoluble fraction
Film-forming solution	G	34 127 661	98.17	1.83	0.00
	G_pH6	33 450 319	96.09	1.92	1.98
	G_pH2	31 649 747	91.10	1.64	7.26
	G5C_pH2	31 783 866	91.41	1.72	6.87
	G5C_pH6	33 113 945	94.96	2.06	2.97
Film	G	37 272 317	96.48	3.52	0.00
	G_pH6	31 436 892	81.26	3.08	15.66
	G_pH2	30 552 163	69.24	12.73	18.03
	G1.5C_pH2	29 486 404	58.09	21.02	20.89
	G3C_pH2	29 699 276	58.89	20.79	20.32
	G5C_pH2	25 354 266	47.10	20.93	31.98
	G5C_pH6	33 057 828	86.05	2.64	11.31

No major differences were found among the size exclusion profiles of the different gliadin film-forming solutions analyzed, especially in the SDS-soluble fraction (**Figure 4.1**). **Table 4.2** shows that more than 90% of the film-forming solutions was soluble in SDS, and that the treatment with DTE and sonication was able to extract only around 2% of the SDS insoluble fraction of the gliadin film-forming solutions. The insoluble fraction (in SDS with DTE and sonication) increased up to 7% for the film-forming solutions in which a pH reduction was produced. In spite of this increase in insolubility, the size distribution profiles indicated that the addition of cinnamaldehyde and the pH modification did not produce a great alteration in the molecular weight profile of the protein when it remained in solution.

The major changes in the size distribution profiles were produced after or during the casting of the film-forming solutions, and were observed in the resulting gliadin films (**Figure 4.2**). This difference between the SE-HPLC profiles of the gliadins in the film-forming solutions and in the resulting films indicates that the cross-linking reaction caused by the cinnamaldehyde took place mainly while the film was drying. This phenomenon was also observed by SDS-PAGE in a previous work (Balaguer et al., 2011b).

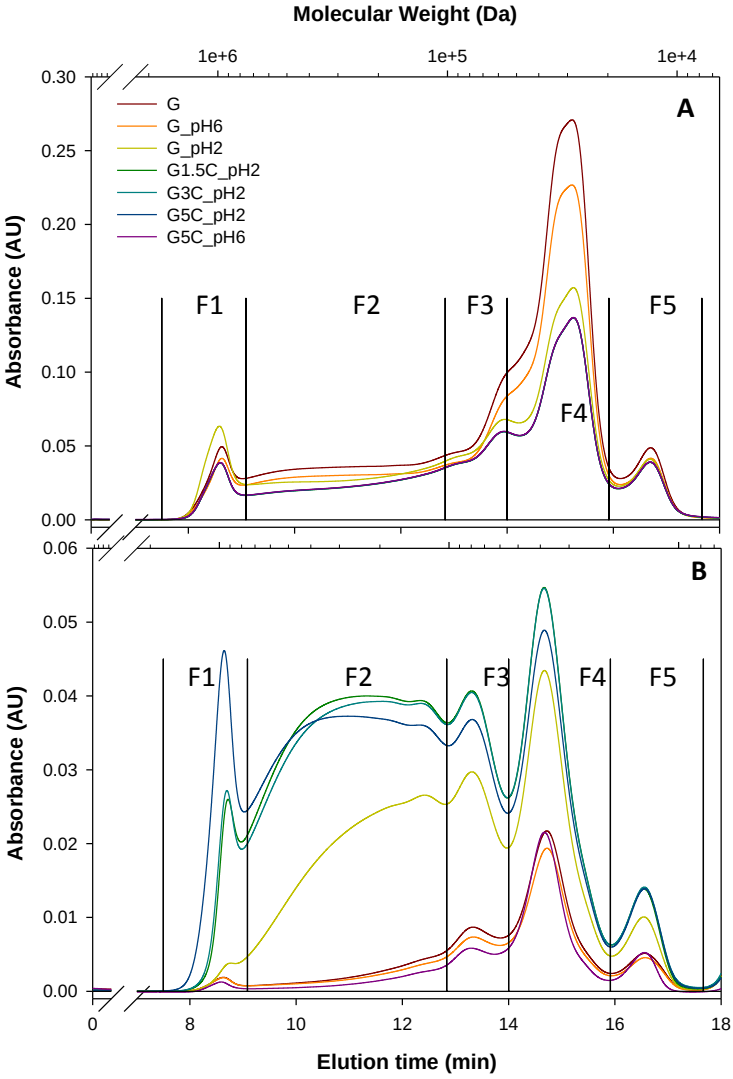

Figure 4.2. Size exclusion distribution profiles of gliadin films: (**A**) SDS-soluble fraction, (**B**) SDS-insoluble fraction extracted with sonication and DTE reduction treatment. Fractions F1 to F5 include: glutenin polymers and large protein aggregates above 680000 Da (F1), and ranging from 95000 to 680000 Da (F2); gliadin monomers ranging from 55000 to 95000 Da (F3), and from 20000 to 55000 Da (F4); and saline-soluble proteins from 6000 to 20000 Da (F5).

The reduction of the pH from 6 (G_pH6) to 2 (G_pH2) produced a decrease of the F4 SDS-soluble fraction corresponding to the gliadins (**Figure 4.2A**), and an increase in the SDS-insoluble fraction (**Figure 4.2B**), in agreement with the previously observed reduction of the intensity of the corresponding band in the SDS-PAGE (Balaguer et al., 2011b). Although

the SDS-insoluble fraction increased, the SDS-DTE-insoluble fraction did not change with the reduction of pH (**Table 4.2**). This result indicates that the reduction of the pH induced the formation of protein aggregates with a molecular weight of around 400 kDa (**Figure 4.2B**, fraction F2) which could still be solubilized by the action of sonication and the reduction treatment with DTE (**Table 4.2**).

The addition of cinnamaldehyde at the native pH (G5C_pH6) did not produce a significant modification of the SE-HPLC profile. In contrast, the combination of cinnamaldehyde addition and pH reduction (GXC_pH2) reduced the area of the F4 fraction from the SDS-soluble part (**Figure 4.2A**), increased the area of the SDS-insoluble fraction, especially the higher molecular weight fractions F1 and F2 (**Figure 4.2B**), and considerably increased the SDS-DTE-insoluble fraction (**Table 4.2**). This effect can be attributed to the cross-linking capacity of cinnamaldehyde, which gave rise to higher molecular weight protein aggregates owing to polymerization of monomeric gliadins (increasing connectivity between polypeptide chains), thus developing insoluble polymer structures. The amount of cinnamaldehyde employed also had an influence on the final size distribution profile, because the sample with the highest concentration of cinnamaldehyde, G5C_pH2, had a greater F1 SDS-insoluble fraction area, which corresponds to polymers of molecular weight above 680 kDa (**Figure 4.2B**), and presented less than 50% of SDS-soluble proteins in comparison with the 80% of the control gliadin film, G_pH6.

4.3.1.2. ATR-FTIR

The FTIR analysis was performed in order to evaluate the effect of the chemical modifications on the secondary structure of the protein conformation in the film-forming solutions and in the films, and also the evolution during the drying step to form the film. **Figure 4.3** shows the spectra obtained for the G_pH6 film (film made without changing the native pH and without cinnamaldehyde addition). The broad band in the 3600–3000 cm^{-1} region is ascribed to N-H stretching vibrations and the group of bands in the 3000–2800 cm^{-1} region corresponds to the characteristic C-H vibrations (Secundo and Guerrieri, 2005). Characteristic protein bands Amide I, Amide II, and Amide III appeared in the infrared spectra. The absorption associated with the Amide I band (1600–1700 cm^{-1}) leads to stretching vibrations of the C=O bond of the amide group. Because both the C=O and the N-H functions are involved in the hydrogen bonding that takes place between the different elements of secondary structure, the locations of both the Amide I and the Amide II bands

are sensitive to the secondary structure content of a protein. The Fourier deconvoluted spectrum of the Amide I band exhibits three bands, at 1623, 1652, and 1675 cm^{-1}. The 1675 cm^{-1} band is assigned to the β-turn conformation, whereas the prominent band at 1652 cm^{-1} is assigned to the α-helical conformation, although the spectral contribution from the unordered conformation cannot be excluded at this frequency. The low-frequency amide I band at about 1620 cm^{-1} is generally associated with the presence of intermolecular β-sheet networks (Pézolet et al., 1992) and is usually observed during protein aggregation (Boye et al., 1995).

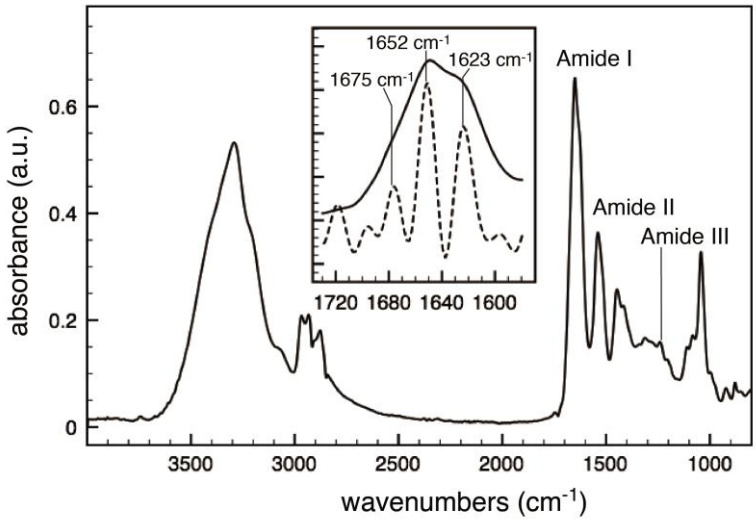

Figure 4.3. ATR-FTIR spectrum of dried G_pH6 film with a zoom view of (—) original and (---) Fourier deconvoluted infrared spectrum in the amide I region.

Figure 4.4 shows the evolution of the spectra in the amide I region from the film-forming solution during the drying step until the generation of the film. The signal of the amide I band clearly improved with time. A rearrangement of the conformation was prompted by the increase of the protein concentration owing to solvent evaporation. In agreement with other authors (Lefèvre et al., 2005; Mangavel et al., 2001), the major feature of this evolution was the transition from a mixture of different secondary structures, with an important contribution of α-helical and irregular structure to the formation of hydrogen bonded β-sheets.

Regarding the influence of pH, the folding of the protein chain through secondary structures is promoted at the isoelectric point of protein because of the change of their net charge at the other pH values (Chourpa et al., 2006). Considering the pI value of gliadin in the range of 6.5-8 (Haugaard and Johnson, 1930; Wu and Dimler, 1963), the side-chain repulsions that appear at pH 2 have the effect of slowing down the folding of protein. As consequence, the kinetics of protein folding, followed by the evolution spectral fingerprint of amide I, appear faster at pH 6 that at pH 2 but the final spectra obtained on the dried films G_pH6 and G_pH2 did not exhibit any significant difference in the intensity of bands at 1623 and 1652 cm^{-1}.

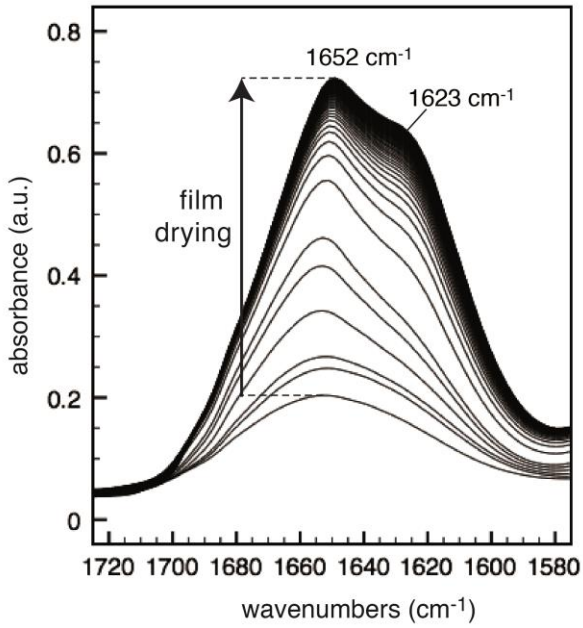

Figure 4.4. ATR-FTIR spectra in the amide I region of G_pH6 film during film drying.

The influence of cinnamaldehyde on the gliadin structuration process was investigated through the amide I spectrum analysis. **Figure 4.5** shows the difference spectra resulting from the subtraction of spectral fingerprint obtained from films with and without cinnamaldehyde at different pHs. The results reveal marked differences according to the pH of the film-forming solution. The low amplitude spectral signal at pH 6 reflected the absence of influence of cinnamaldehyde on structuration of gliadin at that pH. In contrast,

cinnamaldehyde addition induced major conformational changes of proteins at pH 2 with, in particular, a concomitant increase in intensity of the band at 1617 and a decrease at 1658 cm^{-1}. These spectral modifications reflect the formation of β-sheet, which would be shaped to the detriment of the initial α-helical structure. In agreement with the size exclusion results, therefore, cinnamaldehyde seems to promote the network formation of proteins through intermolecular β-sheets.

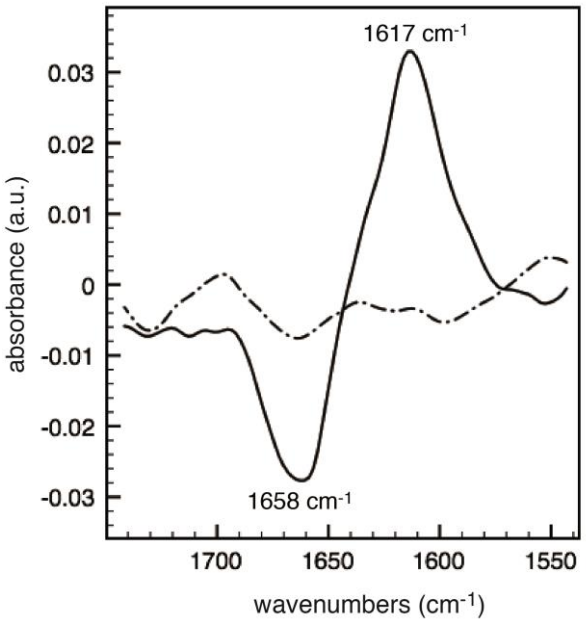

Figure 4.5. Difference spectra of films obtained by addition of cinnamaldehyde into the film-forming solution at (—) pH 2 and (–·–) pH 6.

4.3.1.3. Migration tests

Gliadin film treated with 5% of cinnamaldehyde maintained its integrity after 10 days of immersion at 40 °C in all the food simulants tested. **Figure 4.6** shows a visual probe of film resistance after 10 days of immersion at 40 °C in the food simulants employed.

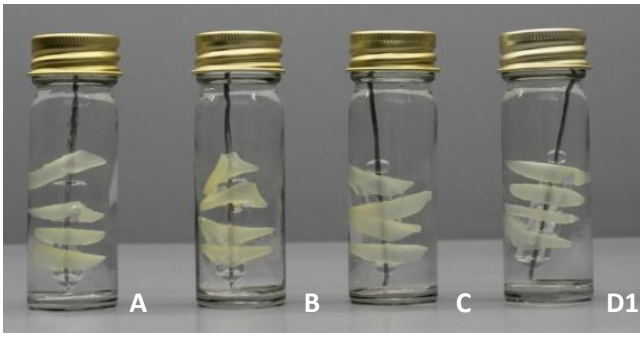

Figure 4.6. Resistance of gliadin film cross-linked with 5% of cinnamaldehyde after 10 days of contact at 40 °C with several food simulants.

As stated by the regulation 10/2011/EC, plastic materials and articles must not transfer their constituents to food simulants in quantities exceeding 10 mg of total constituents released per dm^2 of food contact surface. On the other hand, according to the regulation on active and intelligent materials and articles intended to come into contact with food (450/2009/EC), the overall migration should not include the amount of active substance released. The method used here to calculate the overall migration does not include volatile substances such as cinnamaldehyde, because the conditions fixed for the evaporation of the simulants lead to the evaporation of the possible cinnamaldehyde migrated. Therefore, the overall migration corresponds mostly to the gliadin proteins, and some glycerol residue (0.80 ± 0.13% g glycerol residue/100 g glycerol migrated).

Table 4.3 shows the overall migration for gliadin films with the highest degree of cross-linking (G5C_pH2) into various food simulants after 10 days of contact at 40 °C. The values in all the food simulants were hardly over the regulation limit, therefore it was not necessary to test the films with lower cross-linking degrees. The reduction of the pH seemed to favor the migration of gliadins into the acidic simulant. It is known that at pHs far from the isoelectric point (6.5–8 (Haugaard and Johnson, 1930; Wu and Dimler, 1963)) side-chain repulsions of induced net charges lead to conformational changes in protein structure due to possible unfolding, rupture of hydrogen bonds, and alteration of hydrophobic interactions (Chourpa et al., 2006), which could give rise to greater solubilization of protein. Furthermore, a solution with 50% v/v ethanol is close to 70% v/v ethanol, in which gliadins are soluble, thus leading to a higher migration than using a lower ethanol percentage.

The results for the overall migration are much lower than those obtained for common gluten films or gluten films containing 5% montmorillonite (Mauricio-Iglesias et al., 2010). The loss of non-volatile mass from the film to the food simulants accounted for 1.6% in simulant A, 3.1% in simulant B, 1.1% in simulant C, and 3.0% in simulant D1, far below the values obtained by Mauricio-Iglesias et al. (2010), which were around 10% in water, and 20% in 3% acetic acid and 15% ethanol for gluten films. The achievement of this remarkable reduction in migration was a result of the high degree of cross-linking obtained in the gliadins with cinnamaldehyde treatment.

Table 4.3. Overall migration of a gliadin film cross-linked with 5% of cinnamaldehyde after 10 days of contact at 40 °C with the food simulants. Limit of overall migration: 10 mg/dm^2 (10/2011/EC)

Food simulant	Overall migration (mg/dm^2)
A: 10% Ethanol	15.13 ± 2.80
B: 3% Acetic acid	30.06 ± 5.36
C: 20% Ethanol	15.24 ± 0.44
D1: 50% Ethanol	28.81 ± 10.07

It is important to point out that the extreme conditions (temperature, time, and liquid media) set out in the regulation and the high hydrophilicity of these biomaterials result in higher migration values in comparison with conventional plastic materials. The need for the development and standardization of tests conceived for such materials under different conditions has been defended by other authors (Dainelli et al., 2008; Mauricio-Iglesias et al., 2010).

4.3.2. Evaluation of free cinnamaldehyde in gliadin films after cross-linking reaction and drying step

Strong retention of the active agent in the matrix during film production is very necessary in order to exert antimicrobial activity in the packaged system. In the case of gliadins treated with cinnamaldehyde at pH 2, a cross-linking reaction irreversibly links some of the aldehyde with the protein, as has been shown by SE-HPLC and also by SDS-PAGE, protein solubility assessment with bicinchoninic acid assay, MDSC, cross-linking density, etc. (Balaguer et al., 2011a; Balaguer et al., 2011b). This endows cinnamaldehyde-treated gliadin films with improved functional properties in comparison with untreated films: better water resistance, higher mechanical strength, and enhanced water vapor and

oxygen barrier properties. However, this phenomenon may reduce the quantity of free compound available to act as an antimicrobial agent. Therefore, the residual quantity of cinnamaldehyde entrapped by weak bonding that remained in the films after the drying step at 37 °C and 50% RH as a result of weak bonding was evaluated.

Figure 4.7 depicts the quantity of free cinnamaldehyde (mg/g film) as a function of the initial percentage added to the film-forming solution, ranging from 0.5 to 40% (g cinnamaldehyde/100 g protein). The difference between the theoretical quantity expected and the experimental quantity obtained corresponds not only to the cinnamaldehyde that acts as cross-linker but also to the losses that are produced during the steps of manufacturing and drying the film-forming solution.

For the films more specifically studied, G1.5C_pH2, G3C_pH2, and G5C_pH2, the initial amounts of free cinnamaldehyde were 1.8 ± 0.3, 4.8 ± 0.1, and 11.0 ± 0.8 mg/g film, respectively.

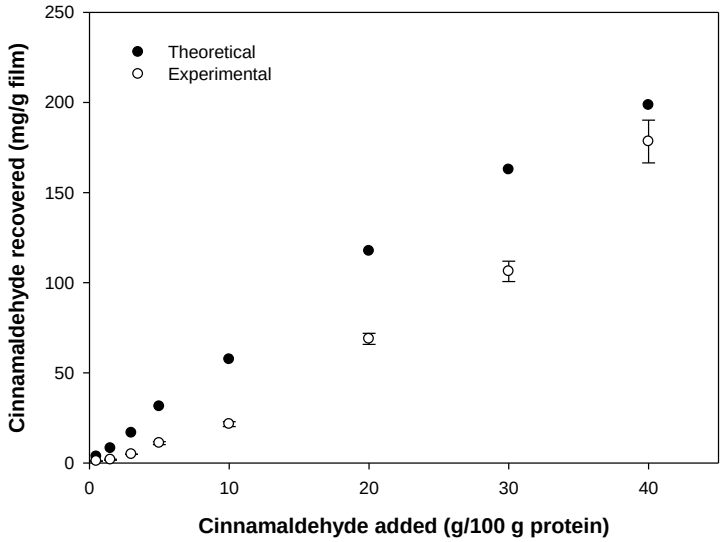

Figure 4.7. Concentration of free cinnamaldehyde in the film (mg/g film) as a function of the concentration of cinnamaldehyde added to the film-forming solution (g/100 g protein). The theoretical amount was calculated taking into account the surface density of the compound (g cinnamaldehyde/cm^2 film), and the surface density of the film at 50% RH (g film/cm^2 film).

The experimental amount of cinnamaldehyde recovered did not follow a linear trend. As the percentage added to the film-forming solution increased, the amount of free cinnamaldehyde present in the film increased exponentially.

The recovery percentage increased from 22% for the film containing 1.5% of cinnamaldehyde to 90% for the film containing 40% of cinnamaldehyde. One explanation for this might be that most of the cinnamaldehyde added is used initially as a cross-linker, remaining covalently and irreversibly bonded with the protein, leaving a smaller amount of free cinnamaldehyde reversibly linked with the protein by weak bonds. However, a recovery of 100% is difficult to achieve also because of the losses that occur during the drying step.

A linear fit with a good determination coefficient (R^2 = 0.9996) was obtained in the region from 1.5% to 10% of cinnamaldehyde added to the film-forming solution:

$$Cinn_{recovered} = 0.4042 \cdot Cinn_{added} - 1.6884 \qquad (\mathbf{4.7})$$

both cinnamaldehyde concentrations being expressed in mg/g film (**Figure 4.8**). From this correlation, the amount of free cinnamaldehyde available to be released from the film as a function of the initial amount added can be calculated. One interesting value obtained from this correlation is the minimum amount of cinnamaldehyde that should be added in order to have free cinnamaldehyde available in the film, which is when the cinnamaldehyde recovered starts to be positive (x-intercept). The x-intercept zone is depicted in detail as an inset graph of **Figure 4.8**. From **Equation 4.7** the x-intercept resulted in 4.17 mg of cinnamaldehyde/g of film, thus this amount is lost during the drying step or as a result of participation in the cross-linking reaction.

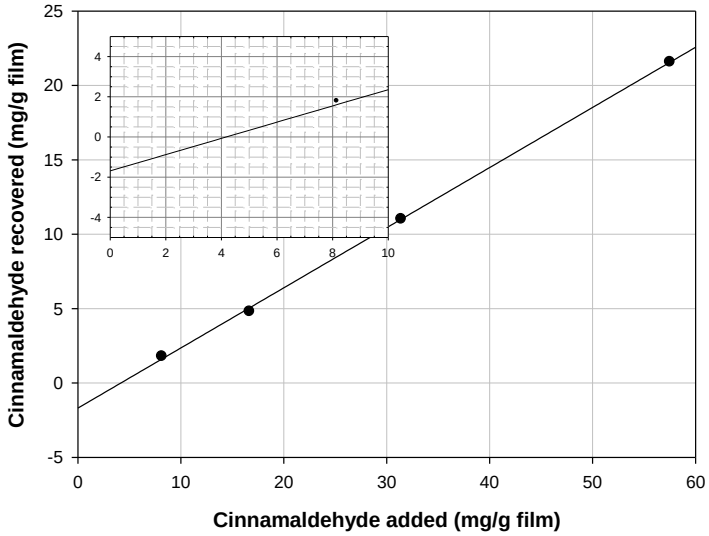

Figure 4.8. Concentration of free cinnamaldehyde (mg/g film) as a function of the concentration of cinnamaldehyde added to the film (mg/g film). Linear fit is shown in **Equation 4.7**. The concentration added was calculated taking into account the surface density of the compound (g cinnamaldehyde/cm^2 film), and the surface density of the film at 50% RH (g film/cm^2 film). Inset graph: detail of the x-intercept which represents the minimum amount of cinnamaldehyde that should be added in order to have free cinnamaldehyde available in the film.

Previous results in paper coated with soy protein containing cinnamaldehyde showed a loss of volatile of 60% and 64% with initial concentrations of 10% and 30% of cinnamaldehyde (w/w) in the coating solution, respectively (Ben Arfa et al., 2007). For gluten paper coatings containing carvacrol the losses found were around 23–24% (Mascheroni et al., 2010; Mascheroni et al., 2011), and no cross-linking can be involved in the case of this compound, which also had a higher retention than cinnamaldehyde in soy protein coatings (Ben Arfa et al., 2007). Usually, the interactions established between aroma compounds and proteins are reversible, involving hydrophobic and hydrogen bonding (Guichard, 2006). In the case of aldehydes, however, reversible covalent bonds with proteins through Schiff base formation have been widely reported (Metz et al., 2004).

4.3.3. Kinetics of cinnamaldehyde release from gliadin films and estimated apparent diffusivity

4.3.3.1. Influence of cinnamaldehyde concentration

Figure 4.9 shows the kinetics of cinnamaldehyde release from gliadin films incorporating different percentages of cinnamaldehyde at 90% RH and 20 °C. The release kinetic at 90% RH was very rapid for all the films, and, although the initial concentrations were different, almost total release was reached after 5 days. It can be observed that a higher concentration of cinnamaldehyde could be recovered from the film in the first hours of the release experiment (second point). This could be due to exposure of the film to a higher humidity (from 50% to 90% RH), which opens the matrix and facilitates extraction.

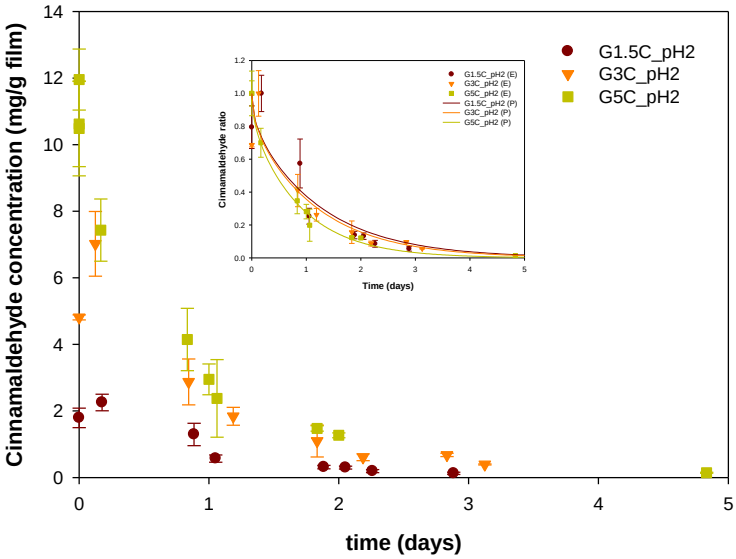

Figure 4.9. Kinetics of cinnamaldehyde release from cross-linked gliadin films at 90% RH and 20 °C. Inset graph: Experimental data (symbols), and predicted values (line).

Apparent diffusivities of cinnamaldehyde were estimated by adjusting **Equation 4.5** to the experimental data. The second point was taken as the maximum concentration. The estimated apparent diffusivities expressed as mean ± standard deviation of three replicates are summarized in **Table 4.4**. The *D* values obtained are independent of the initial concentration of cinnamaldehyde incorporated. Modifications in *D* values were observed when strong interactions between the matrix and the molecule occurred, inducing

plasticization and increasing polymer and molecule mobility (Dury-Brun et al., 2007; Follain et al., 2010). However, for the concentrations studied there are no strong interactions between free cinnamaldehyde and gliadin proteins, and therefore Fick's laws can be used to predict the transfer.

Table 4.4. Apparent diffusivity of cinnamaldehyde in cross-linked gliadin films at 90% RH and 20 °C. Film thickness: 100 ± 10 μm.

Sample	$D \cdot 10^{15}$ (m^2/s)	RMSE
G1.5C_pH2	8.91 ± 1.75	0.1292
G3C_pH2	9.65 ± 1.44	0.0912
G5C_pH2	13.1 ± 1.7*	0.0571

Values reported are the means ± standard deviations
* Statistically significant difference between films with different degrees of cross-linking ($p \leq 0.05$).

Conversely, some influence related with the different cross-linking degrees of the matrices was expected, as has been documented for oxygen and water vapor diffusivities (Balaguer et al., 2013). However, in this case the matrix with the highest cross-linking degree, expected to have the lowest *D* value, has the highest amount of permeant (cinnamaldehyde). It is possible that the cross-linking effect is counterbalanced by the potential plasticization effect of cinnamaldehyde at high concentrations, which favor release (Quezada Gallo et al., 1998).

4.3.3.2. Influence of relative humidity

Figure 4.10 shows the kinetics of cinnamaldehyde release from a gliadin film incorporating 5% of cinnamaldehyde (G5C_pH2) at different relative humidities (30%, 50%, and 90% RH) and 20 °C. The release of cinnamaldehyde from the gliadin matrix was notably affected by the relative humidity of the environment. The higher the relative humidity, the faster the release kinetic of cinnamaldehyde was. Owing to the hydrophilic nature of gliadins, sorption of water promotes plasticization of the film and release of the volatile compound entrapped within the polymer network. This effect can be used to trigger release of the aroma compound and to control the release rate. Therefore the films can be stored at low relative humidity conditions to avoid loss of cinnamaldehyde before their use. On the other hand, the high relative humidity conditions present inside packaged food, often associated with microorganism development, trigger release of the antimicrobial volatile compound when it is required.

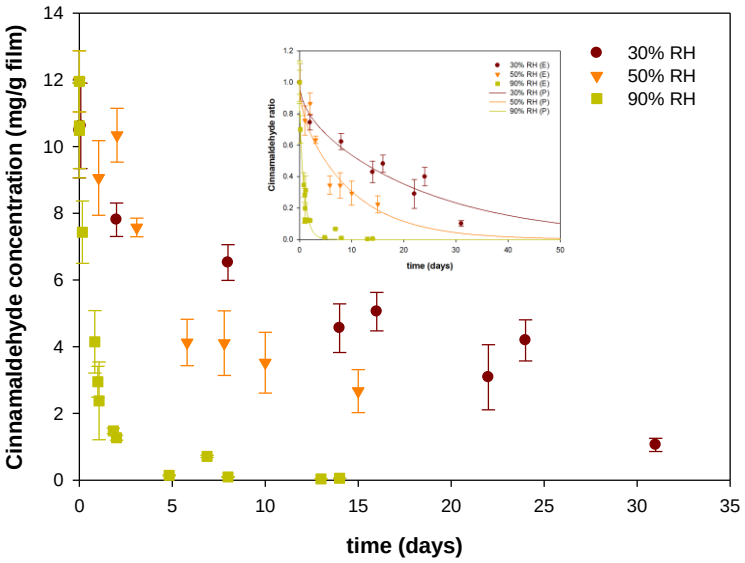

Figure 4.10. Kinetics of cinnamaldehyde release from G5C_pH2 film at different relative humidities and 20 °C. Inset graph: Experimental data (symbols), and predicted values (line).

The release of cinnamaldehyde was well modeled by **Equation 4.5**. The RMSE values, which represent the accuracy of the model, were always in the same range as or lower than the experimental errors (0.1 to 0.8 mg/g). At 30% RH, 15 days are needed to reach the release of half of the initial free cinnamaldehyde amount, contrary to what happens at 90% RH, where only half a day is needed. **Table 4.5** gives the apparent diffusivities estimated as a function of the relative humidity. The increase of cinnamaldehyde diffusivity with relative humidity was 26-fold for a variation between 30% and 90% RH. The effect of relative humidity on diffusivity was similar to what happened in the case of carvacrol included in wheat gluten coated paper (20-fold) (Mascheroni et al., 2011). Moreover, the absolute *D* values were in the same order of magnitude for cinnamaldehyde and gliadin than for carvacrol and gluten. Diffusivity depends not only on the size, shape, and polarity of the permeant molecule, but also on the density, the structural organization of the macromolecular network, and the polymer-chain segmental mobility. Therefore, this similarity between these different permeants in related matrices (gliadin and wheat gluten) may be explained by the different cross-linking degree of cinnamaldehyde-treated gliadins versus gluten; since taking into account the hydrophobic nature of the permeants, according to its log *P* cinnamaldehyde is less hydrophobic than carvacrol (1.82 vs 3.52), weaker hydrophobic interactions can be established with protein and cinnamaldehyde, and

although the solubility of cinnamaldehyde in water is relatively low, a small part of cinnamaldehyde could be solubilized in the water sorbed in the matrix and could diffuse together with it. Therefore, the new entanglements generated in the gliadin matrix prevented from a faster release of cinnamaldehyde.

Table 4.5. Apparent diffusivity of cinnamaldehyde in G5C_pH2 film at different relative humidities and 20 °C. Film thickness: 100 ± 10 μm.

% RH	$D \cdot 10^{15}$ (m^2/s)	RMSE
30	0.488 ± 0.053^{a}	0.0742
50	1.15 ± 0.17^{b}	0.0922
90	13.1 ± 1.7^{c}	0.0571

Values reported are the means ± standard deviations.
a-c Different lowercase letters in the same column indicate a statistically significant difference between films with different degrees of cross-linking ($p \leq 0.05$).

In the case of oxygen diffusivity for the G5C_pH2 film, the values ranged from 0.78·10–13 and 2.1·10–13 to 11.6·10–13 (m2/s) for 35%, 50%, and 75% RH, respectively (Balaguer et al., 2013). This permeant does not interact with protein and its diffusivity is only affected by the plasticization of the matrix, showing a similar behavior to cinnamaldehyde. However, in the case of water vapor the D values for the entire RH range ranged from 0.1·10–13 to 1.9·10–13 (m2/s), depicting a bell-like curve for all the gliadin films evaluated, being concentration-dependent, influenced by a high number of simultaneously occurring phenomena, such as plasticization of the matrix, and water clustering (Balaguer et al., 2013).

4.4. CONCLUSIONS

Cinnamaldehyde treatment endowed gliadin films with i) higher weight distribution profiles, lower solubility, and reduced overall migration into food simulants as a consequence of polymerization of gliadin units by covalent bonding; and with ii) the ability to release the cinnamaldehyde entrapped in the matrix by weak bonding when the films were exposed to high relative humidity conditions, or to retain this volatile active agent whenever low relative humidity was maintained. The diffusivity of cinnamaldehyde was greatly affected by relative humidity, providing a mechanism for control of its triggering

and release rate. Despite the losses of active agent that took place during the film manufacturing process, a significant amount of volatile was retained. Therefore, subsequent antimicrobial tests should be carried out in order to check their efficacy against bacterial and fungal growth.

4.5. REFERENCES

Angellier-Coussy, H., Torres-Giner, S., Morel, M. H., Gontard, N., and Gastaldi, E. 2008. Functional properties of thermoformed wheat gluten/montmorillonite materials with respect to formulation and processing conditions. *Journal of Applied Polymer Science, 107*(1), 487-496.

Balaguer, M. P., Cerisuelo, J. P., Gavara, R., and Hernandez-Muñoz, P. 2013. Mass transport properties of gliadin films: Effect of cross-linking degree, relative humidity, and temperature. *Journal of Membrane Science, 428*, 380-392.

Balaguer, M. P., Gomez-Estaca, J., Gavara, R., and Hernandez-Munoz, P. 2011a. Functional properties of bioplastics made from wheat gliadins modified with cinnamaldehyde. *Journal of Agricultural and Food Chemistry, 59*(12), 6689-6695.

Balaguer, M. P., Gómez-Estaca, J., Gavara, R., and Hernandez-Munoz, P. 2011b. Biochemical properties of bioplastics made from wheat gliadins cross-linked with cinnamaldehyde. *Journal of Agricultural and Food Chemistry, 59*(24), 13212-13220.

Ben Arfa, A., Preziosi-Belloy, L., Chalier, P., and Gontard, N. 2007. Antimicrobial paper based on a soy protein isolate or modified starch coating including carvacrol and cinnamaldehyde. *Journal of Agricultural and Food Chemistry, 55*(6), 2155-2162.

Boye, J. I., Alli, I., Ismail, A. A., Gibbs, B. F., and Konishi, Y. 1995. Factors affecting molecular characteristics of whey protein gelation. *International Dairy Journal, 5*(4), 337-353.

Burt, S. 2004. Essential oils: Their antibacterial properties and potential applications in foods - a review. *International Journal of Food Microbiology, 94*(3), 223-253.

Crank, J., 1975. *The mathematics of diffusion*. 2nd ed.; Oxford University Press, London: 44-69.

Cuq, B., Gontard, N., and Guilbert, S. 1998. Proteins as agricultural polymers for packaging production. *Cereal Chemistry, 75*(1), 1-9.

Chalier, P., Ben Arfa, A., Guillard, V., and Gontard, N. 2009. Moisture and temperature triggered release of a volatile active agent from soy protein coated paper: Effect of glass transition phenomena on carvacrol diffusion coefficient. *Journal of Agricultural and Food Chemistry, 57*(2), 658-665.

Chen, L. H., Reddy, N., Wu, X. Y., and Yang, Y. 2012. Thermoplastic films from wheat proteins. *Industrial Crops and Products, 35*(1), 70-76.

Chourpa, I., Ducel, V., Richard, J., Dubois, P., and Boury, F. 2006. Conformational modifications of alpha gliadin and globulin proteins upon complex coacervates formation with gum arabic as studied by raman microspectroscopy. *Biomacromolecules, 7*(9), 2616-2623.

Dainelli, D., Gontard, N., Spyropoulos, D., Zondervan van den Beuken, E., and Tobback, P. 2008. Active and intelligent food packaging: Legal aspects and safety concerns. *Trends in Food Science & Technology, 19*(Suppl. 1), S99-S108.

Dury-Brun, C., Chalier, P., Desobry, S., and Voilley, A. 2007. Multiple mass transfers of small volatile molecules through flexible food packaging. *Food Reviews International, 23*(3), 199-255.

Follain, N., Valleton, J.-M., Lebrun, L., Alexandre, B., Schaetzel, P., Metayer, M., and Marais, S. 2010. Simulation of kinetic curves in mass transfer phenomena for a concentration-dependent diffusion coefficient in polymer membranes. *Journal of Membrane Science, 349*(1–2), 195-207.

Friedman, M., Henika, P. R., and Mandrell, R. E. 2002. Bactericidal activities of plant essential oils and some of their isolated constituents against *Campylobacter jejuni*, *Escherichia coli, Listeria monocytogenes,* and *Salmonella enterica*. *Journal of Food Protection, 65*(10), 1545-1560.

Gamage, G. R., Park, H. J., and Kim, K. M. 2009. Effectiveness of antimicrobial coated oriented polypropylene/polyethylene films in sprout packaging. *Food Research International, 42*(7), 832-839.

Gill, E. P., Murray, W., and Wright, M. H., 1981. *Practical optimization*. Academic Press: New York.

Gomes, C., Moreira, R. G., and Castell-Perez, E. 2011. Poly (dl-lactide-co-glycolide) (PLGA) nanoparticles with entrapped trans-cinnamaldehyde and eugenol for antimicrobial delivery applications. *Journal of Food Science, 76*(2), S16-S24.

Guichard, E. 2006. Flavour retention and release from protein solutions. *Biotechnology Advances, 24*, 226-229.

Haugaard, G., and Johnson, A. H. 1930. Fractionation of gliadin. *Comptes rendus des travaux du laboratoire Carlsberg, 18*(no. 2), 133-135.

Hernandez-Munoz, P., and Hernandez, R. J. 2001. *Glutenin and gliadin films from wheat gluten: Preparation and properties.* Paper presented at the IFT Annual Meeting, New Orleans, Louisiana.

Hernandez-Munoz, P., Kanavouras, A., Lagaron, J. M., and Gavara, R. 2005. Development and characterization of films based on chemically cross-linked gliadins. *Journal of Agricultural and Food Chemistry, 53*(21), 8216-8223.

Kim, K. M., Hanna, M. A., Weller, C. L., Cho, S.-H., and Choi, S.-G. 2006. Characterization of cinnamaldehyde-supplemented soy protein isolate films. *Food Science and Biotechnology, 15*(4), 631-634.

Kyoungju, K., Yungbum, S., and Kyung Bin, S. 2007. Physical properties of gelidium corneum films treated with cinnamaldehyde. *Journal of Food Science and Nutrition, 12*(2), 122-125.

Lefèvre, T., Subirade, M., and Pézolet, M. 2005. Molecular description of the formation and structure of plasticized globular protein films. *Biomacromolecules, 6*(6), 3209-3219.

Lopez, P., Sanchez, C., Batlle, R., and Nerin, C. 2007. Vapor-phase activities of cinnamon, thyme, and oregano essential oils and key constituents against foodborne microorganisms. *Journal of Agricultural and Food Chemistry, 55*(11), 4348-4356.

Mangavel, C., Barbot, J., Popineau, Y., and Gueguen, J. 2001. Evolution of wheat gliadins conformation during film formation: A Fourier transform infrared study. *Journal of Agricultural and Food Chemistry, 49*(2), 867-872.

Mascheroni, E., Chalier, P., Gontard, N., and Gastaldi, E. 2010. Designing of a wheat gluten/montmorillonite based system as carvacrol carrier: Rheological and structural properties. *Food Hydrocolloids, 24*(4), 406-413.

Mascheroni, E., Guillard, V., Gastaldi, E., Gontard, N., and Chalier, P. 2011. Anti-microbial effectiveness of relative humidity-controlled carvacrol release from wheat gluten/montmorillonite coated papers. *Food Control, 22*(10), 1582-1591.

Mauricio-Iglesias, M., Peyron, S., Guillard, V., and Gontard, N. 2010. Wheat gluten nanocomposite films as food-contact materials: Migration tests and impact of a novel food stabilization technology (high pressure). *Journal of Applied Polymer Science, 116*(5), 2526-2535.

Metz, B., Kersten, G. F. A., Hoogerhout, P., Brugghe, H. F., Timmermans, H. A. M., de Jong, A., Meiring, H., Hove, J. t., Hennink, W. E., Crommelin, D. J. A., and Jiskoot, W. 2004. Identification of formaldehyde-induced modifications in proteins. *Journal of Biological Chemistry, 279*(8), 6235-6243.

Morel, M.-H., Redl, A., and Guilbert, S. 2002a. Mechanism of heat and shear mediated aggregation of wheat gluten protein upon mixing. *Biomacromolecules, 3*(3), 488-497.

Morel, M. H., Redl, A., and Guilbert, S. 2002b. Mechanism of heat and shear mediated aggregation of wheat gluten protein upon mixing. *Biomacromolecules, 3*(3), 488-497.

Pereda, M., Aranguren, M. I., and Marcovich, N. E. 2008. Characterization of chitosan/caseinate films. *Journal of Applied Polymer Science, 107*, 1080-1090.

Pézolet, M., Bonenfant, S., Dousseau, F., and Popineau, Y. 1992. Conformation of wheat gluten proteins. Comparison between functional and solution states as determined by infrared spectroscopy. *FEBS Lett., 299*((3)), 247-250.

Quezada Gallo, J. A., Debeaufort, F., and Voilley, A. 1998. Interactions between aroma and edible films. 1. Permeability of methylcellulose and low-density polyethylene films to methyl ketones. *Journal of Agricultural and Food Chemistry, 47*(1), 108-113.

Redl, A., Morel, M. H., Bonicel, J., Guilbert, S., and Vergnes, B. 1999. Rheological properties of gluten plasticized with glycerol: Dependence on temperature, glycerol content and mixing conditions. *Rheologica Acta, 38*(4), 311-320.

Rhim, J. W., and Ng, P. K. W. 2007. Natural biopolymer-based nanocomposite films for packaging applications. *Critical Reviews in Food Science and Nutrition, 47*(4), 411-433.

Rojas-Grau, M. A., Avena-Bustillos, R. J., Olsen, C., Friedman, M., Henika, P. R., Martin-Belloso, O., Pan, Z., and McHugh, T. H. 2007. Effects of plant essential oils and oil compounds on mechanical, barrier and antimicrobial properties of alginate-apple puree edible films. *Journal of Food Engineering, 81*(3), 634-641.

Sanla-Ead, N., Jangchud, A., Chonhenchob, V., and Suppakul, P. 2012. Antimicrobial activity of cinnamaldehyde and eugenol and their activity after incorporation into cellulose-based packaging films. *Packaging Technology and Science, 25*(1), 7-17.

Secundo, F., and Guerrieri, N. 2005. Atr-ft/ir study on the interactions between gliadins and dextrin and their effects on protein secondary structure. *Journal of Agricultural and Food Chemistry, 53*(5), 1757-1764.

Soares, R. M. D., and Soldi, V. 2010. The influence of different cross-linking reactions and glycerol addition on thermal and mechanical properties of biodegradable gliadin-based film. *Materials Science & Engineering C - Materials for Biological Applications, 30*(5), 691-698.

Song, Y. H., Li, L. F., and Zheng, Q. 2009. Influence of epichlorohydrin modification on structure and properties of wheat gliadin films. *Journal of Agricultural and Food Chemistry, 57*(6), 2295-2301.

Tunc, S., Chollet, E., Chalier, P., Preziosi-Belloy, L., and Gontard, N. 2007. Combined effect of volatile antimicrobial agents on the growth of *Penicillium notatum*. *International Journal of Food Microbiology, 113*(3), 263-270.

Wu, Y. V., and Dimler, R. J. 1963. Hydrogen ion equilibria of wheat glutenin and gliadin. *Archives of Biochemistry and Biophysics, 103*(3), 310-318.

Zhang, X. Q., and Do, M. D. 2009. Plasticization and crosslinking effects of acetone-formaldehyde and tannin resins on wheat protein-based natural polymers. *Carbohydrate Research, 344*(10), 1180-1189.

CHAPTER 5

ANTIFUNGAL PROPERTIES OF GLIADIN FILMS INCORPORATING CINNAMALDEHYDE AND APPLICATION IN ACTIVE FOOD PACKAGING OF BREAD AND CHEESE SPREAD FOODSTUFFS

Balaguer, M.P.; Lopez-Carballo G.; Catala R.; Gavara, R.; and Hernandez-Munoz, P.

International Journal of Food Microbiology, 2013, 166, 369-77

Gliadin films incorporating 1.5, 3 and 5% cinnamaldehyde (g/100 g protein) were tested against food-spoilage fungi Penicillium expansum and Aspergillus niger in vitro, and were employed in an active food packaging system for sliced bread and cheese spread. Gliadin films incorporating cinnamaldehyde were highly effective against fungal growth. P. expansum and A. niger were completely inhibited after storage in vitro for 10 days in the presence of films incorporating 3% cinnamaldehyde. Indeed 1.5% cinnamaldehyde was sufficient in the case of P. expansum. The amount of cinnamaldehyde retained in films after storage for 45 days at 20 °C and 0% RH was also sufficient in most cases to prevent fungal growth in vitro. Active food packaging with gliadin films incorporating 5% cinnamaldehyde increased the shelf-life of both sliced bread and cheese spread. Mold growth was observed on sliced bread after 27 days of storage at 23 °C with active packaging, whereas in the control bread packaged without the active film fungal growth appeared around the fourth day. In the cheese spread, no fungi were observed after 26 days of storage at 4 °C when the product was packaged with the active film. However, growth of fungi was observed in control packaged cheese after 16 days of storage. This work demonstrates a noteworthy potential of these novel bioplastics incorporating natural antimicrobial compounds as innovative solutions to be used in active food packaging to extend shelf-life of food products.

5.1. INTRODUCTION

Nowadays, food industry challenges are focused on diverse requirements. On the one hand, the fulfillment of consumers' demands aimed at increasing food quality from the sensory and nutritional points of view without raising its cost. On the other hand, the reduction of food waste and the improvement of food safety by controlling the growth of food-borne and food-spoilage microorganisms while reducing the use of synthetic preservatives that are associated with health risks and microbial resistance (Naidu, 2000). Fungi are able to grow on diverse foods inducing the development of off-flavors, acidifying, fermenting, discoloring, disintegrating, rotting and rendering nutritious commodities unpalatable or unsafe due to the formation of pathogenic or allergenic toxins (Filtenborg et al., 1996; Pitt and Hocking, 2009).

One novel approach to achieve these needs is based on the use of natural antimicrobial compounds combined with the design of new carrier materials or devices. These active systems should incorporate the antimicrobial agent, trigger its release once necessary, control its rate of release thereby exerting either lethal or inhibitory effects against food pathogens or spoilage microorganisms present in foodstuffs.

Although herbs and spices have been used for centuries in food preservation, a renewed scientific interest has occurred for the last twenty years (Kalemba and Kunicka, 2003). It has been demonstrated that some of their constituents possess greater antimicrobial activities than the essential oils themselves (Burt, 2004; Friedman et al., 2002; Lopez et al., 2007b), hence the use of individual compounds derived from essential oils could reduce the amount of material required for antimicrobial activity. Moreover, numerous individual components of essentials oils, either extracted from plant material or synthetically manufactured, are also categorized as flavoring agents by the European Commission, and as generally recognized as safe (GRAS) by the United States Food and Drug Administration (FDA).

Cinnamaldehyde is an aromatic α,β-unsatured aldehyde, and the major component in essential oils from some cinnamon species (Singh et al., 2007; Wang et al., 2009). It is

registered in the EU flavoring list (FL no. 05.014[1]), and the FDA has classified it as a synthetic GRAS flavoring substance for its intended use (reg no. 182.60[2]).

Cinnamaldehyde has been shown to exert antimicrobial activity against a wide range of microorganism including bacteria, yeasts, and molds (Burt, 2004; Gutierrez et al., 2009; Lopez et al., 2007b; Pauli and Knobloch, 1987; Xing et al., 2010), and to be more effective than other cinnamon essential oil constituents (Khan and Ahmad, 2011; Matan et al., 2011; Utama et al., 2002), especially in vapor phase (Lopez et al., 2007b). Thus, the main advantage of cinnamaldehyde is that direct contact is not required for antimicrobial activity. Its microbicidal activity may be ascribed to the high electrophilic properties of the carbonyl group adjacent to the double bound that make this compound particularly reactive with nucleophiles, such as protein sulfhydryl and amino groups of the microorganism (Neri et al., 2006). Recently, Manso et al. (2013) hypothesized that cinnamon essential oil induces incomplete formation of the conidia of Aspergillus flavus, resulting in inhibited growth, and alternatively, it is also possible that the essential oil causes damage to the conidia after the conidiophore has been formed, resulting in an unstructured vesicle head. These observations are consistent with those observed by other authors when fungi were exposed to essential oils. Abnormalities in the cell wall structure, disrupted and aggregated hyphae, loss of cytoplasm, strong decrease in the number of conidia, and conidiophores with anomalous development have been reported (Helal et al., 2006; Lopez-Malo et al., 2002; Tolouee et al., 2010).

Films, coatings, nanoparticles or devices containing cinnamaldehyde have been produced using a wide variety of raw materials, including cellulose (Sanla-Ead et al., 2012), chitosan (Brasil et al., 2012; Ouattara et al., 2000), pectin (Brasil et al., 2012; Ravishankar et al., 2012; Wang et al., 2010), starch (Ben Arfa et al., 2007; Kechichian et al., 2010), soy protein (Ben Arfa et al., 2007; Gamage et al., 2009), poly(lactic-co-glycolic acid) (Gomes et al., 2011; Zodrow et al., 2012), PP, PE/EVOH (Lopez et al., 2007a), and wax paraffin (Rodriguez-Lafuente et al., 2010; Rodriguez et al., 2008). However, as far as we know there are no studies reported in the literature regarding the use of wheat protein-based materials as carriers of cinnamaldehyde for the development of antimicrobial films.

[1] http://ec.europa.eu/food/food/chemicalsafety/flavouring/database
[2] http://www.ecfr.gov/cgi-bin/text-idx?sid=58029aa65152691d14eab45977de0fb1&c=ecfr&tpl=/ecfrbrowse/Title21/21tab_02.tpl

Most of the active packaging systems containing cinnamaldehyde or cinnamon oil aimed at food applications have shown promising results when tested in vivo. Mild et al. (2011) incorporated cinnamaldehyde in apple-based edible films used to wrap chicken breast and observed great reductions of *Campylobacter jejuni* population without impairment of the sensorial properties of the wrapped product (Du et al., 2012).Reductions in *Escherichia coli O157:H7* and *Salmonella enterica* inoculated in chicken breast, and *Listeria monocytogenes* inoculated in ham were also achieved with these apple-based films containing cinnamaldehyde (Ravishankar et al., 2009). Bologna, regular cooked ham, or pastrami were packaged with chitosan-based films containing cinnamaldehyde; as a result of the application of these films a delay or complete inhibition of the growth of *Enterobacteriaceae* and *Serratia liquefaciens* was obtained (Ouattara et al., 2000). A paper coating based on cinnamon essential oil was highly effective against *Alternaria alternata* inoculated in cherry tomatoes and there were no sensorial changes detected (Rodriguez-Lafuente et al., 2010). Shelf-life of fresh-cut papaya was prolonged by coating with a layer-by-layer edible assembly made of chitosan and pectin incorporating a microencapsulated beta-cyclodextrin/cinnamaldehyde complex (Brasil et al., 2012). Microbial counts of radish, broccoli, and alfalfa sprouts stored in oPP/PE film packages coated with soy protein isolate containing cinnamaldehyde were significantly reduced (Gamage et al., 2009). Cinnamon essential oil incorporated into solid wax paraffin and used as a paper coating showed a strong inhibitory effect on the growth of *Rhizopus stolonifer* inoculated in bread (Rodriguez et al., 2008). However, the antimicrobial effect of cinnamon powders added to cassava-starch films for packaging of bread slices could not be determined since the physico-chemical properties of these biodegradable films were affected by the high relative humidity of bread (Kechichian et al., 2010). No scientific references were found related to the use of cinnamaldehyde in the active packaging of cheese.

The present study is aimed to evaluate the in vitro effectiveness against food-contaminating fungi (*Penicillium expansum* and *Aspergillus niger*) of bioplastics films made from wheat gliadins incorporating cinnamaldehyde, and to provide evidence of their applicability in the design of active food packaging systems for sliced bread and cheese spread foodstuffs.

5.2. MATERIALS AND METHODS

5.2.1. Reagents and microbial strains

Crude wheat gluten (≥ 80% protein), cinnamaldehyde, glycerol, ethanol, and, hydrochloric acid, all laboratory grade, were supplied by Sigma (Madrid, Spain).

Malt Extract Agar (MEA) was purchased from Scharlau (Scharlab S.L., Barcelona, Spain).

P. expansum CECT 2275 and *A. niger* CECT 20156 were used for testing the antimicrobial activity of gliadin films incorporating cinnamaldehyde.

5.2.2. Gliadin-rich fraction extraction from wheat gluten

The gliadin-rich fraction was extracted from the wheat gluten according to the method described by Hernandez-Munoz and Hernandez (2001). Briefly, 100 g of wheat gluten was dispersed in 400 mL of 70% (v/v) ethanol/water mixture, stirred overnight at room temperature, and centrifuged at 5000 rpm for 20 min at 20 °C. The supernatant containing the gliadin-rich fraction was collected and used as the film-forming solution. The amount of protein extracted was around 12–14% (g protein/100 g film-forming solution).

5.2.3. Chemical modification of gliadins

Several cinnamaldehyde concentrations were added to the film-forming solution, namely 1.5% (G1.5C_pH2), 3% (G3C_pH2), and 5% (G5C_pH2) (g cinnamaldehyde/100 g protein). Glycerol was added as plasticizer to the film-forming solutions at 25% (g glycerol/100 g protein). The pH of the mixture containing protein, glycerol, and cinnamaldehyde was adjusted to 2.0 with HCl, the most suitable for producing the cross-linking reaction of gliadins by means of cinnamaldehyde (Balaguer et al., 2013; Balaguer et al., 2011a; Balaguer et al., 2011b), and the mixture was stirred for 30 min to produce a complete homogenization.

5.2.4. Film formation

The film-forming solution was poured onto a horizontal flat Pyrex tray or onto the lid of the plastic Petri dish to allow water and ethanol to evaporate. The weight of film-forming solution used to form the film was calculated in order to obtain a density of 0.01 g protein/cm^2. The films were dried at 37 °C for 24 h, and further conditioned at 50%

RH for 20 h to facilitate peeling off the casting surface. They were stored at 0% RH and 20 °C until use.

The film thickness was measured using a micrometer (Mitutoyo, Kanagawa, Japan) with a sensitivity of ± 2 µm. The mean thickness was 100 ± 12 µm, calculated from measurements taken at ten different locations on each film sample. The surface density of the films was 0.015 ± 0.002 g/cm^2.

5.2.5. Culture preparation

P. expansum and *A. niger* were grown on MEA in plastic Petri dishes (9 cm diameter) for 7 days at 30 °C. Conidia were then collected by flooding the surface of the plates with sterile peptone water and gently scraping the mycelial surface with a spatula. Ten mL of this suspension was transferred to sterile plastic tubes, which were shaken to obtain a homogenous suspension of conidia. The conidial suspensions were adjusted to $1 \cdot 10^6$ spores/mL. The Neubauer improved method (Bright-Line Hemacytometer, Hausser Scientific, Horshan, PA) was used to determinate spore concentration.

5.2.6. Effectiveness of antimicrobial gliadin films against P. expansum and A. niger in vitro

The microatmosphere method was selected for testing the antimicrobial effectiveness of films since it most resembles the likely future application of these films in which no direct contact between film and food is necessary for the former to exert its activity. In this method, the volatile compound migrates from the film into the head-space of the system, thus becoming available to contact to the growth media and the microorganism. The surface of the solid MEA culture medium contained in Petri dishes of 9 cm diameter was inoculated at three equidistant points with 3 µL of conidial suspension. To study the in vitro antifungal capacity films were directly casted over the plate lids using the film-forming solutions previously prepared (G1.5C_pH2, G3C_pH2, G5C_pH2). All film formulations, G1.5C_pH2, G3C_pH2, and G5C_pH2, were tested. Once Petri dishes and lids were assembled, the units were sealed with Parafilm™ to reduce any leakage of the volatile agent. Incubation was done at 30 °C, and colony diameters were measured as a function of time over 10 days. Two perpendicular measures of each colony diameter were made and an average value was obtained. Controls were prepared in the same way but without the lid containing any film. All the tests were performed in triplicate.

Fungal growth data were transformed into percentage inhibition by comparing the colony diameters of the fungi in the antimicrobial tests ($\overline{\emptyset}_{antimicrobial}$) with those measured in the control tests ($\overline{\emptyset}_{control}$), using the equation:

$$Inhibition\ (\%) = 100 - \frac{\overline{\emptyset}_{antimicrobial}}{\overline{\emptyset}_{control}} \cdot 100 \qquad (\mathbf{5.1})$$

5.2.7. Determination of fungicidal/fungistatic capacities of antimicrobial gliadin films

The fungicidal/fungistatic capacities of the films were evaluated after the in vitro tests by studying the inhibition of fungal reproduction and growth. Petri dishes with no fungal growth after exposure to cinnamaldehyde-containing films were assayed. The antimicrobial film was considered fungistatic if growth of the fungus occurred after replacing the lid containing the film with an empty Petri dish lid, that is to say, exposing the fungus to an environment free of the antimicrobial volatile. If no growth was observed after removing the antimicrobial film, the film was considered to be fungicidal.

5.2.8. Exhaustion and storage of the antimicrobial films

After the in vitro assays, in which a continuous release of the antimicrobial volatile was produced during 10 days into the Petri dish system containing MEA inoculated with fungus, the antifungal films were reused in additional in vitro assays against *P. expansum* and *A. niger* to assess their effectiveness and capacity for reuse. These samples are coded as -R.

The capacity of the films to exert their antifungal activity was also evaluated after storage at 20 °C and 0% RH over 45 days. Films were tested in in vitro assays against *P. expansum* and *A. niger*. These samples are coded as -45.

5.2.9. Antimicrobial effectiveness of active gliadin films in sliced white bread

5.2.9.1. Bread production

White bread was produced according to the traditional method using a bread-making machine. The ingredients employed were 500 g of white wheat flour from organic culture (ES-ECO-002 certified by SHC) (Panadería Rincón del Segura S.L., Albacete, Spain), 10 g of dehydrated yeast (VITAM Hefe-Produkt GmbH, Hameln, Germany), 340 mL of water, 6 g of salt and 12.5 g of sugar. After baking, the bread was cooled at ambient temperature for 30 min and sliced into portions of 1 cm thickness by means of a standard bread slicer

(Model TP 60/2, E. Gabarró, Barcelona, Spain). The dimensions of the bread slices were approximately 12 cm × 7 cm and the weight was around 45 g.

5.2.9.2. Bread inoculation

Bread slices were inoculated at three points on the surface with 5 µL of the *P. expansum* conidial suspension prepared as in **Section 5.2.5**. Other slices were not inoculated in order to check the effectiveness of the antifungal films against the fungi naturally present in bread.

5.2.9.3. Bread packaging and storage

Each bread slice, either inoculated or not, was placed in a plastic bag (15 cm × 10 cm) of mono cast polypropylene of 30 µm thickness along with a piece (13 cm × 8 cm) of an antimicrobial gliadin film treated with 5% of cinnamaldehyde (G5C_pH2) (active packaging tests). Control packaging tests were performed in the same way without including the gliadin film. The plastic bags were closed using a manual sealing machine (Sealboy 420 SBM, Rovebloc S.A., Barcelona, Spain) and stored at 23 ± 2 °C and 50% RH. The antifungal effect was evaluated over time by visual inspection of the fungal growth. Antimicrobial packaging was considered effective only if there was a delay in the appearance of fungal growth in comparison with the control. Tests were performed in triplicate.

5.2.10.Antimicrobial effectiveness of active gliadin films in cheese spread

Commercial pasteurized white cheese spread was used in this test. The composition was: 4.7% protein, 4.1% carbohydrate, and 23% lipid. The ingredients were pasteurized cow milk, pasteurized cow cream, salt, stabilizers (E-410 and E-407) and lactic starters.

Approximately 10 g of cheese was spread on the base of Petri dishes (5.5 cm diameter). Each cheese sample was inoculated in the middle with a 5 µL drop of the *P. expansum* conidial suspension prepared as in **Section 5.2.5**. Non-inoculated cheese samples were used as controls to check the effectiveness of the antifungal films against naturally present fungi in cheese. Active packaging tests consisted of Petri dish lids incorporating the antimicrobial films casted in situ; control samples were closed with empty lids. The antimicrobial gliadin film used incorporated 5% cinnamaldehyde (G5C_pH2). Petri dishes were sealed with Parafilm™ and stored at 4 °C. The antifungal effect was evaluated over time by visual inspection. Antimicrobial packaging with the

cinnamaldehyde incorporating-films was considered effective if a delay in fungal growth occurred in comparison to the control packaging. Six replicates of each sample were evaluated.

5.3. RESULTS AND DISCUSSION

5.3.1. Effectiveness of antimicrobial gliadin films in vitro

The growth of *P. expansum* and *A. niger* was evaluated by the microatmosphere method over a 10-day period in MEA Petri dishes in the presence or absence of antimicrobial films containing different concentrations of cinnamaldehyde. **Figure 5.1** shows the antifungal effect of films after 3 days of storage at 30 °C. Antimicrobial gliadin films incorporating cinnamaldehyde were highly effective against fungal growth, *P. expansum* being more sensitive (**Figure 5.11A**) than *A. niger* (**Figure 5.1B**). Inhibition of fungal growth was observed even at low concentrations of cinnamaldehyde. Moreover, when fungal growth did occur in the presence of the antimicrobial agent (**Figure 5.1B**, film G1.5C_pH2) the morphology of the fungal colony was notably affected. As a consequence of the high relative humidity produced by the agar culture medium the protein matrix swelled so that the film dimensions exceeded the lid surface size and wrinkles appeared in the film. Of note, the greatest wrinkles occurred in the films with the least cross-linking. It is expected that plasticization of the films by water due to the high relative humidity inside the Petri dish triggers the release of the antimicrobial volatile retained in the film.

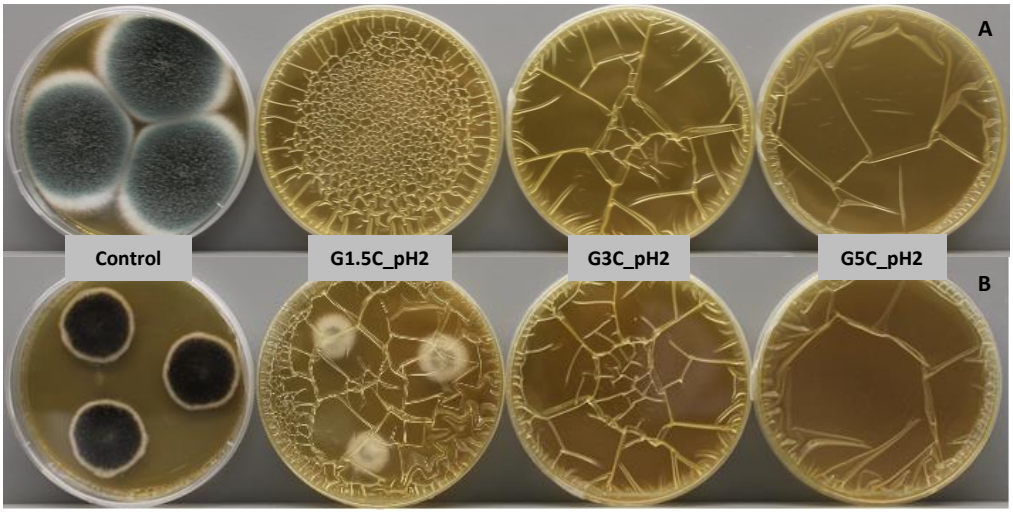

Figure 5.1. Antifungal effect of gliadin films incorporating 1.5%, 3% and 5% of cinnamaldehyde after 3 days of storage at 30 °C against *Penicillium expansum* **(A)** and *Aspergillus niger* **(B)**.

Figure 5.2 shows the changes over time of the percentage inhibition calculated by comparison of colony diameters with those of the control samples (**Equation 5.1**). Film G1.5C_pH2 produced 100% inhibition against *P. expansum* only immediately after casting (G1.5C_pH2-0). After storage for 45 days at 20 °C and 0% RH the efficacy was reduced by 23% (G1.5C_pH2-45) due to the losses of cinnamaldehyde by evaporation throughout this period. The exhaustion of this film was almost complete after its first use since it did not prevent fungal growth upon reuse in additional tests, showing percentages of inhibition between 0% and 20% (G1.5C_pH2-0-R, G1.5C_pH2-45-R). *A. niger* was inhibited by 69% and 42% for G1.5C_pH2-0 and G1.5C_pH2-45, respectively. In the reusing tests films did not shown any activity against *A. niger* (G1.5C_pH2-0-R, G1.5C_pH2-45-R).

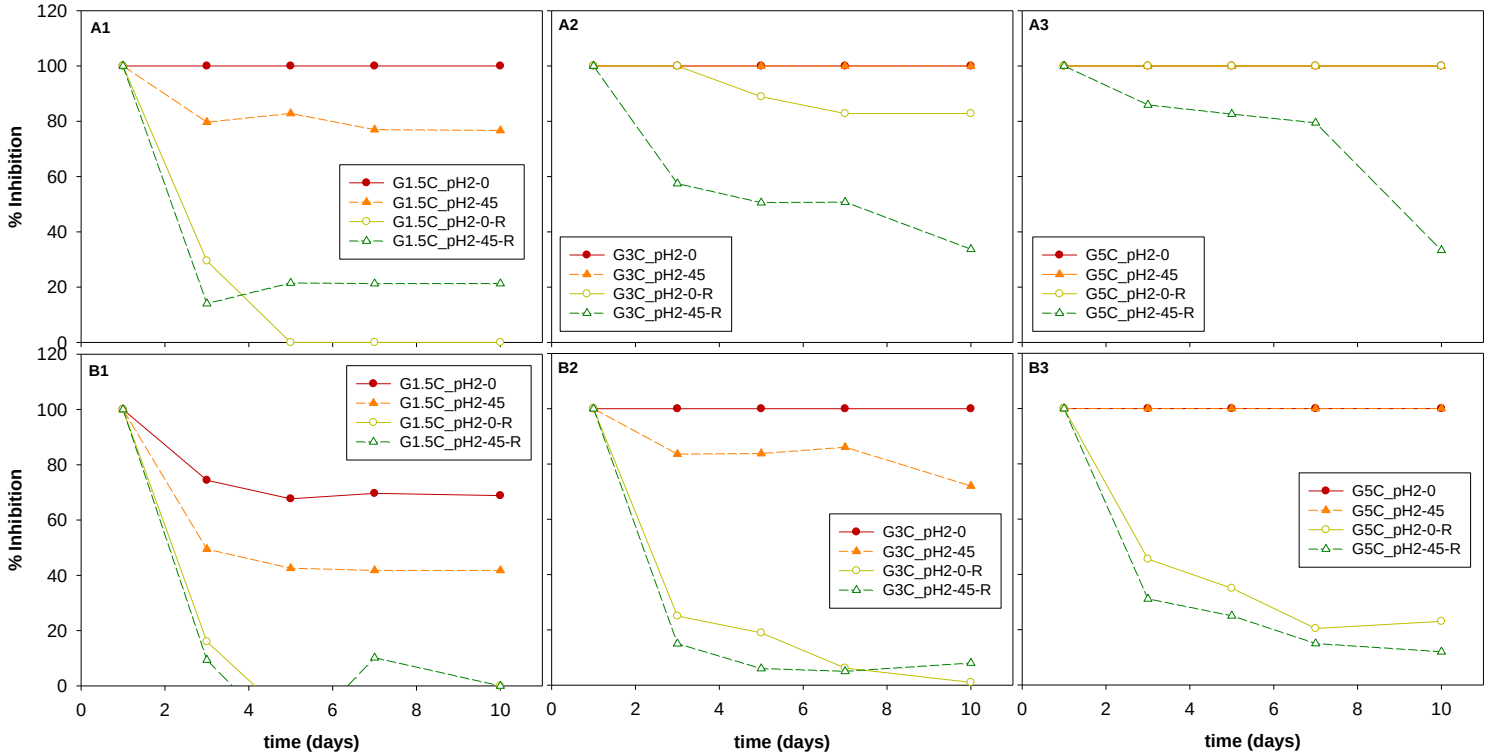

Figure 5.2. Effectiveness *in vitro* of the antifungal gliadin films incorporating cinnamaldehyde against *Penicillium expansum* **(A)** and *Aspergillus niger* **(B)**. GXC_pH2-0: film just produced; GXC_pH2-45: film stored at 0% RH and 20 °C over 45 days; GXC_pH2-0-R: film just produced, and used 10 days at 100% RH and 30 °C; GXC_pH2-45-R: film stored at 0% RH and 20 °C over 45 days, and used 10 days at 100% RH and 30 °C.

Film G3C_pH2 was 100% effective against *P. expansum* regardless of its production time. In the reuse tests, however, there was a great difference between G3C_pH2-0-R and G3C_pH2-45-R since the percentage inhibition decreased from 83 to 34% after a 10-day exposure. The G3C-pH2-0 film totally inhibited growth of *A. niger*, but there was a 30% reduction in its antimicrobial activity after the storage period (G3C-pH2-45). Inhibition of *A. niger* growth was negligible when the film was reused, suggesting that the amount of cinnamaldehyde remaining in the film after its first use is too low to exert any antifungal activity.

Film G5C_pH2 inhibited *P. expansum* growth by 100% in all cases over the 10-day exposure period. Film G5C_pH2-45-R showed a high efficacy of around 80% during the first 7 days of exposure but this was greatly reduced to 33% at day 10. This effect is indicative of its fungistatic capacity. In the case of *A. niger*, films were 100% effective independently of the production time, but after their first use (-R) their efficacy was greatly reduced to values near 20%.

The efficacy of cinnamaldehyde in inhibiting the growth of fungi from the genera *Penicillium* and *Aspergillus* has been demonstrated by several authors. Lopez et al. (2007b) found that *Penicillium islandicum* and *A. flavus* were completely inhibited by 4.36 µL/L and 34.9 µL/L, respectively, of a cinnamaldehyde-fortified cinnamon essential oil in vapor phase, the MIC of cinnamaldehyde against *A. flavus* being 21.8 µL/L. Tunc et al. (2007) found cinnamaldehyde to be one of the strongest inhibitors of *Penicillium notatum* growth (MIC 3.9 µmol/L).

Antimicrobial films of PP incorporating 2% of cinnamaldehyde were also highly effective against mold growth producing complete inhibition of *A. flavus*, *Penicillium commune*, *P. expansum*, *Penicillium nalgiovense*, *Penicillium roqueforti*, and *P. islandicum* (Lopez et al., 2007a). Ben Arfa et al. (2007) include cinnamaldehyde in a paper coating made with soy protein or modified starch, and obtained a 21-day growth delay of *Botrytis cinerea* for concentrations of 5 mg/L.

In the present work, the amount of cinnamaldehyde present in each Petri dish system was 9.5 mg (G1.5C_pH2), 19.1 mg (G3C_pH2) and 31.8 mg (G5C_pH2), respectively, since films were casted to have 0.01 g protein/cm^2. In a previous work, however, it was reported that a percentage of the added cinnamaldehyde remained irreversibly linked to the protein, and some compound losses occurred throughout the film production steps (mixing,

casting, and drying). Therefore, lower amount than the initially added remained free to be released and further exert its antifungal activity (Balaguer et al., 2013). The amount of free cinnamaldehyde remaining in the films after their production was evaluated by solvent extraction with n-pentane followed by gas chromatography quantification (Balaguer et al., 2013). It was shown that the amount of free cinnamaldehyde depended on the initial percentage added, 1.8 ± 0.3, 4.8 ± 0.1, and 11.0 ± 0.8 mg cinnamaldehyde/g film for the films G1.5C_pH2, G3C_pH2, and G5C_pH2, respectively, which represents 20.2%, 26.9%, and 37.0% of the incorporated cinnamaldehyde. According to this percentage of retention, the maximum amount of cinnamaldehyde able to be released into each Petri dish system was 1.9, 5.1, and 11.8 mg, respectively for the films G1.5C_pH2, G3C_pH2, and G5C_pH2. However, it is difficult to know the real concentration or amount released that prevents fungal growth, since, although the volatile is released into the head-space, (i) the agar can absorb a part of the volatile, (ii) some leakage may be expected in the Petri dish because it is not a hermetically-sealed system, (iii) a saturation of the head-space could be achieved before releasing all the compound present in the film, (iv) the partition coefficient of cinnamaldehyde between the film and the air influences the final head-space concentration (Kurek et al., 2013), and (v) the fungi can biotransform or metabolize some cinnamaldehyde into other compounds as has been demonstrated by Ma et al. (2011).

The fungicidal/fungistatic effect of cinnamaldehyde was evaluated. The active agent could exert a lethal effect on the microorganism (fungicidal), or a merely growth inhibition (fungistatic). Fungistatic effects can also be observed if growth takes place after prolonged incubation, probably due to losses of the volatile agent through evaporation. The fungicidal activity observed depended on the concentration of the volatile compound and the fungal species tested. **Table 5.1** summarizes the fungicidal/fungistatic activity against *P. expansum* and *A. niger* of films immediately after production, and films stored for 45 days at 20 °C and 0% RH. Cinnamaldehyde had a lethal effect on *P. expansum* at concentrations in the film higher than 3%, whereas at least 5% concentration was required for inactivation of *A. niger*. Gliadin films incorporating 5% cinnamaldehyde (G5C_pH2) had a lethal effect on *P. expansum* and *A. niger* spores, which are more resistant than fungal hyphae. These films maintained their efficacy after storage of up to 45 days at 20 °C and 0% RH as a result of the high retention of the antimicrobial agent in the protein matrix at low relative humidities.

Table 5.1. Fungicidal/fungistatic activity of cinnamaldehyde incorporated in gliadin films.

Sample	Time produced (days)	*Penicillium expansum*		*Aspergillus niger*	
		Fungistatic	Fungicidal	Fungistatic	Fungicidal
G1.5C_pH2	0	+	-	-	-
	45	+	-	-	-
G3C_pH2	0	+	+	+	-
	45	+	-	-	-
G5C_pH2	0	+	+	+	+
	45	+	+	+	+

+: with effect, -: without effect

Exposure of the antimicrobial film to humid environments, which are commonly found in foodstuffs and promote microbial growth, triggered the release of the volatile compound and, thereby, its antifungal capacity. This work demonstrates that direct contact between the active agent and food is not needed for efficacy Moreover, it is shown that once the equilibrium in the system is achieved, the cinnamaldehyde still present in the film acts as a reservoir, thus opening of the package system does not limit the antimicrobial capacity. However, the growth of fungi in a particular food is governed largely by a series of physical and chemical parameters, such as water activity, hydrogen ion concentration, temperature of both processing and storage, gas tension, specifically of oxygen and carbon dioxide, consistency, nutrient status, and specific solute effects (Pitt and Hocking, 2009). The situation in practice is made more complex by the fact that such factors frequently do not act independently, but synergistically (Pitt and Hocking, 2009). Moreover, the antimicrobial activity of essential oil components is generally modified in food systems, requiring a higher concentration to achieve the same effect as in laboratory media, since the active compound can be retained by the lipid fraction or react with proteins reducing its availability (Burt, 2004). Hence real foodstuffs must be tested to demonstrate antimicrobial potential in situ.

5.3.2. Shelf-life extension of food products by active packaging with gliadin films containing cinnamaldehyde

5.3.2.1. Effectiveness of antimicrobial films in sliced bread

The shelf-life of bakery products is rather short due to firming, staling and molding. Staling is a spontaneous and irreversible phenomenon caused by retrogradation of starch and the

migration of water from the starch to proteins and firming can easily be controlled by correct packaging (Labuza, 1982). Thus, the development of surface molds is the main reason for shelf-life reduction of packaged bakery products.

To extend the shelf-life of these packaged products some strategies have been investigated. Modified atmosphere seems to be an adequate packaging solution but, apart from the need to use high barrier packaging materials (Piergiovanni and Fava, 1997), complete air substitution is also essential to obtain an atmosphere free of oxygen. This is particularly difficult due to the typical texture of bakery products which retain large quantities of air in their porous structures. Even upon overcoming these problems, once the product is opened by the consumer, the modified atmosphere is lost and with it the hurdle to inhibit mold growth. Therefore, new techniques such as active packaging with natural antimicrobials could be a feasible approach.

As film G5C_pH2 showed the best antifungal capacity as well as the best functional properties (Balaguer et al., 2011a), it was selected for further assays performed in a food model. Fungal growth development on the bread slices packaged with or without the antimicrobial films is shown in **Table 5.2**. As the bread formulation did not include any preservative and the flour was organic, fungal growth appeared very early. Active packaging of bread slices was highly effective in delaying fungal growth, and only one sample was slightly contaminated after 28 days of storage. **Figure 5.3** shows the growth of *P. expansum* and fungi naturally present in bread in both the control and the active packaging samples after different storage times.

Table 5.2. Evolution of fungal growth on bread slices after packaging and storage.

Type of packaging	Fungi	Growth delay[1] (days)	Fungal growth[2]		
			Day 7	Day 14	Day 30
Non-Active	Naturally present fungi	5 ± 2 (3)	+	+	+++
	Inoculated with *P. expansum*	3 ± 1 (3)	+	++	+++
Active (G5C_pH2)	Naturally present fungi	28 (1)	-	-	+
	Inoculated with *P. expansum*	-	-	-	-

[1] Number of days until visible fungal growth appeared, between parenthesis: number of contaminated samples
[2] - Absence of fungal growth, + Fungal growth on <25% of the surface, ++ Fungal growth on around 50% of the surface, +++ Fungal growth on >75% the surface

Figure 5.3. Growth of inoculated *Penicillium expansum* and fungi naturally present in **(A)** inoculated bread in control packaging after 14 days, **(B)** uninoculated bread in control packaging after 14 days, **(C)** uninoculated bread in control packaging after 1 month, and **(D)** inoculated bread in active packaging after 1 month (similar to uninoculated bread with active packaging after 1 month, results not shown).

As reported in the literature the water activity of bread is around 0.95, therefore the humidity created in the internal atmosphere represents an excellent mechanism to trigger the release of the antimicrobial compound. According to the release kinetics and the diffusion coefficients estimated in a previous study (Balaguer et al., 2013), it is expected that this release would start rapidly at high relative humidity. Once the partition equilibrium between the concentration of cinnamaldehyde in the film and in the head-space is reached, the film containing the remaining free cinnamaldehyde acts as a reservoir.

The utility of cinnamaldehyde in bread active packaging has been studied by several authors. Rodriguez et al. (2008) developed an antimicrobial paper containing cinnamon essential oil incorporated as a wax coating. The active packaging of bread slices with a paper containing 6% of cinnamon essential oil almost completely inhibited the growth of *R.*

stolonifer after 3 days of storage, and this effect was related to the amount of cinnamaldehyde found in the bread. By contrast, the antimicrobial effectiveness of films based on cassava starch incorporating cinnamon powder developed by Kechichian et al. (2010) was completely unsatisfactory. The authors attributed yeast and mold growth to the high water activity of bread and the suitability of the biodegradable films as a source of carbohydrates and sugars.

Even though the microbiological shelf-life of sliced bread can be extended, it is also necessary to evaluate the sensory and physico-chemical properties to assess the potential of cinnamon essential oil or its constituents in the active packaging of bread. In this regard Gutierrez et al. (2011) evaluated the effect of cinnamon essential oil-based active packaging on the sensorial properties of a gluten-free bread. The results revealed no significant differences between the non-active and active packaging in parameters such as characteristic flavor, cinnamon flavor, cinnamon taste, and sponginess. On the other hand, crumbliness and hardness, undesirable properties for this type of bread, were significantly reduced. Taking this into account, and noting that the nominal amount of antimicrobial incorporated is reduced in our case (0.012 g of cinnamaldehyde vs. 0.0215 or 0.0374 g of cinnamon essential oil in each package), and that the amount of free cinnamaldehyde for G5C_pH2 film is nearly 30% (Balaguer et al., 2013), it is expected that the sensorial properties may not be greatly affected by the presence of the antimicrobial. However, in that study the weight of the sample or the volume of the package was not revealed.

5.3.2.2. Effectiveness of antimicrobial gliadin films in cheese spread

The microbiological quality of cheese has been enhanced using diverse technologies. Among these, modified atmosphere packaging has been widely employed for extending shelf-life (Alam and Goyal, 2011; Del Nobile et al., 2009; Eliot et al., 1998; Irkin, 2011; Khoshgozaran et al., 2012; Mexis et al., 2011; Papaioannou et al., 2007; Rodriguez-Alonso et al., 2011). However, opening the package results in the loss of the modified atmosphere. Therefore, new ways for prolonging cheese shelf-life are focusing on packaging with active materials, more specifically those incorporating naturally occurring antimicrobials (Conte et al., 2007; Ramos et al., 2012; Ture et al., 2011), or combinations of MAP and active packaging (Gammariello et al., 2011; Govaris et al., 2011; Scannell et al., 2000; Winther and Nielsen, 2006).

The antimicrobial gliadin films developed in this work were employed in the active packaging of cheese spread. Their potential to protect against fungal growth was assessed simulating a typical cheese spread tub that was able to incorporate the antifungal film on the inner surface of the lid. It is important to note that evaluation tests were carried out at 4 °C, and that this low temperature delays fungal growth, increasing the lag time, but reducing the release rate and vapor pressure of cinnamaldehyde. In the case of temperature abuse during storage, cinnamaldehyde release would be enhanced due to the increase in vapor pressure with temperature, potentially counteracting increased fungal growth at higher temperatures.

A summary of the development of fungal growth in cheese spread in the presence or absence of initial active packaging during the storage period under refrigeration is shown in **Table 5.3**. Initial appearance of fungal growth in the diverse packaging systems is also presented.

Table 5.3. Evolution of fungal growth on the cheese spread surface stored at 4 °C.

Type of packaging	Fungi	Growth delay[1] (days)	Fungal growth[2]				
			Day 7	Day 14	Day 21	Day 30	Day 45
Non-active	Naturally present fungi	16.3 ± 5.2 (6)	-	+	+	++	+++
	Inoculated *P. expansum*	18.3 ± 5.8 (6)	-	+	+	++	+++
Active (G5C_pH2)	Naturally present fungi	33.5 ± 9.2 (2)	-	-	-	-	+
	Inoculated *P. expansum*	26.3 ± 5.0 (3)	-	-	-	+	+

[1] Number of days until visible fungal growth appeared. Values reported are the means ± standard deviations, and between parentheses the number of contaminated samples is given.
[2] - Absence of fungal growth, + Fungal growth on < 1/3 of the surface, ++ Fungal growth on ca. 1/2 of the surface, +++ Fungal growth on > 2/3 of the surface

Although the sell-by date for packaged cheese spread is around 6 months after its production, once the package is opened by the consumer its shelf-life is greatly reduced. In non-active packaging tests the first visible growth of naturally present fungi was observed 16 ± 5 days after opening, and spread across the cheese surface very rapidly. However, when the cheese spread was actively packaged with gliadin films containing cinnamaldehyde the fungal growth was inhibited for ca. 30 days (**Table 5.3**). **Figure 5.4** shows the fungal growth on cheese spread with active and non-active packaging after 1 month of storage at 4 °C. Similar results were observed in samples of cheese inoculated

with *P. expansum* (results not shown). These results highlight the effectiveness of gliadin films incorporating 5% cinnamaldehyde in extending the shelf-life of cheese spread.

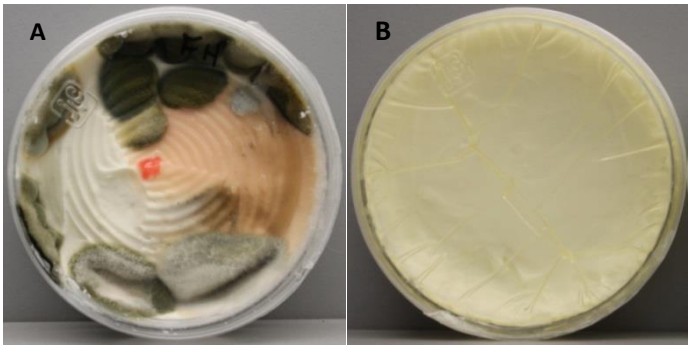

Figure 5.4. Growth of fungi naturally present in cheese spread 1 month after opening, and storage at 4 °C with **(A)** control packaging and with **(B)** active packaging.

Cinnamon and its derivatives have been evaluated as preservative agents in different types of cheese by direct addition. Investigations carried out to assess the efficiency of cinnamon and other plant essential oils in low-fat and full-fat soft cheese against *L. monocytogenes* and *Salmonella enteritidis* showed that cheese composition is essential in determining effectiveness, which increases as the percentage of fat decreases (Smith-Palmer et al., 2001). However, the addition of 1% cinnamon essential oil led to complete inhibition (< 1 log CFU/mL) in both types of cheese. The potential application of an ethanolic extract of cinnamon stick as a natural preservative for cheddar cheese was also evaluated (Shan et al., 2011). The results indicated that the cinnamon extract had antibacterial activity against *L. monocytogenes*, *S. aureus*, and *S. enterica* in cheese, delaying the bacterial growth, and also preventing lipid oxidation for a 9-day storage period. Cinnamon powder exhibited bacteriostatic action on *L. monocytogenes* in cheese (Menon and Garg, 2001). In samples treated with 6% cinnamon *Listeria* counts were reduced by 1–2 log units/g compared with the untreated controls when the cheese was maintained at 30 °C for 7 days and at 7 °C for 15 days. However, the activity of 3% cinnamon was not appreciable in cheese stored at 7 °C.

We have failed to find information in the literature on the prevention of microbial growth in cheese by means of active packaging incorporating cinnamon essential oil, extract, oleoresin, or its major constituent cinnamaldehyde. Among other essential oils used for

fungal control by active packaging in cheese, allyl isothiocyanate (AITC), incorporated in a package label, was shown to be effective against cheese-related fungi (*P. commune*, *P. roqueforti*, and *A. flavus*) when tested on both laboratory media and cheese, extending the shelf-life of Danish cheese from 4 to 28 weeks when two labels were used simultaneously (Winther and Nielsen, 2006). However, cheese stored for up to 12 weeks had an unacceptable mustard flavor, which decreased to an acceptable level between weeks 12 and 28, and a fresher taste without a CO_2 off-flavor compared with the cheese stored under modified atmosphere packaging.

Other natural compounds incorporated into films designed to be applied in antimicrobial active packaging of cheese include natamycin (de Oliveira et al., 2007; dos Santos Pires et al., 2008; Fajardo et al., 2010; Ramos et al., 2012), nisin (dos Santos Pires et al., 2008; Pintado et al., 2010), or lysozyme (Conte et al., 2011; Duan et al., 2007).

5.4. CONCLUSION

Gliadin films incorporating cinnamaldehyde were highly effective against fungal growth both in vitro and in real food systems. The amount of cinnamaldehyde retained in the film after manufacture and storage was enough to exert fungistatic, and in some cases fungicidal activity against *P. expansum* and *A. niger* in vitro. The capacity of these films to extend the shelf-life of bread and cheese spread foodstuffs demonstrated the potential of these novel biomatrices incorporating natural antimicrobials to avoid the application of synthetic chemical preservatives directly onto food. However, further research must be conducted in order to verify if active packaging with cinnamaldehyde imparts new organoleptic features to the foodstuffs which could influence acceptability by consumers.

5.5. REFERENCES

Alam, T., and Goyal, G. K. 2011. Effect of map on microbiological quality of Mozzarella cheese stored in different packages at 7 +/- 1 degrees c. *Journal of Food Science and Technology-Mysore, 48*(1), 120-123.

Balaguer, M. P., Borne, M., Chalier, P., Gontard, N., Morel, M. H., Peyron, S., Gavara, R., and Hernandez-Munoz, P. 2013. Retention and release of cinnamaldehyde from wheat protein matrices. *Biomacromolecules, 14*(5), 1493-1502.

Balaguer, M. P., Gomez-Estaca, J., Gavara, R., and Hernandez-Munoz, P. 2011a. Functional properties of bioplastics made from wheat gliadins modified with cinnamaldehyde. *Journal of Agricultural and Food Chemistry, 59*(12), 6689-6695.

Balaguer, M. P., Gómez-Estaca, J., Gavara, R., and Hernandez-Munoz, P. 2011b. Biochemical properties of bioplastics made from wheat gliadins cross-linked with cinnamaldehyde. *Journal of Agricultural and Food Chemistry, 59*(24), 13212-13220.

Ben Arfa, A., Preziosi-Belloy, L., Chalier, P., and Gontard, N. 2007. Antimicrobial paper based on a soy protein isolate or modified starch coating including carvacrol and cinnamaldehyde. *Journal of Agricultural and Food Chemistry, 55*(6), 2155-2162.

Brasil, I. M., Gomes, C., Puerta-Gomez, A., Castell-Perez, M. E., and Moreira, R. G. 2012. Polysaccharide-based multilayered antimicrobial edible coating enhances quality of fresh-cut papaya. *LWT-Food Science and Technology, 47*(1), 39-45.

Burt, S. 2004. Essential oils: Their antibacterial properties and potential applications in foods - a review. *International Journal of Food Microbiology, 94*(3), 223-253.

Conte, A., Brescia, I., and Del Nobile, M. A. 2011. Lysozyme/edta disodium salt and modified-atmosphere packaging to prolong the shelf life of burrata cheese. *Journal of dairy science, 94*(11), 5289-5297.

Conte, A., Scrocco, C., Sinigaglia, M., and Del Nobile, M. A. 2007. Innovative active packaging systems to prolong the shelf life of Mozzarella cheese. *Journal of dairy science, 90*(5), 2126-2131.

de Oliveira, T. M., Ferreira Soares, N. d. F., Pereira, R. M., and Fraga, K. d. F. 2007. Development and evaluation of antimicrobial natamycin-incorporated film in Gorgonzola cheese conservation. *Packaging Technology and Science, 20*(2), 147-153.

del Nobile, M. A., Conte, A., Incoronato, A. L., and Panza, O. 2009. Modified atmosphere packaging to improve the microbial stability of Ricotta. *African Journal of Microbiology Research, 3*(4), 137-142.

dos Santos Pires, A. C., Ferreira Soares, N. d. F., de Andrade, N. J., Mendes do Silva, L. H., Camilloto, G. P., and Bernardes, P. C. 2008. Development and evaluation of active packaging for sliced Mozzarella preservation. *Packaging Technology and Science, 21*(7), 375-383.

Du, W.-X., Avena-Bustillos, R. J., Woods, R., Breksa, A. P., McHugh, T. H., Friedman, M., Levin, C. E., and Mandrell, R. 2012. Sensory evaluation of baked chicken wrapped with antimicrobial apple and tomato edible films formulated with cinnamaldehyde and carvacrol. *Journal of Agricultural and Food Chemistry, 60*(32), 7799-7804.

Duan, J., Park, S. L., Daeschel, M. A., and Zhao, Y. 2007. Antimicrobial chitosan-lysozyme (CL) films and coatings for enhancing microbial safety of Mozzarella cheese. *Journal of Food Science, 72*(9), M355-M362.

Eliot, S. C., Vuillemard, J. C., and Emond, J. P. 1998. Stability of shredded Mozzarella cheese under modified atmospheres. *Journal of Food Science, 63*(6), 1075-1080.

Fajardo, P., Martins, J. T., Fucinos, C., Pastrana, L., Teixeira, J. A., and Vicente, A. A. 2010. Evaluation of a chitosan-based edible film as carrier of natamycin to improve the storability of Saloio cheese. *Journal of Food Engineering, 101*(4), 349-356.

Filtenborg, O., Frisvad, J. C., and Thrane, U. 1996. Moulds in food spoilage. *International Journal of Food Microbiology, 33*(1), 85-102.

Friedman, M., Henika, P. R., and Mandrell, R. E. 2002. Bactericidal activities of plant essential oils and some of their isolated constituents against *Campylobacter jejuni, Escherichia coli, Listeria monocytogenes,* and *Salmonella enterica*. *Journal of Food Protection, 65*(10), 1545-1560.

Gamage, G. R., Park, H.-J., and Kim, K. M. 2009. Effectiveness of antimicrobial coated oriented polypropylene/polyethylene films in sprout packaging. *Food Research International, 42*(7), 832-839.

Gammariello, D., Conte, A., Attanasio, M., and Del Nobile, M. A. 2011. A study on the synergy of modified atmosphere packaging and chitosan on Stracciatella shelf life. *Journal of Food Process Engineering, 34*(5), 1394-1407.

Gomes, C., Moreira, R. G., and Castell-Perez, E. 2011. Poly (dl-lactide-co-glycolide) (PLGA) nanoparticles with entrapped trans-cinnamaldehyde and eugenol for antimicrobial delivery applications. *Journal of Food Science, 76*(2), S16-S24.

Govaris, A., Botsoglou, E., Sergelidis, D., and Chatzopoulou, P. S. 2011. Antibacterial activity of oregano and thyme essential oils against listeria monocytogenes and escherichia coli o157:H7 in feta cheese packaged under modified atmosphere. *LWTFood Science and Technology, 44*(4), 1240-1244.

Gutierrez, L., Batlle, R., Andujar, S., Sanchez, C., and Nerin, C. 2011. Evaluation of antimicrobial active packaging to increase shelf life of gluten-free sliced bread. *Packaging Technology and Science, 24*(8), 485-494.

Gutierrez, L., Escudero, A., Batlle, R., and Nerin, C. 2009. Effect of mixed antimicrobial agents and flavors in active packaging films. *Journal of Agricultural and Food Chemistry, 57*(18), 8564-8571.

Helal, G. A., Sarhan, M. M., Abu Shahla, A. N., and Abou El-Khair, E. K. 2006. Effects of *cymbopogon citratus* l. Essential oil on the growth, lipid content and morphogenesis of *Aspergillus niger* Ml2-strain. *J Basic Microbiol, 46*(6), 456-469.

Hernandez-Munoz, P., and Hernandez, R. J. 2001. *Glutenin and gliadin films from wheat gluten: Preparation and properties.* Paper presented at the IFT Annual Meeting, New Orleans, Louisiana.

Irkin, R. 2011. Shelf-life of unsalted and light "Lor" whey cheese stored under various packaging conditions: Microbiological and sensory attributes. *Journal of Food Processing and Preservation, 35*(2), 163-178.

Kalemba, D., and Kunicka, A. 2003. Antibacterial and antifungal properties of essential oils. *Current Medicinal Chemistry, 10*(10), 813-829.

Kechichian, V., Ditchfield, C., Veiga-Santos, P., and Tadini, C. C. 2010. Natural antimicrobial ingredients incorporated in biodegradable films based on cassava starch. *LWT-Food Science and Technology, 43*(7), 1088-1094.

Khan, M. S. A., and Ahmad, I. 2011. Antifungal activity of essential oils and their synergy with fluconazole against drug-resistant strains of *Aspergillus fumigatus* and *Trichophyton rubrum*. *Applied Microbiology and Biotechnology, 90*(3), 1083-1094.

Khoshgozaran, S., Azizi, M. H., and Bagheripoor-Fallah, N. 2012. Evaluating the effect of modified atmosphere packaging on cheese characteristics: A review. *Dairy Science & Technology, 92*(1), 1-24.

Kurek, M., Moundanga, S., Favier, C., Galić, K., and Debeaufort, F. 2013. Antimicrobial efficiency of carvacrol vapour related to mass partition coefficient when incorporated in chitosan based films aimed for active packaging. *Food Control, 32*(1), 168-175.

Labuza, T. P., 1982. *Shelf-life dating of foods*. Food & Nutrition Press, Inc.: Connecticut.

Lopez-Malo, A., Alzamora, S. M., and Palou, E. 2002. *Aspergillus flavus* dose-response curves to selected natural and synthetic antimicrobials. *International Journal of Food Microbiology, 73*(2-3), 213-218.

Lopez, P., Sanchez, C., Batlle, R., and Nerin, C. 2007a. Development of flexible antimicrobial films using essential oils as active agents. *Journal of Agricultural and Food Chemistry, 55*(21), 8814-8824.

Lopez, P., Sanchez, C., Batlle, R., and Nerin, C. 2007b. Vapor-phase activities of cinnamon, thyme, and oregano essential oils and key constituents against foodborne microorganisms. *Journal of Agricultural and Food Chemistry, 55*(11), 4348-4356.

Ma, L., Liu, X. M., Liang, J. J., and Zhang, Z. H. 2011. Biotransformations of cinnamaldehyde, cinnamic acid and acetophenone with *Mucor*. *World Journal of Microbiology & Biotechnology, 27*(9), 2133-2137.

Manso, S., Cacho-Nerin, F., Becerril, R., and Nerín, C. 2013. Combined analytical and microbiological tools to study the effect on *Aspergillus flavus* of cinnamon essential oil contained in food packaging. *Food Control, 30*(2), 370-378.

Matan, N., Saengkrajang, W., and Matan, N. 2011. Antifungal activities of essential oils applied by dip-treatment on areca palm (*areca catechu*) leaf sheath and persistence of their potency upon storage. *International Biodeterioration & Biodegradation, 65*(1), 212-216.

Menon, K. V., and Garg, S. R. 2001. Inhibitory effect of clove oil on *Listeria monocytogenes* in meat and cheese. *Food Microbiology, 18*(6), 647-650.

Mexis, S. F., Chouliara, E., and Kontominas, M. G. 2011. Quality evaluation of grated Graviera cheese stored at 4 and 12 degrees c using active and modified atmosphere packaging. *Packaging Technology and Science, 24*(1), 15-29.

Mild, R. M., Joens, L. A., Friedman, M., Olsen, C. W., McHugh, T. H., Law, B., and Ravishankar, S. 2011. Antimicrobial edible apple films inactivate antibiotic resistant and susceptible *Campylobacter jejuni* strains on chicken breast. *Journal of Food Science, 76*(3), M163-M168.

Naidu, A. S. 2000. Overview. In *Natural food antimicrobial systems*, A.S. Naidu, Ed. CRC Press: Boca Raton, Florida.

Neri, F., Mari, M., and Brigati, S. 2006. Control of *Penicillium expansum* by plant volatile compounds. *Plant Pathology, 55*(1), 100-105.

Ouattara, B., Simard, R. E., Piette, G., Begin, A., and Holley, R. A. 2000. Inhibition of surface spoilage bacteria in processed meats by application of antimicrobial films prepared with chitosan. *International Journal of Food Microbiology, 62*(1-2), 139-148.

Papaioannou, G., Chouliara, I., Karatapanis, A. E., Kontominas, M. G., and Savvaidis, I. N. 2007. Shelf-life of a greek whey cheese under modified atmosphere packaging. *International Dairy Journal, 17*(4), 358-364.

Pauli, A., and Knobloch, K. 1987. Inhibitory effects of essential oil components on growth of food-contaminating fungi. *Zeitschrift Fur Lebensmittel-Untersuchung Und-Forschung, 185*(1), 10-13.

Piergiovanni, L., and Fava, P. 1997. Minimizing the residual oxygen in modified atmosphere packaging of bakery products. *Food Additives and Contaminants, 14*(6-7), 765-773.

Pintado, C. M. B. S., Ferreira, M. A. S. S., and Sousa, I. 2010. Control of pathogenic and spoilage microorganisms from cheese surface by whey protein films containing malic acid, nisin and natamycin. *Food Control, 21*(3), 240-246.

Pitt, J. I., and Hocking, A. D., 2009. *Fungi and food spoilage*. Third ed.; Springer: New York.

Ramos, O. L., Pereira, J. O., Silva, S. I., Fernandes, J. C., Franco, M. I., Lopes-da-Silva, J. A., Pintado, M. E., and Malcata, F. X. 2012. Evaluation of antimicrobial edible coatings from a whey protein isolate base to improve the shelf life of cheese. *Journal of Dairy Science, 95*(11), 6282-6292.

Ravishankar, S., Jaroni, D., Zhu, L., Olsen, C., McHugh, T., and Friedman, M. 2012. Inactivation of listeria monocytogenes on ham and bologna using pectin-based apple, carrot, and hibiscus edible films containing carvacrol and cinnamaldehyde. *Journal of Food Science, 77*(7), M377-M382.

Ravishankar, S., Zhu, L., Olsen, C. W., McHugh, T. H., and Friedman, A. 2009. Edible apple film wraps containing plant antimicrobials inactivate foodborne pathogens on meat and poultry products. *Journal of Food Science, 74*(8), M440-M445.

Rodriguez-Alonso, P., Centeno, J. A., and Garabal, J. I. 2011. Biochemical study of industrially produced Arzua-Ulloa semi-soft cows' milk cheese: Effects of storage under vacuum and modified atmospheres with high-nitrogen contents. *International Dairy Journal, 21*(4), 261-271.

Rodriguez-Lafuente, A., Nerin, C., and Batlle, R. 2010. Active paraffin-based paper packaging for extending the shelf life of cherry tomatoes. *Journal of Agricultural and Food Chemistry, 58*(11), 6780-6786.

Rodriguez, A., Nerin, C., and Batlle, R. 2008. New cinnamon-based active paper packaging against *Rhizopus stolonifer* food spoilage. *Journal of Agricultural and Food Chemistry, 56*(15), 6364-6369.

Sanla-Ead, N., Jangchud, A., Chonhenchob, V., and Suppakul, P. 2012. Antimicrobial activity of cinnamaldehyde and eugenol and their activity after incorporation into cellulose-based packaging films. *Packaging Technology and Science, 25*(1), 7-17.

Scannell, A. G. M., Hill, C., Ross, R. P., Marx, S., Hartmeier, W., and Arendt, E. K. 2000. Development of bioactive food packaging materials using immobilised bacteriocins lacticin 3147 and nisaplin (r). *International Journal of Food Microbiology, 60*(2-3), 241-249.

Shan, B., Cai, Y.-Z., Brooks, J. D., and Corke, H. 2011. Potential application of spice and herb extracts as natural preservatives in cheese. *Journal of Medicinal Food, 14*(3), 284-290.

Singh, G., Maurya, S., deLampasona, M. P., and Catalan, C. A. N. 2007. A comparison of chemical, antioxidant and antimicrobial studies of cinnamon leaf and bark volatile oils, oleoresins and their constituents. *Food and Chemical Toxicology, 45*(9), 1650-1661.

Smith-Palmer, A., Stewart, J., and Fyfe, L. 2001. The potential application of plant essential oils as natural food preservatives in soft cheese. *Food Microbiology, 18*(4), 463-470.

Tolouee, M., Alinezhad, S., Saberi, R., Eslamifar, A., Zad, S. J., Jaimand, K., Taeb, J., Rezaee, M. B., Kawachi, M., Shams-Ghahfarokhi, M., and Razzaghi-Abyaneh, M. 2010. Effect of matricaria chamomilla l. Flower essential oil on the growth and ultrastructure of aspergillus niger van tieghem. *International Journal of Food Microbiology, 139*(3), 127-133.

Tunc, S., Chollet, E., Chalier, P., Preziosi-Belloy, L., and Gontard, N. 2007. Combined effect of volatile antimicrobial agents on the growth of *Penicillium notatum*. *International Journal of Food Microbiology, 113*(3), 263-270.

Ture, H., Eroglu, E., Ozen, B., and Soyer, F. 2011. Effect of biopolymers containing natamycin against *Aspergillus niger* and *Penicillium roquefortii* on fresh Kashar cheese. *International Journal of Food Science and Technology, 46*(1), 154-160.

Utama, I. M. S., Wills, R. B. H., Ben-Yehoshua, S., and Kuek, C. 2002. *In vitro* efficacy of plant volatiles for inhibiting the growth of fruit and vegetable decay microorganisms. *Journal of Agricultural and Food Chemistry, 50*(22), 6371-6377.

Wang, R., Wang, R., and Yang, B. 2009. Extraction of essential oils from five cinnamon leaves and identification of their volatile compound compositions. *Innovative Food Science & Emerging Technologies, 10*(2), 289-292.

Wang, X., Liu, H., Wei, J., and Ma, Z. 2010. Effects of oregano oil, carvacrol, cinnamaldehyde, and citral on antimicrobial, mechanical and barrier properties of

carrot puree films. In *Piageng 2010: Photonics and imaging for agricultural engineering*, H. Tan, Ed. Vol. 7752.

Winther, M., and Nielsen, P. V. 2006. Active packaging of cheese with allyl isothiocyanate, an alternative to modified atmosphere packaging. *Journal of Food Protection, 69*(10), 2430-2435.

Xing, Y., Li, X., Xu, Q., Yun, J., and Lu, Y. 2010. Antifungal activities of cinnamon oil against rhizopus nigricans, aspergillus flavus and *Penicillium expansum in vitro* and *in vivo* fruit test. *International Journal of Food Science and Technology, 45*(9), 1837-1842.

Zodrow, K. R., Schiffman, J. D., and Elimelech, M. 2012. Biodegradable polymer (PLGA) coatings featuring cinnamaldehyde and carvacrol mitigate biofilm formation. *Langmuir : the ACS journal of surfaces and colloids, 28*(39), 13993-13999.

CHAPTER 6

COMPOSTABLE PROPERTIES OF ANTIMICROBIAL BIOPLASTICS BASED ON CINNAMALDEHYDE CROSS-LINKED GLIADINS

Balaguer, M.P.; Villanova, J.; Cesar, G.; Gavara, R.; and Hernandez-Munoz, P.

Chemical Engineering Journal, 2015, 262, 447-455

The disintegration, biodegradation and ecotoxicity of cross-linked wheat gliadin films with antimicrobial properties were assessed under controlled composting conditions. Gliadins were chemically modified with different percentages of cinnamaldehyde (1.5%, 3% and 5%) increasing their cross-linking degree and imparting antimicrobial activity. The most cross-linked gliadin film showed a very fast disintegration profile. It completely disintegrated into fine visually indistinguishable residues after 4 days of being inserted in compost medium. Scanning electron microscopy revealed the rapid microbial colonization of the films' surface. Biodegradation was assessed by measuring the amount of carbon dioxide produced in a static system specifically designed for this study. The cross-linking degree of the proteinaceous matrices modified their biodegradation rate without impairing their complete biodegradation. The presence of residual cinnamaldehyde in the films, which can exert antimicrobial activity, did not hamper their biodegradation neither caused ecotoxicity on tomato seeds germination and plant growth.

6.1. INTRODUCTION

In the last decades there has been an increasing interest in the development of renewable materials with biodegradable properties in an attempt to contribute to the sustainable development and to reduce the environmental impact associated with non-biodegradable petroleum-based plastics (Queiroz and Collares-Queiroz, 2009). Many unsubstantiated claims to biodegradability were made in the past as a consequence of the lack of well-identified environmental requirements, and thus the inexistence of well-established testing methods (van der Zee, 2005). However, nowadays diverse standardization organizations have standard test methodologies, where specific disposal pathways, specific time frames and passing criteria are indicated in order to evaluate the suitability of a packaging material for its organic recovery (van der Zee, 2005). These standards tests require high amounts of packaging materials to be tested (around 15 kg) and costly facilities to conduct the assays, thus only final materials with the aim of being certified and placed on the market are usually evaluated. For novel materials developed at laboratory scale and produced in lower quantities some preliminary tests need to be developed to serve as a reference to choose or discard among them.

Composting is the aerobic treatment of the biodegradable parts of packaging waste, which produces stabilized organic residues, under controlled conditions and using microorganisms (94/62/EC). Although recycling could be energetically more favorable than composting in some cases it may not be practical because of excessive sorting and cleaning requirements (Kale et al., 2007). Moreover, the use of compost reduces chemical inputs, suppresses crop diseases, replenishes organic carbon, increases water and nutrient retention, and improves soil productivity (Narayan, 1993).

It is important to note that all compostable plastics are biodegradable, but not all biodegradable plastics are compostable. According to ISO 17088 a compostable plastic is a plastic that undergoes degradation by biological processes during composting to yield carbon dioxide, water, inorganic compounds, and biomass at a rate consistent with other known compostable materials and leaves no visible distinguishable or toxic residues. Therefore, the evaluation of compostability includes three phases: disintegration, biodegradation and ecotoxicity.

Materials based on proteins from plants (wheat gluten, corn zein, and soy protein) and animals (gelatin, keratin, casein, and whey) are renewable and inherently biodegradable (Hernandez-Izquierdo and Krochta, 2008). Among them, gluten proteins present remarkable advantages since they are highly available, have low cost, and can be obtained as by-product from the wheat starch industry, which is steadily rising as starch is used for bioethanol production, and in the manufacturing of other bioplastics such as thermoplastic starch (TPS) and poly (lactic acid) (PLA). However, gluten proteins have poor mechanical and water resistant properties making their modification essential to obtain suitable materials for diverse applications. Their improvement can also lead to changes in their compostability, since their disintegration could be hampered or their biodegradation could be incomplete.

Several authors have studied the biodegradation properties of diverse wheat gluten-based materials (Chevillard et al., 2011; Domenek et al., 2004; Zhang et al., 2010) in different environments such as soil, water, and compost; however, no reports have been found about their compostability.

In this study, the monomeric fraction of wheat gluten, gliadins, was treated with cinnamaldehyde to produce improved protein-based bioplastics. Cinnamaldehyde involved in the chemical cross-linking of the gliadins enhances the functional properties of the resulting films, especially their mechanical and water resistance (Balaguer et al., 2013b; Balaguer et al., 2011a, 2011b), whereas free cinnamaldehyde which eventually do not undergoes covalent bonding between proteins imparts active antimicrobial properties to the films (Balaguer et al., 2013b). Therefore, its incorporation can alter the inherent biodegradation properties of naturally-occurring not-modified materials.

The aim of the present work was to explore the disintegration, biodegradation and ecotoxicity at laboratory scale of the active antimicrobial wheat protein-based bioplastics after its use. To the best of our knowledge, this is the first report that deals with the compostable properties of active antimicrobial bioplastics that can be used in food packaging applications.

6.2. MATERIALS AND METHODS

6.2.1. Reagents

Crude wheat gluten (≥ 80% protein), trans-cinnamaldehyde 99%, glycerol, ethanol, hydrochloric acid, and microcrystalline cellulose with a particle diameter of around 20 μm, all laboratory grade, were supplied by Sigma (Madrid, Spain).

Compost was obtained from a municipal urban solid waste treatment plant where aerobic composting was produced (Tetma, Guadassuar, Spain). The compost selected was between two and four-months old. Initial physico-chemical characteristics were supplied by the manufacturer.

A mixture of peat with siliceous sand, both obtained from Viveros Alegre (Chiva, Spain), was employed as reference substrate in the determination of ecotoxic effects to higher plants. Tomato (*Solanum lycopersicum*) seeds from Vilmorin S.A. (La Ménitré, France) with a seedling emergence of 97%, evaluated with the reference substrate, were purchased at Leroy Merlin (Aldaia, Spain).

6.2.2. Preparation and characterization of antimicrobial cross-linked gliadin films

Antimicrobial films were produced from wheat proteins according to the method described by Balaguer et al. (2011b). Basically, a solution rich in gliadins was extracted from wheat gluten and different percentages of the cross-linker, namely 1.5% (G1.5C_pH2), 3% (G3C_pH2), and 5% (G5C_pH2) (g cinnamaldehyde/100 g protein) were incorporated into the solution. Glycerol was added as a plasticizer at 25% (g/100 g protein). The film-forming solution containing the plasticizer and different amounts of the cross-linker was adjusted at pH 2 with HCl and stirred for 30 min. Films were produced by casting and subsequent evaporation of the solvent at 37 °C for 24 h. A gliadin film produced at the native pH of the gliadin film-forming solution (pH 6) and without cinnamaldehyde addition was employed as the control (G_pH6). The mean film thickness was 100 ± 12 μm measured using a micrometer (Mitutoyo, Kanagawa, Japan), and calculated from measurements taken at ten different locations on each film sample. The grammage of the films was 0.015 ± 0.002 g/cm^2 measured at 50% RH (relative humidity) and 23 °C. Actual concentration of cinnamaldehyde after the production of the films was evaluated in a previous work by solvent extraction followed by gas chromatography determination (Balaguer et al., 2013a). Remaining cinnamaldehyde was present in concentrations lower than 1% (Balaguer et al., 2013a); therefore, biodegradation of this constituent was not necessary to be tested separately.

In previous studies it was shown that cinnamaldehyde release is triggered by the presence of ambient moisture (Balaguer et al., 2013a). Low relative humidity conditions enable the retention of cinnamaldehyde in the gliadin matrix, and high or medium relative humidity conditions trigger its release. Therefore, in order to simulate their potential use as antimicrobial food packaging materials, gliadin films were conditioned during one week at 75% RH and 23 °C (common conditions that can be achieved inside a packaged foodstuff of medium a_w) to trigger the release of cinnamaldehyde, and to achieve a remaining level after their use in accordance to their application. After the simulation step, films were conditioned at 0% RH and 23 °C with P_2O_5 until achieving a constant weight, reporting all data in dry basis.

The carbon content of the film samples was measured with an elemental analyzer EA1108 CE Instruments (Thermo Fisher Scientific, Madrid, Spain).

6.2.3. Compost conditioning and characterization

The compost was sieved discarding fragments ≥ 0.5 cm and large inert objects such as glass, stones, and metal pieces were manually removed to obtain a homogeneous material. The total dry solids content was determined by drying the compost at 105 °C until a constant weight was achieved (**Equation 6.1**). The total volatile solids content was evaluated by placing the dried compost in a muffle at 550 °C during 24 h (**Equation 6.2**).

$$DS\ (\%) = \frac{W_d^{105}}{W_w^i} \times 100 \qquad (\mathbf{6.1})$$

$$VS\ (\%) = \frac{W_d^{105} - W_d^{550}}{W_d^{105}} \times 100 \qquad (\mathbf{6.2})$$

where W_w^i is the initial weight of compost, W_d^{105} is the weight of compost after drying at 105 °C until a constant weight was achieved, W_d^{550} is the weight of compost after drying at 550 °C for 24 h.

The moisture content of the compost was adjusted by adding water, and the pH was measured by mixing 1 part of compost with 5 parts of deionized water (w/w). The mix was shaken and the pH was immediately measured using a pHmeter.

6.2.4. Disintegration tests

A laboratory-scale composting test was used for a qualitative determination of the disintegration of the films. The test was carried out only for the film G5C_pH2, which represents the most unfavorable conditions according to its functional properties (Balaguer et al., 2013b; Balaguer et al., 2011a, 2011b). A composting vessel consisting of a 2-L glass jar filled with compost was employed for the test at 58 °C. Film samples were cut into pieces of 3.8 x 2.7 cm and placed inside plastic slide frames with an interior size of 3.4 x 2.3 cm. The slices frames containing the films were introduced in the composting vessels and withdrawn at different time intervals. The vessels remained open and the surrounding compost was carefully stirred with a glass stick every day in order to maintain aerobic conditions. Water irrigation was done as needed in order to maintain a moisture content of around 80% of the holding capacity of the compost. Films were collected to proceed with the visual inspection and scanning electron microscopy analysis to qualitatively determinate the degree of disintegration.

6.2.4.1. Visual inspection

Collected films were carefully cleaned with a soft brush. A Canon EOS Reflex digital camera was used to take pictures of the remaining films and their pieces.

6.2.4.2. Scanning Electron Microscope (SEM)

The surface morphology of the samples before and after different time intervals of being exposed to the compost disintegration test was studied by scanning electron microscopy using a Hitachi model S-4100 with a BSE Autrata detector and a EMIP 3.0 image capture system (Hitachi, Madrid, Spain). A copper cube was used as a support for the films which were fixed with double-sided carbon tape. The samples were coated with gold–palladium under vacuum in a sputter coating unit. Accelerated voltage of 10 kV and vacuum pressure were used as operating conditions.

6.2.5. Biodegradation tests

The ultimate aerobic biodegradation level of gliadin films was established by testing under controlled composting conditions at laboratory scale. The method was adapted from the ISO standard 14855-1 which is based in the measure of the CO_2 evolved, which is proportional to the percentage of biodegraded substance.

Film samples were ground with a domestic grinder to obtain particles around 1 to 2 mm. The respirometric unit consisted of a hermetic 2-L glass jar (bioreactor), which was modified for the air withdrawal with a rubber septum, and containing two polypropylene flasks of 60-mL capacity (**Figure 6.1**). One of the flasks contained 3 g of dry compost mixed with 50 mg of equivalent carbon of ground dry samples (around 100 mg of sample). Vermiculite (1 g) was added to prevent the compost from becoming compacted and to facilitate oxygen access. The water content of the compost was adjusted to 50%. The compost appeared slightly sticky and free water was observed after pressing the sample, these conditions were maintained through the test by adding water when needed. The other flask contained distilled water in order to maintain the relative humidity at 100% inside the jar to avoid compost drying. The glass vessels were hermetically closed and incubated in the dark at 58 ± 2 °C. Biodegradation experiments included control and blank samples. The control samples were microcrystalline cellulose, a positive reference material well-known by its biodegradation properties, which was mixed with compost. The blank samples corresponded with the compost alone, i.e. without addition of an external carbon source. All experiments were run in triplicate.

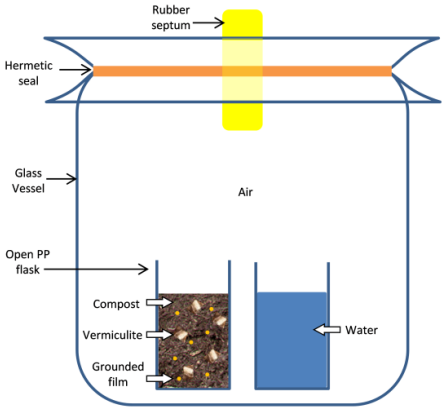

Figure 6.1. Schematic illustration of the bioreactor used in the biodegradation tests.

The CO_2 produced in each bioreactor was measured by withdrawal of 10 mL of the head-space air with a syringe and posterior injection in an O_2 and CO_2 analyzer CheckMaster 2100 (Lippke, Neuwied, Germany). Oxygen concentration was also recorded and always maintained above 6% in order to maintain aerobic conditions.

The theoretical amount of CO_2 that can be produced assuming that all the carbon of the test sample is transformed into CO_2 ($CO_2^{Th}{}_S$) was calculated from **Equation 6.3**:

$$CO_2^{Th}{}_S = W_s \cdot C_s \cdot \frac{MW_{CO_2}}{MW_C} \qquad (\mathbf{6.3})$$

where W_s (g) is the dry weight of film sample introduced in the bioreactor, C_s (g C/g dry sample) is the proportion of organic carbon in the dry film samples, MW_{CO_2} (44 g/mol) is the molecular weight of carbon dioxide, and MW_C (12 g/mol) is the molecular weight of carbon.

The percentage of biodegradation ($\%B$) can be calculated from the cumulative amount of CO_2 produced, expressed as a percentage of the theoretically expected value for total conversion to CO_2 ($CO_2^{Th}{}_S$) by means of **Equation 6.4**:

$$\%B = \frac{\sum CO_{2_S} - \sum CO_{2_B}}{CO_2^{Th}{}_S} \cdot 100 \qquad (\mathbf{6.4})$$

where $\sum CO_{2_S}$ (g) is the cumulative amount of CO_2 produced in the sample bioreactors, and $\sum CO_{2_B}$ (g) is the cumulative amount of CO_2 produced in the blank bioreactors.

Kinetics of biodegradation were modeled by the Hill's equation (**Equation 6.5**) (Calmon et al., 1999; Chevillard et al., 2011):

$$\%B = \%B_{max} \cdot \frac{t^n}{k^n + t^n} \qquad (\mathbf{6.5})$$

where $\%B_{max}$ is the percentage of biodegradation at infinite time, t (days) is time, k (days) is the time at which $\%B = 0.5 \cdot \%B_{max}$, and n the curve radius of the sigmoid function.

6.2.6. Ecotoxicity tests in plants

The determination of ecotoxic effects to higher plants was based on OECD Guideline for testing chemicals 208 "Terrestrial Plant Test: Seedling Emergence and Seedling Growth Test" with the modifications given in the Annex E of EN 13432, which are required for testing compost samples. The method was adapted to laboratory-scale composting conditions as described below.

Ecotoxicity test was carried out only on the film G5C_pH2 since this sample presents the most stringent conditions: the highest cross-linking degree and the highest amount of antimicrobial agent (Balaguer et al., 2013a; Balaguer et al., 2011a, 2011b). A blank compost (C) and a compost containing the test material (C+F) were used for the preparation of the samples. The C+F compost was obtained by mixing in a glass tray 20 g of dry film G5C_pH2 in granules with 600 g of compost. The mixture was stabilized for 14 days at 58 °C to prevent possible toxic effect because of biological activity and immaturity of the compost. Moisture content was controlled during the whole test by adding water when needed. According to EN 13432 the disintegration period can be produced in 12 weeks, therefore this short stabilization period implies severe conditions. The C compost was obtained from the parallel process without addition of the test material.

A seedbed was employed to distribute the samples. Mixtures were prepared with two mixing ratios of the compost (C or C+F) with the reference substrate (RS), namely 1:3 and 1:1 (w/w). Two seeds of tomato were introduced in each cubicle containing 10 g of mixture, and 13 replicates were tested. The use of these smaller pots in comparison with those ones proposed in OECD 208 (500 g of mixed compost and reference substrate) will reduce the soil available for roots and their capacity to explore the soil environment what gives rise to a greater uptake of the possible phytotoxic-degradation products (Boluda et al., 2011).

Water was added until reaching 70% to 100% of the water holding capacity and the seedbeds were incubated at a constant temperature of 25 ± 2 °C in a growth-plant chamber Ibercex Serie F with a photoperiod of 16 h of light/8 h of darkness (Ibercex, Arganda del Rey, Spain). The test was finished 14 days after 50% of the control plants have emerged (23 days). The plants were observed each 3 days for visual phytotoxicity (chlorosis, necrosis, wilting, leaf and stem deformation) and mortality. At the end of the test, the number of seeds germinated and the plant biomass were recorded. Plant biomass was measured as the final fresh weight (including the roots and the shoot) and shoot height, and germination rate was calculated as:

$$Germination\ rate\ (\%) = \frac{Number\ of\ seeds\ germinated}{Number\ of\ seeds\ sowed} \cdot 100 \qquad (\mathbf{6.6})$$

The toxicity was evaluated by comparison of the results of germination and plant biomass in the blank compost and the compost incorporating the film sample.

6.3. RESULTS AND DISCUSSION

6.3.1. Compost characteristics

Table 1 compiles the physico-chemical properties of the compost employed in the tests, which were within the ranges established in the standards.

Table 1. Physico-chemical properties of the compost employed in the tests.

pH	DS (%)	VS (%)	C/N ratio
8.17	67.20 ± 0.67	58.31 ± 0.67	23.70

6.3.2. Disintegration tests

Gliadin film G5C_pH2 showed a very fast disintegration profile in composting conditions, although compost was employed for test instead of the fresh bioresidue proposed in the standard. This condition gives rise to a more unfavorable environment for decomposition, since lower temperatures and lower microorganism charge are achieved. **Figure 6.2** shows physical falling apart of the gliadin bioplastic film into fine visually indistinguishable fragments which was completed in only 4 days.

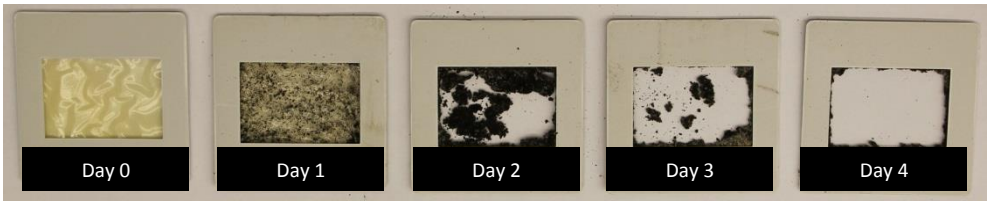

Figure 6.2. Qualitative view of disintegration of gliadin film G5C_pH2 exposed to composting conditions.

This fast disintegration could be related with a bulk erosion of the gliadin matrix coupled with enzymatic cleavage of hydrolysable bonds. The erosion kinetics of insoluble matrices, such as gliadins, is mainly affected by two major phenomena (Peppas and Langer, 1994): (i) the diffusion of water penetrating through the polymer material, and (ii) the degradation rate of the polymer backbone in the presence of water. If the degradation process is faster than the diffusion process, surface erosion will occur since the material surface will quickly degrade before water has time to diffuse and penetrate through the material. If the diffusion process is faster than the degradation process bulk erosion will occur because water penetrates through the material before significant erosion occurs on the surface (Burkersroda et al., 2002).

In gliadin films the diffusion of water into the matrix is very fast, since they are highly hydrophilic materials. Effective water vapor diffusion coefficients (D_{H_2O}) of gliadin films were determined in a previous work (Balaguer et al., 2013b). At high relative humidities, such as composting environments, D_{H_2O} were affected by water clustering phenomena, ranging from $2.7 \cdot 10^{-14}$ m^2/s at 70% RH to $1.03 \cdot 10^{-14}$ m^2/s at 88% RH for the film G5C_pH2 (Balaguer et al., 2013b). The time (t_{diff}) that water needs to travel a distance (x) can be estimated by applying random theory to the motion of water in the polymer (Atkins and De Paula, 2006):

$$t_{diff} = \frac{x^2 \pi}{4 D_{H_2O}} \qquad (\mathbf{6.7})$$

Applying **Equation 6.7** for a film thickness of 100 μm, and 88% RH, water vapor will reach the center of the film in 2.20 days. Concurrently, the cleavage of the protein backbone is actively catalyzed by appropriate enzymes such as proteases that increase the degradation rate in comparison with a passive hydrolysis. Therefore, disintegration phenomena occurred in a very short time scale.

Despite the film employed in the disintegration analyses presented the greatest cross-linking degree achieved by polymerization with cinnamaldehyde treatment (Balaguer et al., 2013a; Balaguer et al., 2011b), the disintegration was faster than that found by other authors for wheat gluten films in compost (Zhang et al., 2010), and in soil (Domenek et al., 2004). Other materials such as PLA needed at least 28 days to fully breakdown according to Rudeekit et al. (2012).

Figure 6.3 shows the SEM images of G5C_pH2 film before and during the disintegration test in composting conditions. Gliadin films presented a smooth surface with some superficial cavities smaller than 5 μm in diameter, probably produced during the solvent evaporation in the manufacturing step (**Figure 6.3.0**). After 1 day in composting conditions the surface became granular as a consequence of erosion produced by water penetration (**Figure 6.3.1B**). After 2 days the first fungi appeared on the surface of the highly eroded gliadin films (**Figure 6.3.2**). After 3 days fungal colonization spread across the gliadin film surface and extracellular enzymes secreted by the fungi started the proteolysis of the protein chains (**Figure 6.3.3B**). After 4 days fungal hyphae predominated in the small fragments of gliadin films recovered (**Figure 6.3.4**); this fungal growth was also visible at macroscopic scale with the formation of a white mycelium network in the compost media.

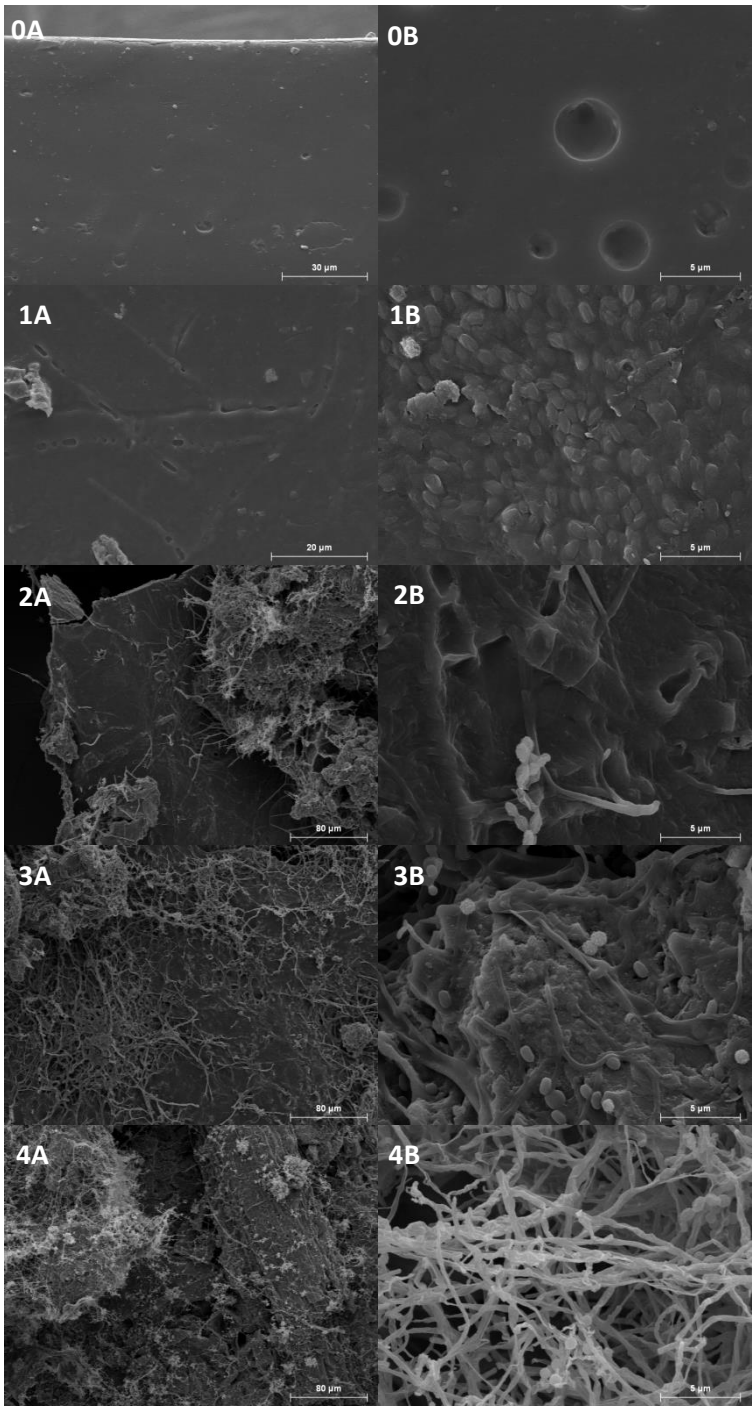

Figure 6.3. SEM images of gliadin film G5C_pH2 before the disintegration test **(0A, 0B)** and after 1 **(1A, 1B)**, 2 **(2A, 2B)**, 3 **(3A, 3B)**, and 4 **(4A, 4B)** days exposed to composting conditions.

6.3.3. Biodegradation tests

Biodegradable polymers generally decompose into carbon dioxide, water, inorganic compounds and biomass, and consume oxygen under aerobic conditions. The theoretical quantity of carbon dioxide that can be produced by the biodegradation of the samples was calculated from the carbon content determined by elemental analysis. **Table 6.2** shows the elemental composition in carbon, hydrogen, sulfur, and nitrogen of the samples analyzed.

Table 6.2. Elemental composition of control gliadin film (G_pH6), active antimicrobial and cross-linked gliadin films (GXC_pH2), positive reference (Cellulose), and commercial compostable film (Starch).

Sample	C (%)	H (%)	S (%)	N (%)
G_pH6	48.63	7.89	0.67	13.13
G1.5C_pH2	48.21	7.70	0.39	12.67
G3C_pH2	48.59	7.84	0.49	12.68
G5C_pH2	49.38	7.68	0.38	12.37
Cellulose	42.92	6.71	0	0
Starch	56.30	7.18	0	0

Figure 6.4 shows the biodegradation kinetics of the control gliadin film (G_pH6), the active antimicrobial and cross-linked gliadin films (G1.5C_pH2, G3C_pH2, and G5C_pH2), the microcrystalline cellulose employed as a positive reference, and the commercial compostable film based on potato starch. Cellulose and starch film displayed the characteristic sigmoidal profile of respirometric tests. Cellulose reached a 100% of biodegradation after 14 days; however, the maximum biodegradation was found after 21 days accounting for 130%. This behavior corresponding to a percentage of biodegradation greater than 100% was also observed for gliadin films in a more pronouncedly way. This effect is known as priming and it occurs if the compost inoculum in the test reactor containing the samples is producing more CO_2 than the compost inoculum in the blank reactors (Kuzyakov et al., 2000). This corresponds with a stimulation of organic matter mineralization that can occur after the addition of easily-decomposable organic matter (Fontaine et al., 2003; Kuzyakov, 2010; Kuzyakov et al., 2000). However, although the mechanism by which priming effects are produced remain unknown, it is believed that it is not an artifact of respirometric studies, as sometimes supposed, but it is a natural process consequence of the interaction of microorganisms and organic matter (Fontaine et al., 2003; Kuzyakov, 2010). Priming effects were also observed in the biodegradation in composting medium of starch-polystyrene foams (Pushpadass et al., 2010), and of L-polylactide-

polycaprolactone co-polymer films (Plackett et al., 2006). The higher priming effects observed in the case of gliadins (140-200%) could be a consequence of their different composition in comparison to the cellulose and starch, as they represent also a source of nitrogen.

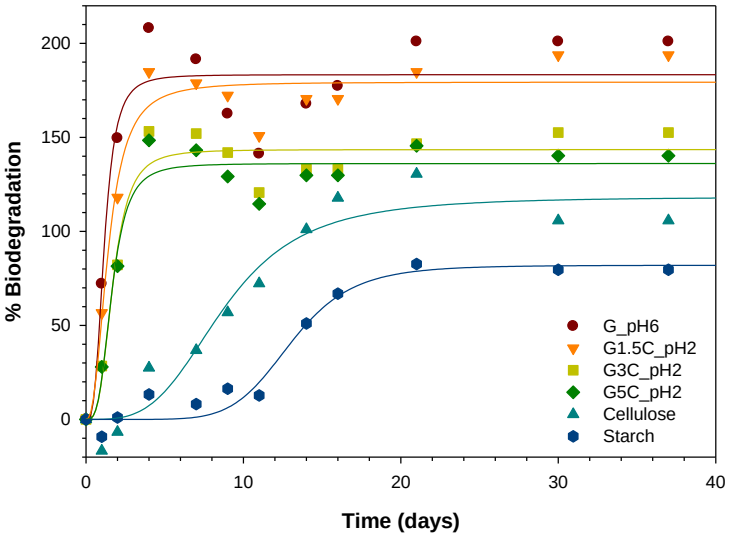

Figure 6.4. Biodegradation kinetics of control gliadin film (G_pH6), active antimicrobial and cross-linked gliadin films (GXC_pH2), positive reference (Cellulose), and commercial compostable film (Starch). Symbols: experimental data, and lines: predicted data by Hill's equation. Standard deviations were ≤ 20%.

The negative beginning in the biodegradation curve of cellulose, also found for the starch-based film, can be ascribed to the initial step of microbial degradation process which consists in the depolymerization or chain cleavage of the macromolecules by extracellular enzymes (van der Zee, 2005). As a result, a lag phase can be observed, corresponding to the time needed for water to diffuse through the matrix, and enzymes to cleave the polymer chains (van der Zee, 2005). Once the polymer fragments are small enough, they can be transported inside the cells where they are metabolized (Kale et al., 2007). In the case of cellulose and starch, both polysaccharides, glycosidases are responsible of the cleavage of glycosidic bonds, more particularly amylases act on starch hydrolyzing the α-1,4 and/or α-1,6 glucoside linkages, and cellulases act on cellulose β-1,4 glucoside linkages (Whitaker, 1994). In the case of gliadins, proteases catalyze the hydrolysis of amide bonds and sometimes the related

hydrolysis of ester linkages (Whitaker, 1994). The coupling of water-induced hydrolysis throughout the polymer's bulk and enzymatic degradation caused by microorganism increased their susceptibility to biodegradation.

Biodegradation profile of gliadin films reached a maximum after 1-2 days and then decreased during 4 days. This behavior was similar to that found for feather keratin films analyzed by Barone and Arikan (2007). However, in the case of gliadin films after this minimum a recovery in the percentage of biodegradation was produced. It is believed that gliadin films were rapidly biodegraded by a growing microbial population achieving very rapid biodegradation rates. This fact could give rise to a sharp reduction of nutrients, and the feedstuff became insufficient for the living microorganisms which were also drastically reduced, diminishing the amount of carbon dioxide produced in comparison with the blank bioreactors. After a lag phase the microbial population was recovered, and continued the biodegradation in the same rate as the blank compost.

The fast biodegradation of gluten-based materials has also been reported in different environments by several authors (Chevillard et al., 2011; Domenek et al., 2004; Zhang et al., 2010). Zhang et al. (2010) examined the biodegradation of a series of chemically modified thermally processed wheat gluten-based polymers according to the standard AS ISO 14855. Most of these materials reached 93-100% biodegradation within 22 days of composting. In the case of control gluten films incorporating 18% of glycerol obtained by compression molding at 130 °C, a 100% of biodegradation was reached in 12 days. Domenek et al. (2004) subjected to biodegradation a large variety of wheat gluten based bioplastics. The biodegradability tests were performed in liquid medium following the international standard ISO 14852 (modified Sturm test). All gluten materials analyzed (cast, hot-molded, and mixed in a two-blade counterrotating mixer) were fully degraded after 36 days in aerobic fermentation, reaching the plateau zone after around 10 days. The mineralization half-life time of 3.8 days in the modified Sturm test situated gluten materials among the fastest degrading polymers. Chevillard et al. (2011) evaluated the biodegradability of wheat gluten-based materials in soil by adapting the US standard ASTM D5988, and found that extruded wheat gluten-based materials biodegraded very rapidly since the maximum degradation rate was observed after only 4 days, and the 50% of the maximum biodegradation was achieved in less than 6 days. However, biodegradation of gliadin films in compost produced higher biodegradation rates than in soil media (Chevillard et al., 2011) or in liquid media (Domenek et al., 2004) for gluten-based materials, probably due to higher temperature of the analysis

which increases the rate of reactions. However, higher biodegradation rates were obtained also in comparison with wheat gluten materials under composting conditions (Zhang et al., 2010). Therefore, gliadins can be more easily degradable by microorganism than gluten, since they represent only the monomeric fraction, and glutenins also present in gluten, the polymeric fraction.

Biodegradation curves were modeled by Hill's equation (**Equation 6.3**), and the fitting parameters are reported in **Table 6.3**. The maximum biodegradation percentages corresponded in all cases, except in the case of the starch-based bioplastic, with values higher than 100%, as a consequence of the priming effects. Gliadin films showed higher percentages of biodegradation (136-183%) than cellulose (118%), and the starch-based bioplastic (82%). Values predicted by Hill's equation were lower than values determined experimentally for gliadins films, opposite to cellulose and starch-based bioplastic. Gliadin films reached 50% of biodegradation in less than 2 days in composting environment as showed by the constant k of Hill's equation. Cellulose reference last almost 9 days, and 4 more days were necessary in the case of the commercial compostable film based on starch.

Table 6.3. Hill's parameters and related biodegradation indicators of control gliadin film (G_pH6), active antimicrobial and cross-linked gliadin films (GXC_pH2), positive reference (Cellulose), and commercial compostable film (Starch).

Sample	Hill's parameters				$\%B_{37}$	r_{max} (%/day)	$t_{r_{max}}$ (days)
	$\%B_{max}$	k (days)	n	R^2			
G_pH6	183	1.16	3.22	0.8984	201	77.4	1
G1.5C_pH2	179	1.41	2.47	0.9562	194	61.4	1
G3C_pH2	143	1.70	3.32	0.9521	153	53.8	1
G5C_pH2	136	1.65	3.34	0.9539	140	53.5	1
Cellulose	118	8.77	3.46	0.9471	106	17.1	2
Starch	82.0	13	6.74	0.9649	79.6	12.8	11

$\%B_{max}$: percentage of biodegradation at infinite time
k: time at which $\%B = 0.5 \cdot \%B_{max}$
n: curve radius of the sigmoid function
$\%B_{37}$: percentage of biodegradation measured at the end of the test
r_{max}: maximum biodegradation rate
$t_{r_{max}}$: time to reach the maximum degradation rate

The chemical treatment with cinnamaldehyde had a pronounced effect on the biodegradability of gliadin films, although all gliadin samples were 100% biodegradable the degree of biodegradation decreased as the percentage of cinnamaldehyde increased. This was in accordance with the cross-linking density determined in a previous work (Balaguer et

al., 2011a). In the same way, the molecular weight profiles, determined by SDS-PAGE (Balaguer et al., 2011b) and by SE-HPLC (Balaguer et al., 2013a), pointed out the appearance of high molecular weight protein aggregates as a consequence of the polymerization of monomeric gliadins in films treated with cinnamaldehyde at pH 2. Therefore, the higher degree of cross-linking achieved produced a more resistant matrix against physico-chemical and biological degradation. In addition, the new linkages created among the polypeptide chains represent new bonds to be cleaved by microorganisms. Moreover, these new bonds could lack of specific enzymes to act on them for depolymerization. On the other hand, polymers with higher molecular weights possess higher glass transition temperatures (T_g) (G5C_pH2 > G3C_pH2 > G1.5C_pH2 > G_pH6) (Balaguer et al., 2011b) what is indicative of a lower conformational flexibility of the polymer chains as a consequence of the greater connectivity between polypeptide chains. Therefore, if rotation of bonds is compromised polymer will not easily fit into the active sites of enzymes, and accessible sites for water hydrolysis will be buried what reduces biodegradation rate (Kale et al., 2007). Indeed, water entrance was more restricted in the matrices with higher cross-linking degrees, which presented lower swelling, measured as water uptake and size increase (Balaguer et al., 2011a), and lower water vapor diffusion coefficients (Balaguer et al., 2013b).

Zhang et al. (2010) also found that chemical cross-linking did slow down the rate or reduce the degree of biodegradation of gluten bioplastics modified with epoxidised soybean oil, acetone-formaldehyde resin, tannin resin, and glycidoxypropyl trimethoxysilane. The segments containing structures derived from the reactions with additives such as tannin or epoxidised soybean oil remained in the degradation residues while the glycidoxypropyl trimethoxysilane agent produced similar to 20% undegraded residues containing silicon-cross-linking structures. Chevillard et al. (2011) investigated the influence of clay nanoparticles on the biodegradability of wheat gluten-based materials. Respirometric experiments showed that the rate of biodegradation of wheat gluten-based materials could be slowed down by adding unmodified montmorillonite without affecting the final biodegradation level whereas the presence of an organically modified montmorillonite did not significantly influence the biodegradation pattern. The authors hypothesized that (i) a reduced water adsorption capacity of the gluten materials in the presence of such fillers, (ii) the establishment of interactions between the nanoclays and the matrix, resulting in a lower availability for the matrix to be biodegraded, and/or (iii) the presence of a tortuous path induced by the nanodispersion of layered silicates leading to a slower diffusion of penetrants

could be responsible of the changes of biodegradability patterns in wheat gluten materials. Conversely, Domenek et al. (2004) did not found differences in the biodegradation profiles in liquid medium of wheat gluten samples having undergone different heat and shear treatments.

Figure 6.5 depicts biodegradation rates obtained from the first derivative and in **Table 6.3**, the maximum biodegradation rate ($\boldsymbol{r_{max}}$), and the time to reach the maximum biodegradation rate ($\boldsymbol{t_{r_{max}}}$) are reported. Cellulose maintained the most constant biodegradation rate of the samples evaluated, reaching a maximum of 17.1%/day after 2 days. The starch-based film showed the slowest biodegradation rate and the greater time lag (11 days). According to biodegradation rates more than 50% of biodegradation of gliadin films was produced in one day, being the maximum rates inversely proportional to the percentage of cinnamaldehyde incorporated, from 77.4 for the film G_pH6 to 53.5 %/day for the film G5C_pH2. Different phases of the biodegradation process can be identified with the maximum and minimum peaks of the derivative curves. Domenek et al. (2004) proposed that this accelerating and slowing-down behavior of the biodegradation could be a result of changes in the culture medium, such as variations in the pH.

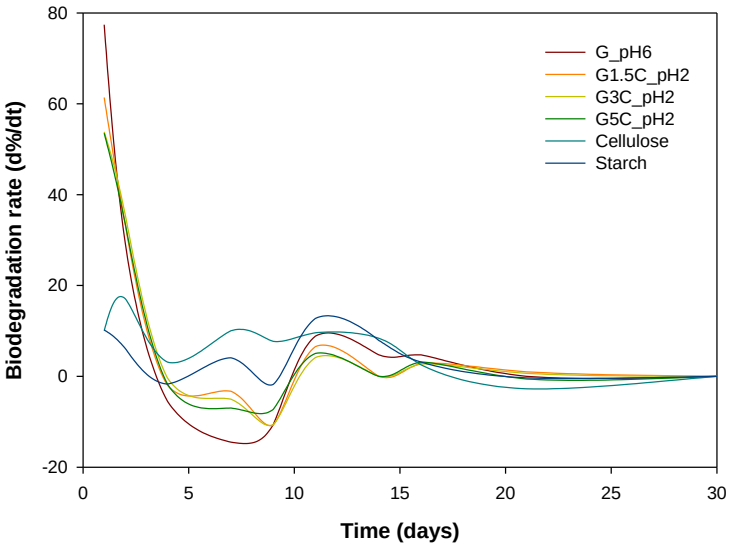

Figure 6.5. Biodegradation rate of control gliadin film (G_pH6), active antimicrobial and cross-linked gliadin films (GXC_pH2), positive reference (Cellulose), and commercial compostable film (Starch).

The release of remaining cinnamaldehyde did not impede gliadin proteins to biodegrade, although its net effect on the inherent biodegradability could not separately be evaluated from the cross-linking effects, since the matrices with the higher cross-linking degrees possess the higher amounts of free cinnamaldehyde (Balaguer et al., 2013a).

6.3.4. Plant ecotoxicity tests

The rate of seedling germination and plant growth of the resulting compost after the addition of the film G5C_pH2 in comparison with the blank compost are shown in **Table 6.4**. The incorporation of a higher proportion of compost with respect to the reference substrate decreased the germination rate, the shoot height and the fresh weight of the plant. Some wilting was also observed when a higher proportion of compost with respect to reference substrate was used. This could be due to the fact that the compost was unstable or immature which may slow plant growth and damage the plant by competing for oxygen or cause phytotoxicity to plants due to insufficient biodegradation of organic matter (Alvarenga et al., 2007; Wu et al., 2000). However, no significant differences were found between blank compost (C) and compost test incorporating the film (C+F), since p-value of F-test was higher or equal to 0.05 in all cases (**Table 6.4**). Relative germination rate and shoot height were not less than 90% of that corresponding to the blank compost (**Table 6.4**). Only fresh weight presented some discrepancies since for low compost proportion test (1:3) the fresh weight was lower and for high proportion (1:1) the fresh weight was higher than for blank compost; however, they were not statistically significant. This variable result can be consequence of a differential irrigation.

Table 6.4. Germination, shoot height and fresh weight of plants in test compost and blank compost in the different test ratios, relative values, and statistical parameters.

Sample	Germination rate (%)	Relative germination rate (%)	Shoot height (cm)	Relative shoot height (%)	F-test	Fresh weight (mg)	Relative fresh weight (%)	F-test
1C:3RS	100.00	92.31	6.37 ± 1.13	97.21	0.43	69.35 ± 19.39	80.69	0.05
1C+F:3RS	92.31		6.19 ± 1.33			55.95 ± 29.18		
1C:1RS	96.15	96.00	5.60 ± 1.13	91.89	0.46	36.15 ± 23.86	106.44	0.12
1C+F:1RS	92.31		5.15 ± 1.31			38.48 ± 17.11		

C: blank compost, C+F: compost with film, RS: reference substrate

Therefore, all the parameters studied agree about the absence of ecotoxicological effects on tomato plants of the compost obtained with gliadin films containing cinnamaldehyde. Although Kopeć et al. (2013) found that the addition of a thermoplastic maize starch to compost caused an increase in its ecotoxicity, observed as a reduction in germination and root growth in comparison with a blank compost, most of the authors do not report ecotoxicity when bioplastics are composted (Degli-Innocenti et al., 2001; Jayasekara et al., 2003; Tuominen et al., 2002; Witt et al., 2001). However, to the best of our knowledge this is the first work that deals with the compostability of active bioplastics with antimicrobial properties. In this case, the presence of remaining cinnamaldehyde did not affect the ecotoxicity of the resulting compost. These results are in line with one of the applications of cinnamaldehyde since it is used as a pesticide commercialized under the name Cinnamite™ and it can be used for the treatment of a wide variety of crops. Despite the high concentration employed in this product (30%) its application to greenhouse-grown herbs only produced some temporary phytotoxic effects which did not reduce their market quality and salability (Cloyd and Cycholl, 2002). Indeed the application of cinnamaldehyde directly in soil is proposed by Yossa et al. (2010) as an effective treatment to reduce the potential transfer of pathogens from soil to fresh produce and, consequently, reduce the fresh produce-related outbreaks.

6.4. CONCLUSIONS

The adaptions conducted to perform the tests at lower scale could serve as a guide for preliminary testing of novel materials produced in lower quantities, serving as a reference to choose or discard among them.

Gliadin films cross-linked with cinnamaldehyde showed good compostable properties at laboratory scale. Fast disintegration into fine indistinguishable fragments took place in compost as a consequence of rapid microbial colonization of films' surface. Biodegradation profiles were affected by the cross-linking degree of the proteinaceous matrices without affecting their complete biodegradation. The resulting compost did not produce any ecotoxicological effect in tomato plants. The presence of residual cinnamaldehyde in the films did not compromise their susceptibility for organic recovery. To the best of our

knowledge, this is the first work that deals with the compostability of antimicrobial bioplastics.

6.5. REFERENCES

Alvarenga, P., Palma, P., Goncalves, A. P., Fernandes, R. M., Cunha-Queda, A. C., Duarte, E., and Vallini, G. 2007. Evaluation of chemical and ecotoxicological characteristics of biodegradable organic residues for application to agricultural land. *Environment International, 33*(4), 505-513.

Atkins, P., and De Paula, J., 2006. *Atkins' Physical chemistry*. W. H. Freeman and Company, NewYork.

Balaguer, M. P., Borne, M., Chalier, P., Gontard, N., Morel, M.-H., Peyron, S., Gavara, R., and Hernández-Muñoz, P. 2013a. Retention and release of cinnamaldehyde from wheat protein matrices. *Biomacromolecules*, 1493-1502.

Balaguer, M. P., Cerisuelo, J. P., Gavara, R., and Hernandez-Muñoz, P. 2013b. Mass transport properties of gliadin films: Effect of cross-linking degree, relative humidity, and temperature. *Journal of Membrane Science, 428*, 380-392.

Balaguer, M. P., Gomez-Estaca, J., Gavara, R., and Hernandez-Munoz, P. 2011a. Biochemical properties of bioplastics made from wheat gliadins cross-linked with cinnamaldehyde. *Journal of Agricultural and Food Chemistry, 59*(24), 13212-13220.

Balaguer, M. P., Gomez-Estaca, J., Gavara, R., and Hernandez-Munoz, P. 2011b. Functional properties of bioplastics made from wheat gliadins modified with cinnamaldehyde. *Journal of Agricultural and Food Chemistry, 59*(12), 6689-6695.

Barone, J. R., and Arikan, O. 2007. Composting and biodegradation of thermally processed feather keratin polymer. *Polymer Degradation and Stability, 92*(5), 859-867.

Boluda, R., Roca-Perez, L., and Marimon, L. 2011. Soil plate bioassay: An effective method to determine ecotoxicological risks. *Chemosphere, 84*(1), 1-8.

Burkersroda, F. V., Schedl, L., and Gopferich, A. 2002. Why degradable polymers undergo surface erosion or bulk erosion. *Biomaterials, 23*, 4221-4231.

Calmon, A., Silvestre, F., Bellon-Maurel, V., Roger, J. M., and Feuilloley, P. 1999. Modelling easily biodegradability of materials in liquid medium-relationship between structure and biodegradability. *Journal of Environmental Polymer Degradation, 7*(3), 135-144.

Cloyd, R. A., and Cycholl, N. L. 2002. Phytotoxicity of selected insecticides on greenhouse-grown herbs. *HortScience, 37*(4), 671-672.

Chevillard, A., Angellier-Coussy, H., Cuq, B., Guillard, V., César, G., Gontard, N., and Gastaldi, E. 2011. How the biodegradability of wheat gluten-based agromaterial can be modulated by adding nanoclays. *Polymer Degradation and Stability, 96*(12), 2088-2097.

Degli-Innocenti, F., Bellia, G., Tosin, M., Kapanen, A., and Itavaara, M. 2001. Detection of toxicity released by biodegradable plastics after composting in activated vermiculite. *Polymer Degradation and Stability, 73*(1), 101-106.

Domenek, S., Feuilloley, P., Gratraud, J., Morel, M.-H., and Guilbert, S. 2004. Biodegradability of wheat gluten based bioplastics. *Chemosphere, 54*(4), 551-559.

Fontaine, S., Mariotti, A., and Abbadie, L. 2003. The priming effect of organic matter: A question of microbial competition? *Soil Biology and Biochemistry, 35*(6), 837-843.

Hernandez-Izquierdo, V. M., and Krochta, J. M. 2008. Thermoplastic processing of proteins for film formation--a review. *Journal of Food Science, 73*(2), R30-39.

Jayasekara, R., Sheridan, S., Lourbakos, E., Beh, H., Christie, G. B. Y., Jenkins, M., Halley, P. B., McGlashan, S., and Lonergan, G. T. 2003. Biodegradation and ecotoxicity evaluation of a bionolle and starch blend and its degradation products in compost. *International Biodeterioration & Biodegradation, 51*(1), 77-81.

Kale, G., Kijchavengkul, T., Auras, R., Rubino, M., Selke, S. E., and Singh, S. P. 2007. Compostability of bioplastic packaging materials: An overview. *Macromolecular Bioscience, 7*(3), 255-277.

Kopeć, M., Gondek, K., and Baran, A. 2013. Assessment of respiration activity and ecotoxicity of composts containing biopolymers. *Ecotoxicology and Environmental Safety, 89*(0), 137-142.

Kuzyakov, Y. 2010. Priming effects: Interactions between living and dead organic matter. *Soil Biology and Biochemistry, 42*(9), 1363-1371.

Kuzyakov, Y., Friedel, J. K., and Stahr, K. 2000. Review of mechanisms and quantification of priming effects. *Soil Biology and Biochemistry, 32*(11–12), 1485-1498.

Narayan, R. 1993. Biodegradation of polymeric materials during composting. In *Science and Engineering of Composting: Design, Environmental, Microbiological and Utilization Aspects*, H. Hoitink, and H. Keener, Eds. Renaissance Publications: Worthington, OH; 339.

Peppas, N. A., and Langer, R. 1994. New challenges in biomaterials. *Science, 263*(5154), 1715-1720.

Plackett, D. V., Holm, V. K., Johansen, P., Ndoni, S., Nielsen, P. V., Sipilainen-Malm, T., Sodergard, A., and Verstichel, S. 2006. Characterization of L-potylactide and L-polylactide-polycaprolactone co-polymer films for use in cheese-packaging applications. *Packaging Technology and Science, 19*(1), 1-24.

Pushpadass, H. A., Weber, R. W., Dumais, J. J., and Hanna, M. A. 2010. Biodegradation characteristics of starch-polystyrene loose-fill foams in a composting medium. *Bioresource Technology, 101*(19), 7258-7264.

Queiroz, A. U. B., and Collares-Queiroz, F. P. 2009. Innovation and industrial trends in bioplastics. *Polymer Reviews, 49*(2), 65-78.

Rudeekit, Y., Siriyota, P., Intaraksa, P., Chaiwutthinan, P., Tajan, M., and Leejarkpai, T. 2012. Compostability and ecotoxicity of poly(lactic acid) and starch blends. *Advanced Materials Research*, 506, 323-326.

Tuominen, J., Kylma, J., Kapanen, A., Venelampi, O., Itävaara, M., and Seppälä, J. 2002. Biodegradation of lactic acid based polymers under controlled composting conditions and evaluation of the ecotoxicological impact. *Biomacromolecules, 3*(3), 445-455.

van der Zee, M. 2005. Biodegradability of polymers – mechanisms and evaluation methods. In *Handbook of biodegradable polymers,* C. Bastioli, Ed., Smithers Rapra Technology: United Kingdom.

Whitaker, J. R., 1994. *Principles of enzymology for the food sciences*. Marcel Dekker, Inc., New York

Witt, U., Einig, T., Yamamoto, M., Kleeberg, I., Deckwer, W. D., and Müller, R. J. 2001. Biodegradation of aliphatic-aromatic copolyesters: Evaluation of the final biodegradability and ecotoxicological impact of degradation intermediates. *Chemosphere, 44*(2), 289-299.

Wu, L., Ma, L. Q., and Martinez, G. A. 2000. Comparison of methods for evaluating stability and maturity of biosolids compost. *Journal of Environment Quality, 29*(2), 424-429.

Yossa, N., Patel, J., Miller, P., and Lo, Y. M. 2010. Antimicrobial activity of essential oils against *Escherichia coli* O157:H7 in organic soil. *Food Control, 21*(11), 1458-1465.

Zhang, X. Q., Gozukara, Y., Sangwan, P., Gao, D. C., and Bateman, S. 2010. Biodegradation of chemically modified wheat gluten-based natural polymer materials. *Polymer Degradation and Stability, 95*(12), 2309-2317.

CHAPTER 7

FUNCTIONAL PROPERTIES AND ANTIFUNGAL ACTIVITY OF FILMS BASED ON GLIADINS CONTAINING CINNAMALDEHYDE AND NATAMYCIN

Balaguer, M.P.; Fajardo, P.; Gartner, H.; Gomez-Estaca, J.; Gavara, R.; Almenar, E.; and Hernandez-Munoz, P.

International Journal of Food Microbiology, 2014, 173(0), 62-71

Gliadin films cross-linked with cinnamaldehyde (1.5, 3, and 5%) and incorporated with natamycin (0.5%) were prepared by casting, and their antifungal activity, water resistance, and barrier properties were characterized. Incorporation of natamycin gave rise to films with greater water uptake, weight loss and diameter gain, and higher water vapor and oxygen permeabilities. These results may be associated to a looser packing of the protein chains as a consequence of the presence of natamycin. The different cross-linking degree of the matrices influenced the natamycin migration to the agar test media, increasing from 13.3 to 23.7 (μg/g of film) as the percentage of cinnamaldehyde was reduced from 5% to 1.5%. Antifungal activity of films was assayed against common food spoilage fungi (Penicillium species, Alternaria solani, Colletotrichum acutatum). The greatest effectiveness was obtained for films containing natamycin and treated with 5% of cinnamaldehyde. The level of cinnamaldehyde reached in the head-space of the test assay showed a diminishing trend as a function of time, which was in agreement with fungal growth and cinnamaldehyde metabolization. Developed active films were used in the packaging of cheese slices showing promising results for their application in active packaging against food spoilage.

7.1. INTRODUCTION

The substitution of synthetic preservatives used in food products by natural antimicrobial compounds has been attracting much attention in the last decade (Burt, 2004; del Nobile et al., 2012; Tajkarimi et al., 2010). Consumers are more aware of the importance of consuming healthy, great quality, and safety-assured food products, so food manufacturers need to find new ways of reducing food waste and sanitary risks associated with microbial contamination. In addition, extension of the shelf-life of food products is desired while complying with the legislation and without generating the marketing drawbacks associated with synthetic preservatives.

Natamycin (**Figure 7.1**) is a fungicide of the polyene macrolide group produced by natural strains of *Streptomyces natalensis* or *Streptococcus lactis*. It is registered in EU food additive list with the number E-235. According to Regulation 1333/2008/EC on food additives, natamycin is only approved as a surface preservative for certain cheese and dried sausage products at a maximum level of 1 mg/dm^2 in the outer 5 mm of the surface, corresponding to 20 mg/kg. Its mechanism of action is binding to sterols (principally ergosterol) in the fungal cell membrane, and as bacteria lack sterols in their membrane they are insensitive to natamycin. Minimum inhibitory concentrations (MIC) of natamycin for molds range from 0.5 to 6 µg/mL, but some species require 10 to 25 µg/mL, and most yeasts are inhibited at concentrations from 1 to 5 µg/mL (Delves-Broughton et al., 2005).

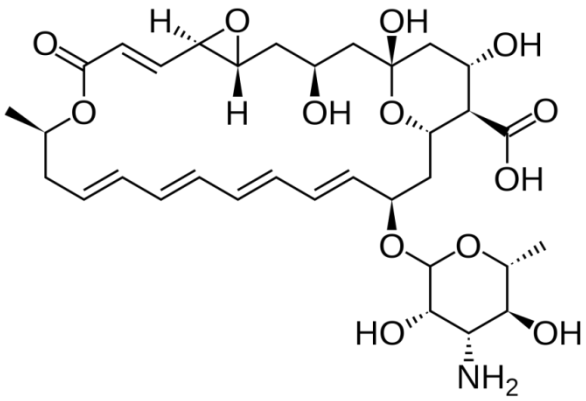

Figure 7.1. Chemical structure of natamycin.

The application of natamycin onto food surfaces by spraying or dipping is not always as effective as expected due to its inactivation by interaction with other components of the food matrix (Fucinos et al., 2012; Reps et al., 2002). Moreover, direct application of antimicrobials onto the food surface may result in a rapid migration to the food bulk, allowing surface fungal growth. The inclusion of natamycin in a polymer matrix for later sustained release to the surface of the food can ensure a minimal concentration of the antimicrobial capable of protecting the food against fungal growth. Moreover, incorporation of natamycin in a polymer matrix can reduce the loss of activity of the compound by interaction with food.

Biopolymers based on renewable resources present a noteworthy potential to retain and release active compounds (Cha and Chinnan, 2004). These biopolymers can be employed in the development of antimicrobial active packaging films which can extend the shelf-life of packaged foods and at the same time contribute to the use of environmentally-friendly materials. In this regard, some biopolymers have been proposed as carriers of natamycin, e.g. cellulose (de Oliveira et al., 2007; dos Santos Pires et al., 2008), wheat gluten and methyl cellulose (Ture et al., 2008), chitosan (Ce et al., 2012; Fajardo et al., 2010), blends of alginate and chitosan (da Silva et al., 2012), whey protein (Pintado et al., 2010; Ramos et al., 2012), and alginate and pectin (Krause Bierhalz et al., 2012).

The cross-linking degree of the polymer employed as carrier of natamycin could be used as a mechanism to modulate its release into the medium. Films based on gliadins chemically modified by treatment with cinnamaldehyde possess different functional properties depending on the cross-linking degree achieved (Balaguer et al., 2013b; Balaguer et al., 2011a, 2011b). Moreover, it has been shown that a part of the cinnamaldehyde incorporated in the gliadin matrix does not cross-link the protein and remains entrapped in the matrix until being released under certain environmental conditions.

The aim of this work has thus been (i) to incorporate natamycin into gliadin films treated with cinnamaldehyde, (ii) to study how natamycin affects some functional properties of the films, (iii) to estimate the release of cinnamaldehyde and natamycin from the films, and (iv) to evaluate the antifungal effectiveness of the developed films *in vitro* and in different kinds of cheese.

7.2. MATERIALS AND METHODS

7.2.1. Reagents and microbial strains

Crude wheat gluten (≥ 80% protein), glycerol, ethanol, hydrochloric acid, and cinnamaldehyde, all laboratory grade, were supplied by Sigma (Madrid, Spain). Pimaricin supplied by VGP, S.L. (Barcelona, Spain) as the source of the active agent natamycin, consisted of 50% natamycin and 50% lactose. In this work, unless otherwise indicated, percentage of natamycin will be expressed as levels of pure natamycin (without lactose).

Potato Dextrose Agar (PDA) was purchased from Sigma (Sigma-Aldrich Corp., Saint Louis, MO, USA).

Fungal strains of *Colletotrichum acutatum* and *Penicillium* species were originally isolated from diseased blueberry fruit, and decayed bread, respectively. *Alternaria solani* was provided by the Department of Plant Pathology of Michigan State University (East Lansing, MI, USA).

7.2.2. Film formation and characterization

7.2.2.1. Gliadin-rich fraction extraction from wheat gluten

The gliadin-rich fraction was extracted from wheat gluten according to Hernandez-Munoz et al. (2003). Briefly, 100 g of wheat gluten was dispersed in 400 mL of 70% (v/v) ethanol/water mixture, stirred overnight at room temperature, and centrifuged at 5000 rpm for 20 min at 20 °C. The supernatant containing the gliadin-rich fraction was collected and used as the film-forming solution.

7.2.2.2. Chemical modification of gliadins

In preliminary studies, the use of cinnamaldehyde as a protein cross-linker was found to be strongly dependent on the pH (Balaguer et al., 2013a; Balaguer et al., 2011a, 2011b). Initially, the pH of the gliadin film forming solution was brought to 2.0 with HCl as the most suitable for polymerization. Then, chemical modification of gliadins was conducted by adding different concentrations of cinnamaldehyde to the film-forming solution, namely 1.5% (G1.5C_pH2), 3% (G3C_pH2) and 5% (G5C_pH2) (g cinnamaldehyde/100 g protein). Glycerol was added as plasticizer at 25% (g glycerol/100 g protein). For films incorporating natamycin (NT-GXC_pH2), 0.5% of natamycin was added to the film-forming solution (g

natamycin/100 g protein). The mixture with all the reagents was stirred at room temperature for 30 min.

7.2.2.3. Film production and conditioning

In order to have 0.01 g of protein/cm^2, measured volumes of the film-forming solution were poured onto a horizontal flat Pyrex tray to allow water and ethanol to evaporate. The films were dried at 37 °C for 24 h. The dried films were peeled off the casting surface. The film thickness was measured using a micrometer (Mitutoyo, Kanagawa, Japan) with a sensitivity of ± 2 µm. The mean thickness was calculated from measurements taken at ten different locations on each film sample. The films were stored 1 month at 30% RH and 23 °C before testing. The surface density of the resulting films was 0.0195 ± 0.0065 g/cm^2.

7.2.2.4. Water uptake, weight loss and diameter gain

Film specimens were cut into circles with a diameter of 2.5 cm (initial diameter, $\emptyset^i$), and dried over P_2O_5 in a desiccator until they reached constant weight. At this point the moisture content in the film samples was assumed to be close to zero. Samples were accurately weighed (initial dry weight, W_d^i) and immersed in test tubes containing 10 mL of distilled water. The tubes were shaken in an orbital shaker at 180 rpm at 23 °C for 24 h. The film specimens were then removed from the solutions, blotted with absorbent paper to remove any remaining water from the surface, and weighed (final wet weight, W_w^f). The diameter (final diameter, $\emptyset^f$) was measured using a Vernier caliper. The film samples were replaced in the desiccator with P_2O_5 until they reached a constant weight (final dry weight, W_d^f). The percentage of water uptake, weight loss and diameter gain of the films was calculated as:

$$\text{Water uptake (\%)} = \frac{W_w^f - W_d^f}{W_d^f} \cdot 100 \qquad (\mathbf{7.1})$$

$$\text{Weight loss (\%)} = \frac{W_d^i - W_d^f}{W_d^i} \cdot 100 \qquad (\mathbf{7.2})$$

$$\Delta\emptyset\ (\%) = \frac{\emptyset^f - \emptyset^i}{\emptyset^i} \cdot 100 \qquad (\mathbf{7.3})$$

7.2.2.5. Barrier properties

7.2.2.5.1. Water permeability

Water vapor transmission rate [kg/(m^2·s)] through the films was measured using a Mocon PERMATRAN-W® Model 3/33 (Lippke, Neuwied, Germany). It operates according to ASTM F1249 (ASTM, 2006) and uses an infrared sensor. The film samples were double-masked with aluminum foil, leaving a circular uncovered effective film area of 5 cm^2. Testing was performed at 23 °C with a relative humidity gradient of 50% to 0% (in dry nitrogen) across the film. At least four samples of each type of film were measured. The water vapor permeability coefficient in (kg·m)/(m^2·s·Pa) can be calculated from the transmission rate values measured as follows:

$$P = \frac{Q \cdot l}{A \cdot t \cdot \Delta p} \qquad (\mathbf{7.4})$$

where Q is the amount of permeant (kg) passing through a film of thickness l (m) and area A (m^2), t is the time (s), and Δp is the partial pressure differential across the film (Pa). Δp is calculated from the water vapor partial pressure at 23 °C and a RH gradient of 50-0%.

7.2.2.5.2. Oxygen permeability

The oxygen transmission rates [m^3/(m^2·s)] through the films were measured using a Mocon OX-TRAN® Model 2/21 (Lippke, Neuwied, Germany). It operates according to ASTM D3985 (ASTM, 2005) and uses a coulometric sensor (COULOX®). The film samples were double-masked with aluminum foil, leaving a circular uncovered effective film area of 5 cm^2. Testing was performed at 23 °C and at a constant relative humidity of 50%. At least four samples of each type of film produced were measured. Transmission rate values are reported as oxygen permeability coefficient in (m^3·m)/(m^2·s·Pa), calculated as in **Equation 7.4**.

7.2.2.6. Determination of natamycin migration from the films to the agar media

The amount of natamycin migrated was calculated as the difference between the initial amount of compound extracted from the film and the amount extracted from the film after 7 days of contact with the agar media, in order to correlate natamycin migration with

the antifungal tests. Due to the greater stability and solubility of natamycin in methanol compared to water (Delves-Broughton et al., 2005) an extraction procedure using methanol as solvent was selected to determine the amount of natamycin in the film. Films were cut in pieces of 2.5 cm of diameter, and weighed accurately. Each piece of film was placed in a dark test tube, to prevent the photolysis of natamycin, containing 10 mL of methanol. During the extraction the piece of film was completely immersed, with both sides in contact with the solvent, and with continuous agitation. After 24 h an aliquot was withdrawn, and analyzed by High Performance Liquid Chromatography (HPLC). The quantitative analysis was performed on a 1200 series HPLC equipped with an SPD-M10Avp diode array detector, a DGU-14A degasser, an SCL-10Avp system controller, and a Class-VP v.6.14 chromatography data system (Agilent Technologies, Las Rozas, Spain). A stainless steel column, Gemini C18 110A, 4.6 x 150 mm, 5 µm particle size, from Phenomenex (Torrance, CA), was used. The method was based on that of Hanusova et al. (2010). The mobile phase was acetonitrile:acetate buffer (pH 4.3) 35:65 (v/v) with a flow rate of 0.4 mL/min at temperature of 23 °C. Peaks were detected by measurement of absorbance at 304 nm. The concentration of natamycin was calculated from a calibration curve of natamycin in methanol for concentrations ranging from 0.05 to 5 ppm.

7.2.2.7. Determination of cinnamaldehyde level evolution in the head-space of the assay system

An assay system was elaborated to determine the amount of cinnamaldehyde released from the films to the head-space of the system. The system consisted of a glass jar with a volume of 0.5 L which was modified placing a septum in the cap of the jar for the withdrawal of the volatile. The surface of a film with a diameter of 2 cm (weight of 55.7 ± 1.5 mg) was put in contact with the agar media contained in a 5 cm diameter Petri dish which was placed at the bottom of the jar, immediately after the system was hermetically closed with a screw cap. This assembly rendered the film the moisture necessary to trigger the release of cinnamaldehyde to the head-space of the jar. The release of cinnamaldehyde to the head-space was monitored for seven days at 23 °C. The concentration of cinnamaldehyde was estimated by sampling of the jar head-space using a solid-phase microextraction (SPME) head-space sampling method combined with gas chromatography (GC) analysis. Samples from the head-space were taken at days 0, 1, 3, 5, and 7 with a 100 µm polydimethylsiloxane SPME fiber (Supelco, Bellefonte, PA) through the septum in the screw cap. The fiber was exposed to the jar head-space for 20 min at 23

°C, and the trapped volatiles were immediately desorbed for 5 min at 250 °C at the splitless injection port of the GC instrument Hewlett-Packard 6890 series (Agilent Technologies, Palo Alto, CA) equipped with a flame ionization detector (FID) and a HP-5 column (30 m × 0.25 mm × 0.25 µm film thickness).

7.2.3. Efficacy of gliadin films containing cinnamaldehyde and natamycin against fungal growth in vitro

7.2.3.1. Culture preparation

Cultures of *A. solani*, *C. acutatum* and *Penicillium* spp. were grown on PDA in plastic Petri dishes (9 cm diameter) for 14 days at 23 °C. Conidia were then collected by flooding the surface of the plates with sterile peptone water and gently scraping the mycelial surface with a spatula. 10 mL of this suspension was transferred to sterile plastic tubes, which were shaken to obtain a homogenous suspension of conidia. The conidial suspensions were adjusted to $1{\cdot}10^6$ spores/mL. The Neubauer improved method (Bright-Line Hemacytometer, Hausser Scientific, Horshan, PA) was used to determinate spore concentration.

7.2.3.2. Bio-assay system preparation

The systems prepared in section 2.2.7 were inoculated with the selected fungi. For that, 10 µL droplets of conidial suspensions of each fungus were spread onto 5 cm diameter Petri dishes containing the solidified PDA media. Inoculated Petri dishes were then placed inside the glass jars and a piece of gliadin film with a diameter of 2 cm was placed over the inoculated Petri dish. The jars were closed hermetically with screw caps. Inoculated Petri dishes without film were used as the control. All the jars were stored for 7 days at 23 °C. Tests were performed in triplicate.

7.2.3.3. Measurement of fungal growth

Growth of the cultures in both control and bio-assay systems was evaluated at days 1, 3, 5, and 7 measuring the diameter of the inhibition halo of fungal growth around the film placed on the agar surface ($\overline{\emptyset}_{no\ growth}$). Because of the optical transparency of both the glass and Petri dish, these measurements could be made without opening the jars. The effectiveness of gliadin films containing cinnamaldehyde and natamycin against fungal growth was expressed as the percentage of inhibition:

$$Inhibition\ (\%) = \frac{\overline{\emptyset}_{no\ growth}}{\overline{\emptyset}_{total}} \cdot 100 \qquad (\mathbf{7.5})$$

where $\overline{\emptyset}_{total}$ is the diameter of the Petri dish (5 cm).

7.2.3.4. Determination of cinnamaldehyde levels in the head-space of bio-assay systems

The evolution of cinnamaldehyde level inside the bio-assay systems was conducted following the method described in **section 7.2.2.7.**

7.2.3.5. Determination of cinnamaldehyde-metabolized products by *C. acutatum*

Control bio-assay systems as described above containing *C. acutatum* were stored at 23 °C. After seven days, 1 µL of cinnamaldehyde was injected into each jar (three jars in total) through the septum on the screw caps using a 10 µL syringe (Sigma Aldrich, USA). Head-space composition was analyzed after 1 and 5 days post injection of cinnamaldehyde using a 100 µm polydimethylsiloxane SPME fiber and gas chromatography/mass spectrometry (GC/MS) in order to identify the unknown compounds resulting from the metabolization of cinnamaldehyde by *C. acutatum*. The SPME fiber was conditioned in the injector port of the GC/MS at 250 °C for 0.5 h, exposed to the head-space in the jars for 20 min, and immediately desorbed in the splitless injection port of the GC/MS at 220 °C for 5 min while cryofocusing with liquid nitrogen. GC/MS analysis was performed using a Hewlett-Packard 6980 series GC instrument (Hewlett-Packard, USA) coupled with a Pegasus time of flight mass spectrometer (TOFMS) (LECO Corporation, USA). The GC system was operated using an OmegaWax 250 capillary GC column (30 m x 0.25 mm x 0.25 µm) (Supelco, USA). The initial oven temperature was maintained at 70 °C for 1 min and ramped at a rate of 5 °C/min until a temperature of 85 °C, then increased at 10 °C/min until a temperature of 170 °C, with a final increase of 20 °C/min until 220 °C which was maintained for 3 min. The total run time for each sample was 18.0 min. Cinnamaldehyde and the unknown metabolites were observed on the total ion current chromatograph (TIC) ranging from 29 to 270 mass units and were identified based on their selected masses and verified by a library search using Pegasus Chroma TOF software. For comparison, the jars were also injected into the GC/FID used for the determination of the cinnamaldehyde levels. The same conditions as those in the determination of the cinnamaldehyde levels were used.

7.2.4. Efficacy of gliadin films containing cinnamaldehyde and natamycin against fungal growth in cheese

Two kinds of sliced cheese (soft and semi-hard cheeses), which were acquired at a local market, were employed for the experiments. The water activity and pH of each cheese were determined for comparison purposes. Water activity was measured by means of a FAST lab automatic water activity analyzer from GBX (Bourg de Peage, France). The pH was determined by homogenizing 10 g of cheese with 90 mL of distilled water, then the mixture was allowed to stand at room temperature for 10 min with occasional shaking and the pH was measured.

Two independent experiments were performed to evaluate the effectiveness of films in inhibiting fungal growth on cheese. In the first one, cheese slices of 2 mm in thickness and 5.5 cm in diameter were introduced into Petri dishes of the same size, and then surface inoculated by spreading 10 µL of a $1 \cdot 10^6$ spores/mL solution of *Penicillium* spp. Film G5C_pH2 and NT-G5C_pH2 having 16 mm of diameter were placed over the cheese surface, and the lids put on Petri dishes were sealed with Parafilm® to diminish water losses by evaporation. The samples were stored at 20 °C. The antifungal effect of the films was evaluated by visual inspection after 7 days of storage.

A second experiment was performed in order to evaluate the fungicide/fungistatic effect of the films on the microbiota of the cheeses, thus films were not previously inoculated. Circular cuts of semi-hard cheese with a diameter of 5.5 cm were introduced into Petri dishes. Then, circular pieces of film G5C_pH2 and NT-G5CpH2 were placed covering the entire cheese surface, the lids put on and the Petri dishes sealed with Parafilm®. The samples were stored at 20 °C and the antifungal effect was evaluated by visual inspection. To evaluate the fungicide/fungistatic effect, two methodologies were used: on one hand, films were removed from the cheese surface after 14 days of contact and mold growth was observed after 3 days at 20 °C; on the other hand, small portions of cheese were randomly taken from the slice, placed on the surface of PDA plates and incubated at 30 °C for 3 days. The absence of growth would be indicative of a fungicidal effect, whereas fungal growth would be indicative of a fungistatic effect.

7.2.5. Statistical analysis

Statistical analysis of the results was performed with SPSS commercial software (SPSS Inc, Chicago, IL, USA). A one-way analysis of variance (ANOVA) was carried out. Differences between means were assessed on the basis of confidence intervals using the Tukey test at a level of significance of $p \leq 0.05$. The propagation of uncertainty was used to calculate the standard deviations when the experimental values were combined in a function.

7.3. RESULTS AND DISCUSSION

7.3.1. Film formation and characterization

Gliadin films cross-linked with different amounts of cinnamaldehyde and incorporating 0.5% of natamycin were stable in water, homogeneous and transparent having a yellow color to the naked eye. The thickness of the films was around 115 ± 19 μm and no statistical differences ($p > 0.05$) were observed with respect to gliadin films without natamycin. It is remarkable to point out that in previous trials the addition of higher concentrations of natamycin, namely 2.5% and 5%, into the film-forming solution produced turbidity, and when the pH was adjusted to 2.0 some crystals appeared in the solution and remained in the films. Indeed, films treated with 1.5 and 3% cinnamaldehyde incorporating natamycin at 2.5 and 5% lost their integrity in water. A possible explanation for this is that natamycin or lactose (impurity of the preparation) might be hampering protein cross-linking, weakening the matrix, and preventing from a more compact molecular packing. Therefore, according to these previous results a concentration of 0.5% of natamycin was chosen.

7.3.1.1. Water uptake, weight loss and diameter gain

In previous works it was shown that as the percentage of cinnamaldehyde increased, gliadin films were generally more resistant to water giving rise to lower water uptake, lower weight loss, and lower diameter gain (Balaguer et al., 2011a, 2011b). **Table 7.1** shows the water uptake, the weight loss and the diameter gain of gliadin films cross-linked with cinnamaldehyde containing (+NT) or not (-NT) natamycin, after 24 h of immersion in distilled water at 23 °C. The addition of natamycin to the films cross-linked with cinnamaldehyde produced significant modifications ($p \leq 0.05$) in all the parameters

evaluated. Natamycin and lactose could be retaining higher amounts of water (Krause Bierhalz et al., 2012), and at the same time could be reducing the cohesiveness of the matrix what facilitates the entrance of water, increasing the water uptake of films incorporated with natamycin. This effect is also evidenced as a greater diameter gain achieved for the films with natamycin. The weight loss in gliadin films was related mostly with the migration of glycerol and to a minor extent with the release of small protein chains into the medium, since films did not lose their integrity but remained very brittle after drying upon immersion. The greater weight loss in films with natamycin was enhanced owing to the lower retention of all the compounds present in the film as a result of the formation of a looser matrix because of the presence of natamycin.

Table 7.1. Water uptake, weight loss and diameter gain of gliadin films cross-linked with cinnamaldehyde with (+NT) or without (-NT) natamycin, after 24 h of immersion in distilled water at 23 °C.

Sample	Water Uptake (%)		Weight Loss (%)		Diameter gain (%)	
	-NT	+NT	-NT	+NT	-NT	+NT
G1.5C_pH2	72.01 ± 8.80^{a*}	150.54 ± 8.28^{a}	23.83 ± 1.00^{a*}	26.21 ± 0.90^{a}	5.33 ± 2.31^{a*}	20.07 ± 1.50^{a}
G3C_pH2	54.98 ± 1.63^{b*}	96.86 ± 4.09^{b}	21.98 ± 0.23^{a*}	23.94 ± 0.94^{b}	5.56 ± 1.39^{a*}	18.03 ± 1.25^{a}
G5C_pH2	47.99 ± 2.06^{c*}	66.93 ± 5.84^{c}	21.57 ± 0.08^{a*}	23.63 ± 0.36^{b}	1.78 ± 1.54^{b*}	8.20 ± 3.17^{b}

Values reported are the means ± standard deviations (n = 3, 95% confidence interval).
$^{a-c}$ Different lowercase letters in the same column indicate a statistically significant difference between films with different degree of cross-linking ($p \leq 0.05$).
* In the same row indicates a statistically significant difference between films with or without natamycin ($p \leq 0.05$).

7.3.1.2. Barrier properties

In a previous study it was shown that higher amounts of cinnamaldehyde enhanced the barrier properties of gliadin films due to the formation of a more cross-linked matrix that restricted chain mobility and produced a more compact structure (Balaguer et al., 2013b). **Table 7.2** shows the water vapor and oxygen permeability values of gliadin films cross-linked with different amounts of cinnamaldehyde incorporating natamycin (+NT) and their comparison with films without natamycin (-NT). The incorporation of natamycin reduced the barrier properties of films cross-linked with cinnamaldehyde; however significant differences ($p \leq 0.05$) were found only for the films with the greater percentage of cinnamaldehyde. This result may be associated with a looser packing of the protein chains

as a consequence of the presence of natamycin and lactose, which increased the free volume of the polymeric structure and thus enhanced permeability.

Table 7.2. Water vapor permeability (WVP) and oxygen permeability (O2P) values of gliadin films cross-linked with different amounts of cinnamaldehyde incorporating (+NT) or not (-NT) natamycin at 23 °C.

Sample	$WVP \cdot 10^{14}$ [(kg·m)/(m²·s·Pa)] ΔRH=50%–0%		$O_2P \cdot 10^{19}$ [(m³·m)/(m²·s·Pa)] RH=50%	
	-NT	+NT	-NT	+NT
G1.5C_pH2	3.95 ± 0.22^{b}	3.82 ± 0.07^{a}	2.52 ± 0.17^{b}	3.21 ± 0.59^{bc}
G3C_pH2	3.75 ± 0.43^{b}	3.83 ± 0.05^{a}	2.44 ± 0.05^{b}	2.65 ± 0.34^{ab}
G5C_pH2	2.98 ± 0.55^{a*}	3.89 ± 0.04^{a}	1.79 ± 0.21^{a*}	2.44 ± 0.42^{a}

Values reported are the means ± standard deviations (n = 4, 95% confidence interval).
$^{a-c}$ Different lowercase letters in the same column indicate a statistically significant difference between films with different degree of cross-linking ($p \leq 0.05$).
* In the same row indicates a statistically significant difference between films with or without natamycin ($p \leq 0.05$).

Krause Bierhalz et al. (2012) also observed that the incorporation of natamycin in single or composite films based on alginate and pectin caused a significant increase ($p \leq 0.05$) in water vapor permeability. Whereas Fajardo et al. (2010) found that natamycin incorporation (0.5 mg/mL) into chitosan films did not affect significantly ($p > 0.05$) the water vapor permeability value but did slightly and significantly increase oxygen permeability ($p \leq 0.05$). Ture et al. (2009) prepared wheat gluten and methyl cellulose films with different amounts of natamycin without finding significant ($p > 0.05$) changes in water vapor permeability upon its incorporation.

7.3.1.3. Natamycin migration into the agar

The amount of natamycin recovered from the cross-linked films by extraction with methanol, before and after the contact with the agar and the calculated migration of natamycin from the films into the agar is shown in **Table 7.3**. The nominal amount of natamycin per gram of film was around 2.56 mg/g film (equivalent to 0.05 mg natamycin/cm^2 film taking into account an average surface density of 19.5 ± 6.5 mg/cm^2 for the films evaluated). However, the maximal amount of natamycin extracted with methanol was 0.032 mg/g film, what represents around 1.25% of the theoretical amount incorporated into the film. Other authors also found a similar value (2.6% of the nominal amount) for coated polyethylene films with polyvinyldichloride or nitrocellulose lacquer

containing natamycin (Hanusova et al., 2010). This low value for the natamycin extraction could be due to the low pH of the film-forming which could be affecting the stability of natamycin. Natamycin is stable at pH values from 4.5 to 9, but not at extreme pHs as 2 or 10 (Raab, 1972). At low pH values, degradation of natamycin produces mycosamine and at least three additional inactive compounds (Brik, 1976).

Table 7.3. Amounts of natamycin extracted from the film and estimated migration to the agar.

Sample	µg NT/g film experimental before contact	µg NT/g film experimental after contact	Experimental migration		% Migration
			µg NT/g film	mg NT/dm² film*	
NT-G1.5C_pH2	31.9 ± 1.4[a]	8.2 ± 2.8[a]	23.7 ± 3.2	0.0463 ± 0.0062	74.39
NT-G3C_pH2	24.0 ± 2.5[b]	8.4 ± 0.9[a]	15.7 ± 2.6	0.0306 ± 0.0051	65.15
NT-G5C_pH2	20.0 ± 0.2[c]	6.7 ± 0.4[a]	13.3 ± 0.5	0.0260 ± 0.0009	66.64

Values reported are the means ± standard deviations (n = 3, 95% confidence interval).
The standard deviation of the experimental migration was calculated using the propagation of uncertainty.
[a-c] Different lowercase letters in the same column indicate a statistically significant difference between films with different degree of cross-linking ($p \leq 0.05$).
*Average surface density of the films (g film/dm²) was used for in this conversion

The amount of natamycin extracted from the film before contact with the agar was progressively reduced as the percentage of cinnamaldehyde increased ($p \leq 0.05$). The formation of a more cross-linked network in films treated with a greater amount of cinnamaldehyde prevented a higher extraction of natamycin, enhancing its retention. After films had been in contact with the agar the amount of natamycin remaining in the matrix was reduced and showed similar values for all the films ($p > 0.05$). The amount of natamycin migrated from the films to the agar was dependent on the cross-linking degree. The formation of a more compact structure due to chemical treatment with cinnamaldehyde was responsible of a higher retention of natamycin inside the protein matrix. These results highlight the noteworthy potential of these gliadin film matrices with different cross-linking degrees achieved with cinnamaldehyde treatment as carrier systems to control the amount of the active compound released.

Despite the low amount of active compound able to migrate from the films, natamycin is very effective against mold and yeast growth. According to the manufacturer information, MICs of natamycin are 0.1-0.2 µg/mL for *Aspergillus clavatus*, 1.0-2.0 µg/mL for *Botrytis cinerea*, 2.5 µg/mL for *Aspergillus niger*, 5.0 µg/mL for *Penicillium expansum*, 10 µg/mL for

Fusarium spp., and 1.5-2.0 µg/mL for *Candida albicans*, 2.5 µg/mL for *Saccharomyces cerevisiae*, and 5.0 µg/mL for *Saccharomyces sake*.

7.3.1.4. Cinnamaldehyde level evolution in the head-space of the assay system

Blank assay systems containing only the films were prepared as described in materials and methods **section 7.2.2.7** in order to follow the cinnamaldehyde level evolution in the head-space of the assay system. Due to the hydrophilic nature of gliadins, water contained in the agar was sorbed by proteins enabling swelling of the matrix and release of free cinnamaldehyde. **Figure 7.2** shows the chromatographic area evolution of cinnamaldehyde released from films containing or not natamycin over a 7-day storage period. In the right axis the equivalence in mg of cinnamaldehyde per L of air in the assay system is given. As expected, the films treated with higher concentrations of cinnamaldehyde released a greater amount of the compound into the head-space of the assay systems. It can also be observed that the level of cinnamaldehyde in the head-space decreased with time. This could be due to diverse factors: (i) cinnamaldehyde vapor released to the head-space is absorbed by the agar medium, (ii) condensation to liquid phase takes place, and (iii) some transformation of cinnamaldehyde into other compounds (such as cinnamic acid) could also occur.

Concentration of cinnamaldehyde present in the head-space of the assay system after 24 h of storage at 23 °C for the films G1.5C_pH2, G3C_pH2, and G5C_pH2 was 0.05, 0.16, and 0.24 mg cinnamaldehyde/L air, respectively. Although, these concentrations were lower than expected, it is important to remark that the films were not tested as soon as they were prepared, instead a storage period of 1 month at low relative humidity preceded their evaluation. In the case of films NT-G1.5C_pH2, NT-G3C_pH2, and NT-G5C_pH2 the concentrations of cinnamaldehyde in the assay systems were increased to 0.08, 0.19, 0.36 mg cinnamaldehyde/L air, respectively. The slightly higher amount of cinnamaldehyde released from the films containing natamycin could also be related with the formation of a less cross-linked matrix due to some steric hindrance of natamycin and lactose that resulted in a higher amount of free cinnamaldehyde, and simultaneously the development of a looser structure that prompted cinnamaldehyde release.

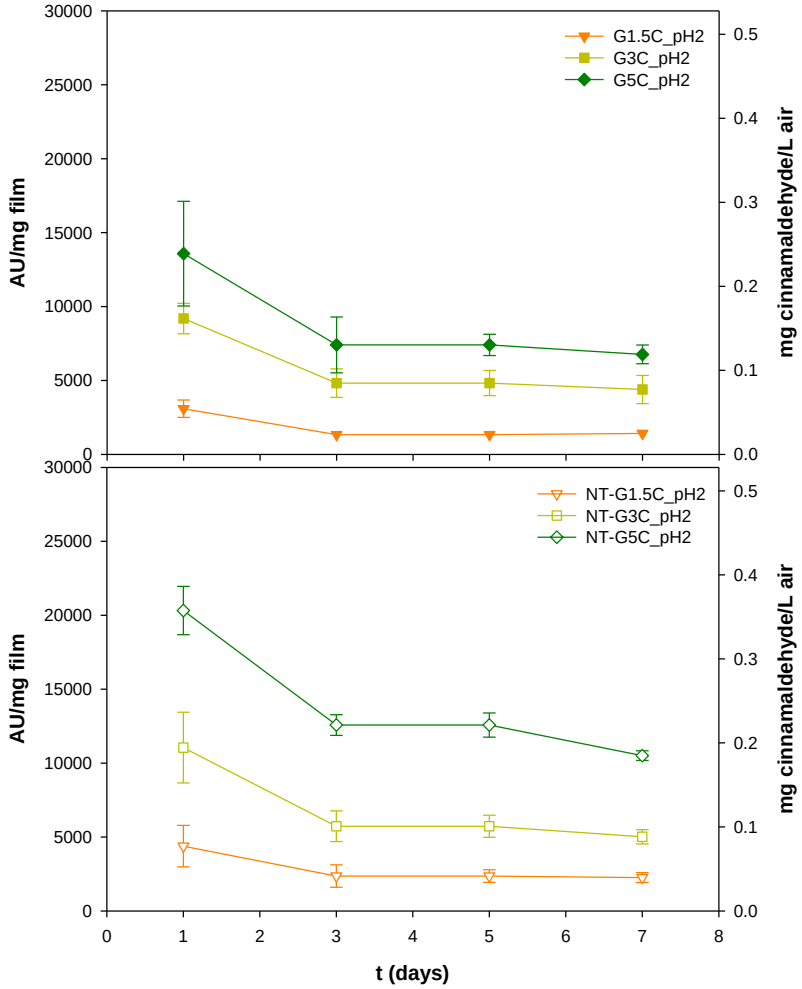

Figure 7.2. Cinnamaldehyde level evolution in the head-space of the blank assay systems: **(A)** antifungal films containing cinnamaldehyde (GXC_pH2), and **(B)** antifungal films containing cinnamaldehyde and natamycin (NT-GXC_pH2), over a 7-day storage period at 23 °C. The left axis represents the chromatographic area units per mg of film. The right axis shows the concentration of cinnamaldehyde in the air of the head-space (relative error 11.72%).

7.3.2. Efficacy of gliadin films containing cinnamaldehyde and natamycin against fungal growth

7.3.2.1. Antifungal activity

The percentages of inhibition of gliadin films treated with 1.5, 3 and 5% of cinnamaldehyde and incorporating 0.5% or no natamycin against *Penicillium* spp., *A. solani*, and *C. acutatum* are shown in **Figure 7.3**. The effectiveness of the films depended of the type of fungus evaluated, with *Penicillium* spp. the most sensitive, and showing the highest rates of inhibition. The incorporation of natamycin into the films increased in some cases the percentages of inhibition reached, and even a delay in the appearance of fungal growth. After a storage period of 7 days at 23 °C, the film G5C_pH2 produced a 33% growth inhibition for *Penicillium* spp., and around 28% and 16% for *C. acutatum* and *A. solani*, respectively. The incorporation of natamycin (NT-G5C_pH2) increased the percentage of inhibition of *Penicillium* spp. up to 73%, however, no significant differences in the inhibition ($p > 0.05$) were found for the other fungi.

Films with lower concentrations of cinnamaldehyde with or without natamycin were not effective against fungal growth, especially against the less sensitive fungi. In this work the effect of natamycin only was not evaluated since the films without cinnamaldehyde-treatment lost their integrity at high relative humidity conditions or when immersed in water (Balaguer et al., 2011a, 2011b); however, some synergistic effect of cinnamaldehyde and natamycin could be taking place in the film NT-G5C_pH2 against the growth of susceptible strains. Evidence for this synergistic effect can be seen in that films containing 0.5% of natamycin and the lowest concentration of cinnamaldehyde did not inhibit fungal growth (0% inhibition), which implies that 0.5% natamycin alone was not effective. On the other hand, the film with 5% cinnamaldehyde and without natamycin produced 33% fungal growth inhibition, but the film with 0.5% natamycin and 5% cinnamaldehyde raised the percentage of inhibition to 73%.The synergistic activity of natamycin with components from essential oils has been shown by other authors. In the work presented by Ture et al. (2008) rosemary extract did not show any inhibitory antifungal activity alone, and although natamycin incorporated into films at a concentration of 1.5 mg per 10 g film solution was not effective against *A. niger*, combination of natamycin at the same concentration with rosemary extract in the films inhibited the growth of this mold, showing that both compounds acted synergistically to prevent the growth of *A. niger*. Enhancement of antifungal effect of natamycin has been also reported in combination with other preservative systems, such as potassium sorbate (Mann and Beuchat, 2008), fusidic acid (Akiyama et al., 1980), and concentrations above 6% of sodium chloride (Arroyo-Lopez et al., 2012).

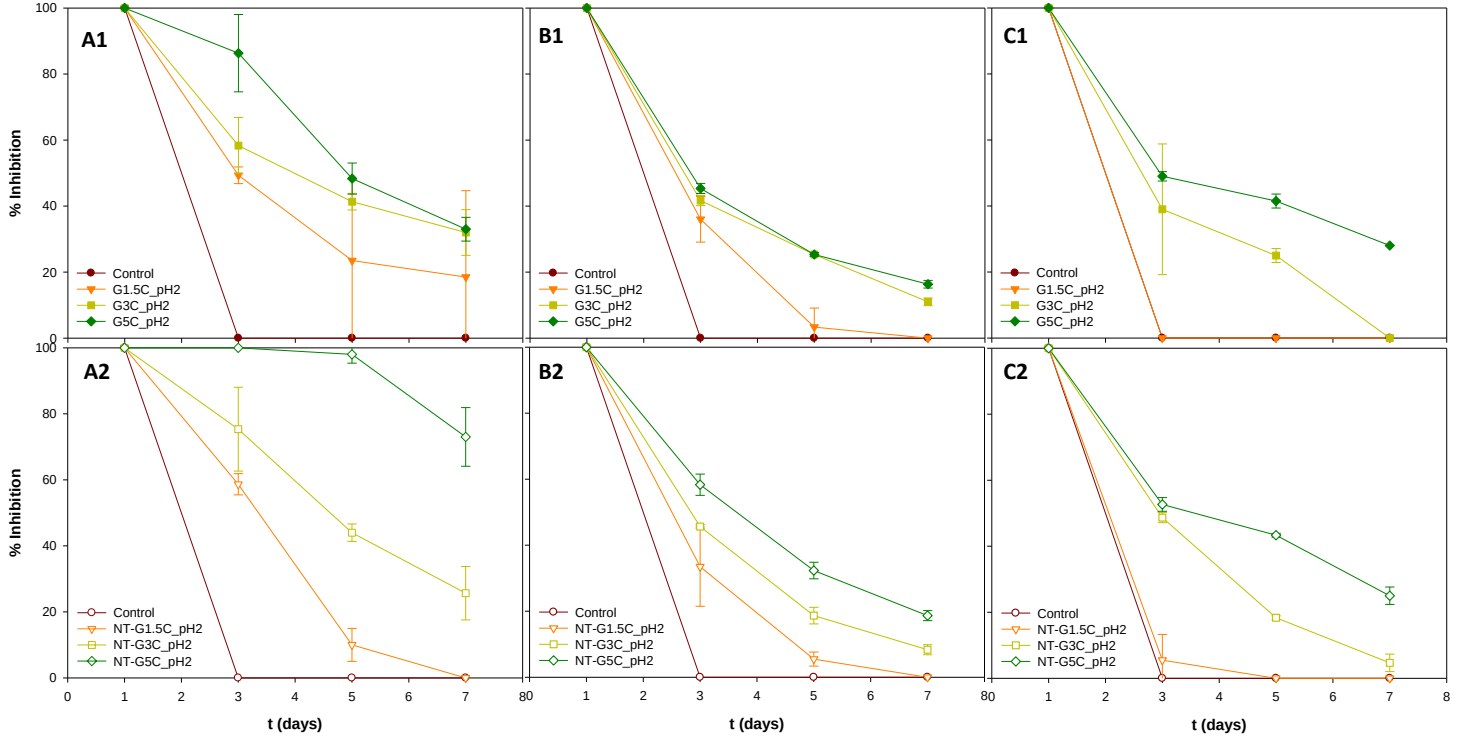

Figure 7.3. Percentage of inhibition of *Penicillium* species **(A)**, *Alternaria solani* **(B)**, *and Colletotrichum acutatum* **(C)** during exposure to antifungal films containing cinnamaldehyde **(1)**, and cinnamaldehyde and natamycin **(2)** over a 7-day storage period at 23 °C.

7.3.2.2. Cinnamaldehyde level evolution in the head-space of bio-assay systems

The percentages of fungal growth inhibition were evaluated in parallel with the cinnamaldehyde level in the head-space of the bio-assay system. **Figure 7.4** shows the chromatographic areas of cinnamaldehyde measured in the head-space of the bio-assay systems containing the fungi. This simultaneous analysis of the results reveals that the initial amount of cinnamaldehyde in the head-space was lower for the tests with *A. solani* and *C. acutatum*. In agreement, Almenar et al. (2007) reported a rapid decline in the concentration of acetaldehyde in bio-assay systems containing *B. cinerea* but not in those containing *Alternaria alternata* and *C. acutatum*. The difference was attributed to a faster growth rate for *B. cinerea* compared to *A. alternata* and *C. acutatum*, which increased its absorption area. After 3 days of storage the cinnamaldehyde level was greatly reduced in most of the cases. This reduction also observed to a minor extent in the blank assay systems could be enhanced due to the metabolization of cinnamaldehyde by the fungus. Therefore, in the test where the fungus was more inhibited a higher level of cinnamaldehyde was present, and *vice versa*.

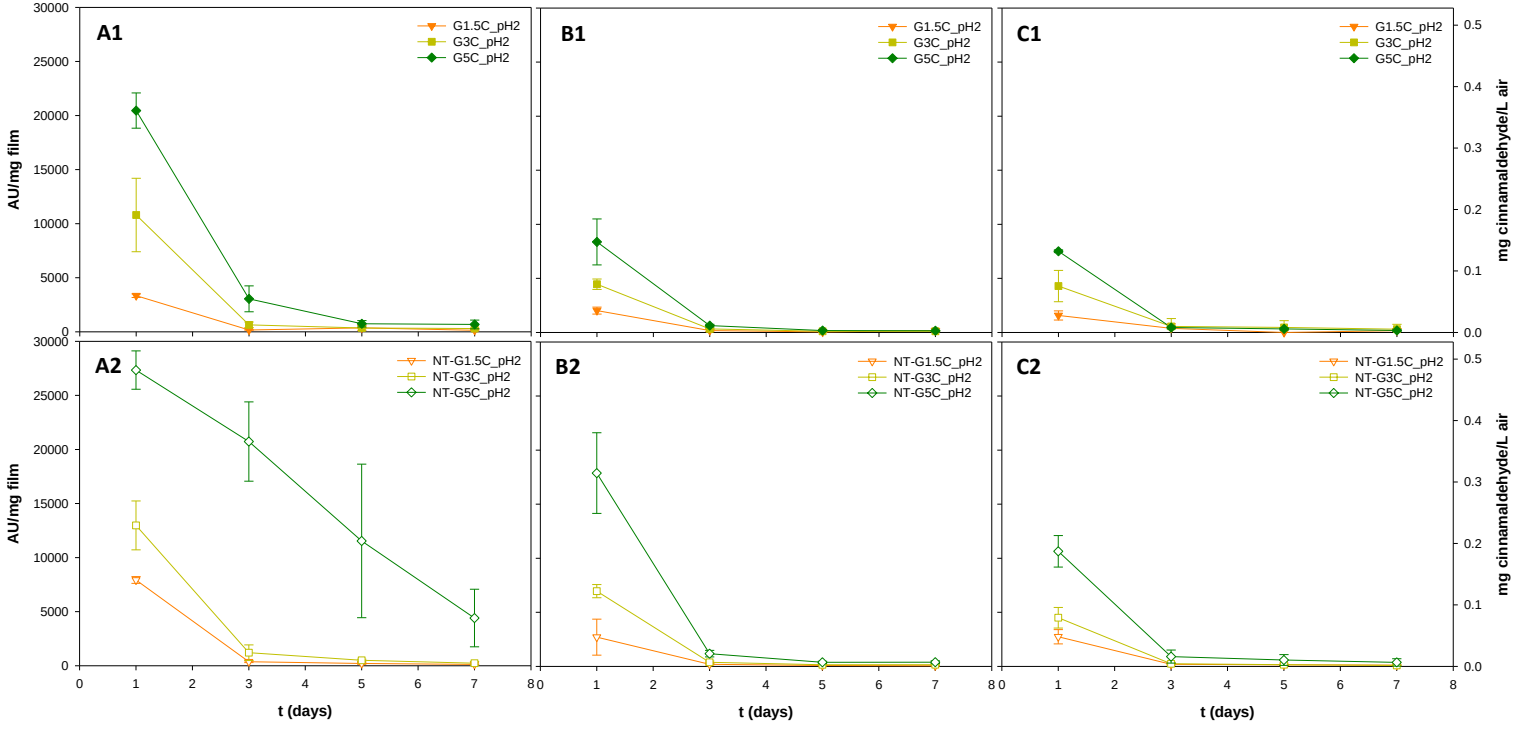

Figure 7.4. Cinnamaldehyde level evolution in the head-space of the bio-assay systems containing: *Penicillium* species **(A)**, *Alternaria solani* **(B)**, and *Colletotrichum acutatum* **(C)** during exposure to antifungal films containing cinnamaldehyde **(1)**, and cinnamaldehyde and natamycin **(2)** over a 7-day storage period at 23 °C. The left axis represents the chromatographic area units per mg of film. The right axis shows the concentration of cinnamaldehyde in the air of the head-space (relative error 11.72%).

7.3.2.3. Metabolic products from cinnamaldehyde produced by *C. acutatum*

Metabolic products from cinnamaldehyde produced by *C. acutatum* were determined. *C. acutatum* broke cinnamaldehyde down into two volatile metabolites which were detected and identified by GC/MS. **Figure 7.5A** shows the total ion current chromatograph (TIC) of the head-space in the jars after 1 day of *C. acutatum* exposure to cinnamaldehyde. Only one peak was detected. However, two new peaks were detected in the head-space of the jars after 5 days of *C. acutatum* exposure to cinnamaldehyde (**Figure 7.5B**). The first peak is carbon dioxide as identified by the GC/MS library. This is a result of microorganism respiration as well as by-product production resulting from the breakdown of cinnamaldehyde. The second and third peaks were identified as styrene and cinnamaldehyde, respectively, by the GC/MS library. The selected masses of both cinnamaldehyde (mass 131) and styrene (mass 104) were used to confirm that the compounds identified by the GC/MS library were cinnamaldehyde and styrene (**Figure 7.6**). These results are in agreement with the GC/FID results (**Figure 7.5C**) which show the same peaks belonging to both cinnamaldehyde and styrene. The peak corresponding to carbon dioxide was not present in the GC/FID chromatogram (**Figure 7.5C**) as flame ionization detectors are not able to detect carbon dioxide. The peak corresponding to styrene was switched to the right due to the different chromatography conditions used. Currently there is no information in the literature on *C. acutatum* being able to convert cinnamaldehyde into styrene. However, the conversion of cinnamaldehyde to styrene has been reported for *Penicillium* species and some yeasts (Adda et al., 1989). A possible mechanism for this reaction has been discussed which involves the conversion of cinnamaldehyde to styrene by a yeast mutant (Chen and Peppler, 1956). In the initial step of the mechanism, cinnamaldehyde dehydrogenase converts cinnamaldehyde to cinnamic acid, and then a decarboxylase reaction converts cinnamic acid to styrene with carbon dioxide as a by-product. A species of *Trichoderma* has also been reported to convert cinnamaldehyde into styrene as well as 1,3-pentadiene (Pinches and Apps, 2007). Due to the detection and identification of the volatile compounds cinnamaldehyde, styrene, and carbon dioxide by GC/MS, it is speculated that *C. acutatum* also has the ability to breakdown cinnamaldehyde and produce styrene as a metabolite.

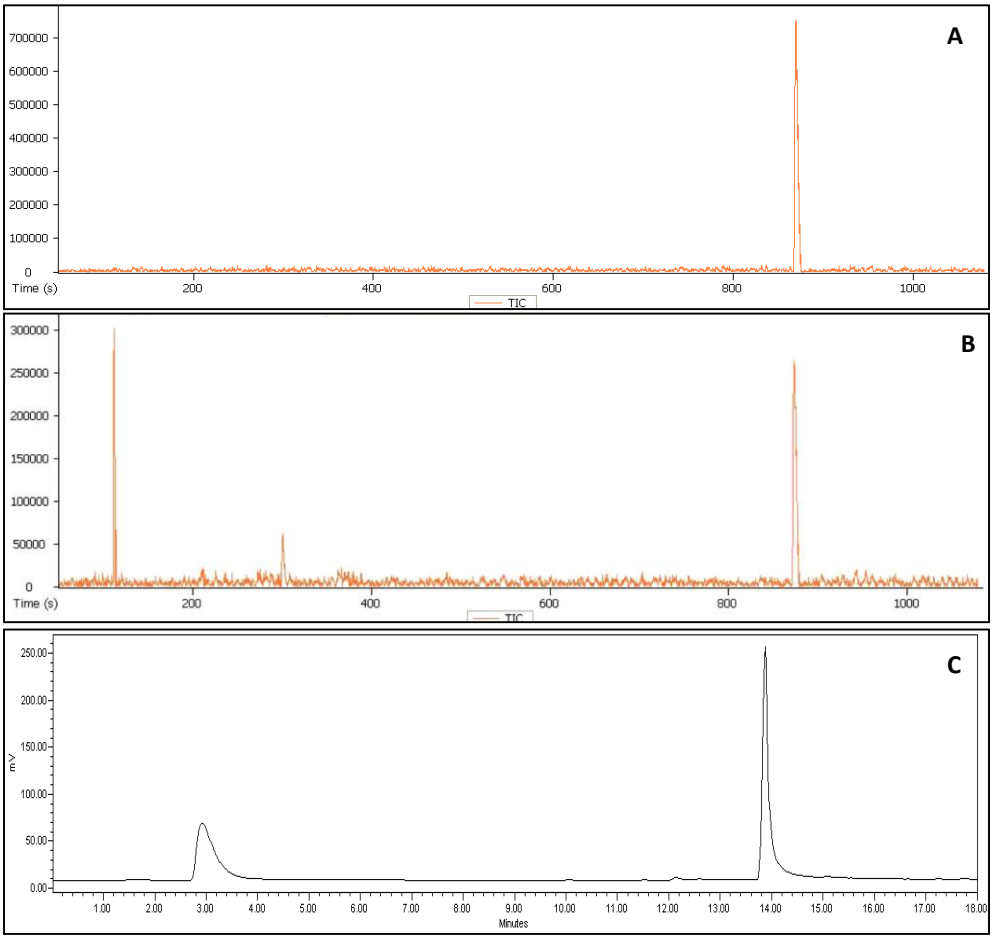

Figure 7.5. Total ion current chromatogram of TOFMS after 1 (A), and 5 (B) days post cinnamaldehyde injection, and GC/FID chromatogram after 5 days post cinnamaldehyde injection (C).

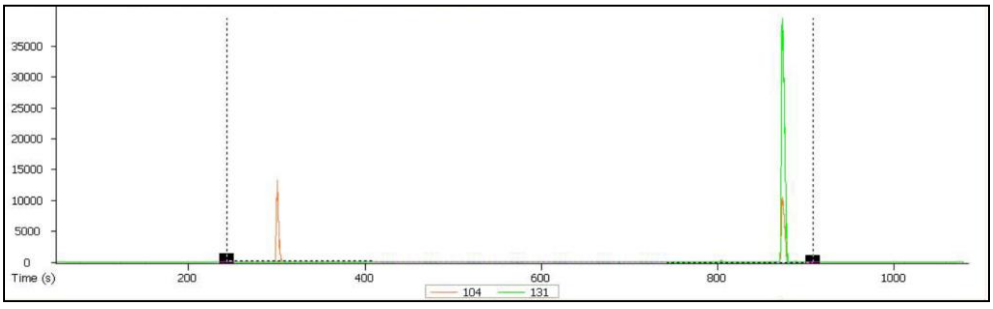

Figure 7.6. Mass spectrometer profile with selected masses: mass 131 indicates cinnamaldehyde and mass 104 indicates styrene.

7.3.3. Antifungal effect of gliadin films containing cinnamaldehyde and natamycin in cheese

Soft and semi-hard cheeses employed in the present work were characterized in terms of their water activity and pH and the results are shown in **Table 7.4**. Both the pH and the water activity were lower for the semi-hard cheese ($p \leq 0.05$) than for the soft cheese. Both pH and water activity are factors that affect microbial growth during storage (Pitt and Hocking, 2009). Additionally, the water activity is expected to trigger the release of the antimicrobial compound present in the films, since gliadin films are hydrophilic materials whose mass transport properties are highly influenced by environmental moisture (Balaguer et al., 2013a).

Table 7.4. Water activity and pH values of cheeses employed.

Type of cheese	Water activity	pH
Soft cheese	0.962 ± 0.002[b]	5.83 ±0.03[b]
Semi-hard cheese	0.947 ± 0.001[a]	5.60 ± 0.11[a]

Values reported are means ± standard deviations (n = 3)
[a-b] Different letters in the same column indicate significant differences ($p \leq 0.05$) between samples.

The antifungal activity of films G5C_pH2 and NT-G5C_pH2 over the inoculated soft and semi-hard cheese is shown in **Figure 7.7**. *Penicillium* spp. was able to grow in both kinds of cheese (**Figure 7.7A** and **7.7D**). For the soft cheese, fungal growth was totally inhibited at the film/cheese interface, and partially inhibited on the rest of the plate, but inhibition halos were not observed (**Figure 7.7B** and **7.7C**). On the contrary, for semi-hard cheese the inhibition was limited only to the film/cheese interface (**Figure 7.7E** and **7.7F**). Regarding the effect of natamycin, no differences were observed between G5C_pH2 and NT-G5C_pH2 films irrespective of the type of cheese. This indicates that under experimental conditions natamycin did not exert an additional antifungal effect. The differences observed between both types of cheese may be attributed to the different water activity, as the antimicrobial effectiveness of edible films made of biopolymers such as gliadins is highly dependent on the presence of water. It is well known that water molecules act as plasticizers, thus causing an increase of free volume of the film matrix which favors the release of the active substances incorporated (Balaguer et al., 2013a). In the case of semi-hard cheese, the lower water activity may produce a lower cinnamaldehyde release; therefore limiting the inhibition to the film/cheese interface. So from these results,

together with those of water activity, it can be stated that the higher the water activity of the cheese, the higher the fungal inhibition when exposed to the present films.

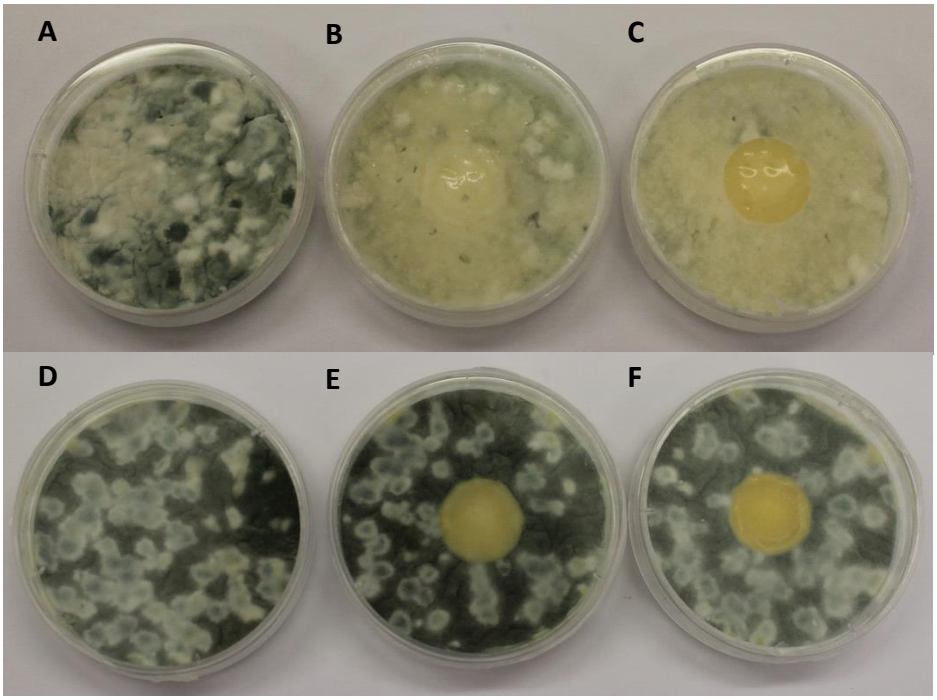

Figure 7.7. Antifungal activity over inoculated soft sliced cheese **(A, B, C)** and inoculated semi-hard cheese **(D, E, F)** of G5C_pH2 **(B, E)** and NT-G5C_pH2 **(C, F)** films. **A** and **D** are controls without film. Photographs were taken after 7 days of storage at 20 °C.

A second experiment was conducted in order to elucidate whether the antifungal effect observed was fungicidal or fungistatic. In this case the cheeses were not inoculated because in a previous experiment the growth of naturally present molds was observed, presumable belonging to *Penicillium* genus. Naturally present microorganisms are generally assumed to be more resistant to antimicrobials, so that this approach would be more reliable. No mold growth was observed on cheese when it was completely covered either with G5C_pH2 or NT-G5C_pH2 film after 14 days of storage at 20 °C, whereas uncovered cheese clearly showed fungal growth (**Figure 7.8**). When films were removed, fungal growth was observed both after cheese incubation at 30 °C on PDA plate and after cheese storage at 20 °C, without differences between films. This indicates that the antimicrobial effect of the films was fungistatic, regardless of the presence of natamycin.

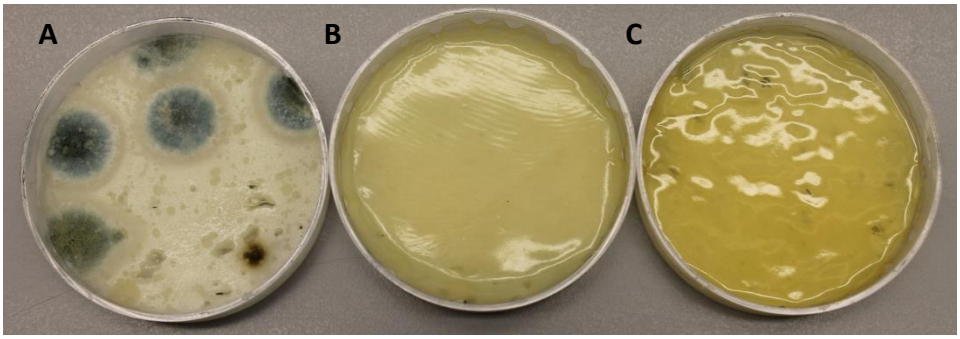

Figure 7.8. Antifungal activity over semi-hard cheese covered with G5C_pH2 film **(B)** and NT-G5C_pH2 film **(C)**. **A** is a control without film. Photographs were taken after 14 days of storage at 20 °C.

There are many reports showing the efficacy of natamycin release systems for cheese preservation. Pintado et al. (2010) inhibited *Penicillium* spp. *in vitro* with a film of whey protein isolate incorporating natamycin. Similar results were found by Pires et al. (2008), who evaluated the *in vitro* antimicrobial effect of a cellulose-based film incorporating natamycin over *Penicillium* spp. and *Geotrichum* spp.. Additionally, these authors applied the developed films to the preservation of Mozzarella slices and they found a reduction of the counts of yeasts and molds of 2 log units, achieving a shelf-life extension of 6 days, compared to the control sample. Ture et al. (2011) evaluated the antimicrobial effect of natamycin added to methyl cellulose and wheat gluten films over *Penicillium roqueforti* and *A. niger*, which were inoculated on the surface of fresh kashar cheese. The authors found a 2 log reduction for *A. niger*, however, *P. roqueforti* was not inhibited, in spite of being sensitive to the film when tested *in vitro* (Ture et al., 2008). The difference between *in vitro* and in food tests was attributed by the authors to the better growth of *Penicillium* in the cheese than in the agar media. Similar inhibitory effects of molds on kashar cheese caused by natamycin released from a film were found by Var et al. (2006), as well as over other cheeses such as Gouda, Edam, Saloio, Blatacke zlato and Gorgonzola (de Oliveira et al., 2007; Fajardo et al., 2010; Hanusova et al., 2010; Reps et al., 2002). The aforementioned studies dealt with soft, semi-soft or semi-hard cheeses, but we were unable to find in the literature any report on the antifungal effects of films incorporated with natamycin on hard cheeses. This is probably because such hydrophilic release systems need the presence of water to trigger the release of the active compounds incorporated.

7.4. CONCLUSION

Gliadin films chemically-treated with cinnamaldehyde and incorporating 0.5% natamycin maintained their integrity in water and were good barriers against oxygen permeation. The different cross-linking degrees achieved by cinnamaldehyde treatment were able to modify the amount of natamycin migrated. The combination of cinnamaldehyde and natamycin gave rise to antifungal bioplastic films against common food spoilage microorganisms both in vitro and in a real foodstuff. This work highlights the effectiveness of these environmentally-friendly films for its use in active food packaging.

7.5. REFERENCES

Adda, J., Dekimpe, J., Vassal, L., and Spinnler, H. E. 1989. Production de styrène par penicillium camemberti thom. *Lait, 69*(2), 115-120.

Akiyama, S. I., Tabuki, T., Kaneko, M., Komiyama, S., and Kuwano, M. 1980. Classification of polyene antibiotics according to their synergistic effect in combination with bleomycin A2 or fusidic acid. *Antimicrobial Agents and Chemotherapy, 18*(2), 226-230.

Almenar, E., Auras, R., Wharton, P., Rubino, M., and Harte, B. 2007. Release of acetaldehyde from beta-cyclodextrins inhibits postharvest decay fungi in vitro. *Journal of Agricultural and Food Chemistry, 55*(17), 7205-7212.

Arroyo-Lopez, F. N., Bautista-Gallego, J., Romero-Gil, V., Rodriguez-Gomez, F., and Garrido-Fernandez, A. 2012. Growth/no growth interfaces of table olive related yeasts for natamycin, citric acid and sodium chloride. *International Journal of Food Microbiology, 155*(3), 257-262.

ASTM. 2005. D3985. Standard test method for oxygen gas transmission rate through plastic film and sheeting using coulometric sensor.

ASTM. 2006. F1249. Standard test method for water vapor transmission rate through plastic film and sheeting using a modulated infrared sensor.

Balaguer, M. P., Borne, M., Chalier, P., Gontard, N., Morel, M. H., Peyron, S., Gavara, R., and Hernandez-Munoz, P. 2013a. Retention and release of cinnamaldehyde from wheat protein matrices. *Biomacromolecules, 14*(5), 1493-1502.

Balaguer, M. P., Cerisuelo, J. P., Gavara, R., and Hernandez-Muñoz, P. 2013b. Mass transport properties of gliadin films: Effect of cross-linking degree, relative humidity, and temperature. *Journal of Membrane Science, 428*, 380-392.

Balaguer, M. P., Gomez-Estaca, J., Gavara, R., and Hernandez-Munoz, P. 2011a. Biochemical properties of bioplastics made from wheat gliadins cross-linked with cinnamaldehyde. *Journal of Agricultural and Food Chemistry, 59*(24), 13212-13220.

Balaguer, M. P., Gomez-Estaca, J., Gavara, R., and Hernandez-Munoz, P. 2011b. Functional properties of bioplastics made from wheat gliadins modified with cinnamaldehyde. *Journal of Agricultural and Food Chemistry, 59*(12), 6689-6695.

Brik, H. 1976. New high-molecular decomposition products of natamycin (pimaricin) with intact lactone-ring. *The Journal of antibiotics, 29*(6), 632-637.

Burt, S. 2004. Essential oils: Their antibacterial properties and potential applications in foods - a review. *International Journal of Food Microbiology, 94*(3), 223-253.

Ce, N., Norena, C. P. Z., and Brandelli, A. 2012. Antimicrobial activity of chitosan films containing nisin, peptide p34, and natamycin. *Cyta-Journal of Food, 10*(1), 21-26.

Cha, D. S., and Chinnan, M. S. 2004. Biopolymer-based antimicrobial packaging: A review. *Critical Reviews in Food Science and Nutrition, 44*(4), 223-237.

Chen, S. L., and Peppler, H. J. 1956. Conversion of cinnamaldehyde to styrene by a yeast mutant. *Journal of Biological Chemistry, 221*(1), 101-106.

da Silva, M. A., Krause Bierhalz, A. C., and Kieckbusch, T. G. 2012. Modelling natamycin release from alginate/chitosan active films. *International Journal of Food Science and Technology, 47*(4), 740-746.

de Oliveira, T. M., de Fátima Ferreira Soares, N., Pereira, R. M., and de Freitas Fraga, K. 2007. Development and evaluation of antimicrobial natamycin-incorporated film in Gorgonzola cheese conservation. *Packaging Technology and Science, 20*(2), 147-153.

del Nobile, M. A., Lucera, A., Costa, C., and Conte, A. 2012. Food applications of natural antimicrobial compounds. *Frontiers in Microbiology, 3*.

Delves-Broughton, J., Thomas, L. V., Doan, C. H., and Davidson, P. M. 2005. Natamycin. In *Antimicrobials in Food, third edition*, CRC Press, Boca Raton, FL, USA: 275-289.

dos Santos Pires, A. C., Ferreira Soares, N. d. F., de Andrade, N. J., Mendes do Silva, L. H., Camilloto, G. P., and Bernardes, P. C. 2008. Development and evaluation of active

packaging for sliced Mozzarella preservation. *Packaging Technology and Science, 21*(7), 375-383.

Fajardo, P., Martins, J. T., Fucinos, C., Pastrana, L., Teixeira, J. A., and Vicente, A. A. 2010. Evaluation of a chitosan-based edible film as carrier of natamycin to improve the storability of Saloio cheese. *Journal of Food Engineering, 101*(4), 349-356.

Fucinos, C., Guerra, N. P., Teijon, J. M., Pastrana, L. M., Rua, M. L., and Katime, I. 2012. Use of poly(N-isopropylacrylamide) nanohydrogels for the controlled release of pimaricin in active packaging. *Journal of Food Science, 77*(7), N21-N28.

Hanusova, K., Stastna, M., Votavova, L., Klaudisova, K., Dobias, J., Voldrich, M., and Marek, M. 2010. Polymer films releasing nisin and/or natamycin from polyvinyldichloride lacquer coating: Nisin and natamycin migration, efficiency in cheese packaging. *Journal of Food Engineering, 99*(4), 491-496.

Hernandez-Munoz, P., Kanavouras, A., Ng, P. K. W., and Gavara, R. 2003. Development and characterization of biodegradable films made from wheat gluten protein fractions. *Journal of Agricultural and Food Chemistry, 51*(26), 7647-7654.

Krause Bierhalz, A. C., da Silva, M. A., and Kieckbusch, T. G. 2012. Natamycin release from alginate/pectin films for food packaging applications. *Journal of Food Engineering, 110*(1), 18-25.

Mann, D. A., and Beuchat, L. R. 2008. Combinations of antimycotics to inhibit the growth of molds capable of producing 1,3-pentadiene. *Food Microbiology, 25*(1), 144-153.

Pinches, S. E., and Apps, P. 2007. Production in food of 1,3-pentadiene and styrene by *Trichoderma* species. *Int J Food Microbiol, 116*(1), 182-185.

Pintado, C. M. B. S., Ferreira, M. A. S. S., and Sousa, I. 2010. Control of pathogenic and spoilage microorganisms from cheese surface by whey protein films containing malic acid, nisin and natamycin. *Food Control, 21*(3), 240-246.

Pitt, J. I., and Hocking, A. D., 2009. *Fungi and food spoilage*. Third ed.; Springer: New York.

Raab, W., 1972. *Natamycin (pimaricin): Its properties and possibilities in medicine*. Georg Thieme Publishers,: Stuttgart, Germany.

Ramos, O. L., Silva, S. I., Soares, J. C., Fernandes, J. C., Fatima Pocas, M., Pintado, M. E., and Xavier Malcata, F. 2012. Features and performance of edible films, obtained from whey protein isolate formulated with antimicrobial compounds. *Food Research International, 45*(1), 351-361.

Reps, A., Drychowski, L. J., Tomasik, J., and Winiewska, K. 2002. Natamycin in ripening cheeses. *Pakistan Journal of Nutrition, 1*(5), 243-247.

Tajkarimi, M. M., Ibrahim, S. A., and Cliver, D. O. 2010. Antimicrobial herb and spice compounds in food. *Food Control, 21*(9), 1199-1218.

Ture, H., Eroglu, E., Oezen, B., and Soyer, F. 2009. Physical properties of biopolymers containing natamycin and rosemary extract. *International Journal of Food Science and Technology, 44*(2), 402-408.

Ture, H., Eroglu, E., Ozen, B., and Soyer, F. 2011. Effect of biopolymers containing natamycin against *Aspergillus niger* and *Penicillium roquefortii* on fresh Kashar cheese. *International Journal of Food Science and Technology, 46*(1), 154-160.

Ture, H., Eroglu, E., Soyer, F., and Ozen, B. 2008. Antifungal activity of biopolymers containing natamycin and rosemary extract against *Aspergillus niger* and *Penicillium roquefortii*. *International Journal of Food Science and Technology, 43*(11), 2026-2032.

Var, I., Erginkaya, Z., Güven, M., and Kabak, B. 2006. Effects of antifungal agent and packaging material on microflora of Kashar cheese during storage period. *Food Control, 17*(2), 132-136.

CHAPTER 8

CHEMICALLY MODIFIED GLIADINS AS SUSTAINED RELEASE SYSTEMS FOR LYSOZYME

Fajardo, P.; Balaguer, M.P.; Gomez-Estaca, J.; Gavara, R.; and Hernandez-Munoz, P.

Food Hydrocolloids, 2014, 41, 53-59

The aim of this work has been to study the effectiveness of gliadin films cross-linked with cinnamaldehyde as systems for the release of the natural antimicrobial compound lysozyme. Prior to the incorporation of lysozyme, the gliadin film-forming solution was treated with different percentages of cinnamaldehyde as cross-linker, and glycerol was added as plasticizer. The effect of the concentration of the cross-linker on the swelling capacity and kinetics of release of the antimicrobial agent from the protein matrix was evaluated at pH 6.2. The antimicrobial activity of the films was assayed against Listeria innocua. The gliadin films cross-linked with cinnamaldehyde incorporating lysozyme preserved their integrity in water. The release rate of the antimicrobial agent was controlled by the reticulation of the protein matrix, thus a greater degree of cross-linking led to slower release of the active agent. Films with a loosely cross-linked structure released a greater amount of lysozyme, exhibiting greater antimicrobial activity.

8.1. INTRODUCTION

Consumers demand for safe, high-quality food products has led to growing interest in the development of active antimicrobial packaging systems. Active packaging can be defined as a type of packaging in which the package, the product, and the environment interact to prolong shelf-life or ensure safety or sensory properties, while maintaining the quality of the product (Suppakul et al., 2003). The antimicrobial agent can be included in sachets or labels that form part of the packaging system, or they may be included in the package walls, the latter being the more promising development. The amount of active substance released to the packaged product is crucial and must be determined, because high concentrations of a released compound in food could cause sensorial or toxicological problems, whereas low concentrations would not be effective (Conte et al., 2006). In this connection, a considerable effort is being made to develop sustained active compound release systems for many applications (Buonocore et al., 2004; Chen et al., 2006; Gemili et al., 2009; Mastromatteo et al., 2010). Thanks to sustained release systems, it is expected that a minimum inhibitory concentration of the antimicrobial agent will be maintained at the food surface longer than if an equivalent amount of antimicrobial was directly spread or sprayed on the food surface (Min et al., 2008). Films made from hydrophilic polymers swell in the presence of water which gives rise to the relaxation of polymer matrix favoring the diffusion of the antimicrobial agent to the release medium. A possible way to modulate the release of antimicrobials incorporated into hydrophilic films that has shown good results consists on increasing the cross-linking density of the polymer network and subsequent slow release of the active agent due to a decrease in water swelling (Buonocore et al., 2004). Gluten is a noteworthy biomaterial for a wide range of technological applications, also as food packaging material (Cornell and Hoveling, 1998). However, gluten is insoluble in water and poorly soluble in ethanol.

Gluten proteins are mainly composed of glutenins, a high molecular weight fraction that tend to form large aggregates hindering gluten processability, and gliadins, a family of low molecular weight proteins. Previous studies of gluten proteins have shown that gliadins and glutenins can be exploited separately in order to maximize their range of industrial uses (Hernandez-Munoz et al., 2003). According to this, gliadins, which can be extracted with ethanol solutions (60-70%) in which they are highly stable and present excellent film-forming properties (Balaguer et al., 2011b), represent a more suitable fraction for processing. Gliadin

films are very glossy and transparent but have poor mechanical resistance and lose their integrity upon immersion in water (Hernandez-Munoz et al., 2003). Various physical, enzymatic, and chemical treatments can be applied in order to improve their properties owing to the susceptibility to modification of the diverse reactive sites groups present in amino acids (Krochta, 2002). Cinnamaldehyde has recently been shown as a good alternative to other toxic cross-linkers, such as formaldehyde, glutaraldehyde and glyoxal, to improve the physico-chemical performance of gliadin films (Balaguer et al., 2013b; Balaguer et al., 2011a, 2011b).

Gliadins appear to be highly promising proteins for the development of matrices with a very interesting controlled release potency of diverse molecules (Arangoa et al., 2001; Balaguer et al., 2014; Duclairoir et al., 1999; Duclairoir et al., 2002; Ezpeleta et al., 1996; Gulfam et al., 2012; Kajal and Misra, 2011; Ramteke and Jain, 2008; Stella et al., 1995; Zhou, 2008a, 2008b).

Lysozyme (LZ) is a naturally occurring enzyme present in several foods which has specific hydrolytic activity against bacterial cell walls, and it is not toxic to humans (Losso et al., 2000). Lysozyme is biocidal against Gram-positive bacteria by hydrolyzing the β-1,4 linkage between N-acetylmuramic acid and N-acetyl-glucosamine in the peptidoglycan of the cell wall. Consequently, Gram-negative bacteria are not sensitive to lysozyme because their cell walls are poor or lacking in peptidoglycan. Various synthetic or natural polymeric structures have been tested as lysozyme carriers: polyvinyl alcohol beads, nylon pellets, and cellulose triacetate films (Appendini, 1997); polyvinyl alcohol films (Conte et al., 2006); plasma-treated polyethylene films (Conte et al., 2008); chitosan (Duan et al., 2007; Park et al., 2004); cellulose and polyacrylamide (Datta et al., 1973); whey protein isolate films (Min et al., 2008); alginate and carrageenan (Cha et al., 2002); sodium caseinate (Mendes de Souza et al., 2010); soy protein (Padgett et al., 1998); and corn zein (Mecitoglu et al., 2006; Padgett et al., 1998). To the best of our knowledge, there is no previous report on the use of gluten or gliadin films as lysozyme carriers.

The objective of the present work was to characterize the release kinetics of lysozyme from gliadin films cross-linked with cinnamaldehyde as a function of the degree of cross-linking achieved, as well as to evaluate their antimicrobial activity against *Listeria innocua*. The effect of lysozyme incorporation on both the mechanical and barrier properties (water vapor and oxygen) of the films was also evaluated.

8.2. MATERIALS AND METHODS

8.2.1. Reagents and bacterial strains

Crude wheat gluten, glycerol, trans-cinnamaldehyde 99%, and lysozyme from chicken egg white were obtained from Sigma (Sigma-Aldrich Química, S.A., Madrid, Spain). Tryptic soy agar (TSA) and Tryptic soy broth (TSB) were purchased from Scharlau (Scharlab S.L., Barcelona, Spain).

L. innocua CECT 910 T was obtained from the Spanish Type Culture Collection (Valencia, Spain) and it was used for testing the antimicrobial activity of lysozyme-gliadin films. Lyophilized *Micrococcus lysodeikticus* ATCC 4698 used for lysozyme release measurement was purchased from Sigma (Sigma-Aldrich Química, S.A., Madrid, Spain).

8.2.2. Extraction of gliadin-rich fraction

The extraction of the gliadin-rich fraction was carried out according to the method of Hernandez-Munoz et al. (2003). Briefly, 100 g of crude wheat gluten was dispersed in 400 mL of 70% (v/v) ethanol/water, stirred overnight at room temperature, and centrifuged at 5000 rpm for 20 min at 20 °C. The resulting supernatant, containing the gliadin-rich fraction, 15% of protein (w/v), was collected and used as the gliadin film-forming solution.

8.2.3. Chemical modification of gliadins

In preliminary studies, the use of cinnamaldehyde as a protein cross-linker was found to be strongly dependent on the pH (Balaguer et al., 2013a; Balaguer et al., 2011a, 2011b). Initially, the pH of the gliadin film forming solution was brought to 2.0 with HCl as the most suitable for polymerization. Then, chemical modification of gliadins was conducted by adding different concentrations of cinnamaldehyde to the film-forming solution, namely 1.5% (G1.5C_pH2), 3% (G3C_pH2) and 5% (G5C_pH2) (g cinnamaldehyde/100 g protein). Glycerol was added as plasticizer at 25% (g glycerol/100 g protein). For films incorporating lysozyme (LZ-GXC_pH2), 10% (g lysozyme/100 g protein) was added. Lysozyme was dissolved into sterile deionized water (15% w/v) using gentle vortexing to obtain a clear colorless solution, and later transferred into the pH-adjusted film-forming solution, maintaining the percentage of ethanol in the film forming solution above 60% to avoid the precipitation of gliadins. The mixture with all the reagents was stirred at room temperature for 30 min.

8.2.4. Film formation and conditioning

The film-forming solutions were poured onto horizontal flat trays to allow water and ethanol to evaporate. To standardize the concentration of gliadin in the films, a density of 0.01 g of gliadin/cm^2 was used in all cases. The films were dried at 37 ± 2 °C for 24 h. The dried films were peeled off the casting surface and preconditioned in a chamber at 23 ± 2 °C and 53 ± 2% RH for at least 18 h.

Film thickness was measured using a micrometer (Mitutoyo, Kanagawa, Japan) with a sensitivity of ± 2 µm. The average film thickness was measured randomly at eight different locations on each film sample.

8.2.5. Swelling, weight loss, and dimensional stability of antimicrobial gliadin films after immersion in water

Films were cut into circles with a diameter of 2.5 cm ($\emptyset^i$) and conditioned for 10 days in a desiccator containing phosphorus pentoxide (0% RH and 23 °C). Pre-weighed (w^i_{dry}) dry film samples were immersed in beakers containing 10 mL of 0.1M phosphate buffer at pH 6.2 and 23 °C. At each sampling time films were removed from the buffer, blotted with a Whatman paper and weighed again (w^f_{wet}). The films were placed back into the desiccator until they reached a constant weight, which was used as the final dry weight (w^f_{dry}) of the film. The degree of swelling (S) was evaluated using the following equation:

$$S(\%) = \frac{w^f_{wet} - w^f_{dry}}{w^f_{dry}} \cdot 100 \qquad (\mathbf{8.1})$$

The diameter of the wet samples ($\emptyset^f$) was measured with a digital caliper to calculate the diameter increase percentage ($\Delta\emptyset$) as a measure of dimensional stability using the following equation:

$$\Delta\emptyset\ (\%) = \frac{\emptyset^f - \emptyset^i}{\emptyset^i} \cdot 100 \qquad (\mathbf{8.2})$$

The weight loss percentage (WL) of each film sample was calculated using the following equation:

$$\text{WL}(\%) = \frac{w_{dry}^{i} - w_{dry}^{f}}{w_{dry}^{i}} \cdot 100 \qquad (\mathbf{8.3})$$

Tests for each type of film were repeated three times.

8.2.6. Release of lysozyme from antimicrobial gliadin films

Films were cut into circles with a diameter of 2.5 cm. The diffusion was carried out in a beaker with a stainless steel net inside covering the bottom of the beaker (6.5 cm) and protecting the antimicrobial film from a magnetic bar used for stirring the medium. Twenty pieces of film (weighing approximately 1.4 g) were immersed in 100 mL of 0.1 M phosphate buffer (pH 6.2) at 20 °C. In order to follow the release kinetic of lysozyme from the film, aliquots of 500 µL were withdrawn from the dissolution medium at various time intervals.

Lysozyme activity in the medium was determined by the method of Shugar (1952), following the lysis of *M. lysodeikticus* for 5 min at 450 nm at 25 °C. The cells of *M. lysodeikticus* were suspended (0.015% w/v) in 66 mM phosphate buffer at pH 6.2. The slope of the initial decrease in turbidity was used to quantify the enzymatic activity. One unit of enzyme produced a ΔA at 450 nm of 0.001 per minute at pH 6.2 and 25 °C. The amount of lysozyme released was then reported as units of lysozyme released per cm^2 of film.

8.2.7. Antimicrobial properties of gliadin films

To keep the same proportion as in the release assay, two pieces of antimicrobial film were immersed in 10 mL of TSB buffered at pH 6.2 with 0.1 M phosphate buffer. The medium was inoculated with 100 µL of an overnight culture of *L. innocua* and incubated at 20 °C for 32 hours. Total viable counts were determined by a pour plate method using TSA after serial 10-fold dilution in 0.1% peptone water at 8, 24, and 32 hours and plates were incubated at 37 °C for 24 h. The same procedure was carried out with films without lysozyme (control films). Moreover, control films were incubated in TSB without inoculation with *L. innocua* to check possible contamination of the films. The results were expressed as the logarithmic reduction of colony forming units per mL (CFU/mL) of the gliadin films containing lysozyme with respect to the control gliadin films.

8.2.8. Mechanical properties

A Mecmesin MultiTest 1-í (Landes Poli Ibérica S.L., Barcelona) equipped with a 250 N static load cell was used to evaluate the maximum tensile strength (σ_m), percentage of elongation at break (ε_b), and Young's Modulus (E) of the films according to ASTM standard method D882 (ASTM, 2009). The films were conditioned at 53 ± 2% RH and 23 ± 2 °C for one week in a desiccator containing a saturated salt solution of magnesium nitrate ($Mg(NO_3)_2 \cdot 6H_2O$). Film samples were cut into strips 2.54 cm wide and 8 cm long. The grip separation was set at 5 cm and the cross-head speed at 25 mm/min. At least 10 samples of each type of film were evaluated. The tensile properties were calculated from the plot of stress (tensile force/initial cross-section area) versus strain (elongation as a fraction of the original length).

8.2.9. Water vapor permeability

Water vapor permeability (WVP) tests were carried out at 23 °C and a RH gradient of 0-53% using permeability cups (Elcometer, Manchester, UK) according to ISO 2528-95 (ISO, 1995). Samples were conditioned before testing at 53 ± 2% RH and 23 ± 2 °C. Aluminum cups were filled with silica gel and sealed with vacuum silicon grease (Sigma-Aldrich Química, S.A., Madrid, Spain) and the film to be tested. The film was fixed with a flat Viton ring, an aluminum ring, and three press-screws. The cups containing silica gel were then stored in a desiccator containing a saturated salt solution of magnesium nitrate ($Mg(NO_3)_2 \cdot 6H_2O$) to ensure the required RH. The cups were weighed daily using an electronic balance to record moisture gain, and the slope of weight increment versus time at steady state provided water vapor transmission rate (WVTR) [g/(m^2·s)]. All the samples were measured in quadruplicate. The water vapor permeability coefficient in (kg·m)/(m^2·s·Pa) can be calculated from the transmission rate values measured as follows:

$$P = \frac{Q \cdot l}{A \cdot t \cdot \Delta p} \qquad (\mathbf{8.4})$$

where Q is the amount of permeant (kg) passing through a film of thickness l (m) and area A (m^2), t is time (s), and Δp is the partial pressure differential across the film (Pa). Δp is calculated from the water vapor partial pressure at the temperature selected and the RH gradients.

8.2.10.Oxygen permeability

Oxygen transmission rate (OTR) [$cm^3/(m^2 \cdot s)$] through the films was measured using an OX-TRAN Model 2/21 Mocon (Lippke, Neuwied, Germany). It operates according to ASTM D3985-05 (ASTM, 2005). Film samples were double-masked with aluminum foil masks, leaving a circular uncovered effective film area of 5 cm^2. Testing was performed at 23 °C and constant RH of 50%. At least four samples of each type of film produced were measured. The samples were conditioned in the cells for 24 h, then oxygen transmission rate values were determined every 45 min, until there were 10 replicates. Transmission rate values are reported as oxygen permeability coefficient in [$(m^3 \cdot m)/(m^2 \cdot s \cdot Pa)$], calculated as in **Equation 8.4**.

8.2.11.Statistical analysis

Comparisons between samples were analyzed using Student's *t*-test ($p \leq 0.05$). Model fits to experimental data and determination of lysozyme diffusion parameters were performed according to the least-squares method (quasi-Newton) provided by the macro 'Solver' of Microsoft Excel 2010.

8.3. RESULTS AND DISCUSSION

In previous studies the suitability of cinnamaldehyde as a natural cross-linker for improving the functional properties of gliadin films has been shown (Balaguer et al., 2011b). The cross-linking effect, which was proportional to the amount of cinnamaldehyde added, was evidenced by a great improvement in the mechanical strength of the films without impairment of their elongation properties, complete resistance after water immersion with negligible loss of weight attributable to protein and an increase in the glass transition temperature compared to the control films (Balaguer et al., 2011b). Sodium Dodecyl Sulfate – Polyacrylamide Gel Electrophoresis (SDS-PAGE) and Size Exclusion – High Performance Liquid Chromatography (SE-HPLC) were used to provide chemical evidence of the cross-linking of gliadins with cinnamaldehyde (Balaguer et al., 2013a; Balaguer et al., 2011a). Moreover, after evaluation of free amino groups, a combination of a Schiff base and a Michael addition between the amino groups of the protein and the cinnamaldehyde was

proposed as a feasible cross-linking mechanism, although the participation of other groups was not ruled out (Balaguer et al., 2011a).

8.3.1. Film formation

The gliadin film-forming solution at pH 2 was miscible with water-soluble lysozyme, providing a homogeneous dispersion. The resulting films were homogeneous to the naked eye and highly transparent, independently of the degree of cross-linking, with a uniform thickness of 112 ± 6 μm. No significant differences in film thickness were observed between different degrees of cross-linking ($p \leq 0.05$) or between gliadin and LZ-gliadin films ($p \leq 0.05$).

8.3.2. Swelling, dimensional stability, and weight loss of antimicrobial gliadin films after immersion in phosphate buffer

Values of swelling, diameter increase, and weight loss of the films after immersion in phosphate buffer are shown in **Figure 8.1**. Gliadin films without cinnamaldehyde lost their integrity when immersed in an aqueous medium for 24 h (Balaguer et al., 2011b), then only cross-linked films have been studied. The films swelled quickly and after 30 minutes no differences were observed between different incubation times. The percentages of swelling and diameter increase were significantly ($p \leq 0.05$) affected by the cross-linking degree of the matrix. The greater the concentration of cross-linker added, the lower the water uptake and diameter increase. The weight loss of cross-linked films was around 24% and this was slightly altered by cross-linker concentration. This loss of weight was mainly due to the diffusion of hydrophilic glycerol into the aqueous medium, which was confirmed by the lack of flexibility of the films after drying. The different behavior of the films after their immersion in a liquid medium could modify the percentage of active agent released from the protein matrix.

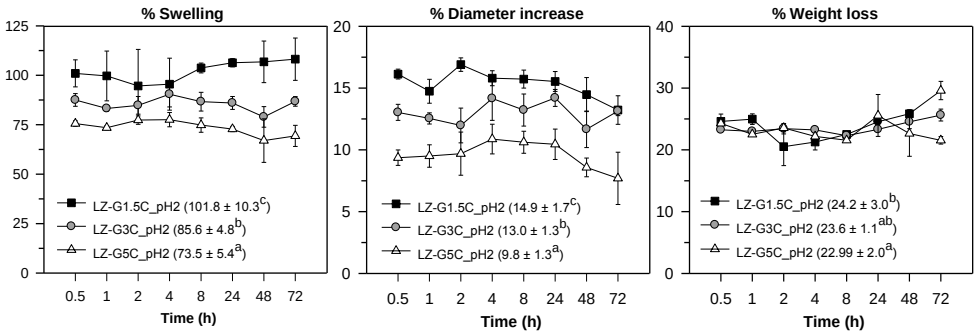

Figure 8.1. Swelling, dimensional stability, weight loss and of films cross-linked with different amounts of cinnamaldehyde containing lysozyme after immersion in pH 6.2 phosphate buffer at 23 °C. Values reported are the means ± standard deviations (n = 24, 3 replicates at 8 different times, 95% confidence interval). $^{a–c}$ Different lowercase letters in the figure indicate a statistically significant difference between films with different degree of cross-linking ($p \leq 0.05$).

8.3.3. Release of lysozyme from films cross-linked with cinnamaldehyde

A slow release of the antimicrobial agent is desired to keep optimal levels of the agent on the food surface over time; in addition, some immobilized antimicrobial activity is also beneficial to maintain film sterility during storage of foods. **Figure 8.2** shows the cumulative percentage of released lysozyme into pH 6.2 phosphate buffer medium at 20 °C. After 115 hours the maximum activity released for film LZ-G5C_pH2 reached 4554 units/cm^2 of film, which corresponds to 8% of the total lysozyme incorporated into the film.

Lysozyme can be retained in the film owing to interaction with protein matrix. Moreover, a loss of enzyme activity caused by the film forming process should not be considered since the films were dried at mild temperature conditions (37 °C for 24 h), and, although the enzyme was incorporated into the gliadin solution at pH 2, in a previous paper only a slight decrease in activity was reported when lysozyme was subjected to acidic pHs (Mendes de Souza et al., 2010).

Since film swelling is inversely proportional to the degree of cross-linking (Balaguer et al., 2011a), it was expected that those matrices treated with lower amounts of cinnamaldehyde, which present a looser structure, facilitated the release of the carried lysozyme due to a greater film matrix relaxation. As was expected, the maximum lysozyme released increased to 18% (10243 units/cm^2), and 48% (26887 units/cm^2) for the films LZ-G3C_pH2, and LZ-G1.5C_pH2, respectively (**Figure 8.2**).

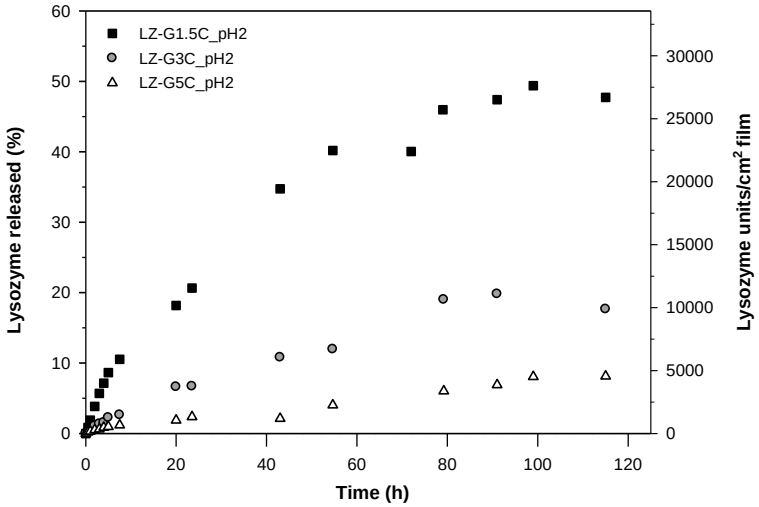

Figure 8.2. Release kinetics of lysozyme from gliadin films cross-linked with different amounts of cinnamaldehyde into pH 6.2 phosphate buffer at 20 °C.

The diffusion of the active agent in the film was modeled using Fick's second law:

$$\frac{\partial C}{\partial t} = D\frac{\partial^2 C}{\partial x^2} \qquad (\mathbf{8.5})$$

The initial and boundary conditions were based on the following hypothesis:

(1) The thickness of the film is l, with $-l/2 < x < +l/2$;

(2) The process is controlled by diffusion through the thickness of the film (no external resistance to mass transfer);

(3) The diffusivity is supposed to be constant and the initial concentration of the diffusing substance is uniform;

(4) The volume of liquid is larger than that of the film;

(5) Because of the convection in the liquid, the concentration of lysozyme is uniform in the liquid at any time ($C_{liquid,\infty}$).

$$t = 0 \qquad -\frac{l}{2} < x < +\frac{l}{2} \qquad C = C_0 \qquad (\mathbf{8.6})$$

$$t > 0 \qquad x = -\frac{l}{2}, +\frac{l}{2} \qquad C = C_{L,\infty} \qquad (\mathbf{8.7})$$

The solution of **Equation 8.4** under the above specified conditions was obtained by Crank (Crank, 1975). It describes the kinetics of a diffusing substance into the sheet of thickness l in contact with a liquid of infinite volume, and can be applied in order to calculate an apparent diffusion coefficient (D) (**Equation 8.8**). Two types of solutions to the differential equation have been described:

i) series of the error function, suitable for numerical solution at short times, i. e. in the early stages of the diffusion process $M_t/M_\infty < 0.5$:

$$\frac{M_t}{M_\infty} = 2\left(\frac{D \cdot t}{l^2}\right)^{\frac{1}{2}} \cdot \left\{\pi^{-\frac{1}{2}} + 2 \cdot \sum_{n=1}^{\infty} (-1)^n \cdot ierfc\ \frac{n \cdot l}{\sqrt{(D \cdot t)}}\right\} \quad (\mathbf{8.8})$$

$$ierfc\ x = \frac{1}{\pi^{\frac{1}{2}}} \cdot e^{-x^2} - x \cdot erfc\ x \qquad (\mathbf{8.9})$$

where M_t and M_∞ are the cumulative amounts of lysozyme (units/cm^2) released at time t, and at infinite time, respectively, and $erfc$ is the error-function complement.

ii) or trigonometric series that converge better for long times, i.e. when the diffusion process has progressed until later states $M_t/M_\infty > 0.5$:

$$\frac{M_t}{M_\infty} = 1 - \frac{8}{\pi^2} \sum_{n=0}^{\infty} \frac{1}{(2n+1)^2} exp\left[-\frac{(2n+1)^2 \pi^2}{l^2} Dt\right] \quad (\mathbf{8.10})$$

As can be observed in **Figure 8.2**, after 120 h the release of lysozyme from cross-linked films was less than 50% and thus error function was used to calculate diffusion parameters. **Figure 8.3** depicts the experimental and the predicted data by the Crank's solution for short times (**Equation 8.8**).

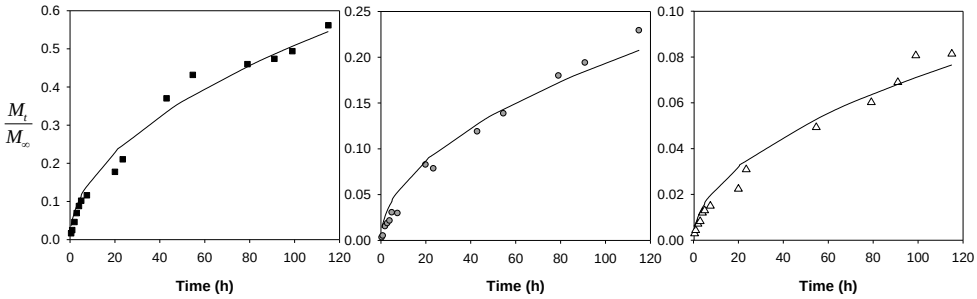

Figure 8.3. Experimental (symbols) and predicted (lines) data of lysozyme release kinetics from gliadin films cross-linked with cinnamaldehyde into pH 6.2 phosphate buffer at 20 °C. M_t/M_∞ is expressed in units of lysozyme released from the film at time t/units of lysozyme released at equilibrium.

The values obtained for the apparent diffusion coefficients calculated from **Equation 8.8** are shown in **Table 8.1**. The higher value obtained for the film LZ-G1.5C_pH2 revealed a faster diffusion of lysozyme in this film as a consequence of a less cross-linked structure. A statistically significant decrease ($p \leq 0.05$) in the value of D was observed as the percentage of cinnamaldehyde increased, without finding significant differences ($p > 0.05$) among films with the higher cross-linking degree LZ-G3C_pH2, and LZ-G5C_pH2. This result indicates that gliadin films cross-linked with cinnamaldehyde can be used to modulate the release of lysozyme. This behavior was also observed in gelatin films cross-linked with genipin as lysozyme carrier (Ma et al., 2013) and confirms the applicability of naturally-occurring cross-linking agents to develop sustained active-compound-release systems for food packaging, as an alternative to other toxic cross-linkers used with the same objective, i.e. glyoxal in lysozyme-PVOH films (Buonocore et al., 2003).

Table 8.1. Model parameters obtained from the fitting of Crank's solution for short times (**Equation 8.8**) to the experimental lysozyme release data.

Parameters	LZ-G1.5C_pH2	LZ-G3C_pH2	LZ-G5C_pH2
M_{120} (units/cm²)	26887	10243	4554
l (µm)	115	109	112
$D \cdot 10^{15}$ (cm²/s)	4.62 ± 0.83[a]	0.47 ± 0.29[b]	0.06 ± 0.05[b]
R^2	0.991	0.991	0.982

Values reported are the means ± standard deviations.
[a-c] Different lowercase letters in the same row indicate a statistically significant difference between films with different degrees of cross-linker ($p \leq 0.05$).

The release of active molecules varies widely depending on the type of polymer, the concentration of lysozyme loaded in the film, the temperature, and properties of the release medium. In general, diffusion coefficients of lysozyme in gliadin films were smaller than those obtained for other hydrophilic polymers evaluated by diverse authors (Buonocore et al., 2003; Cozzolino et al., 2013; Gemili et al., 2009).

8.3.4. Antimicrobial assay

The antimicrobial activity of gliadin films incorporating lysozyme was tested against *L. innocua,* and it is shown in **Figure 8.4**. In general, films containing 10% LZ significantly ($p \leq 0.05$) reduced the number of colony forming units per mL with respect to the control films only containing cinnamaldehyde. However, the greatest logarithmic reductions were obtained with the film LZ-G1.5C_pH2. These results highlight that films with a loosely cross-linked structure able to release a greater amount of lysozyme, can exert a greater antimicrobial activity.

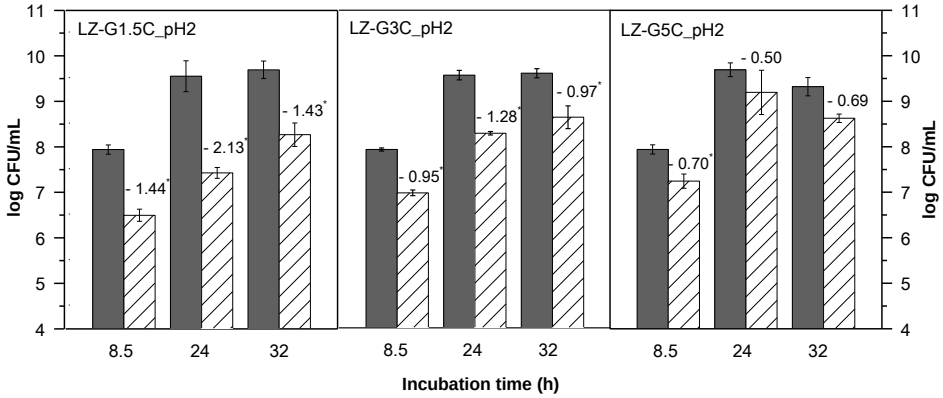

Figure 8.4. Antimicrobial activity, expressed as log CFU/mL, against *Listeria innocua* of films cross-linked with different amounts of cinnamaldehyde. Gray columns: control gliadin films cross-linked with cinnamaldehyde, white columns: gliadin films cross-linked with cinnamaldehyde containing 10% lysozyme. The numbers indicate the logarithmic reduction observed in the LZ-gliadin films with respect to the control gliadin films. * An asterisk indicates a statistically significant difference ($p \leq 0.05$).

8.3.5. Mechanical properties

The maximum tensile strength (σ_m), the percentage of elongation at break (ε_b) and the Young's Modulus (*E*) of the films are shown in **Table 8.2**. In general, a higher amount of cinnamaldehyde produced films with improved mechanical properties (Balaguer et al., 2011b), higher σ_m and *E*, but lower ε_b. When lysozyme was incorporated into the gliadin films a significant ($p \leq 0.05$) decrease in ε_b and a significant ($p \leq 0.05$) increase in *E* were observed. An increase in σ_m was also observed, being significant for films cross-linked with 1.5% of cinnamaldehyde. These results suggest that a denser and tighter polymer network was achieved when lysozyme was incorporated into gliadin films cross-linked with cinnamaldehyde. This effect was also found by Min et al. (2005) when lysozyme was incorporated into whey protein films, exhibiting higher *E* values and lower ε_b than the control films without lysozyme. It seems that lysozyme exerts an antiplasticizing effect on the protein films when it is incorporated at low concentrations. This antiplasticizing effect can be due to the capacity of these proteins to interact together forming complexes. However, when lysozyme was added to chitosan films the σ_m decreased (Park et al., 2004), but the ε_b followed the same decreasing behavior. Similarly, decreases in σ_m and ε_b of Na-alginate and kappa-carrageenan based films were reported with 5% and 10% lysozyme incorporation in the film matrix (Cha et al., 2002). i.e. in these films lysozyme exerts a plasticizing effect. The different behavior observed for lysozyme in proteinaceous or non-proteinaceous films can be due to a greater interaction capacity between lysozyme and amino groups of protein films. For caseinate films containing 1% lysozyme (w/w) Mendes de Souza et al. (2010) reported a negligible decrease in σ_m and ε_b.

Table 8.2. Maximum tensile strength (σ_m), percentage of elongation at break (ε_b), and Young's modulus (*E*) of gliadin films with different degrees of cross-linking, without lysozyme (−LZ), and with 10% lysozyme (+LZ), at 50% RH and 23 °C.

Sample	σ_m (MPa)		ε_b (%)		*E* (MPa)	
	−LZ	+LZ	−LZ	+LZ	−LZ	+LZ
G1.5C_pH2	5.2 ± 0.8^{a}	$7.0 \pm 0.2^{a*}$	248.4 ± 13.7^{c}	$188.9 \pm 16.3^{c*}$	34.9 ± 6.5^{a}	$98.8 \pm 10.3^{a*}$
G3C_pH2	7.7 ± 0.8^{b}	8.9 ± 2.0^{b}	179.9 ± 7.9^{b}	$156.6 \pm 17.9^{b*}$	63.9 ± 21.7^{b}	$131.0 \pm 22.6^{b*}$
G5C_pH2	9.9 ± 1.2^{c}	11.0 ± 1.2^{c}	145.6 ± 12.4^{a}	$120.7 \pm 11.9^{a*}$	112.1 ± 10.9^{c}	$196.2 \pm 27.5^{c*}$

Values reported are the means ± standard deviations (n = 10, 95% confidence interval).
[a-c] Different lowercase letters in the same column indicate a statistically significant difference between films with different degrees of cross-linker ($p \leq 0.05$).
[*] An asterisk in the same row indicates a statistically significant difference between films with or without lysozyme ($p \leq 0.05$).

8.3.6. Barrier properties

Water vapor and oxygen permeability values of films cross-linked with cinnamaldehyde and of these films incorporating lysozyme are given in **Table 8.3**. In general, the lowest ($p \leq 0.05$) values of permeability to oxygen and water were found for films treated with a greater amount of cinnamaldehyde, in concordance with the results obtained in gliadin films without lysozyme (Balaguer et al., 2013b). The addition of 10% lysozyme did not have a significant ($p > 0.05$) effect on the barrier properties of the films. These results are in accordance with those found by Park et al. (2004) for chitosan films and by Bower et al. (2006) for gelatin films, in which water vapor permeability was not significantly affected by the incorporation of lysozyme.

Table 8.3. Water vapor and oxygen permeability coefficients of gliadin films with different degrees of cross-linking, without lysozyme (−LZ), and with 10% lysozyme (+LZ), at 23 °C.

Sample	$WVP \cdot 10^{14}$ [(kg·m)/(m²·s·Pa)] ΔRH=50%–0%		$O_2P \cdot 10^{19}$ [(m³·m)/(m²·s·Pa)] RH=50%	
	−LZ	+LZ	−LZ	+LZ
G1.5C_pH2	3.95 ± 0.22^{b}	3.66 ± 0.24^{b}	2.52 ± 0.18^{b}	2.50 ± 0.04^{c}
G3C_pH2	3.75 ± 0.43^{ab}	3.76 ± 0.33^{b}	2.44 ± 0.05^{b}	2.31 ± 0.07^{b}
G5C_pH2	3.33 ± 0.15^{a}	3.22 ± 0.16^{a}	1.79 ± 0.22^{a}	1.81 ± 0.12^{a}

Values reported are the means ± standard deviations (n = 4, 95% confidence interval).
$^{a\text{-}c}$ Different lowercase letters in the same column indicate e a statistically significant difference between films with different degrees of cross-linker ($p \leq 0.05$).
*An asterisk in the same row indicates a statistically significant difference between films with or without lysozyme ($p \leq 0.05$).

8.4. CONCLUSION

Gliadin films preserved their integrity in water after modification with cinnamaldehyde and addition of lysozyme. The degree of swelling of the protein matrix decreased as the concentration of cross-linker increased. The release rate of the antimicrobial agent was controlled by the reticulation of the protein matrix, thus a greater degree of cross-linking led to slower release of the active agent. The greatest amount of antimicrobial agent released from the film to the medium was obtained for the film with a loosely cross-linked structure, which consequently exerted the highest antimicrobial activity against the microorganism evaluated. The potential of gliadin films cross-linked with cinnamaldehyde as carrier systems that can modulate the release of lysozyme was demonstrated.

8.5. REFERENCES

Appendini, P. 1997. Immobilization of lysozyme on food contact polymers as potential antimicrobial films. *Packaging technology & science, 10*(5), 271-279.

Arangoa, M. A., Campanero, M. A., Renedo, M. J., Ponchel, G., and Irache, J. M. 2001. Gliadin nanoparticles as carriers for the oral administration of lipophilic drugs. Relationships between bioadhesion and pharmacokinetics. *Pharmaceutical Research, 18*(11), 1521-1527.

ASTM. 2005. D3985. Standard test method for oxygen gas transmission rate through plastic film and sheeting using coulometric sensor.

ASTM. 2009. D882. Standard test method for tensile properties of thin plastic sheeting.

Balaguer, M. P., Borne, M., Chalier, P., Gontard, N., Morel, M. H., Peyron, S., Gavara, R., and Hernandez-Munoz, P. 2013a. Retention and release of cinnamaldehyde from wheat protein matrices. *Biomacromolecules, 14*(5), 1493-1502.

Balaguer, M. P., Cerisuelo, J. P., Gavara, R., and Hernandez-Muñoz, P. 2013b. Mass transport properties of gliadin films: Effect of cross-linking degree, relative humidity, and temperature. *Journal of Membrane Science, 428*, 380-392.

Balaguer, M. P., Fajardo, P., Gartner, H., Gomez-Estaca, J., Gavara, R., Almenar, E., and Hernandez-Munoz, P. 2014. Functional properties and antifungal activity of films based on gliadins containing cinnamaldehyde and natamycin. *International Journal of Food Microbiology, 173*(0), 62-71.

Balaguer, M. P., Gomez-Estaca, J., Gavara, R., and Hernandez-Munoz, P. 2011a. Biochemical properties of bioplastics made from wheat gliadins cross-linked with cinnamaldehyde. *Journal of Agricultural and Food Chemistry, 59*(24), 13212-13220.

Balaguer, M. P., Gomez-Estaca, J., Gavara, R., and Hernandez-Munoz, P. 2011b. Functional properties of bioplastics made from wheat gliadins modified with cinnamaldehyde. *Journal of Agricultural and Food Chemistry, 59*(12), 6689-6695.

Bower, C. K., Avena-Bustillos, R. J., Olsen, C. W., McHugh, T. H., and Bechtel, P. J. 2006. Characterization of fish-skin gelatin gels and films containing the antimicrobial enzyme lysozyme. *Journal of Food Science, 71*(5), M141-M145.

Buonocore, G. G., Del Nobile, M. A., Panizza, A., Bove, S., Battaglia, G., and Nicolais, L. 2003. Modeling the lysozyme release kinetics from antimicrobial films intended for food packaging applications. *Journal of Food Science, 68*(4), 1365-1370.

Buonocore, G. G., Sinigaglia, M., Corbo, M. R., Bevilacqua, A., La Notte, E., and del Nobile, M. A. 2004. Controlled release of antimicrobial compounds from highly swellable polymers. *Journal of Food Protection, 67*(6), 1190-1194.

Conte, A., Buonocore, G. G., Bevilacqua, A., Sinigaglia, M., and del Nobile, M. A. 2006. Immobilization of lysozyme on polyvinylalcohol films for active packaging applications. *Journal of Food Protection, 69*(4), 866-870.

Conte, A., Buonocore, G. G., Sinigaglia, M., Lopez, L. C., Favia, P., D'Agostino, R., and del Nobile, M. A. 2008. Antimicrobial activity of immobilized lysozyme on plasma-treated polyethylene films. *Journal of Food Protection, 71*(1), 119-125.

Cornell, H. J., and Hoveling, A. W., 1998. *Wheat: Chemistry and utilization*. Technomic Publishing Company, Inc.: Lancaster, PA, USA.

Cozzolino, C. A., Nilsson, F., Iotti, M., Sacchi, B., Piga, A., and Farris, S. 2013. Exploiting the nano-sized features of microfibrillated cellulose (MFC) for the development of controlled-release packaging. *Colloids and Surfaces B: Biointerfaces, 110*, 208-216.

Crank, J., 1975. *The mathematics of diffusion*. 2nd ed.; Oxford University Press, London: 44-69.

Cha, D. S., Choi, J. H., Chinnan, M. S., and Park, H. J. 2002. Antimicrobial films based on Na-alginate and kappa-carrageenan. *Lebensmittel-Wissenschaft Und - Technologie-Food Science and Technology, 35*(8), 715-719.

Chen, L. Y., Remondetto, G. E., and Subirade, M. 2006. Food protein-based materials as nutraceutical delivery systems. *Trends in Food Science & Technology, 17*(5), 272-283.

Datta, R., Armiger, W., and Ollis, D. 1973. Lysis of micrococcus-lysodeikticus by lysozyme covalently immobilized on cellulose and polyacrylamide. *Biotechnology and Bioengineering, 15*(5), 993-1006.

Duan, J., Park, S., Daeschel, M., and Zhao, Y. 2007. Antimicrobial chitosan-lysozyme (CL) films and coatings for enhancing microbial safety of Mozzarella cheese. *Journal of Food Science, 72*(9), M355-M362.

Duclairoir, C., Irache, J. M., Nakache, E., Orecchioni, A. M., Chabenat, C., and Popineau, Y. 1999. Gliadin nanoparticles: Formation, all-trans-retinoic acid entrapment and release, size optimization. *Polymer International, 48*(4), 327-333.

Duclairoir, C., Orecchioni, A. M., Depraetere, P., and Nakache, E. 2002. Alpha-tocopherol encapsulation and in vitro release from wheat gliadin nanoparticles. *Journal of Microencapsulation, 19*(1), 53-60.

Ezpeleta, I., Irache, J. M., Stainmesse, S., Chabenat, C., Gueguen, J., Popineau, Y., and Orecchioni, A. M. 1996. Gliadin nanoparticles for the controlled release of all-trans-retinoic acid. *International Journal of Pharmaceutics, 131*(2), 191-200.

Gemili, S., Yemenicioglu, A., and Altinkaya, S. A. 2009. Development of cellulose acetate based antimicrobial food packaging materials for controlled release of lysozyme. *Journal of Food Engineering, 90*(4), 453-462.

Gulfam, M., Kim, J.-e., Lee, J. M., Ku, B., Chung, B. H., and Chung, B. G. 2012. Anticancer drug-loaded gliadin nanoparticles induce apoptosis in breast cancer cells. *Langmuir, 28*(21), 8216-8223.

Hernandez-Munoz, P., Kanavouras, A., Ng, P. K. W., and Gavara, R. 2003. Development and characterization of biodegradable films made from wheat gluten protein fractions. *Journal of Agricultural and Food Chemistry, 51*(26), 7647-7654.

ISO. 1995. 2528. Sheet materials - Determination of water vapour transmission rate - gravimetric (dish) method.

Kajal, H., and Misra, A. 2011. Preparation of tetanus toxoid and ovalbumin loaded gliadin nanoparticles for oral immunization. *Journal of Biomedical Nanotechnology, 7*(1), 211-212.

Krochta, J. M. 2002. Proteins as raw materials for films and coatings. In *Protein-Based Films and Coatings*, CRC Press: Boca Raton.

Losso, J. N., Nakai, S., and Charte, E. A. 2000. Lysozyme. In *Natural food antimicrobial systems*, N. AS, Ed. CRC Press: Boca Raton.

Ma, W., Tang, C. H., Yin, S. W., Yang, X. Q., and Qi, J. R. 2013. Genipin-crosslinked gelatin films as controlled releasing carriers of lysozyme. *Food Research International, 51*(1), 321-324.

Mastromatteo, M., Conte, A., and Del Nobile, M. A. 2010. Advances in controlled release devices for food packaging applications. *Trends in Food Science & Technology, 21*(12), 591-598.

Mecitoglu, C., Yemenicioglu, A., Arslanoglu, A., Elmaci, Z. S., Korel, F., and Cetin, A. E. 2006. Incorporation of partially purified hen egg white lysozyme into zein films for antimicrobial food packaging. *Food Research International, 39*(1), 12-21.

Mendes de Souza, P., Fernandez, A., Lopez-Carballo, G., Gavara, R., and Hernandez-Munoz, P. 2010. Modified sodium caseinate films as releasing carriers of lysozyme. *Food hydrocolloids, 24*(4), 300-306.

Min, S., Harris, L. J., Han, J. H., and Krochta, J. M. 2005. *Listeria monocytogenes* inhibition by whey protein films and coatings incorporating lysozyme. *Journal of Food Protection, 68*(11), 2317-2325.

Min, S., Rumsey, T. R., and Krochta, J. M. 2008. Diffusion of the antimicrobial lysozyme from a whey protein coating on smoked salmon. *Journal of Food Engineering, 84*(1), 39-47.

Padgett, T., Han, I., and Dawson, P. 1998. Incorporation of food-grade antimicrobial compounds into biodegradable packaging films. *Journal of Food Protection, 61*(10), 1330-1335.

Park, S., Daeschel, M., and Zhao, Y. 2004. Functional properties of antimicrobial lysozyme-chitosan composite films. *Journal of Food Science, 69*(8), M215-M221.

Ramteke, S., and Jain, N. K. 2008. Clarithromycin- and omeprazole-containing gliadin nanoparticles for the treatment of *Helicobacter pylori*. *Journal of Drug Targeting, 16*(1), 65-72.

Shugar, D. 1952. The measurement of lysozyme activity and the ultra-violet inactivation of lysozyme. *Biochimica Et Biophysica Acta, 8*(3), 302-309.

Stella, V., Vallee, P., Albrecht, P., and Postaire, E. 1995. Gliadin films 1. Preparation and in-vitro evaluation as a carrier for controlled drug-release. *International Journal of Pharmaceutics, 121*(1), 117-121.

Suppakul, P., Miltz, J., Sonneveld, K., and Bigger, S. W. 2003. Active packaging technologies with an emphasis on antimicrobial packaging and its applications. *Journal of Food Science, 68*(2), 408-420.

Zhou, Y. 2008a. Nanocomposite for preparing medicine for treating hepatitis, comprises silibinin and carrier material wheat gliadin having predetermined grain size. CN101317840-A; CN101317840-B.

IV. GENERAL DISCUSSION

The present Doctoral Thesis deals with the development, characterization, and application of new antimicrobial bioplastic films based on chemically cross-linked wheat gliadins designed for food packaging applications.

The selection of gliadins as the matrix for the production of biobased and biodegradable films was based on:

1) The use of by-products. The wheat gluten which was used as raw material for the extraction of gliadins is a by-product in the starch industry[1].

2) Abundant availability. Worldwide annual production of wheat is around 700 million tons[2], the vast majority used for human food and livestock feed. Since starch production in Europe was 10 million tons in 2012[3], the production of wheat gluten could be estimated as about 2.3 million tons per year. Indeed, production of starch is steadily rising[4] because it is used to obtain bioethanol, and as raw material for the manufacture of other bioplastics such as thermoplastic starch (TPS) and poly(lactic acid) (PLA).

3) Low cost. The price of vital wheat gluten ranges from 0.5 to 1.2 €/kg[5], being a cost-competitive raw material.

4) Low environmental impact. Wheat gluten films offer better environmental performance compared with PLA and LDPE films[6]. The extraction of gliadins by means of aqueous ethanol solutions at ambient temperature followed by centrifugation and decantation and the manufacture of film by a coating processing is environmentally more compatible and sustainable than the production of other polymers and the preparation of film-forming solutions where more toxic solvents such as chloroform or ethyl acetate and mild/high temperatures are used.

[1] http://www.iwga.net/what_is_wg.htm

[2] http://www.igc.int/es/grainsupdate/sd.aspx?crop=Wheat

[3] http://www.aaf-eu.org/european-starch-industry

[4] http://www.aaf-eu.org

[5] http://spanish.alibaba.com/product-list/gluten/pid100008856--glutens.html

[6] Deng, Y., Achten, W. M. J., Van Acker, K., and Duflou, J. R. 2013. Life cycle assessment of wheat gluten powder and derived packaging film. *Biofuels, Bioproducts and Biorefining*.

5) High solubility and stability. Gliadins are soluble in ethanol 70% (v/v) and are easily extracted from wheat or gluten, achieving a high extraction yield. Film-forming hydroalcoholic solutions can be stored for a long period of time without alteration of protein properties.

6) Film-forming ability. Gliadins present excellent film-forming properties, and the films produced are extremely homogeneous, transparent, and glossy.

7) Water insolubility but water sensitivity. Although gliadins are insoluble in water, their water sensitivity can be used as a trigger mechanism for the release of molecules previously incorporated into the matrix, which could lead to the production of active films.

8) Inherent compostability. Proteins are biobased materials which are biodegradable in various media. Gliadins are disintegrated and biodegraded in composting environments at a rate consistent with other known compostable materials and without leaving visible distinguishable or toxic residues, thus fulfilling the requirements stated in EN 13432.

Despite all these benefits, gliadin films are very brittle and need to be plasticized, and their physical properties such as mechanical resistance and water vapor barrier should be improved in order to provide a real alternative to conventional polymeric materials. Accordingly, gliadins were modified with cinnamaldehyde (**Figure 1.1**), a naturally-occurring α,β-unsaturated aldehyde which is the major component of cinnamon bark essential oil. The cross-linking reaction was found to be pH-dependent and pH 2 was shown to be the optimum pH according to the resulting functional properties of the films produced by solution-casting.

The molecular weight profiles obtained by Sodium Dodecyl Sulfate–Polyacrylamide Gel Electrophoresis (SDS-PAGE) (**Figure 2.1**), and Size Exclusion–High Performance Liquid Chromatography (SE-HPLC) (**Figure 4.2**) provided biochemical evidence of cross-linking of gliadins by cinnamaldehyde. The formation of a polymerized network of gliadins was evidenced by: (i) protein aggregates of high molecular weight that did not enter the gel, (ii) reduction of bands intensity of fractions corresponding to gliadins (35 to 50 kDa) in the SDS-PAGE analysis, and (iii) an increase in higher molecular weight fractions (> 680 kDa) in the SDS-insoluble fraction in SE-HPLC.

Both analyses also highlighted that the cross-linking reaction took place while the film was drying, since no differences were found in the molecular weight profiles of the film-forming solutions. This was also revealed by Attenuated Total Reflectance–Fourier Transform Infrared Spectroscopy (ATR-FTIR). Indeed, conformational changes in the protein structure, reflected as formation of intermolecular β-sheets to the detriment of the initial α-helical structure, were clearly distinguished (**Figure 4.5**).

The studies of protein solubility in various media (phosphate buffer, SDS, 2-ME, DTE) disclosed the limited participation of non-covalent bonds and disulfide bridges in stabilizing the cross-linked protein structure (**Table 1.1**, **Table 2.1**, **Table 4.2**, **Figure 2.2**). The involvement of amino groups in the cinnamaldehyde cross-linking reaction was evaluated by determining the content of free amino groups in the film-forming solutions at various pHs, and in the films treated at pH 2 with various amounts of cinnamaldehyde (**Figure 2.4**), along with the analysis of amino acid composition (**Figure 2.5**).

The results from the various assays carried out proved that films made from acidified gliadins (pH 2) were weaker, and in some way denatured (lower Young's modulus, lower elongation at break, lower glass transition temperature, lower peak decomposition temperature, lower cross-linking density, higher solubility, etc.). It is known that at pHs far from the isoelectric point net charges induce side-chain repulsion that leads to conformational changes, protein unfolding, rupture of hydrogen bonds, and alteration of hydrophobic interactions. These changes in the native conformation of the protein can favor the exposure of reactive groups that are otherwise buried. This was also proved by analysis of free amino groups, which were present in a higher concentration at pH 2, and whose amount decreased after addition of cinnamaldehyde (**Figure 2.4**).

Amino acid analysis was carried out to evaluate modifications in the amino acid molar composition as a consequence of the reaction of cinnamaldehyde with protein residues. The downward tendency of glutamine could be indicative of a reaction between its amino/amide group with cinnamaldehyde (**Figure 2.5**).

In view of these results, a possible mechanism of wheat gliadin cross-linking by means of cinnamaldehyde was proposed (**Figure 2.3**). The combination of a Schiff base and a Michael addition between the amino groups of the protein and cinnamaldehyde could be a feasible mechanism; however, the participation of other reactive side groups such as thiol or phenol could not be ruled out.

Treatment of gliadins with cinnamaldehyde at pH 2 led to a slight change in the color of the films, increasing the yellowish component. At pH 6, cinnamaldehyde did not act as a cross-linker for gliadins and the films developed acquired a vivid yellow color due to the formation of a Schiff base (C=N) and thus the presence of a conjugated double bond (**Figure B.1**).

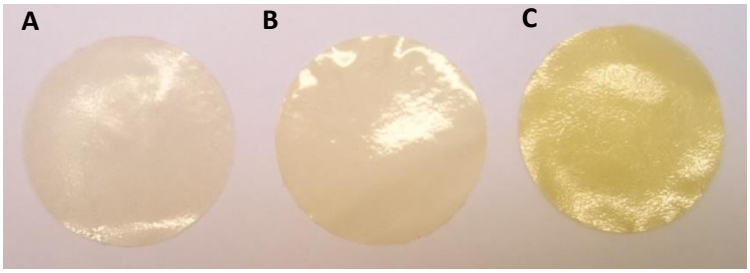

Figure B.1. Visual appearance of gliadin films: **(A)** Non-cross-linked gliadin film (G_pH6), **(B)** Cross-linked gliadin film (G5C_pH2), **(C)** Non-cross-linked gliadin film (G5C_pH6).

Mechanical properties of cross-linked films improved considerably compared with control gliadin films. The maximum tensile strength increased from 1.6 to 9.9 MPa measured at 50% RH, and Young's modulus rose to 112 MPa, 470% more than gliadin film G_pH6 (**Table 1.2**). The elongation at break decreased to 146%, almost 60% lower than that of the control film, which could be considered as a preservation of their viscous properties (**Table 1.2**). These results were related with the cross-linking density achieved (**Table 2.1**), which was proportional to the percentage of cinnamaldehyde incorporated. Mechanical properties were highly affected by the relative humidity (**Figure 1.4** and **Table 1.2**). Water vapor produces a high level of plasticization, reducing intermolecular forces between polypeptide chains and increasing the free volume of the network.

After cinnamaldehyde treatment at pH 2, water stability increased enormously because the films became water resistant (**Figure B.2**). Water uptake was inversely proportional to the amount of cross-linker added (**Table 2.1**), and weight loss of cross-linked films was mostly due to glycerol migration to the aqueous media (**Table 1.3**), because dissolved protein was nearly 10 mg/g film (**Figure 2.2**). Moreover, long-term water stability studies revealed that cross-linked gliadin films did not suffer considerable physical changes when immersed for up to 20-30 days in aqueous medium, and did not disintegrate for at least 5 months (**Figure 2.6**). The enzymatic degradation under simulated gastric and intestinal

conditions in which the proteolytic enzymes pepsin and trypsin were employed showed that the films may be degraded in the stomach only if low cross-linking treatment is applied (**Figure 2.7**).

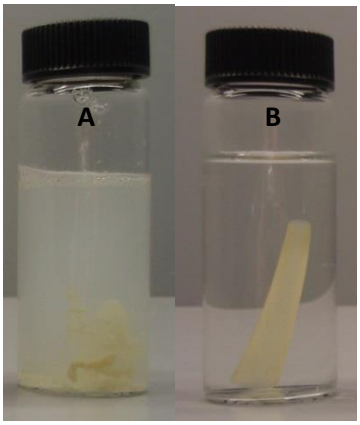

Figure B.2. Water resistance: **(A)** Non-cross-linked gliadin film (G_pH6), **(B)** Cross-linked gliadin film (G5C_pH2).

The increase in the glass transition temperature obtained by Modulated Differential Scanning Calorimetry (MDSC) of cross-linked gliadin films in comparison with the control gliadin film produced at pH 2 revealed a reduction in the mobility of the polymer chains as a consequence of the restrictions imposed by the new intermolecular bonds created among gliadins (**Table 1.4**). The peak decomposition temperatures measured by Thermogravimetric Analysis (TGA) also reflected an increase in the thermal stability of the cross-linked polymer in comparison with G_pH2 (**Table 1.4**). A small loss of weight at cinnamaldehyde decomposition temperature was also detected, and attributed to free cinnamaldehyde remaining in the matrix and not involved in the cross-linking reaction (**Figure 1.5**).

Another important achievement was that chemical modification of gliadins by means of cinnamaldehyde improved barrier properties of the films against water vapor, oxygen, and carbon dioxide (**Figure 3.1**, **Figure 3.11**, **Figure 3.12**). The formation of a more reticulated network reduced permeability by up to 64% (35%-0% ΔRH), 75% (35% RH), and 79% (75% RH), respectively, for water vapor, oxygen, and carbon dioxide. Barrier properties were highly influenced by relative humidity. The values of water permeability ranged from

$6.6 \cdot 10^{-15}$ to $3.4 \cdot 10^{-13}$ (kg·m)/(m^2·s·Pa), depending on the degree of cross-linking and relative humidity (**Figure 3.1**). The increase in the relative humidity gradient from 35%-0% to 90%-0% raised the permeability 50-fold, being less influenced than the oxygen permeability coefficient, which increased 150-fold (**Figure 3.8**). Oxygen permeabilities were up to 3 orders of magnitude lower than those for polyolefin films (**Table 3.4**), ranging from $5 \cdot 10^{-20}$ to $2.1 \cdot 10^{-17}$ (m^3·m)/(m^2·s·Pa). Carbon dioxide permeabilities ranged from $6.6 \cdot 10^{-19}$ to $1.7 \cdot 10^{-17}$ (m^3·m)/(m^2·s·Pa), and, contrary to what was found for water vapor and oxygen, the differences in carbon dioxide permeability with respect to the control films were greater at higher relative humidity.

Water vapor mass transport phenomena were found to be highly complex in gliadin films owing to their hydrophilic nature. Water vapor sorption isotherms were fitted with a non-linear model (D'Arcy and Watt) (**Figure 3.3**, **Figure 3.4**, and **Table 3.3**). Water vapor diffusivity was concentration-dependent (**Figure 3.6** and **Figure 3.7**), because the amount of water diffusing molecules highly affected various properties of the protein matrix (such as degree of plasticization, water clustering, availability of free active sites, chain segmental motion, free volume, state of the amorphous region, and glass transition temperature) that influenced water diffusion through the film. Water vapor diffusivity values were in the range of 1 to $20 \cdot 10^{-20}$ (m^2/s), and were affected by the degree of cross-linking. Temperature-dependence of water vapor permeability presented a discontinuity when the Arrhenius law was applied, which could be indicative of a change of state in the matrix. The influences of activation energy of permeation and diffusion, heats of solution, condensation, and mixing, and pre-exponential factor of the Arrhenius law were discussed in detail, and attention was drawn to the difficulty of distinguishing between temperature-dependent effects and concentration-dependent effects.

Oxygen mass transport phenomena fitted ideally with Arrhenius (**Figure 3.9**), and the diffusion coefficient was dependent on the relative humidity and on the degree of cross-linking, with values in the range of $7.8 \cdot 10^{-14}$ to $1.7 \cdot 10^{-12}$ (m^2/s) (**Figure 3.10** and **Figure 3.11**).

The amount of free cinnamaldehyde, that is, aldehyde molecules not participating in the cross-linking reaction, was evaluated by solvent extraction and gas chromatography. Despite the losses incurred in the film processing and the amount that remained covalently bonded to the protein, the addition of 1.5, 3, and 5% of cinnamaldehyde (g/100 g protein)

produced 0.18, 0.48, and 1.1% of free cinnamaldehyde (g/100 g film), respectively (**Figure 4.8**). The diffusion coefficients of cinnamaldehyde at 90% RH were estimated to be around $9\text{-}13\cdot10^{-15}$ (m^2/s); however, the possible effect of the degree of cross-linking, observed for oxygen and water vapor diffusivities, was counterbalanced by the potential cinnamaldehyde plasticization effect at high concentrations (**Figure 4.9** and **Table 4.4**). The effect of relative humidity on the kinetic release of cinnamaldehyde from gliadin films was noteworthy. The cinnamaldehyde diffusion coefficient rose from $4.9\cdot10^{-16}$ at 30% RH to $1.3\cdot10^{-14}$ at 90% RH (m^2/s) (**Figure 4.10** and **Table 4.5**). This water sensitivity provides: (i) a triggering mechanism for the release of the cinnamaldehyde entrapped in the matrix by weak bonds when the films are exposed at high relative humidities, which are typical conditions present in some packaged foodstuffs, and (ii) a method for retaining this volatile compound whenever low relative humidity is maintained, preventing its depletion from the time of film production to that of application.

Overall migration in food simulants was determined according to Regulation 10/2011/EC (**Table 4.3**). Although the values were hardly over the regulation limit of 10 mg/dm^2, it is important to point out that they correspond mostly to gliadin proteins, which do not present a risk for the vast majority of the population.

Cinnamaldehyde antimicrobial properties have been demonstrated by many authors (**Table I.4** and **Table I.5**). The resulting films were tested *in vitro* against common food-spoilage fungi, *Penicillium expansum* and *Aspergillus niger*, and were employed in the active packaging of sliced bread and cheese spread. The results showed that the films were highly effective *in vitro* against mold growth by means of vapor diffusion, i.e. without direct contact (**Figure 5.1**). Films incorporating 1.5% cinnamaldehyde were sufficient to inhibit the growth of *P. expansum* for 10 days, whereas to inhibit the growth of *A. niger* films with at least 3% cinnamaldehyde were needed (**Figure 5.2**). Films incorporating 5% cinnamaldehyde were shown to be fungicidal against both species (**Table 5.1**).

Active packaging of both bread and cheese with films incorporating 5% cinnamaldehyde reduced microbial spoilage, thus increasing their shelf-life. Mold growth was evident after 4 days when bread was packed without the active films; whereas the lag time increased up to 28 days when active packaging was employed (**Table 5.2**). In the case of cheese spread the lag time increased by 10 days; from 16 with control packaging to 26 days with active packaging (**Table 5.3**).

Despite the promising antimicrobial activity obtained, further research must be conducted in order to verify whether active packaging with cinnamaldehyde imparts new organoleptic features compatible with the foodstuffs that do not modify consumer acceptability.

The proven antimicrobial efficacy together with the improved functional properties, especially water resistance, might have modified their inherent biodegradable nature. However, compostability studies based on EN 13432 with modifications showed organic recycling as a feasible end-of-life option, because disintegration and biodegradation in composting conditions and ecotoxicity of the resulting compost were favorable. The most cross-linked gliadin films showed a very fast disintegration behavior, being converted into fine, visually indistinguishable residues in only four days after being placed in compost media (**Figure 6.1**). The rapid microbial colonization of the surface of the films was revealed by Scanning Electron Microscopy (SEM) (**Figure 6.2**). Biodegradation kinetics were influenced by the degree of cross-linking of the proteinaceous matrices; however, biodegradation was complete independently of it (**Figure 6.3**). The presence of remaining free cinnamaldehyde in the films, which could be released and exert antimicrobial activity, did not hamper their biodegradation and did not cause ecotoxicity in tomato seed germination and plant growth (**Table 6.2**).

After chemical modification of the gliadin matrix, it was possible to achieve different levels of water swelling without disintegration, depending on the degree of cross-linking attained. This property, together with the inherent water sensitivity of gliadins, was used to employ new films as carriers and sustained release matrices for other naturally-occurring antimicrobials apart from cinnamaldehyde, being capable of modulating the release of these molecules as a function of the extent of cross-linking. Natamycin (0.5% g NT/100 g protein) and lysozyme (10% g LZ/100 g protein) were selected and incorporated into the films. The functional properties and antimicrobial efficacy of the resulting films were investigated.

Natamycin incorporation into cross-linked films gave rise to a more water sensitive matrix: greater water uptake, weight loss, and diameter gain by swelling (**Table 7.1**), and higher water vapor and oxygen permeabilities (**Table 7.2**). The looser packing of protein chains as a consequence of the presence of natamycin produced matrices with lower resistance to mass transfer and less stability in liquid medium compared with control gliadin films cross-linked with cinnamaldehyde. The different degree of cross-linking of the matrices

influenced natamycin migration to agar test media, increasing from 13.3 to 23.7 (μg/g film) as the percentage of cinnamaldehyde was reduced from 5% to 1.5% (**Table 7.3**). However, greater antifungal activity against *Penicillium* species was obtained for films treated with 5% of cinnamaldehyde and containing natamycin (**Figure 7.3**). For the other fungi, *Alternaria solani,* and *Colletotrichum acutatum*, no significant differences were found with the addition of natamycin (**Figure 7.3**). The level of cinnamaldehyde reached in the head-space of the test assay showed a diminishing trend as a function of time (**Figure 7.4**), which was in agreement with fungal growth and cinnamaldehyde metabolization. Fungi converted cinnamaldehyde into styrene as a consequence of its metabolization. The antimicrobial performance was evaluated in cheese slices with promising results, because no growth was observed in the zones covered by the antimicrobial films (**Figure 7.7** and **Figure 7.8**).

Incorporation of lysozyme did not affect barrier properties (**Table 8.3**), whereas mechanical properties were improved, suggesting that a denser and tighter polymer network was achieved when lysozyme was incorporated into cross-linked gliadin films (**Table 8.2**). Interactions between polypeptide chains of lysozyme and gliadins could be taking place. In accordance with the natamycin results, films with a lower degree of cross-linking released a greater amount of lysozyme, reaching 50% of migration for the film cross-linked with 1.5% cinnamaldehyde (**Figure 8.2**). The release kinetics were also controlled by the reticulation of the protein matrix. Both results are related with the degree of swelling of the protein matrix, which produces relaxation of the matrix, favoring diffusion of the antimicrobial agent to the medium. Therefore, diffusion coefficients of lysozyme ranged from $4.62 \cdot 10^{-15}$ to $0.06 \cdot 10^{-15}$ cm^2/s for films LZ-G1.5C_pH2 and G5C_pH2, respectively (**Table 8.1**). The antimicrobial activity in liquid medium against *Listeria innocua* was in agreement with the amount of lysozyme released (**Figure 8.4**).

V. CONCLUSIONS

1. Gliadin proteins were cross-linked by chemical treatment with cinnamaldehyde at acidic pH during the film-casting process. Solvent evaporation gave rise to an increase in protein concentration, which eased the cross-linking reaction. The formation of covalent bonds among polypeptide chains polymerized “monomeric” gliadins and reticulated the protein matrix. The degree of cross-linking achieved was proportional to the amount of cinnamaldehyde added. The combination of Schiff bases and Michael additions between the amino groups of gliadins and cinnamaldehyde could represent a feasible mechanism for the cross-linking reaction. However, the participation of other reactive side groups could not be ruled out. In addition, some reformation of disulfide bonds through sulfhydryl-disulfide interchange reactions and air reoxidation, and non-covalent interactions (hydrophobic and hydrogen bonding) as well as new physical entanglements also contributed to the film structure.

2. The resulting cross-linked gliadin-based films possessed greater mechanical strength and stiffness, without impairment of their elongation capacity. Water resistance, measured as solubility, swelling, weight loss, and dimensional stability, showed significant improvements with respect to control films, which lost their integrity in liquid medium. Migration to food simulants was slightly over the regulation limit (10 mg/dm^2), but a remarkable reduction was achieved in comparison with other gluten-based films.

3. Reduction of water vapor, oxygen, and carbon dioxide permeability was achieved with cinnamaldehyde-treatment, providing a powerful strategy for improving barrier properties. As a consequence of the hydrophilicity of the films, water vapor transport phenomena deviated substantially from the ideal behavior because: a) water vapor permeability showed a discontinuity when the Arrhenius law was applied, indicating possible changes in the state of the amorphous phase of the matrix; b) water vapor sorption isotherms followed a non-linear profile, fitting the D’Arcy and Watt model; and c) water vapor diffusivity was concentration-dependent with a bell-like profile, increasing as a consequence of matrix plasticization and decreasing owing to water clustering. At low relative humidity, oxygen and carbon dioxide permeabilities were up to 3-log units lower, and selective permeation to carbon dioxide vs. oxygen up to 3-fold greater than for common polyolefin films.

4. Thermal properties evaluated by thermogravimetry and modulated differential scanning calorimetry revealed some denaturation and loss of thermal stability of proteins exposed to acidic conditions. Side-chain repulsions induced by net charges, generated at pHs far from the isoelectric point, produced conformational changes in the structure of the protein. Protein unfolding, rupture of hydrogen bonds, and hydrophobic interactions facilitated chain mobility, lowering glass transition temperature and decomposition temperature. However, when proteins were treated with cinnamaldehyde, the value of both parameters increased as a consequence of the greater cross-linking density and molecular weight reached. Free cinnamaldehyde not participating in the cross-linking reaction remained entrapped in the protein matrix by weak bonding at low relative humidity conditions. At intermediate and high relative humidity conditions, moisture triggered the release of cinnamaldehyde, with the diffusion coefficient being greatly affected. Hence, protein water sensitivity provides a mechanism with a noteworthy potential for retaining the active compound in the films before their use, and for triggering its release when needed.

5. The inherent biodegradability of gliadins was not hampered even for samples with the greatest degree of cross-linking and despite the possible presence of residual free cinnamaldehyde. The films were able to disintegrate very quickly under composting conditions and the resulting compost did not exert any ecotoxic effect against tomato plants. Therefore, the films showed compostable ability, which represents a sustainable and environmentally-friendly end-of-life option.

6. Gliadin films incorporating cinnamaldehyde inhibited fungal growth of *Penicillium expansum* and *Aspergillus niger in vitro* by vapor diffusion. The films exerted a fungistatic and in some cases a fungicidal effect against both fungal species. Active packaging of sliced bread and cheese spread with cinnamaldehyde-containing films delayed microbial spoilage by prolonging lag phase and slowing down the growth rate, and thus extended the shelf-life of both foodstuffs. However, further research must be conducted in order to verify whether active packaging with cinnamaldehyde produces an organoleptic impact compatible with foodstuffs and their acceptance by consumers.

7. Natamycin and lysozyme were incorporated satisfactorily in cross-linked films. The degree of cross-linking achieved was able to modify the release of both antimicrobial compounds as films with a looser structure were able to release higher amounts of the

antimicrobial compounds. Incorporation of natamycin gave rise to films with greater water uptake, weight loss, and diameter gain, and higher water vapor and oxygen permeabilities, probably owing to lower packing of protein chains caused by the presence of natamycin. The films showed moderate antifungal activity against common food spoilage fungi (*Penicillium species*, *Alternaria solani*, and *Colletotrichum acutatum*) in *in vitro* assays by disc diffusion. Fungi metabolized cinnamaldehyde into styrene, reducing its concentration in the head-space. In active packaging tests with a real product, cheese slices showed no fungal growth in the zones covered by the antimicrobial films.

8. Incorporation of lysozyme did not affect barrier properties, whereas mechanical properties were improved, suggesting the formation of a denser and tighter polymer network, possibly owing to interactions established between polypeptide chains of lysozyme and gliadins. The antimicrobial activity in liquid medium against *Listeria innocua* was in agreement with the amount of lysozyme released.